The Reductive Amination of Ethanol using Supported Metal Catalysts

By

Gary Stanton Sewell - BSc (Chem. Eng.)

Submitted to the University of Cape Town in fulfilment of the requirements for the degree of

DOCTOR OF PHILOSOPHY

Department of Chemical Engineering
University of Cape Town
Rondebosch
Cape Town
South Africa

14 August 1996

Acknowledgements

I would like to thank my supervisors Dr Eric van Steen and Professor Cyril O'Connor for their guidance and encouragement without which this thesis would not have been possible. My thanks also go to Dr Klaus Moller for the fruitful discussions and to Professor Mark Dry for his help with aspects of metal catalysis.

I would like to thank Rob for the great times, Tony for his friendship, Jannie for his cool hairstyle and Rein for having a comfortable couch. Thanks to Dave for introducing me to the finer intricacies of toolboxes, to Ashley for his unending optimism and to Peter for always losing at pool. To the "Young Ones", Chappie, St. John, Frank, Andrew, Mary and Frans, thanks for the great parties and may the department survive you.

To the catalysis ladies Pam and Leslie, thank you for all of your help with ordering and with the literature. Also to the electrical and mechanical workshops for their help in constructing my rig and to the cleaner staff for preventing my lab from becoming a Class 3 hazard. Special thanks also to Katarina for all the chemisorption work.

I would like to thank the FRD and the Catalysis Research Unit for postgraduate funding and AECI, especially Norbert Behrens, for allowing me the time to complete my postgraduate studies.

Lastly, I wish to thank my parents Keith and Maureen who have supported me throughout and Debbie for being such a great sister.

Synopsis

Silica supported cobalt, nickel and copper are efficient catalysts for the reductive amination of ethanol using ammonia. High selectivity to ethylamine product was obtained between reaction temperatures of 140 and 200°C, between ammonia to ethanol molar ratios ranging from 1 to 4 and between hydrogen to ethanol molar ratios ranging from 2 to 5. Depending on the partial pressures of the ethanol, ammonia and hydrogen feeds, different ethylamine selectivities were obtained. The degree of amine substitution was decreased (*i.e.* increasing MEA and decreasing DEA and TEA selectivities) by increasing the ammonia partial pressure or by decreasing either the ethanol or hydrogen partial pressures.

At a reaction temperature of 180°C, a WHSV of 2 g_{EtOH}/g_{cat}·h and an EtOH : NH_3 : H_2 : N_2 molar feed ratio of 1 : 2 : 4.1 : 13.6, the steady state ethanol conversion activity was seen to decrease from 41 to 22 to 5 mol% as the metal was changed from nickel to cobalt to copper. These differences were caused largely by changes in metallic dispersion and metal reducibility, with the overall metallic surface area decreasing in the same order. When the specific activity of the catalysts was calculated, it was seen that the turnover frequency decreased from 0.11 to 0.09 to 0.05 molecules of ethanol per active site per second as the metal was changed from cobalt to nickel to copper. On this basis, it was concluded that principally cobalt is the best catalyst for the reductive amination reaction.

The rate of ethylamine formation during reductive amination was modelled using Langmuir-Hinshelwood kinetics since power rate law models proved inadequate in describing the behaviour of the cobalt, nickel and copper catalysts. Although previous kinetic studies indicated that the rate of alcohol dehydrogenation was the rate limiting step during reductive amination [Kryukov *et al*, 1967; Baiker *et al*, 1983], this was not observed for the silica supported cobalt, nickel and copper catalysts. In the case of the Co/SiO_2 catalyst, the rate determining step for the formation of MEA was described by the rate of surface reaction between ethanol and ammonia whereas the rates of DEA and TEA formation could be described by kinetic expressions formulated for a case in which the rate of ethanol adsorption was the controlling step. It was also found that the cobalt catalyst was partially deactivated

during amination due to the formation of cobalt nitride. The formation of cobalt nitride increased with increasing ammonia partial pressure but decreased with increasing hydrogen partial pressure. The formation of cobalt nitride was only significant below hydrogen to ammonia molar ratios of 2.5 : 1 however and in order to obtain maximum catalyst utilization, it is recommended that cobalt catalysts are operated at higher hydrogen to ammonia molar ratios.

With Ni/SiO_2, the rates of MEA, DEA and TEA formation could be described using kinetic expressions formulated for a case where the rate of surface reaction was the controlling step. In order to obtain a good prediction of the experimental behaviour of the nickel catalyst, the kinetic expression describing the rate of MEA formation had to be modified by decreasing the power on the adsorption term from 2 to 1. This would indicate that MEA is formed via an Eley-Rideal mechanism over nickel catalysts where a gas phase molecule reacts with an adsorbed surface species. This mechanism was not supported by the other experimental evidence and it is possible that the assumed series reaction mechanism was too simple. As with the cobalt catalyst, the amination behaviour of the nickel catalyst could not be described by expressions developed for a case in which the rate of alcohol dehydrogenation was the rate limiting step.

For the Cu/SiO_2 catalyst, the rates of MEA and DEA formation were best described by kinetic expressions derived for a case in which the rate controlling step was that of ethanol adsorption whereas the rate of TEA formation was best described by a kinetic expression in which the reaction between adsorbed ethanol and DEA was the controlling step. As a consequence of the series nature of the amination reaction and the low MEA selectivities obtained using this metal, it was found that the rates of MEA and DEA formation were almost identical within the range investigated.

The differences in ethylamine selectivity were ascribed to the difference in the strengths of adsorption (as estimated from the kinetic regressions) of ethanol and ammonia on the three metals. Depending on the relative surface concentrations of ethanol and ammonia, different degrees of amine substitution were obtained. The decrease in the NH_3 : EtOH surface

concentration as the metal was changed from nickel to cobalt to copper results in a decrease in the specific MEA selectivity and an increase in the specific selectivity to DEA and TEA.

Since cobalt was found to show the greatest specific activity for ethanol conversion during the reductive amination of ethanol using ammonia, the influence of a variety of parameters during catalyst preparation and activation on the catalytic performance were evaluated. It was seen that changing the preparation and activation procedures of a series of cobalt catalysts resulted in considerable changes to both the activity and the selectivity of the catalysts. The changes in activity were directly related to the reduced metallic surface area of the catalysts indicating that cobalt is the active catalytic component. The changes in metallic surface area were due to changes in the metallic dispersion and changes in the reducibility of the supported cobalt. The changes in metallic dispersion were largely due to thermal effects (*i.e.* the time and temperature of the calcination/reduction procedure) however significant changes in metallic dispersion were also obtained by changing the type of support which indicates that the chemical interaction between the metal precursor and the carrier metal is important. Changes in metal reducibility were caused by the formation of difficult to reduce cobalt-support species, the amount of which depended strongly on the chemical composition of the carrier material. The extent of reduction of cobalt catalysts decreased from 42 to 40 to 32 to 8 % as the aluminium content of the carrier material was increased from 0 to 4 to 13 to 100 wt%. The high extent of reduction of the SiO_2 supported cobalt catalyst coupled with a relatively high dispersion (8 %) resulted in this catalyst having the greatest activity. At a temperature of 180°C, a space velocity of 1 g_{EtOH}/g_{cat}·h and an EtOH : NH_3 : H_2 : N_2 molar ratio of 1 : 2 : 8.6 : 17.6, the ethanol conversion of the Co/SiO_2 catalyst was 66 %. In contrast, the magnesia supported cobalt catalyst showed a conversion of less than 2 % at identical reaction conditions due to the very low extent of metal reduction on this catalyst.

Considerable differences in the specific ethylamine selectivity (*i.e.* the selectivity at the same reactant conversion) were also obtained upon changing the type of catalyst preparation and activation procedure. It was shown that the specific MEA selectivity decreased from 67 to 43%, the specific DEA selectivity increased from 30 to 50% and the specific TEA selectivity increased from 3 to 7% as the metal surface area of the catalyst was increased from 0.55 to

1.3 m^2/g_{cat}. Since the specific activity for the conversion of ethanol was not affected by the metal surface area, it could be deduced that the specific rate of ammonia consumption decreased with increasing metallic surface area. The only physical parameter able to be correlated with the change in ethylamine selectivity was the reversibility of hydrogen adsorption [Zowtiak and Bartholomew, 1983; Reuel and Bartholomew, 1984] as measured using hydrogen chemisorption. The reversibility of hydrogen adsorption which is defined as the percentage of hydrogen atoms which cannot be removed by a 15 minute evacuation at the temperature of adsorption decreased with increasing metal surface area of the reduced cobalt catalysts. The decrease in the reversibility of hydrogen adsorption corresponds to a decrease in the concentration of "strong" adsorption sites relative to "weak" adsorption sites. This decrease in the relative concentration of "strong" adsorption sites therefore corresponds to a decrease in the specific rate of ammonia consumption which indicates that the adsorption and reaction of ammonia on supported cobalt may be determined by the strength of the adsorption site.

Temperature programmed reduction of SiO_2 supported cobalt catalysts showed the presence of 6 types of reducible cobalt species. Depending on the cobalt precursor, the impregnating solution, the support surface area, the calcination temperature and the calcination atmosphere, various cobalt species were obtained. The hydrogen consumption occurring between temperatures of 180 and 240°C was ascribed to the reduction of residual cobalt nitrate, between 270 and 330°C to the reduction of trivalent cobalt species, between 350 and 390°C to the reduction of the cobalt oxide CoO and between 450 and 520°C to the reduction of divalent cobalt ions interacting with cobalt silicate species. The high temperature hydrogen consumption occurring between 650 and 780°C was ascribed to the reduction of various cobalt hydrosilicate species whereas the hydrogen consumption occurring between 880 and 990°C was ascribed to cobalt silicate reduction.

Cobalt silicate species were proposed to originate via the interaction between dissolved cobalt ions and support silanol groups. This was deduced from the fact that by increasing the silica surface area (and therefore the number of silanol groups) from 300 to 750 m^2/g, an increase in the cobalt silicate content from 8 to 29 mol% was observed. Also, by decreasing the

residual water content of the catalyst precursor by increasing the severity of the drying conditions from 1 hour at 60°C to 48 hours at 150°C, a decrease in the cobalt silicate content from 14 to 2 mol% was observed. The importance of water in the formation of cobalt silicate species was underlined by using DMSO as an impregnation solvent. DMSO is a strong chelating agent which removes water associated with the dissolved cobalt ion and the TPR spectrum of this catalyst did not show hydrogen consumption caused by cobalt silicate reduction.

Table of Contents

Page

2. Experimental

Page

3. Results

Page

Page

Page

List of Figures

Page

Page

Page

Page

List of Tables

Page

Page

Nomenclature

C_m - total number of active sites on reduced metal catalyst [-]

d_p - average particle diameter [nm]

k_a - rate of reactant adsorption [mmol/g_{cat}·h·kPa^2]

K_a - equilibrium adsorption constant [-]

k_d - rate of product desorption [mmol/g_{cat}·h·kPa^2]

K_d - equilibrium desorption constant [-]

k_s - rate of surface reaction [mmol/g_{cat}·h·kPa^2]

K_s - reaction equilibrium constant [-]

N_{Av} - Avogadro's number [molecules/mol]

N_{Co} - number of cobalt atoms [atoms]

r_i - rate of ethylamine formation [mmol/g_{cat}·h]

V_{irr} - hydrogen uptake of reduced metal catalysts not able to removed by a 15 min evacuation [sccm/g_{cat}]

V_{total} - total hydrogen uptake of reduced metal catalysts in [sccm/g_{cat}]

CHAPTER 1

INTRODUCTION

1. Introduction

The final aim of any industrial catalytic process is to optimize not only the catalytic activity but also the selectivity to the desired product. In order to achieve this goal, a comprehensive understanding of both the functioning of the catalyst and the reaction pathway is required. These catalytic reactions normally proceed through at least three steps, namely, the adsorption of the reactants, reaction via the formation of intermediates and desorption of the formed products. Each of these steps may be rate determining and may depend either on the conditions of reaction or on the nature of the catalyst surface. To increase the yield of the desired product whilst maintaining high activity thus requires a comprehensive understanding of the nature of the catalyst surface and the mechanism of the reaction pathway.

The synthesis of aliphatic amines via the reductive amination of alcohols is typically catalysed by supported metal catalysts [Kirk-Othmer, 1992; Baiker and Kijenski, 1985]. Depending on the specific catalyst formulation procedure and the reaction conditions employed, considerable differences in the activity and selectivity of the amination reaction are observed. This introduction serves to provide a background on the synthesis of aliphatic amines as well as on the supported metal catalysts which are used in this study.

1.1. Uses and Demand for Alkylamines

Alkylamines are derivatives of ammonia where one, two or three of the hydrogen atoms are replaced by an alkyl chain to form primary, secondary or tertiary amines respectively. The length of the alkyl substituents may be of similar or differing lengths. The lower alkylamines (*i.e.* those having alkyl groups with less than 6 carbon atoms) are toxic, colourless gases or liquids which are highly flammable and have strong odours. Like ammonia, alkylamines exhibit basic properties due to the donation of the unshared pair of electrons which is associated with the nitrogen atom. Substitution of hydrogen by an alkyl group increases the tendency of the molecule to share or donate the electron pair, thus making the molecule more basic. Primary amines are therefore stronger bases than ammonia and secondary amines are stronger bases than primary amines. Steric hindrance during donation of the electron pair can

sometimes result in tertiary amines being weaker bases than secondary amines. The k_b values of selected alkylamines are presented in Table 1.1.

Alkylamines have a wide range of applicability as reactants in the synthesis of industrial chemical intermediates and end products [Kirk-Othmer, 1992]. Methylamines are used in the synthesis of pharmaceuticals, photographic developers, pesticides, solvents, rubber vulcanizers and choline, an animal and poultry supplement. The ethylamines, next higher homologues of the methylamines, generally have similar applicability. In addition, they are also used as reactants in the synthesis of dyestuffs, emulsifiers, insecticides, surfactants and as condensing agents in the polymer industry. Propylamines are used in the production of textile and leather finishing resins, as petroleum additives and as corrosion inhibitors whereas the butylamines are used to form soaps with fatty acids. Higher alkylamines are used extensively as intermediates in the synthesis of dyestuffs, emulsifying agents, pesticides, pharmaceuticals and speciality items.

Alkylamines are produced in large tonnages by the basic organic synthesis industry (Table 1.1.). Methylamines are produced in the largest tonnages with dimethylamine constituting the largest fraction of methylamine production. Since the ratio of amines produced is seldom in the ratio required for industrial consumption, unwanted product amines are separated and recycled to the reactor where they inhibit the formation of these amines. In this way, process output can be adjusted to meet industrial requirements. Ethylamines are produced in tonnages lower than that of the methylamines but greater than that of the longer chained alkylamines. Of the ethylamines, monoethylamine has the greatest application and the molar ratio of mono-, di- and triethylamine produced is 73 : 16 : 11. As with methylamine production, separation and recycling of unwanted amines is used to tailor the product distribution in order to meet industrial requirements. Isopropylamine and diisobutylamine are produced in significant quantities, probably for speciality markets. Scales of manufacture for higher alkylamines are relatively low.

Table 1.1. Scale of manufacture, price and basicity of various alkylamines [Kirk-Othmer, 1992]

Compound	Scale of Manufacture (t/y)	Price ($/kg)	$k_b \times 10^4$
Monomethylamine	32 000	1.04	4.26
Dimethylamine	80 000	1.04	6.03
Trimethylamine	15 000	1.04	0.63
Monoethylamine	20 000	2.68	5.62
Diethylamine	7 000	2.67	1.29
Triethylamine	6 500	2.76	5.75
n-Propylamine	500	2.45	2.51
Dipropylamine	17 000	2.69	7.9
Tripropylamine	small	3.59	n.a.
Isopropylamine	23 000	2.16	4.27
n-Butylamine	1 900	2.76	4.07
Dibutylamine	3 000	2.89	5.12
Tributylamine	700	3.48	n.a.
Diisobutlyamine	18 000	2.76	n.a.

n.a. - not available

1.2. The Catalytic Synthesis of Alkylamines

Many methods are known for the manufacture of amines from a variety of starting materials. The particular process used depends upon the type of amine desired, the availability and price of raw materials, the economic viability of the plant as well as the market for byproducts. The following processes are listed in order of importance, as measured by annual production [Kirk-Othmer, 1992].

1.2.1. Reaction of ammonia and an alcohol over a dehydration catalyst

For dehydrative amination, a mixture of ammonia and the alcohol is passed continuously over the catalyst in a gas-solid heterogeneous reaction. The reactor used is of a fixed, multiple bed configuration and operates at temperatures ranging between 300 and 500°C and at pressures of 8 - 36 bar. The ammonia to alcohol molar ratio is varied between 2 : 1 to 6 : 1 in order to obtain the desired ratio of product amines and the gas hourly space velocity is maintained between 500 and 1500 vol/vol. Even though adjustment of the ammonia to alcohol feed ratio results in changes in the selectivity of the reaction, the ratio of product amines (*i.e.* primary, secondary and tertiary) is seldom in the ratio as desired by industry. Consequently, unwanted product amines are separated and recycled in order to further suppress their formation.

Typical catalysts used are alumina, silica-alumina, silica, titania and various metal phosphates [Kirk-Othmer, 1992]. More recently, zeolite catalysts such as mordenite, rho and ZK-5 have been applied for the dehydrative amination of alcohols, especially in the instance of methylamine synthesis. The steric constraints imposed by the crystalline structure of the zeolite catalyst inhibit the formation of bulkier, more substituted amines. The use of these catalysts results in a product amine ratio more in line with industrial requirements therefore saving on separation and recycle costs. The principal disadvantage of synthesizing amines using dehydration catalysts is the occurrence of a number of side reactions. Dehydration of the reactant alcohol [Klyuev and Khikedel, 1980] used to be a significant problem encountered using acid catalysts however catalytic improvements have reduced the negative impact of this side reaction. Figure 1.1. shows a flowsheet for a typical reactor and separation train.

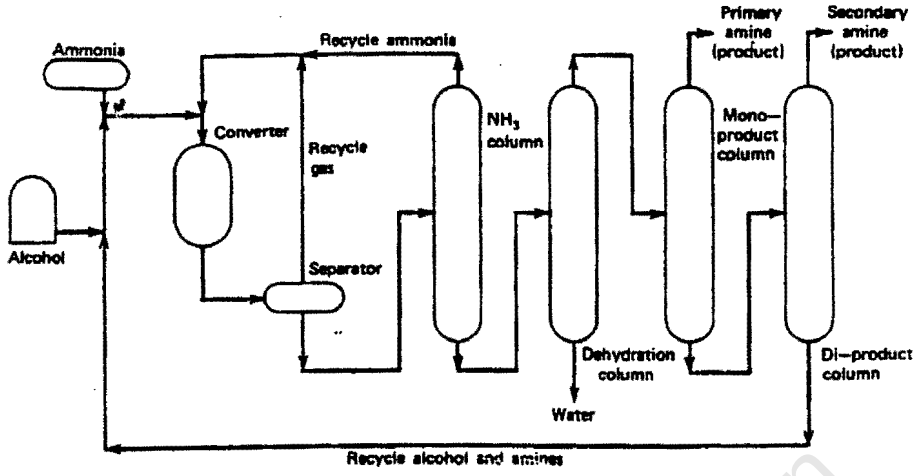

Figure 1.1. Typical ammonia-alcohol reactor and separation train [Kirk-Othmer, 1976]

1.2.2. Reaction of ammonia and an alcohol over a dehydrogenation catalyst

In this process, ammonia, hydrogen and the alcohol are passed continuously over the catalyst in a gas-solid heterogeneous reaction at temperatures between 130 and 250°C, pressures between 8 and 36 bar and space velocities ranging from 500 to 1500 vol/vol. The lower temperature required for the reductive amination reaction reduces the energy requirements of the amination process in comparison to dehydrative amination. The ammonia to alcohol molar ratio is varied between 2 : 1 to 6 : 1 in order to adjust the composition of the product spectrum and the hydrogen to alcohol molar ratio is kept in a similar range. Hydrogen is added in order to prevent catalyst deactivation [Baiker and Kijenski, 1985] and there is no net consumption of hydrogen during the reaction.

Typical catalysts include supported silver, nickel, copper and cobalt [Kirk-Othmer, 1992]. Under the reaction conditions listed above, these catalysts give high conversions and good selectivity to amines. The main byproducts obtained from this reaction are nitriles and amides. As with the first method, recycle of these unwanted byproducts prevents a continuous loss of feed.

1.2.3. Reaction of ammonia and a carbonyl compound over a hydrogenation catalyst

The amination of carbonyl compounds is conducted under similar conditions and using similar catalysts as in the amination of alcohols using ammonia. Unlike the reductive amination of alcohols however, there is a net consumption of hydrogen. The heat generated from the hydrogenation reaction and the pressure drop due to hydrogen consumption must consequently be balanced by careful reactor design. Since aldehydes and ketones are usually more expensive than the corresponding alcohols, this method is principally used as an alternative during shortages or for when the specific amine is only available by this route [Kirk-Othmer, 1992].

1.2.4. Reaction of ammonia and an olefin over an acid catalyst

The addition of ammonia to olefins is a promising alternative to conventional synthesis procedures due to the lack of coproducts (water) during reaction. Previously, metal amide catalysts [Howk *et al*, 1954] were used for the direct amination of olefins however more recently, zeolites have found application for this reaction due to their strong acidity [Deeba *et al*, 1987; Mizuno *et al*, 1994]. The zeolites tested by these authors included erionite, mordenite, offretite, chabazite, ZSM-5, H-Y and β-zeolite.

The reaction temperatures used for this reaction range from 150°C for the metal amide catalysts up to 400°C for the zeolite catalysts. Although the amine selectivity of the zeolite catalysts is high, olefin conversions are thermodynamically restrained (typically lower than 10 %). In order to increase the equilibrium olefin conversion, extremely high pressures are required. The high feed recycle ratio and the high pressures required impact negatively on the economic viability of this process.

1.2.5. Other methods of synthesis

Many other processes have been published or patented describing the production of alkylamines. These processes include the addition of hydrogen cyanide to an olefin, the

reaction of ammonia and alkyl halides [Kirk-Othmer, 1992], the reduction of nitriles using hydrogen [Shulman *et al*, 1961] and the reaction of CO, H_2 and NH_3 over promoted iron catalysts [Reck *et al*, 1967]. None of these procedures is used for large scale production at the present time.

1.3. Reductive Amination

Although the amination of alcohols using acid catalysts is the most widely used technique for commercially synthesizing alkylamines at present, the high selectivity of the reductive amination reaction (*i.e.* alcohol, ammonia and hydrogen over a dehydrogenation catalyst) as well as the relatively mild operating conditions make the route a promising one for industrial application. This reaction has gained increasing importance in recent years since it constitutes an economical way for the synthesis, in particular, of long-chain aliphatic amines [Baiker and Kijenski, 1985].

1.3.1. Effect of Reaction Parameters

In any catalytic process, specific reaction conditions are selected in order to optimize the yield of a particular product. The particular selection depends on the reactor configuration adopted as well as the type of catalyst used. Although considerable research on reductive amination has been conducted using batch or semi-batch reactors [Baiker and Kijenski, 1985], it has been shown that continuous fixed bed reactors are more efficient for this particular process [Baiker and Richarz, 1977]. On this basis, all subsequent parameters will be discussed with respect to this configuration.

1.3.1.1. Influence of the molar reactant ratio

The molar ratio of the reactants (alcohol and ammonia/amine) plays a decisive role in the selectivity of the reductive amination reaction. Depending on both the reactants and the desired amine, either a stoichiometric excess of alcohol or ammonia is necessary. An excess of ammonia is conducive to primary amine formation whereas an excess of reactant alcohol

favours secondary and tertiary amine synthesis [Fowlkes *et al*, 1980]. By changing the starting composition of a mixture of ethanol and ammonia, the changes in the equilibrium ethylamine selectivity were evaluated (Figure 1.2.).

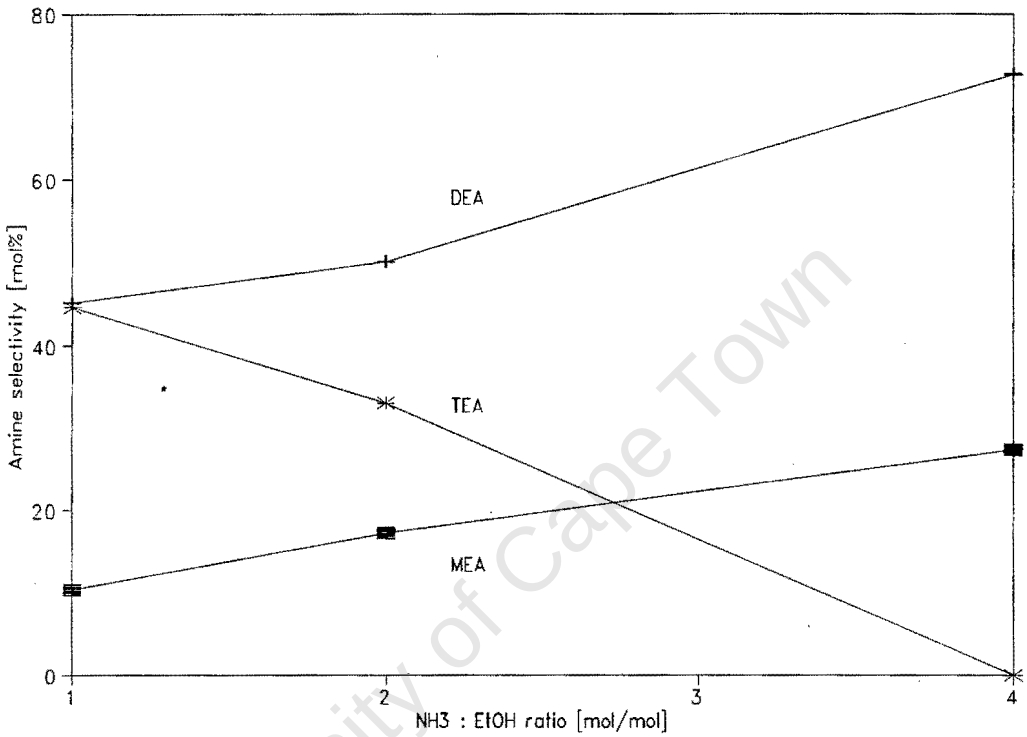

Figure 1.2. Effect of reactant ratio on equilibrium ethylamine selectivity
(T = 180°C, P = 1 bar)

Increasing the ammonia to ethanol molar ratio from 1 : 1 to 4 : 1 resulted in an increase in the MEA selectivity from 10 to 27 mol% whereas the TEA selectivity decreased from 45 to less than 1 mol%. The equilibrium DEA selectivity increased from 45 to 73 mol% indicating that DEA was the thermodynamically favoured ethylamine product under these conditions. At equilibrium, the ethanol conversion was almost complete and the residual reaction mixture consisted of the three product ethylamines, unreacted ammonia and water formed as a coproduct during amination. Side reactions to form aldehydes and nitriles were not considered in the equilibrium calculations since these were not found to influence the final composition considerably [Pasek *et al*, 1972].

Since a number of reactions in the amination process occur on the catalyst surface and are therefore affected by adsorption-desorption equilibria, it is to be expected that increasing the ammonia to alcohol molar ratio will result in a greater surface coverage by ammonia. This has been shown to result in a decrease in the alcohol conversion and an increase in the primary amine selectivity during the reductive amination of ethanol using ammonia [Best, 1978]. Besides altering amine selectivity, stoichiometric excesses of ammonia are also used as a "heat sink" for maintaining the reaction temperature and to minimize side reactions such as amine reforming, amine dehydrogenation and deamination [Heft *et al*, 1990]. The reactions to form the three ethylamines are all slightly exothermic and the heats of reaction for MEA, DEA and TEA formation are -6.6, -32.0 and -32.5 kJ/mol respectively.

1.3.1.2. Influence of the hydrogen partial pressure

It has been shown that the overall rate of reductive amination is determined by the rate of abstraction of the α-hydrogen from the reactant alcohol [Kryukov *et al*, 1967; Kliger *et al*, 1975; Baiker *et al*, 1983]. Despite this, the overall rate of alcohol conversion has been found not to be significantly affected by the hydrogen pressure and the hydrogen pressure is insignificant in the kinetic rate expression [Smeykal, 1936; Heft *et al*, 1990]. Although the hydrogen pressure does not affect the overall rate of alcohol conversion, it does influence the product selectivity by suppressing the rate of disproportionation of reactant and product amines [Baiker and Kijenski, 1985]. High hydrogen pressures have however been reported to decrease amination selectivity by increasing byproduct hydrocarbon formation [Fowlkes *et al*, 1980] through hydrocracking of the reactant alcohol.

The main function of hydrogen is to inhibit catalyst deactivation caused by metal nitride and metal carbide formation [Baiker and Kijenski, 1985]. The minimum hydrogen pressures required depend on the type of metal catalyst as well as the particular reaction conditions used. For supported cobalt catalysts, hydrogen must be present to the extent of at least 10 mole percent at all times in order to ensure efficient catalyst utilization [Gardner and Clark, 1980]. In the absence of hydrogen, both the activity and selectivity of the reductive amination reaction are decreased. Figure 1.3. illustrates the influence of hydrogen on the activity and

selectivity of an alumina supported copper catalyst for the amination of dodecanol with dimethylamine [Baiker, 1981]. The decreased activity in the absence of hydrogen was ascribed to the formation of copper nitride which is inactive for the reductive amination reaction. The activity and selectivity of this catalyst is returned to its original values upon restoring the hydrogen flow indicating that the deactivation process is reversible.

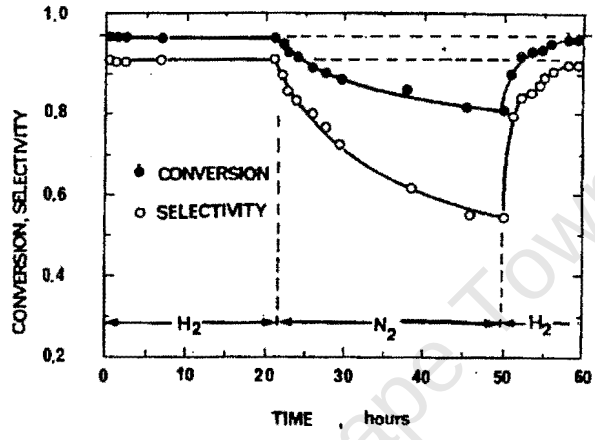

Figure 1.3. Influence of hydrogen on the activity and selectivity of Cu/Al_2O_3 for the amination of dodecanol with dimethylamine [Baiker, 1981]

1.3.1.3. Influence of reactant dilution and the total pressure

Dilution of the reactant mixture with an inert gas may be used to avoid mass transfer limitations or heat transfer problems. Although reactant dilution can benefit mass and heat transfer during reaction, it also results in a decrease in reactant concentration. Disproportionation of reactant and product amines, which decreases the selectivity of the reductive amination reaction, is inhibited by the reactant alcohol [Baiker and Kijenski, 1985]. A lowering of the alcohol concentration will result in a decrease in the extent of surface coverage of the alcohol on the catalyst surface thus weakening the inhibiting effect of alcohol on amine reforming. Lower surface coverages of the reactant alcohol will also decrease the conversion and thus negatively affect the efficiency of catalyst utilization. Both the conversion and the selectivity of benzyl alcohol amination using dimethylamine decreased upon dilution of the reaction mixture with nitrogen [Kijenski *et al*, 1984].

The balanced reaction stoichiometry of the reductive amination reaction indicates that the total reaction pressure should have no influence upon the product selectivity. It has been shown that the selectivity of dodecanol amination with dimethylamine decreased as the pressure was increased [Baiker and Richarz, 1977]. The decrease in selectivity was attributed to increased disproportionation activity at higher pressures. The use of high pressures may be of benefit in that it would be expected to decrease the rate of certain unwanted side reactions such as hydrocracking, amine dehydrogenation and deamination.

1.3.1.4. Influence of the reaction temperature

The reaction temperature at which the reductive amination of alcohols is carried out is critical and should be maintained between 140 and 225°C [Gardner and Clark, 1981]. Below 140°C, the reaction rate is too slow to be practical whereas above 225°C, losses occur due to undesirable side reactions. These side reactions include alcohol dehydration, the deamination of product amines as well as nitrile and hydrocarbon formation. Hydrocarbon formation is believed to be partially responsible for catalyst deactivation due to the deposition of carbonaceous material [Fowlkes *et al*, 1980] and should thus be minimized.

Increasing the reaction temperature results in an increase in the alcohol conversion at the expense of the selectivity. The decrease in catalyst selectivity with increasing reaction temperature is largely due to the increased rate of disproportionation between reactant and product amines [Baiker and Richarz, 1977]. Figure 1.4. illustrates the influence of the temperature of reaction on the conversion and selectivity of a SiO_2 supported copper catalyst for the amination of dodecanol with dimethylamine. The decrease in the alcohol conversion at temperatures greater than 340°C was attributed to excessive catalyst decay [Baiker and Richarz, 1977].

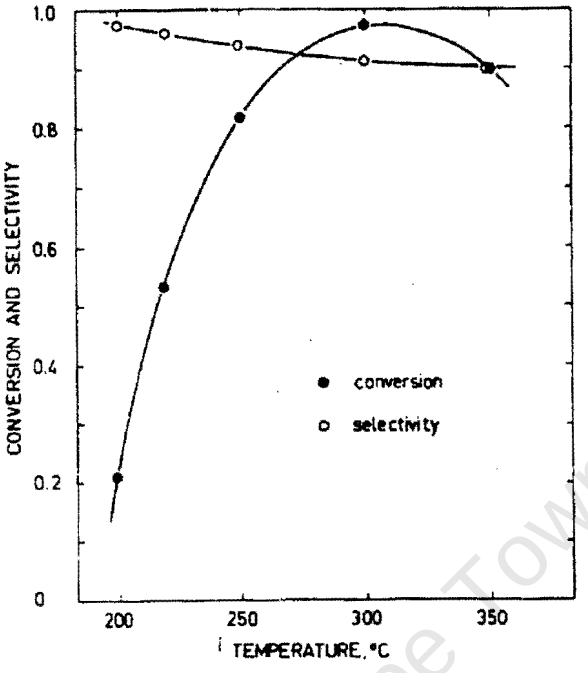

Figure 1.4. Effect of the reaction temperature on the activity and selectivity of Cu/SiO_2 for the amination of dodecanol with dimethylamine [Baiker and Richarz, 1977]

The influence of the reaction temperature on the ethylamine equilibrium selectivity was investigated by varying the reaction temperature of a mixture of ammonia and ethanol (Figure 1.5.). The starting molar ratio of the ammonia and ethanol reactants was 2 : 1. At equilibrium, the MEA selectivity increased from 12 to 20 mol%, the DEA selectivity increased from 47 to 51 mol% and the TEA selectivity decreased from 41 to 29 mol% as the reaction temperature was increased from 140 to 200°C. The ethanol conversion was almost complete at equilibrium however residual ammonia was still present since an excess of this species was used in the reaction mixture.

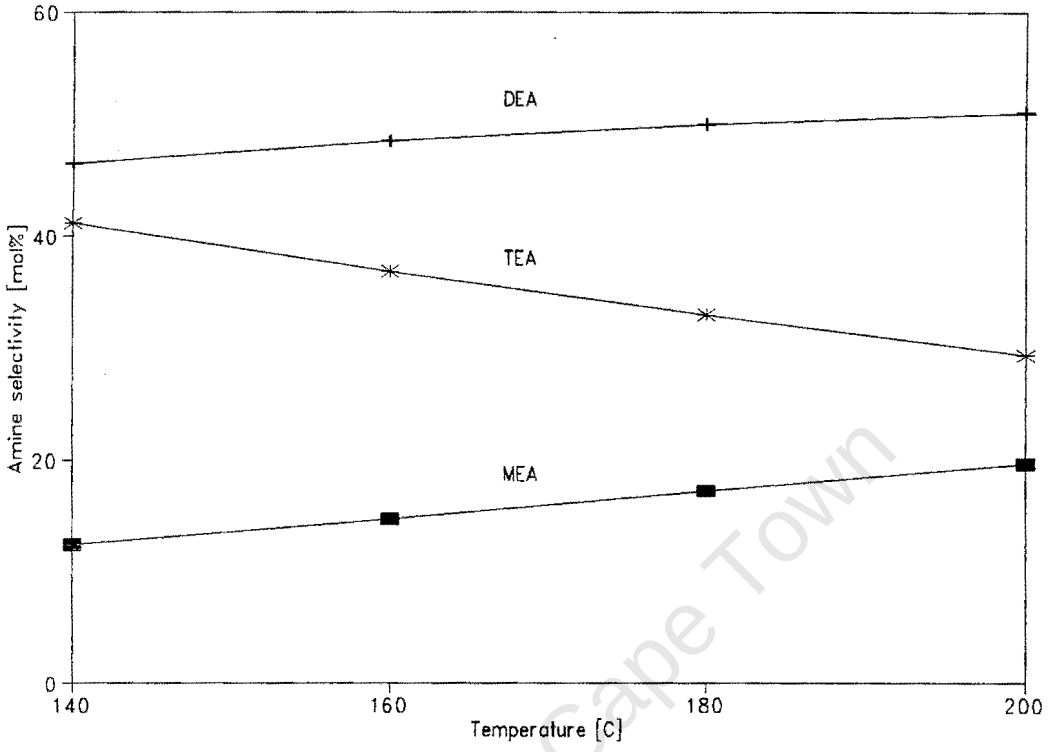

Figure 1.5. Effect of temperature on equilibrium ethylamine selectivity
(NH_3 : EtOH = 2 : 1, P = 1 bar)

1.3.2. Mechanism of Reductive Amination

In the presence of hydrogenation/dehydrogenation catalysts, alcohols react with ammonia or amines (primary or secondary) to form the corresponding amines. The amination of alcohols can be looked upon as a series reaction which produces water as a coproduct. The reaction stoichiometry is illustrated below.

$$CH_3CH_2OH + NH_3 \rightleftarrows CH_3CH_2NH_2 + H_2O \quad [1]$$

$$CH_3CH_2OH + CH_3CH_2NH_2 \rightleftarrows (CH_3CH_2)_2NH + H_2O \quad [2]$$

$$CH_3CH_2OH + (CH_3CH_2)_2NH \rightleftarrows (CH_3CH_2)_3N + H_2O \quad [3]$$

Apart from amines, unsaturated and saturated hydrocarbons, nitriles, aldehydes, ketones and

ethers are also detected in the reaction product [Klyuev and Khikedel, 1980]. There is no unanimous view concerning the formation of these compounds and whether these species are reaction intermediates or the products of side reactions occurring during amination.

Unlike ammonia, primary or secondary amines, tertiary amines do not react with alcohols [Baiker and Kijenski, 1985]. It was therefore postulated that the primary function of the metal catalyst was to dehydrogenate the alcohol to form the corresponding aldehyde or ketone via reaction [4] [Schwegler and Adkins, 1939; Gruyot and Fournier, 1929]. The aldehyde or ketone may then condense with ammonia via reaction [5] to form an imine which may be hydrogenated to the primary amine as illustrated by reaction [6]. Further reaction of product amines with the carbonyl compound formed in reaction [4] gives rise to secondary and tertiary amines via the intermediate Schiff bases (reactions [7] - [9]).

$$RCH_2OH \rightleftarrows RCHO + H_2 \qquad [4]$$

$$NH_3 + RCHO \rightleftarrows RCH{=}NH + H_2O \qquad [5]$$

$$RCH{=}NH + H_2 \rightleftarrows RCH_2NH_2 \qquad [6]$$

$$RCH_2NH_2 + RCHO \rightleftarrows RCH_2N{=}CHR + H_2O \qquad [7]$$

$$RCH_2N{=}CHR + H_2 \rightleftarrows (RCH_2)_2NH \qquad [8]$$

$$RCH_2N{=}CHR + RCHO + H_2 \rightleftarrows (RCH_2)_3N + H_2O \qquad [9]$$

By studying the interaction of labelled ethanol with ammonia, it was noted that the ethanol is initially dehydrogenated, with the abstraction of the hydrogen atoms from the α - position in the alcohol being the rate limiting process [Kryukov *et al*, 1967; Bashkirov *et al*, 1971; Kliger *et al*, 1975]. The β - hydrogen atoms in the alcohol are not involved in the rate limiting step. The reaction mechanism as elucidated via isotopic labelling studies is therefore in agreement with the reaction mechanism as proposed by Schwegler and Adkins [1939]. Addition of carbonyl compounds formed through alcohol dehydrogenation to ammonia, primary or secondary amines results in the formation of primary, secondary and tertiary amines respectively. The proposed reaction path is depicted through reactions [10] - [20] where $\ast$ is an active catalyst site.

$RCH_2OH + * \rightleftarrows RCH_2OH*$ [10]

$H_2 + * \rightleftarrows H_2*$ [11]

$NH_3 + * \rightleftarrows NH_3*$ [12]

$RCH_2OH* \rightleftarrows RCHO* + H_2*$ [13]

$RCHO* + NH_3* \rightleftarrows RCH{=}NH* + H_2O*$ [14]

$RCH{=}NH* + H_2* \rightleftarrows RCH_2NH_2* + *$ [15]

$RCHO* + RCH_2NH_2* \rightleftarrows RCH{=}NCH_2R* + H_2O*$ [16]

$RCH{=}NCH_2R* + H_2* \rightleftarrows (RCH_2)_2NH* + *$ [17]

$RCH_2NH_2* \rightleftarrows RCH_2NH_2 + *$ [18]

$(RCH_2)_2NH* \rightleftarrows (RCH_2)_2NH + *$ [19]

$H_2O* \rightleftarrows H_2O + *$ [20]

It was established that neither ammonia nor primary or secondary amines influence the rate of reaction whereas the addition of water greatly reduced the rate of amination [Kryukov *et al*, 1967]. In the mechanism proposed by these authors, the rate of alcohol dehydrogenation (reaction [13]) is postulated to be slow whereas the remaining stages are fast or at equilibrium. Since water is not directly involved in the proposed rate limiting step, it should not influence the rate of amination significantly. Unless water is strongly adsorbed on the catalyst surface (thereby reducing the number of available active sites), there thus appears to be a contradiction in the argument forwarded by these researchers.

Similar mechanisms have been proposed for the reaction between octanol and ammonia [Kliger *et al*, 1975] and the reaction between octanol and dimethylamine [Baiker *et al*, 1983]. Besides determining that the rate of abstraction of the α-hydrogen from the alcohol was the rate determining step via isotopic labelling studies, the intermediate aldehyde was also identified. The mechanism proposed above is therefore the most likely reaction pathway during reductive amination.

1.3.3. Catalysts used for Reductive Amination

The reductive amination of alcohols using transition metal catalysts is a well established

process. The literature concerning ethanol amination however is scarce and occurs predominantly in patent literature [Heft *et al*, 1990; Best, 1978; Gardner and Clark, 1981; Fowlkes and de Pinillos, 1979; Deeba, 1988]. The performance of selected catalysts for the reductive amination of ethanol is listed below.

Table 1.2. Catalysts used for reductive amination

Catalyst	N : R : H[1] (mol : mol)	P (bar)	T (°C)	x_{EtOH}[2] (%)	M : D : T[3] (mol %)	Reference
40% Ni/Al_2O_3	1:1:1.4	16	170	43.4	46:38:11	Gardner *et al*, 1981
59% Ni/Kieselguhr	1:1:1.4	16	170	44	49:40:11	Gardner *et al*, 1981
24% Co/Kieselguhr	1:1:1.4	16	170	65	47:37:16	Gardner *et al*, 1981
36% Co/Al_2O_3	1:1:1.4	16	170	64	23:58:19	Gardner *et al*, 1981
5% Co/Y-Zeolite	2:1:2	19	210	71	58:37:5	Deeba, 1988
25% Co/SiO_2	2:1:2	19	180	73	37:43:20	Deeba, 1988
25% Co/SiO_2	2:1:2	19	200	92	30:50:20	Deeba, 1988
35% Co/Ca-Al_2O_3	1:1:1	16	193	63	26:54:20	Heft *et al*, 1990
35% Co/Ca-Al_2O_3	1:1.3:1	16	193	82	25:54:21	Heft *et al*, 1990
8% NiRe/$SiO_2Al_2O_3$	10:1	14	190	17	96:2:2	Best, 1978
34% Co/Al_2O_3	2:1:1	17	216	88	47:44:7	Fowlkes *et al*, 1979
34% Co/Al_2O_3	4:1:1	17	216	96	52:40:7	Fowlkes *et al*, 1979
57% Ni/Al_2O_3	4:1:1	17	216	88	41:42:6	Fowlkes *et al*, 1979
57% Ni/Al_2O_3	5:1:4	20	150	81	43:47:10	Engelhard Report
34% Ni/Al_2O_3	5:1:4	20	150	52	58:37:5	Engelhard Report

[1] Molar ratio of ammonia, ethanol and hydrogen in the feed
[2] Molar conversion of ethanol
[3] Molar selectivity of monoethylamine (M), diethylamine (D) and triethylamine (T)

Gardner and Clark [1980] compared the performance of supported cobalt and nickel catalysts. Both metals were highly selective to ethylamine product (carbon efficiency > 99%) however the cobalt catalysts showed greater activity at similar operating conditions. Both the metal

loadings and the support surface areas were varied, making it impossible to compare the specific activities of each metal however. The molar ratio of monoethylamine (MEA), diethylamine (DEA) and triethylamine (TEA) in the reaction product varied with the metal support, with the kieselguhr-supported metals producing a less substituted amine product than their alumina-supported counterparts (*i.e.* more MEA and less TEA).

Deeba [1988] compared the performance of cobalt supported on silica and zeolite Y. The silica-supported cobalt catalyst was more active than the zeolite-supported catalyst at similar operating conditions, most likely due to the higher metal loading (25 wt% compared to 5 wt%). An enhanced selectivity to MEA and DEA and a diminished selectivity to TEA was observed when using the Co/Y-Zeolite catalyst. This was attributed to steric constraints imposed on the amination reaction by the crystalline zeolite structure. Increasing the reaction temperature increased ethanol conversion, decreased MEA selectivity and increased DEA and TEA selectivities for both catalysts, in accordance with the series nature of the amination reaction. Increasing the hydrogen pressure increased the ethanol conversion slightly but the selectivities to individual ethylamine products were largely unaffected.

Heft *et al* [1990] used a 25 wt% Co/Ca-Al_2O_3 catalyst for the amination of ethanol using diethylamine. High selectivity to triethylamine was obtained with little reforming to monoethylamine. An increase in diethylamine conversion was achieved by increasing the reaction temperature and by increasing the ethanol to diethylamine reactant ratio. Although activity increased with temperature, an increase in amine reforming to monoethylamine was also observed. Substitution of the diethylamine in the feed with ammonia resulted in a product MEA : DEA : TEA ratio of 25 : 54 : 21, which was stated to be equilibrium controlled. An increase in the molar feed ratio of ethanol to ammonia resulted in an increase in ethanol conversion however the product selectivities remained essentially unchanged. This is in contradiction to thermodynamic equilibrium predictions [Pasek *et al*, 1972] which show decreasing MEA and increasing DEA and TEA selectivities with increasing ethanol to ammonia feed ratio.

Best [1976] used a nickel-rhenium catalyst containing boron and supported on silica-alumina

for the reaction of ethanol with ammonia. After 2 hours, the ethanol conversion was only 17% however the MEA selectivity was very high. The high MEA selectivity may be attributed to the low ethanol conversions and to the high ammonia to ethanol molar feed ratio (10 : 1).

Fowlkes and de Pinillos [1979] evaluated the performance of a 34% Co/Al_2O_3 catalyst with various commercially available nickel catalysts. Under similar operating conditions, the alumina supported cobalt catalyst had a greater activity than the commercial nickel catalysts tested. At similar conversions, the cobalt catalyst produced a less substituted ethylamine product (*i.e.* a higher MEA selectivity and lower DEA and TEA selectivities) than the nickel catalysts and byproduct formation was lower. Ethanol conversion was seen to increase with increasing ammonia to ethanol feed ratio and the selectivity to MEA was increased. Although increasing the ammonia to ethanol feed ratio resulted in increased activity and increased MEA yields, it was also shown to increase the formation of the unwanted byproduct acetonitrile.

In a private report from Engelhard [1985], the performance of a number of nickel catalysts were evaluated. It was shown that an increase in temperature resulted in an increase in the conversion of ethanol, an increase in the yields of DEA and TEA and a decrease in the yield of MEA. Decreasing the hydrogen pressure increased ethanol conversion and MEA selectivity whereas DEA and TEA selectivities were suppressed slightly. Although changes in the type of nickel catalyst did not affect the selectivity to individual amines significantly, the overall activity varied significantly. These differences were not discussed or investigated.

In summary, it appears that cobalt is more efficient than nickel for the reductive amination of ethanol using ammonia [Gardner and Clark, 1980; Fowlkes and de Pinillos, 1979], although the specific activities of each metal cannot be determined from the literature available. Besides being more active, cobalt catalysts produce higher yields of monoethylamine [Fowlkes and de Pinillos, 1979]. This is beneficial since MEA is used in larger tonnages by the basic organic synthesis industry as compared to DEA and TEA [Kirk-Othmer, 1992]. The type of metal support used influences the yield of individual ethylamines

[Gardner and Clark, 1980] and the use of crystalline aluminosilicate supports appears particularly beneficial to the MEA yield [Deeba, 1988]. MEA yields may be further increased by increasing the ammonia to ethanol molar feed ratio. This however impacts negatively on the recycling costs of unreacted feed and can result in an increase in byproduct formation [Fowlkes and de Pinillos, 1979].

1.3.4. Catalyst Deactivation

Catalyst deactivation is of paramount importance in many industrial processes since the decline in activity with time results in a decrease in the economic viability of the process. The mechanisms of deactivation are complex and are often not well understood. A decline in activity may be observed due to the deposition of carbonaceous material which in turn leads to coverage of the active site and to pore blockage. In the instance of microporous materials such as zeolites, severe diffusional restrictions may arise. Besides the deposition of carbonaceous material, a decrease in the active catalytic surface area may result due to the agglomeration of metal crystallites (sintering), which in turn will result in a decrease in catalytic activity.

1.3.4.1. Deactivation behaviour during amination

The catalytic amination of alcohols and the disproportionation of amines using supported metal catalysts is usually carried out in the presence of hydrogen [Baiker *et al*, 1984]. Hydrogen is added in order to maintain catalyst activity and it is important to note that there is no net consumption of hydrogen in the amination reaction. Replacement of hydrogen in the feed with an inert carrier such as helium results in a severe decrease in both the activity and selectivity of copper, nickel and cobalt catalysts. This phenomenon has been attributed to deactivation of the metal catalyst in the absence of hydrogen [Baiker *et al*, 1984].

Three different processes have been identified as leading to deactivation of supported metal catalysts during the reductive amination of alcohols, *viz.* the sintering of metal crystallites [Baiker and Richarz, 1978], the formation of metal nitrides [Baiker, 1981] and the deposition

of carbonaceous material [Baiker *et al*, 1984; Anderson and Clark, 1966].

1.3.4.2. Deactivation by Sintering

The agglomeration of metal crystallites (sintering) during a reaction results in a decrease in the active metal surface area which in turn results in a less active catalyst. Using the amination of dodecanol with dimethylamine as a test reaction, the activity of supported copper catalysts was shown to decrease with time on stream [Baiker and Richarz, 1978]. The catalytic activity of γ - alumina (59 m^2/g) and silica (240 m^2/g) supported catalysts was reasonably stable over a testing period of 1000 hours, however the activity of a kaolin (43 m^2/g) supported copper catalyst decreased sharply with time on stream (Figure 1.6.). The decrease in activity was attributed to the formation of agglomerates by thermal diffusive fusion of the supported metal crystallites, as shown by X-ray diffraction. Mercury porosimetry and electron microscopy showed no evidence for deactivation due to macrostructural changes.

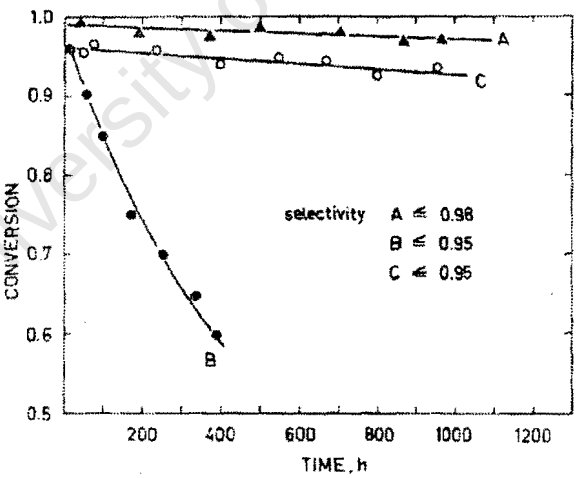

Figure 1.6. Time on stream conversion of Al_2O_3 (A), kaolin (B) and SiO_2 (C) supported copper catalysts [Baiker and Richarz, 1978]

The inherent ability of the support to stabilize the metal crystallites towards sintering is clearly important in preparing an active and stable catalyst. Prevention of metal particle migration is not necessarily dependent on the surface area of the support (e.g. γ-alumina and

kaolin) and is determined by the level of interaction between the reduced metal and the carrier material.

1.3.4.3. Deactivation by metal nitride formation

The stability as well as the attractive mechanical and electrical properties of certain metal nitrides has attracted a considerable amount of investigation [Troth, 1971]. In contrast, the low stability of copper, nickel and cobalt nitrides has resulted in little effort being expended in the investigation of these materials. The formation of metal nitrides has been shown to impair the use of these metals as catalysts for reactions involving ammonia or amines, such as during reductive amination [Baiker and Maciejewski, 1984].

These metal nitrides can be formed either by direct interaction with ammonia or by reaction of the product amines with the metal surface according to the following reactions (Me = metal, R = alkyl).

$$NH_3 + 3\ Me \rightleftarrows Me_3N + 1.5\ H_2 \qquad [1]$$

$$3\ R_2NH + 3\ Me \rightleftarrows Me_3N + 2\ R_3N + 1.5\ H_2 \qquad [2]$$

$$2\ RNH_2 + 3\ Me \rightleftarrows Me_3N + R_2NH + 1.5\ H_2 \qquad [3]$$

$$1.5\ RNH_2 + 3\ Me \rightleftarrows Me_3N + 0.5\ R_3N + 1.5\ H_2 \qquad [4]$$

These reactions leading to metal nitride formation are all thermodynamically feasible under typical conditions selected for reductive amination, and it thus likely that all of these reactions contribute to metal nitride formation [Baiker and Kijenski, 1985]. These authors stated that only a small hydrogen pressure may be sufficient to prevent nitride formation however the actual hydrogen pressure required to prevent nitride formation was not quantified.

Nitrogen incorporation into the metal lattice was observed at 175°C for copper and at temperatures as low as 125°C for nickel [Baiker and Maciejewski, 1984]. The formation of stable metal nitrides was found to be confined to narrow temperature ranges however. The

highest rates for copper nitride formation were between 270 and 300°C whereas nickel nitride formation was predominant at temperatures between 360 and 390°C [Baiker and Kijenski, 1984]. Below this range, the rate of nitride formation was very low and above this range, decomposition of the nitride predominated. The thermal stability of copper nitride is illustrated in Figure 1.7. which represents the mass changes of a copper sample in a 50 ml/min ammonia stream.

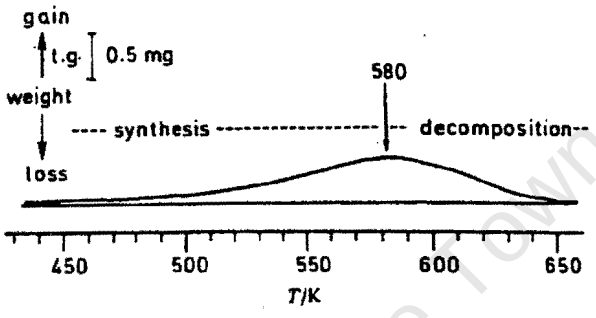

Figure 1.7. Thermogravimetric measurement of copper nitride formation and decomposition [Baiker and Maciejewski, 1984]

The temperatures of maximum nitride formation are significantly higher than the temperatures usually applied for reductive amination, indicating that any nitride formation occurring would be slow. The stability of these metal nitride compounds was found to be diminished in the presence of hydrogen. By exposing nitrided catalyst samples to a flowing stream of hydrogen, copper nitride was only stable at temperatures lower than 105°C and nickel nitride was only stable at temperatures lower than 155°C. Figure 1.8. illustrates the thermal stability of copper nitride in a hydrogen atmosphere and in an ammonia atmosphere. From this figure it is clear that the stability of metal nitrides is strongly dependent on the gas phase composition and that the stability of these compounds will vary with varying ammonia and hydrogen partial pressures during amination.

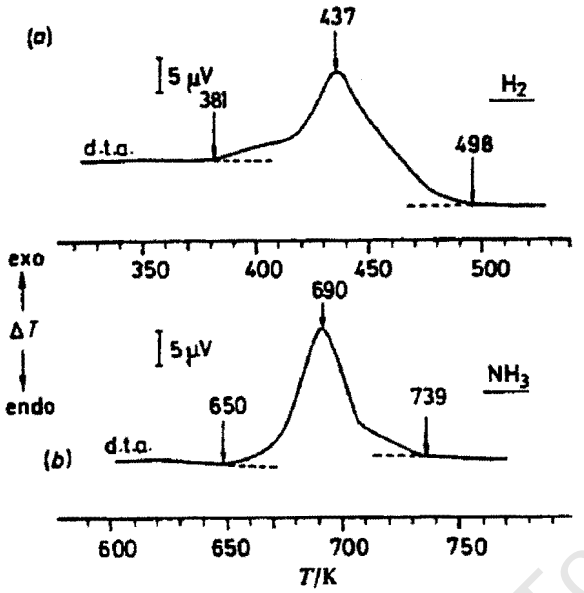

Figure 1.8. Thermal stability of copper nitride in hydrogen and ammonia atmospheres [Baiker and Maciejewski, 1984]

Nitrogen desorption spectra of metal catalysts previously exposed to ammonia indicated that the stability of the metal nitrides in an inert atmosphere was of the order Co_3N > Ni_3N > Cu_3N [Baiker, 1981]. Although the presence of hydrogen has been shown to inhibit metal nitride formation under typical amination reaction conditions, the stability of these materials in the presence of both hydrogen and ammonia has not been fully evaluated. The possibility of metal nitride formation under typical amination conditions can therefore not be ruled out.

1.3.4.4. Deactivation by carbon deposition

The deposition of carbonaceous material can deactivate catalysts in a number of ways. Extensive carbon deposition can result in pore mouth blockage which can prevent reactant molecules from reaching active catalytic centres deeper within the pore of the catalyst. This phenomenon is usually associated with a decrease in the BET surface area and a change in the pore size distribution. Surface coverage of active sites by carbonaceous material prevents the adsorption and reaction of molecules and can be detected by lower adsorbate uptakes

during chemisorption. Reaction of carbon with the supported metal to form catalytically inactive metal carbide compounds may also be responsible for a decline in activity. Extensive carbide formation can be identified by X-ray diffraction.

Using the catalysed disproportionation of methylamine and dimethylamine as a test reaction, the deactivation of copper, nickel and cobalt catalysts was investigated [Baiker *et al*, 1984]. With copper, loss in activity with time on stream was attributed to metal particle sintering and nitride formation. With the nickel and cobalt catalysts, pore mouth blocking and metal carbide formation was found to further contribute to the deactivation process. From the temperature programmed hydrogenation spectra, two distinct carbon species were observed and these were allocated as amorphous carbon and metal carbide species. The deposition of carbon on these two metals in comparison to copper was attributed to the higher hydrocracking activity (*i.e.* the ability for C-C cleavage) of these metals.

1.4. Supported Metal Catalysts

Transition metals catalyse a large variety of important industrial processes in the chemical industry, in petroleum refining, in exhaust emission control, in gas purification and in alternative fuel production. Bulk metal catalysts pose severe drawbacks in terms of catalyst efficiency (*i.e.* activity per weight of active component) and are therefore costly. Furthermore, these catalysts show low thermal stability which leads to surface area losses caused by sintering.

To overcome these disadvantages, the active metallic component is often deposited onto a high surface area carrier, such as a refractory inorganic oxide. This not only produces highly efficient catalysts with high metal dispersions but also improves the thermal stability (and therefore the life) of the catalyst due to the separation of metal particles and the interaction of such particles with the support. In the instance of structure sensitive reactions (*i.e.* the reaction pattern changes with changing structure of the metal particle or the type of crystallographic face exposed), the selectivity may be enhanced due to the stabilization of different particle morphologies by the support [Haberlandt, 1990].

1.4.1. Preparation of Supported Metal Catalysts

The preparation of supported metal catalysts is a complicated procedure and links the fields of inorganic chemistry, colloid and surface chemistry as well as cluster chemistry [Foger, 1985]. The optimal goal of this preparation is to make a catalyst in which the active phase (the metal) is highly dispersed so as to achieve a large surface area, and thus a high activity per weight of the active component. In general, these supported metal catalysts are prepared in a multistep process as outlined below.

(a) Distribution of the precursor compound over the support surface
(b) Drying and calcination of the catalyst precursor
(c) Activation of the metallic component by reduction

1.4.1.1. Introduction of the precursor compound

In order to manufacture catalysts in an efficient and reproducible manner, it is essential to gain control over parameters such as the metal loading, the metal dispersion and the metal location in the final catalyst. Numerous procedures for introducing the metal to the support material have been applied, including impregnation, precipitation, co-precipitation, ion exchange, chemical vapour deposition and solid state ion exchange. Due to its simplicity, impregnation has been the preferred method of catalyst preparation used in this study.

Two types of impregnation procedures may be used for introducing the metal compound to the support material, *viz.* incipient wetness impregnation and dipping impregnation.

With incipient wetness impregnation, the support is wetted with a volume of a solution containing the metal that corresponds to the pore volume of the particular support. Although this process is technically simple, it is limited in that multiple steps are necessary when the metal precursor has a low solubility. Dipping impregnation on the other hand involves the immersion of the support into a solution containing the metal compound. This technique is mainly applied where the precursor interacts with the support and consequently the metal

loading is determined by the concentration of adsorption sites on the support surface. The interaction between the deposited salt and the support is generally small, however, which leads to metal migration during calcination and reduction and a consequent decrease in the metal dispersion [Bell, 1987].

Capillary forces are responsible for drawing the liquid into the pores of the support during impregnation. The capillary pressure is given by the equation $p_c = 4\gamma\cos\theta/d$ where γ is the surface tension, θ is the contact angle and d is the diameter of the capillary pore. The small pore diameters and the low contact angles result in extremely high capillary pressures (up to 1000 atm) which ensure that complete wetting of the support occurs rapidly [Bell, 1987]. At these pressures, only a small fraction of the pore volume remains filled with gas and gas solubility is increased considerably, thus facilitating removal.

1.4.2. Influence of the type of support

The selection of the carrier is of significant importance in designing supported metal catalysts and is governed by such parameters as surface area, characteristic porosity, mechanical strength and thermal and chemical stability [Foger, 1985]. If catalytic functions are utilized, maximum activity and selectivity are desirable. The support materials selected are frequently inorganic oxides and can be classified according to the following groupings [Foger, 1985]:

(a) Inert supports such as SiO_2, which supply high surface areas for the dispersion of the metal component.
(b) Catalytically active supports such as Al_2O_3, SiO_2-Al_2O_3 and zeolites which are frequently used and make up approximately 80% of all industrial supports.
(c) Supports which influence the active component by strong interactions, including the partially reducible oxides TiO_2, Nb_2O_5 and V_2O_5.
(d) Structural supports such as the monoliths used for motor vehicle exhaust gas purification.

To avoid the excessively high pressure drops encountered with powders, the support materials are usually formed into spheres, granules, extrudates or cylinders before industrial

application. The mechanical strength of the catalysts may be increased by fusion and by the addition of binders in order to prevent degradation during catalytic processing.

1.4.2.1. Surface properties of supports

The surface of inorganic oxides is comprised predominantly of oxygen atoms, hydroxyl groups and, to a lesser extent, exposed metal atoms. The chemical properties of these species and the manner in which they interact with the metal precursors is strongly affected by the amount of charge localization. Oxygen atoms behave as Lewis bases, metal cations as Lewis acids and hydroxyl groups can act as either acids or bases. Acidic oxides have mainly a covalent bond whereas basic oxides have mainly an ionic bond [Bell, 1987].

1.4.2.2. Surface charge in solution

When oxide particles are suspended in aqueous solutions, such as during the impregnation step, a surface polarization results in net electrical surface charges. These surface charges have been associated with dissociation of surface hydroxyl groups and with readsorption of hydroxo complexes formed by partial dissolution of the oxide particle [Parks and DeBruyn, 1962]. Both processes involve H^+ and OH^- ions and are therefore dependent on the solution pH. In an acidic medium, the surface is positively charged (δ-OH_2^+) and will preferentially adsorb anions whereas in an alkaline solution, the particles carry a negative charge (δ-O^-) and adsorb cations [Foger, 1985]. Clearly, at some intermediate pH value, the surface of the support will have no net surface charge. The point of zero net charge is called the isoelectric point and is important when selecting the type of metal precursor (anionic or cationic) and the pH of deposition.

According to their surface charge in solution, support materials can be classified within the pH range 1-14 as [Foger, 1985]:

(a) Cation adsorbers such as silicas, silica-aluminas and zeolites

(b) Anion adsorbers such as magnesia

(c) Amphoteric supports such as alumina, chromia and titania

1.4.2.3. Surface functionalities and catalytic properties

The surfaces of inorganic oxides expose oxygen ions, hydroxyl groups and incompletely coordinated cations in various configurations, in close relation to the chemical and thermal treatment of the oxides [Foger, 1985]. These functionalities supply anchoring sites for metal precursor compounds during catalyst preparation as well as acting as active catalytic sites in multifunctional catalysts. The catalytic properties of the support materials rise from their acid-base properties [Benesi and Winquist, 1977] and/or their oxidation-reduction functions [Rosynek, 1977].

1.4.2.4. Interaction of the metal compound with the support surface

The common substrates used to support metal particles are inorganic oxides, and ion exchange processes with protons or surface hydroxyl groups act to anchor the metal precursor compound to the support surface. These interactions are predominantly controlled by the following parameters [Brunelle, 1978]:

(a) The type of support and the state of the surface, *i.e.* the number of functional groups and their acidity/basicity.
(b) The nature of the impregnating solution, *i.e.* the type and concentration of the metal compound, the pH and the presence of competing ions.

It was shown earlier that surface polarization of the oxide particles results in the particles carrying a positive or a negative charge, depending on their environment. This dictates whether the oxide particles will preferentially adsorb anions or cations. The equilibria for cation (C^+) and anion (A^-) adsorption can be represented by the following equations [Foger, 1985]:

$$S\text{-}OH + C^+ \rightleftarrows S\text{-}O^-C^+ + H^+$$

$$S\text{-}OH + A^- + H_2O \rightleftarrows S\text{-}OH_2^+A^- + OH^-$$

For a given support, the equilibria and the strength of interaction in both processes are determined by the pH of the impregnating solution, *i.e.* cation uptake increases with increasing pH and anion uptake decreases with increasing pH. Too high a pH might lead to metal hydroxide precipitation however and should be avoided if encountered. The affinity for exchange is also dependent on the nature of the particular ion. For cations, this affinity is a function of both the charge and the radius and follows the general rule [Foger, 1985]:

$$M^{4+} > M^{3+} > M^{2+} > M^{1+} \approx H^+$$

The affinity for anion exchange increases with the polarisability of the anions as well as with the anionic charge, as illustrated with the halides below.

$$I^- > Br^- > Cl^- > F^-$$

$$SO_4^{2-} > Cl^-$$

Since the aim of most catalyst preparations is to distribute the metal evenly throughout the support granule, care must be taken not to prepare catalysts with non-uniform metal distributions. Non-uniform metal distributions are generally established either during the impregnation step or during drying, although some redistribution of the active phase may occur during catalyst activation [Komiyama *et al*, 1980]. The resultant distribution depends on both the adsorptive strength of the compound and the nature of the support surface.

In the case of a strong interaction between the metal compound and the support, most of the compound is adsorbed near the pore mouth resulting in a large concentration gradient from the surface to the centre of the carrier material (egg shell distribution). In order to obtain an even distribution of the metal compound throughout the carrier, it is necessary to supply enough of the compound to saturate every adsorption site, to allow long contact times (only successful if desorption is possible) or to add competing ions (chromatographic adsorption).

Chromatographic adsorption comprises the addition of another ion to the impregnating solution which then competes for the adsorption sites on the support surface [Shyr and Ernst, 1980]. The addition of a competing ion of similar adsorptive strength to the metal compound will result in a uniform distribution profile whereas the addition of a competing ion with a strong affinity for the carrier surface will result in a higher metal concentration in the core of the carrier. This results in a so-called "egg-yolk" distribution.

In the case of a weak interaction between the metal compound and the support, a uniform concentration profile is achieved during the impregnation step. Due to the weak interaction, redistribution of the metal compound during drying is common [Foger, 1985]. At high heating rates, the gas-liquid interface proceeds towards the centre of the pellet with uniform deposition of the metal precursor occurring at the liquid meniscus. At low heating rates, the metal compound diffuses into the remaining liquid, which results in its deposition at the centre of the pellet. To avoid segregation of the metal compound during drying, it is thus necessary to select high heating rates [Fenelov *et al*, 1979] or to increase the solution viscosity, which inhibits redistribution of the active phase [Kotter and Riekert, 1979].

1.4.3. Catalyst Activation

The activation of supported metal catalysts generally comprises the drying of the catalyst precursor followed by calcination and reduction. Each procedure may affect the metal distribution of the final catalyst and activation conditions must be carefully selected in order to obtain a highly active catalyst.

1.4.3.1. Drying

Drying constitutes a mild thermal treatment generally in the temperature range of 80 to 200°C which is principally aimed at the removal of the solvent used in precursor deposition [Foger, 1985]. The influence of drying on the spatial distribution of the metal compound must be considered, especially in the case where the interaction between the metal precursor and the carrier is weak. As discussed previously, the rate of drying can result in an

accumulation of the active phase either towards the carrier centre or the carrier surface.

1.4.3.2. Calcination

Calcination constitutes a high temperature treatment with the aim of decomposing the precursor compound. With compounds such as metal carbonyls, thermal treatment alone is sufficient to obtain the active metallic state. More frequently though, a subsequent reduction process is required to activate the catalyst. Calcination is generally carried out under oxidizing conditions and may bring about the following transformations [Foger, 1985]:

(a) Precursor decomposition to form the metal oxide
(b) Reaction of the formed oxide with the support
(c) Sintering of either the precursor or the formed oxide

Clearly, the calcination process may have marked effects on both metal reducibility and metal dispersion. As a specific example, the metal dispersion of alumina supported platinum catalysts first increases and then decreases with increasing calcination temperature [Bournonville *et al*, 1982]. The reducibility of supported cobalt catalysts decreases however with increasing calcination temperatures due to increased incorporation of cobalt ions into alumina lattice sites where they are not easily reduced [Arnoldy and Moulijn, 1985].

1.4.3.3. Reduction

The final activation of a supported metal catalyst consists of the transformation of the oxide into the metallic state, and is usually accomplished by reduction in hydrogen. The metal compounds present on the support before reduction are usually present as oxides formed through calcination or as the salts themselves (*e.g.* metal halides). The reduction processes of oxides and halides are depicted below.

$$MO_{(s)} + H_{2(g)} \rightarrow M_{(s)} + H_2O_{(g)}$$
$$2\ MX_{(s)} + H_{2(g)} \rightarrow 2\ M_{(s)} + 2\ HX_{(g)}$$

The standard free energy of the above metal oxide reduction reaction may be expressed by the following equation :

$$\Delta G = \Delta G^{\circ} + RT \log \frac{p_{H_2O}}{p_{H_2}}$$

Reduction is thermodynamically only possible if the standard free energy (ΔG) of reduction is negative. This may occur due to a strong negative ΔG° value or due to a very small water partial pressure. The standard free energy change (ΔG°) of the reduction of a number of metal oxides as a function of temperature is shown in Figure 1.9. From this figure, it is evident that the reduction of a number of metal oxides is not thermodynamically favoured. By lowering the water partial pressure sufficiently (*i.e.* by increasing the flowrate of the reducing gas), it is possible to reduce materials having positive ΔG° values.

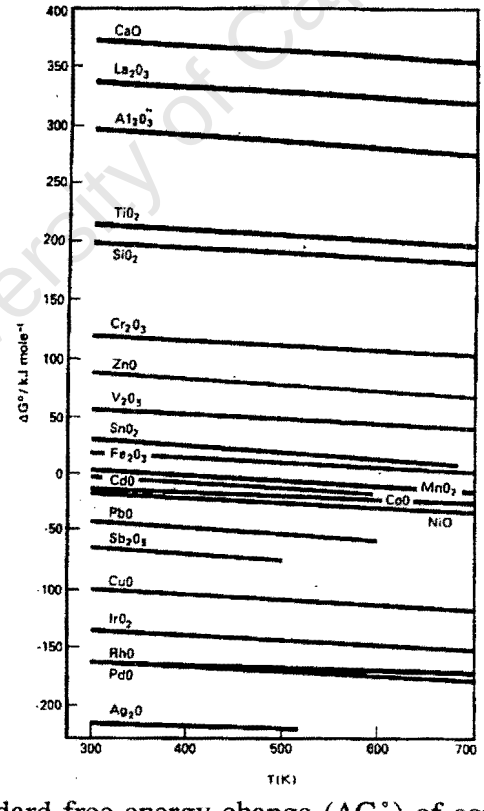

Figure 1.9. Standard free energy change (ΔG°) of complete metal oxide reduction as a function of temperature [Hurst *et al*, 1982]

Reduction processes fall into the category of topochemical reactions which are reactions where the initiation process proceeds at distinct sites (potential centres) on the surface of a solid. The formation of these potential centres is followed by propagation of the reaction zone from such a centre through the solid until complete conversion is achieved [Foger, 1985]. Upon contact of a metal oxide with hydrogen, oxygen ions are removed from the oxide lattice and vacancies are created. As soon as the concentration of such vacancies reaches a critical value, the lattice rearranges and metal nuclei are formed. These nuclei grow, new nuclei are formed and the reaction continues until all of the oxide is consumed. Two models for the reduction reactions have been proposed, *viz.* the nucleation model and the contracting sphere model.

In the nucleation model, the rate limiting step is the nucleation process. After an induction period, the reaction rate increases due to the appearance of new nuclei and the growth of existing ones. At a certain stage, the nuclei contact each other forming a metallic skin around the oxide particle and the reaction rate begins to decrease. Figure 1.10 illustrates the characteristic reduction profiles obtained for the nucleation model where α is the degree of reduction.

The contracting sphere model assumes that the reaction proceeds evenly on the entire surface and that the interface decreases continuously as the reaction proceeds. The model may therefore be applied to the final stages of the nucleation model (after the formation of a continuous metal skin) or to a reduction reaction with instantaneous nucleation. The reduction characteristics of the contracting sphere model are illustrated in Figure 1.11.

The distinction between the nucleation and contracting sphere model is somewhat artificial in that the contracting sphere model starts with very rapid nucleation while the nucleation mechanisms finish by an essentially shrinking core mechanism. The two models exist in order to distinguish between the instance where the reaction interface (and hence rate) increases in the early stages of reduction and the instance where the reaction interface decreases continuously throughout the reduction.

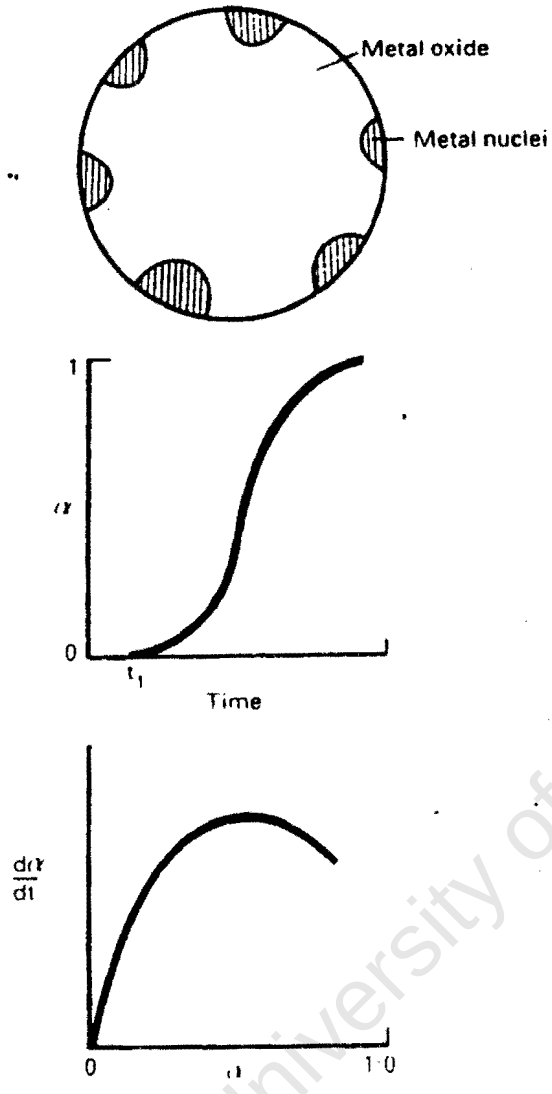

Figure 1.10. Reduction by nucleation mechanism [Hurst *et al*, 1982]

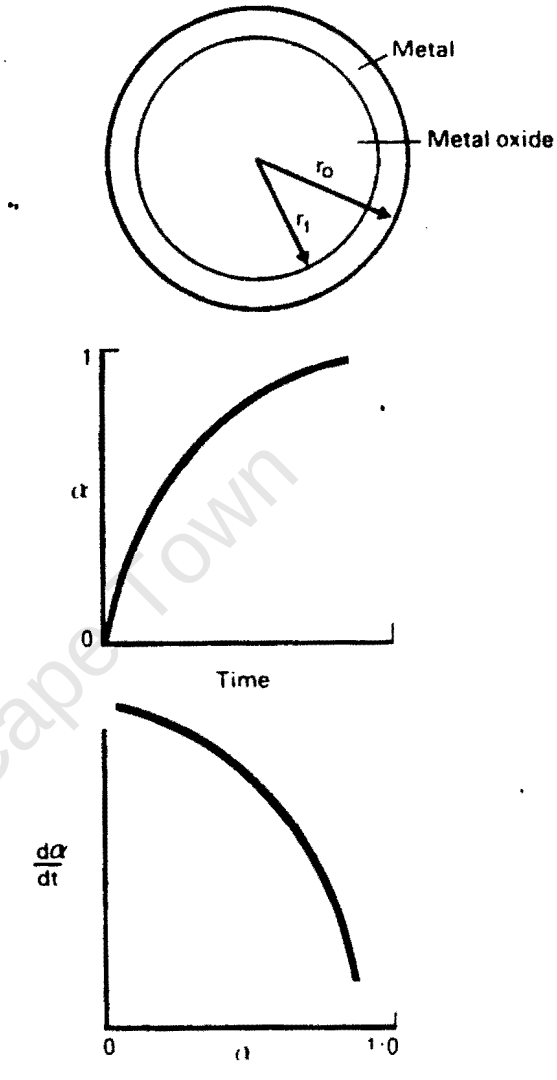

Figure 1.11. Reduction by contracting sphere model [Hurst *et al*, 1982]

It is possible to accelerate a reduction reaction either by promoting nucleation (which can be achieved by increasing the number of potential nucleation sites) or by supplying a more active reducing agent (such as atomic hydrogen). The formation of atomic hydrogen requires the presence of Group VIII metals and accordingly many reduction reactions are autocatalytic [Boldyrev *et al*, 1979].

Metal oxides supported on carrier materials such as γ-Al_2O_3 and SiO_2 may exhibit different reduction behaviours compared with the corresponding unsupported oxides. Reduction may be either hindered or promoted depending on the nature of the oxide/support interaction. In

general, the reduction rates of supported oxides are lower than compared to their unsupported bulk phases due to dispersion effects (nucleation is dependent on particle size and atomic hydrogen has limited mobility) [Foger, 1985]. Acceleration of the rate of reduction of supported oxides may be achieved by the addition of promoters which act as a source of atomic hydrogen however this can only be effective if the promoter and the supported oxide are in intimate contact.

1.4.4. Metal Support Interactions

For most industrial applications, supports are sought which possess high surface area, high chemical and thermal stability and good mechanical strength. While it was originally thought that the active phase was simply an inert carrier for the active phase (metal), it has become evident that the type and nature of the support can result in significant changes in both the activity and selectivity of catalytic reactions. The explanation of this support effect is not trivial, and one has to investigate simultaneously the influence of support, metal loading and dispersion, catalyst preparation and pretreatment as well as the extent of reduction in order to understand these support effects [Bartholomew *et al*, 1980].

Furthermore, the unambiguous identification of a metal's modification by a metal-support interaction is complicated by other phenomena which give rise to "support effects". These include particle size effects [Foger, 1985], poisoning of the metal by support impurities [Fuentes and Figueras, 1978], diffusion of the metal into the support or encapsulation of metal particles by the support [Tatarchuk and Dumesic, 1981] and spillover and reverse spillover effects [Dowden, 1980]. In this context, a metal-support interaction has been defined as a direct influence of the support on the chemisorptive and catalytic properties of the metal phase either by stabilizing unusual metal particle structures, by changing the electronic properties due to electron transfer process between the metal particles and the support, or chemical bonding (compound formation) between the metal and the support [Foger, 1985].

1.4.4.1. Classification of metal-support interactions

Bond [1982] proposed a classification of metal-support effects in which he distinguished between weak (WMSI), medium (MMSI) and strong (SMSI) metal-support interactions. The WMSI occurs predominantly with transition metals supported on "non-reducible" oxides such as SiO_2, Al_2O_3 and MgO, and bonding between the metal and the support is weak and of the van der Waals type [Anderson, 1975]. The weak bonding between the metal and the support is expected to exert little influence on the catalytic and adsorptive properties of the metal, however it may force very small particles to adopt structures different to those observed with metal particles formed in "free space". This effect is of obvious importance when considering structure sensitive reactions such as ethane hydrogenolysis [Bond, 1982].

The MMSI state is classified as those effects which are observed when metal particles are supported in or on zeolites. In this case, metal particles inside zeolite channels are electrophilic (electron deficient) due to electron transfer from the metal to acceptor sites on the support surface [Foger, 1985]. This electrophilic character increases with increasing acidity of the zeolite and with the presence of multivalent cations. Electrophilic metals will thus exhibit a lower affinity for electron acceptor molecules (such as oxygen or sulphur) whereas the affinity for donor molecules (such as ammonia and hydrocarbons) will be enhanced.

The SMSI state is used to explain the modification of the chemisorptive and catalytic properties of metals supported on certain reducible oxides (TiO_2, Nb_2O_5, Ta_2O_5 and V_2O_3) after high temperature reduction in hydrogen (500°C). The SMSI state has similarly been observed with transition metals supported on "non-reducible" oxides however reduction temperatures in excess of 800°C were required [Praliaud and Martin, 1981]. Metals in the SMSI state usually exhibit the following features [Foger, 1985]:

(a) greatly diminished H_2 and CO adsorption
(b) unchanged O_2 chemisorption
(c) enhanced N_2 chemisorption

(d) decreased activities for hydrocarbon hydrogenolysis, isomerization and hydrogenation reactions

(e) enhanced activities for reactions involving CO (*e.g.* Fischer-Tropsch Synthesis)

The extent to which the chemisorption and reaction properties are modified depends on the severity of reduction, the type of support - the temperature necessary to induce SMSI increases in the order $TiO_2 > Al_2O_3 > SiO_2$ [Foger, 1985], the metal involved and the metal dispersion - the SMSI effect is more pronounced for highly dispersed catalysts [Ko *et al*, 1982].

A number of mechanistic concepts have been proposed to account for SMSI effects. These include strongly adsorbed hydrogen [Menon and Froment, 1981], intermetallic compound formation [Otter and Dautzenberg, 1978], electronic changes due to electron interchange processes between metal particles and the support [Horsley, 1979] and possibly by structural changes [Baker, 1982]. In contrast to the MMSI state, "electron rich" metal particles are formed by a charge transfer from the partially reduced carrier to the metal [Fung, 1982]. The negative charge on the metal atoms reduces their ability to adsorb H_2 or CO as evidenced by the suppression of uptakes during chemisorption.

Foger (1985) suggested that the SMSI effects on reducible oxides (n-type semi-conductors) and on non-reducible oxides (non-conductors) are of different origin. With reducible oxides, electron transfer from the support to the metal leads to negatively charged metal particles whereas with non-reducible oxides, the support and metal atoms form intermetallic compounds. Although the effects of SMSI are beginning to be understood, the origin of this phenomenon is still unclear and remains the subject of current interest.

1.4.5. Catalyst Characterization

The success of catalyst preparation and modification depends on the suitable characterization of that catalyst in order to evaluate its physico-chemical properties. There are many techniques available for this purpose including X-ray powder diffraction, electron

microscopy, photoelectron spectroscopy and infrared spectroscopy. These techniques are generally limited however as they are not generally applicable to the characterization of catalysts under typical working conditions. Temperature programmed reduction and hydrogen chemisorption are useful techniques for the characterization of supported metal catalysts as they provide a measure of the catalyst reducibility and the exposed metal surface area of the catalyst.

1.4.5.1. Temperature programmed reduction

Temperature programmed reduction (TPR) is a highly sensitive although destructive technique which does not depend on any specific property of the catalyst other than that the species under study be in a reducible condition. TPR experiments can be used to determine the most effective reduction conditions, to identify the supported precursor phases and their interaction with the support or to characterize bimetallic systems.

1.4.5.1.1. Instrumentation and experimental apparatus

At the beginning of a TPR experiment, gas flows over a fixed amount of solid at a temperature low enough to prevent reaction. The temperature of the solid is then increased at a linear rate and the rate of reaction is monitored. The rate of reaction may be monitored by measuring concentration or pressure changes or by measuring weight changes of the solid [Hurst *et al*, 1982].

Thermal conductivity detectors are used when the rate of reaction is monitored by measuring concentration changes in the reducing gas. Because hydrogen has been used for the reduction, the uptake is determined by measuring the difference in the thermal conductivity of the gas before and after reduction. This is achieved by using low concentrations of hydrogen in nitrogen. The experimental procedure adopted consists of placing a weighed amount of the sample in a reactor connected to the TPR apparatus. Before the TPR measurements, this sample may be subjected to various pretreatment procedures by utilizing the gas handling system and the reactor furnace. During TPR, a gas stream consisting of a low concentration

of hydrogen mixed in nitrogen (*ca.* 5% H_2/N_2) is passed through a deoxygenation trap before entry into the temperature controlled reactor. The outlet stream from the reactor is then passed through a cold trap or a molecular sieve trap in order to remove products formed during the reduction reaction before entry into one arm of the thermal conductivity detector (TCD). Either nitrogen or the reducing gas mixture may be passed through the other arm of the TCD. The differences in thermal conductivity measured by the detector are due to changes in the concentration of hydrogen in the reducing gas. Since the gas flow is constant, the hydrogen concentration is proportional to the rate of reduction. A typical apparatus used for TPR measurements using thermal conductivity detectors is illustrated in Figure 1.12.

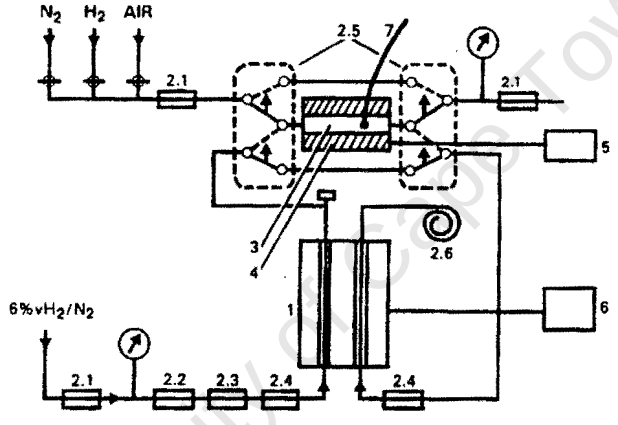

1: Thermal conductivity cell. 2.1: Zambs Negretti reduction valve. 2.2: Pt/Al_2O_3 catalyst. 2.3: Molecular sieves (Linde 5A). 2.4: Dewar (193 K). 2.5: Gas flow switch. 2.6: Brake capillary. 3: Reactor. 4: Oven or furnace. 5: Temperature programmer. 6: Chart recorder. 7: Thermocouple.

Figure 1.12. Typical TPR apparatus using thermal conductivity detection [Hurst *et al*, 1982]

Monitoring of the reaction rate during TPR by measuring pressure changes in the reacting gas is conducted using a recirculation reactor [Jacobs *et al*, 1976]. The apparatus used for these measurements is illustrated in Figure 1.13.

A pressure transducer is used to monitor the changes in the pressure of the reducing gas in the recirculation reactor as the temperature is raised linearly. The pressure changes can be correlated to the hydrogen consumption caused by reduction of the metal oxide and the reaction rates during TPR can be determined. Pressure monitoring cannot be performed continuously due to pump pulsations. Before each pressure measurement, it is therefore

necessary to stop the circulation pump until the pressure reading is constant.

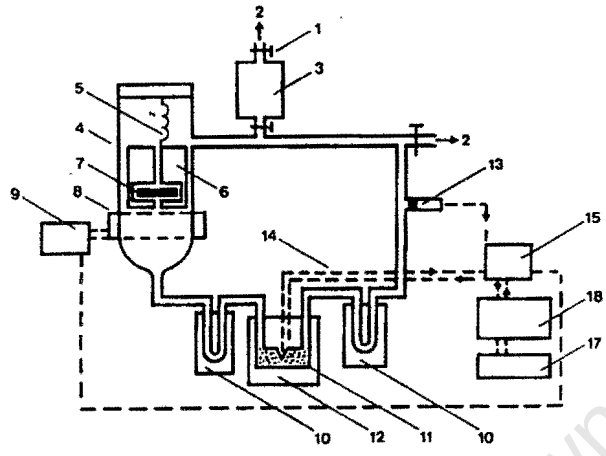

1: Stopcock. 2: To vacuum and gas handling system. 3: Calibrated volume. 4: Circulation pump with variable flow rate (up to 2.5 L/min). 5: Spring. 6: Piston. 7: Valve. 8: Solenoid. 9: Pump control. 10: Cold trap (198 K). 11: Reactor. 12: Stirred air furnace. 13: Pressure transducer. 14: Thermocouple. 15: Microprocessor. 16: Desk computer. 17: Printer-plotter.

Figure 1.13. TPR apparatus using recirculation reactor [Jacobs *et al*, 1976]

Measurement of the weight change of the solid during TPR may be used to calculate the rate of reduction [Banerjee *et al*, 1974]. The sample is contained in a glass bucket hanging from a two-section helical quartz spring which is enclosed in an all glass housing. The degree of extension of the quartz spring is correlated to the sample weight and can be used to monitor the weight change (and therefore the hydrogen consumption) during TPR. During the experiment, purified hydrogen is fed into the sample chamber through an inlet at the top of the bucket. Water formed through metal oxide reduction is removed by the reducing gas through an outlet at the bottom of the chamber. The sample is heated by a non-inductively wound furnace around the sample chamber.

1.4.5.1.2. Effect of experimental parameters

Typical TPR characteristics such as the temperature corresponding to the maximum of the reduction profile and the shape of the profile itself are affected by factors extrinsic to the technique, such as mass transfer limitations, and by the experimental operating variables. By

eliminating extrinsic factors, Monti and Baiker proposed the use of a characteristic number $K = S_o/V \cdot C_o$ to aid in selecting the values for the operating variables during TPR [Monti and Baiker, 1983]. S_o is defined as the initial amount of the reducible species in the sample (μmol), V is the total flow rate (ml/s) and C_o is the initial hydrogen concentration in the feed (μmol/ml). In order to obtain optimum reduction profiles, K values were limited to the range 55 to 140 s for heating rates of between 6 and 18°C/min. Below K values of 55 s, the sensitivity was too low and at K values exceeding 140 s, the quantity of hydrogen consumed was too large resulting in a violation of the assumption of a linear concentration profile.

Malet and Caballero modified the characteristic K value by taking into account the rate of heating β [Malet and Caballero, 1988]. The proposed parameter $P = \beta \cdot S_o/V \cdot C_o$, with β the heating rate in °C/min, was found to result in optimal reduction profiles at P values less than 60. Higher P values resulted in distorted curves with flattened maxima caused by near complete consumption of the hydrogen in the feed. Increasing the heating rate was found to result in an increase in the temperature of maximum hydrogen consumption [Fierro *et al*, 1994].

1.4.5.2. Chemisorption

The ultimate objective during the preparation of supported metal catalysts is to maximize the specific metal surface areas (*i.e.* the number of metal atoms exposed to the gas phase). In order to compare the success or failure of various catalyst preparations, it is necessary to be able to obtain an accurate measurement of the exposed surface area of the supported metal. Although measurement of the number of surface metal atoms may be obtained indirectly using techniques such as X-ray diffraction (XRD), small-angle-X-ray scattering (SAXS) and transmission electron microscopy (TEM), it is desirable to obtain a direct measurement of the number of surface atoms using selective chemisorption.

The technique consists of the adsorption of a selected gas under conditions which permits the formation of a chemisorbed monolayer on the metal without any significant contribution of the support. This monolayer coverage can be measured using volumetric, gravimetric or

chromatographic techniques as well as by titrations [Foger, 1985]. Measurement of the adsorbate uptake required for monolayer coverage allows the number of surface atoms, the exposed surface area and the average particle size to be calculated. Table 1.3. contains the chemisorption properties of some typical transition metals [Myasaki, 1980].

Table 1.3. Chemisorption properties of transition metals [Myasaki, 1980]

Metal	Dissociative adsorption	Associative adsorption
Hf, Ta, Zr, Nb, W, Ti, V, Mn, Cr, Mo	H_2, O_2, N_2, NO, CO	
Fe, Re	H_2, O_2, N_2, NO, CO	NO, CO
Ni, Co, Tc	H_2, O_2, NO, CO	NO, CO
Os, Ir, Ru, Pt, Rh, Pd	H_2, O_2, NO	NO, CO

The stoichiometry of adsorption may be obtained by comparison of the chemisorption surface areas with BET surface areas of metal powders, films or foils; or by comparison with calculated metal surface areas from particle sizes measured by methods like TEM, XRD line broadening or SAXS. A combination of these techniques is usually favoured since adsorption stoichiometries sometimes exhibit a particle size dependency, XRD line broadening is weighted towards larger particles and electron microscopy may not fully discriminate small particles.

Selective chemisorption on bi- or multimetallic catalysts requires the consideration of three separate cases. If the chemisorption properties of both metals are similar, the technique cannot selectively discriminate between the surface areas of the individual metals. This is most common in the instance of combinations of noble metals such as Pt-Ir or Pt-Rh. If only one metal chemisorbs the selected adsorbate, the total surface area must be estimated indirectly using another method such as XRD, TEM or SAXS. This occurrence is commonly obtained with combinations of Group VIII - Group Ib metals such as Pt-Au and Ru-Cu. A further possibility is that the metals exhibit different chemisorption properties towards the

adsorbing gases, *e.g.* the stoichiometry of chemisorption of the two metals differ. In this instance it may be necessary to alter the selection of adsorbates or adsorption conditions in order to calculate the surface composition of the catalyst.

1.4.5.2.1. Activated adsorption

For each adsorption process, there is a characteristic velocity which is determined by the same factors which govern a chemical reaction, *e.g.* the temperature, pressure, concentration and nature of the adsorbing surface. As in the instance of a chemical reaction, an activation energy of adsorption may be described. Changes in the activation energy of the adsorption process will therefore alter the rate of chemisorption. Consequently, adsorption processes with high activation energies will occur more slowly than adsorption processes with low activation energies.

The Langmuir adsorption of a diatomic gas (X_2) on a surface site (S) may occur either by adsorption as molecules or as adsorption as individual atoms. The two processes may be represented by the following equations :

$$S + X_2 \rightleftarrows S{\cdot}X_2 \qquad (1)$$

$$2\,S + X_2 \rightleftarrows 2\,S{\cdot}X \qquad (2)$$

According to the Langmuir concept of adsorption, the relative rates of adsorption and desorption define the average time which molecules occupy the surface. Defining Q as the heat of adsorption and E as the activation energy of adsorption, the average time which the molecules will occupy the surface is given by the following equation [Taylor, 1930]:

$$Average\ time = \frac{A\ e^{-E/R\,T}}{B\ e^{-(Q\,+\,E)/R\,T}} = (A/B)\ e^{Q/R\,T}$$

From this equation it can be seen that the relative magnitudes of the heats of adsorption of the two reactions (Q_1 and Q_2) will largely determine the positions of the adsorption-temperature isobars. Figure 1.14. gives a schematic representation of the isobars obtained

when Q_2 is greater than Q_1.

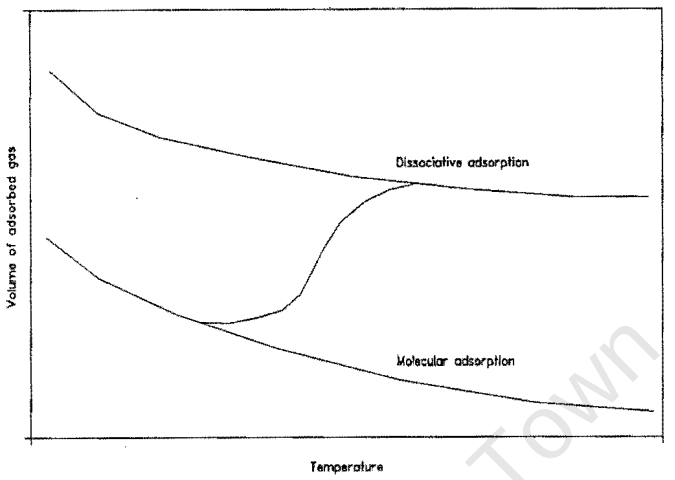

Figure 1.14. Isobars for adsorption processes with different activation energies [Taylor, 1930]

If the activation energy for dissociative adsorption (E_2) is much larger than the activation energy of molecular adsorption (E_1), it may occur over a given range of temperatures that the rate of reaction 2 will be negligibly slow compared with that of reaction 1. Under such conditions, the experimental results will follow the lower curve. As the temperature is raised, there will be the normal decrease in the adsorption of X_2. Simultaneously however, there will be an increase in the velocity of reaction 2 so that, at sufficiently high temperatures, the experimental values obtained will be practically exclusively due to the dissociative adsorption and will follow the upper curve. Between the two extremes, an intermediate region will exist where the adsorption at a given pressure will increase with increasing temperature.

As a specific example, the adsorption of hydrogen on polycrystalline cobalt has been found to be an activated process [Zowtiak *et al*, 1983; Zowtiak and Bartholomew, 1983; Reuel and Bartholomew, 1984]. For unsupported cobalt, a maximum uptake of hydrogen was measured after adsorption at 100°C and the total hydrogen uptake was 1.3 times greater than the uptake at 25°C. The temperature at which maximum adsorption occurs increases from 100 to 125

to 150 to 200°C as the support is changed from SiO_2 to Al_2O_3 to C to TiO_2 indicating that the energy of activation varies with the type of cobalt support. The adsorption temperature of maximum hydrogen uptake also increased with decreasing metal loading.

The fact that the activation energy for hydrogen adsorption increases in the order unsupported Co, Co/SiO_2, Co/Al_2O_3 and as the metal loading is decreased suggests that the activation barrier for dissociative adsorption on cobalt increases with increasing degree of metal-support interaction [Zowtiak and Bartholomew, 1983]. Since the preparation procedure often affects the dispersion (and therefore the degree of metal-support intimacy), differences in catalyst formulation are expected to result in changes in the activation energy of hydrogen adsorption.

Hydrogen adsorption on cobalt is also highly reversible and the degree of reversibility varies with the type of support, the metal loading and the preparation procedure. Reversible adsorption pertains to that hydrogen adsorbed which has a low heat of adsorption and a small activation energy of adsorption [Taylor, 1931]. This hydrogen is weakly adsorbed and may be removed simply under vacuum. The degree of reversibility of hydrogen adsorption on cobalt varies between 15 and 90% [Zowtiak and Bartholomew, 1985] and therefore the choice of adsorption technique affects the measured hydrogen uptake considerably. Using a flow technique measures only irreversibly adsorbed hydrogen whereas a static volumetric technique measures both reversible and irreversible hydrogen adsorption.

By comparing calculated measured surface areas using a combination of XRD, TEM and hydrogen adsorption, it was found that the stoichiometry of hydrogen adsorption was one hydrogen atom per surface cobalt atom [Reuel and Bartholomew, 1984]. This adsorption stoichiometry was only valid however if the total adsorption at the temperature of maximum uptake was considered. To measure the total hydrogen uptake (*i.e.* reversibly and irreversibly adsorbed hydrogen) the static volumetric adsorption technique must be used. The temperature at which maximum adsorption occurs varies with varying catalyst formulation and therefore varies from catalyst to catalyst. Failure to measure the hydrogen uptake using these guidelines will therefore result in spurious measurements of metal surface areas for cobalt based catalysts.

On the other hand, CO adsorption on cobalt is non-activated and reversible [Reuel and Bartholomew, 1984]. It was found that the adsorption stoichiometry varied from 0.4 to 2.3 molecules of CO per cobalt atom however depending on the type of support, the metal loading and the preparation procedure. This technique does not therefore provide accurate indications of cobalt surface area and dispersion.

CHAPTER 2

EXPERIMENTAL

2.1. Catalyst Synthesis

All catalysts used in this study were prepared by the incipient wetness technique. The concentrations of the impregnating solutions were adjusted so that the metal loading would be 9 wt %. Unless otherwise stated, the catalysts were dried at 80°C in an oven for 16 hours. The dried catalyst precursor was then crushed and sieved into a size fraction between 150 and 250 μm before storage in a desiccator.

Differences in catalyst preparation procedure were based on the type of metal impregnated, the type of metal precursor, the solvent of impregnation and the type of metal support. Table 2.1. lists the materials of preparation as well as the nomenclature used for the various catalysts.

High purity metal salts were used for impregnation of the various inorganic oxide supports. $Co(NO_3)_2 \cdot 6H_2O$ and $Co(CH_3CO_2)_2 \cdot 4H_2O$ were supplied by Merck, $CoCl_2 \cdot 4H_2O$ was obtained from Lasechem, $CoSO_4 \cdot 7H_2O$ from BDH Chemicals and $Ni(NO_3)_2 \cdot 6H_2O$ and $Cu(NO_3)_2 \cdot 3H_2O$ were obtained from May and Baker and Riedel-de Haën respectively. The methanol and acetone solvents were supplied by BDH Chemicals, the ethanol and butanol from Merck and the propanol and butanol from Lasechem. All water used was de-ionized. The SiO_2 and MgO supports were supplied from Merck (Darmstadt, Germany) and the γ-Al_2O_3 and SiO_2-Al_2O_3 supports were supplied by Kalichemie (Hannover, Germany). Table 2.2. lists the physical characteristics of the support materials.

Table 2.1. Composition and nomenclature of catalysts

Catalyst Name	Metal Precursor	Solvent	Support
Co/SiO_2	$Co(NO_3)_2$	Water	Silica
Ni/SiO_2	$Ni(NO_3)_2$	Water	Silica
Cu/SiO_2	$Cu(NO_3)_2$	Water	Silica
Co/Al_2O_3	$Co(NO_3)_2$	Water	Alumina
$Co/1SiO_2$-Al_2O_3	$Co(NO_3)_2$	Water	Silica-Alumina
$Co/4SiO_2$-Al_2O_3	$Co(NO_3)_2$	Water	Silica-Alumina
$Co/9SiO_2$-Al_2O_3	$Co(NO_3)_2$	Water	Silica-Alumina
$Co/13SiO_2$-Al_2O_3	$Co(NO_3)_2$	Water	Silica-Alumina
Co/MgO	$Co(NO_3)_2$	Water	Magnesia
$Co(A)/SiO_2$	$Co(CH_3CO_2)_2$	Water	Silica
$Co(Cl)/SiO_2$	$CoCl_2$	Water	Silica
$Co(S)/SiO_2$	$CoSO_4$	Water	Silica
$Co(Me)/SiO_2$	$Co(NO_3)_2$	Methanol	Silica
$Co(Et)/SiO_2$	$Co(NO_3)_2$	Ethanol	Silica
$Co(Pr)/SiO_2$	$Co(NO_3)_2$	Propanol	Silica
$Co(Bu)/SiO_2$	$Co(NO_3)_2$	Butanol	Silica
$Co(DMSO)/SiO_2$	$Co(NO_3)_2$	Dimethylsulfone	Silica
$Co(DMF)/SiO_2$	$Co(NO_3)_2$	Dimethylformamide	Silica
$Co(Ac)/SiO_2$	$Co(NO_3)_2$	Acetone	Silica

Table 2.2. Characteristics of inorganic oxide supports

Support	Surface Area (m^2/g)	Pore Volume (cm^3/g)	Pore Diameter (Å)	Aluminium Content (wt%)	Vendor
SiO_2	289	1.16	160	0	Merck
SiO_2	480	1.44	60	0	Merck
SiO_2	675	1.35	40	0	Merck
SiO_2	750	0.75	21	0	Merck
SiO_2-1Al_2O_3	491	1.21	98	1	Kalichemie
SiO_2-4Al_2O_3	563	0.82	58	4	Kalichemie
SiO_2-9Al_2O_3	461	0.48	42	9	Kalichemie
SiO_2-13Al_2O_3	516	0.47	36	13	Kalichemie
Al_2O_3	209	0.45	85	100	Kalichemie
MgO	33	0.14	148	0	Merck

2.2. Catalyst Characterization

Catalyst characterization is an integral step in the design of catalysts as it aids in the linking of catalytic performance with the structural and electronic properties of the active material. The catalysts in this study were characterized using thermochemical, adsorptive and spectroscopic techniques. The thermochemical characterization techniques included temperature programmed reduction (TPR), temperature programmed oxidation (TPO) and thermogravimetric differential thermal analysis (TG-DTA). Adsorptive characterization techniques applied were hydrogen chemisorption and N_2 BET and the spectroscopic techniques used were X-ray diffraction (XRD) and atomic absorption spectroscopy (AAS).

2.2.1. Thermochemical Characterization Techniques

2.2.1.1. Temperature programmed reduction

The reduction behaviours of the catalysts used in this study were measured using a temperature programmed reduction (TPR) apparatus constructed of stainless steel valves and fittings and containing a quartz microreactor (Figure 2.1.).

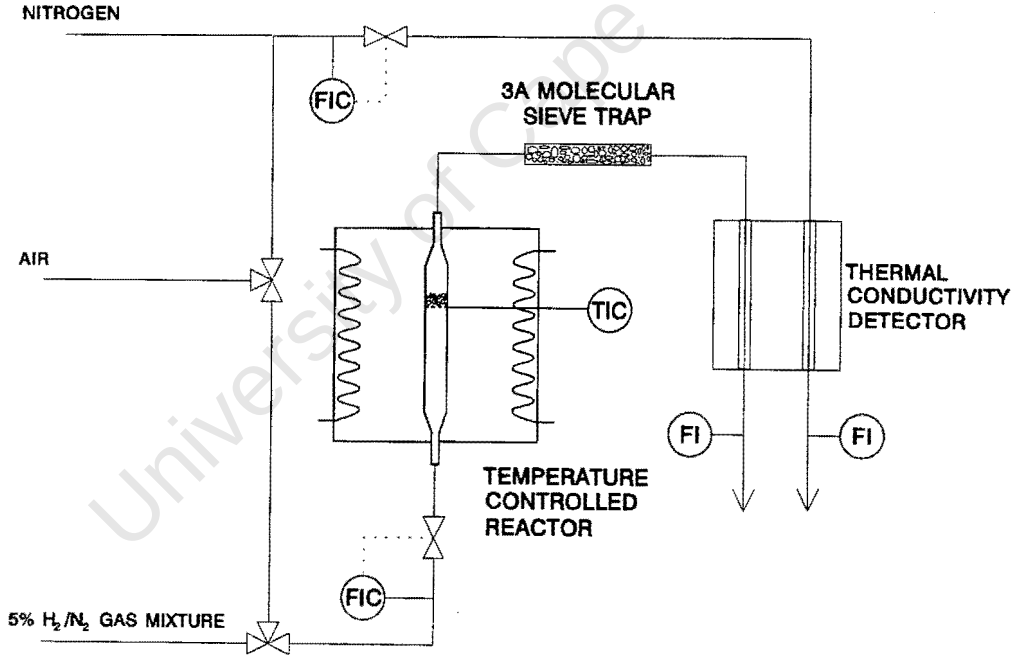

Figure 2.1. Schematic of temperature programmed reduction apparatus
(FI = flow indication, FIC = flow indication and control, TIC = temperature indication and control)

Accurate delivery of the reducing gas (6.2% H_2/N_2) and the TCD reference gas (N_2) was enabled using Brooks Series 9650 mass flow controllers. Calibration of the mass flow

controllers was performed with the aid of soap bubblemeters. Air used for calcination was introduced via the use of a three way valve.

The catalyst sample was placed in a quartz reactor containing a porous frit over which the catalyst particles were spread. The quartz reactor contained a thermowell into which a thermocouple could be inserted allowing temperature control from within the catalyst bed. Connection of the reactor to the stainless steel tubing was performed using Cajon® fittings. The product stream from the reactor was diverted through a 3Å molecular sieve trap in order to remove any water formed through metal oxide reduction before passing through the one arm of the thermal conductivity detector (TCD). A mass flow controlled stream of nitrogen was diverted through the second arm of the TCD as a reference flow. The hydrogen consumption during TPR was calculated by measuring the concentration of hydrogen in the reactor outlet stream as a function of the reduction temperature using a linear temperature programme and a constant inlet flow (water vapour trapped in the molecular sieve trap does not influence the overall flowrate significantly using the selected operating conditions).

In a typical experiment, the catalyst precursor (typically 0.15 g in the instance of the supported catalysts) was loaded into the quartz microreactor which was heated in a 60 ml(NTP)/min N_2 stream to 100°C at 10°C/min. At this temperature, the TCD was turned on and stabilized for at least 4 hours. Upon obtaining a stable signal from the TCD, the reducing gas (60 ml(NTP)/min 6.2% H_2/N_2) was diverted through the reactor and the temperature was raised linearly from 100°C to 1000°C at 10°C/min. The temperature was maintained at 1000°C for 30 minutes in order to ensure complete reduction of the metal catalysts. Data was captured using a microcomputer for further analysis. In instances where precalcination of the catalyst was required, this procedure was performed *in situ* using either air or N_2 prior to the TPR experiment.

The TPR system was calibrated by reduction of the bulk unsupported cobalt oxide Co_3O_4 [Paryjczak *et al*, 1980]. The cobalt oxide used for the calibration procedure was prepared by heating the nitrate salt of cobalt in a muffle furnace at 500°C for 3 hours. The TPR

calibration and the method of signal integration during TPR is detailed in Appendix I.

2.2.1.2. Temperature programmed oxidation

Temperature programmed oxidation (TPO) was used to determine the extent of metal reduction of the supported cobalt catalysts in this study. The extent of metal reduction of supported cobalt catalysts is difficult to determine by measuring the hydrogen consumption during TPR because of the complicated stoichiometry of the reduction (*i.e.* besides the reduction of unknown quantities of divalent and trivalent cobalt ions, reduction of the nitrate ion might also occur).

TPO of unsupported cobalt metal (Figure 2.2.) is characterized by two oxygen consumption maxima occurring at 300 and 580°C, corresponding to the sequential oxidation of metallic cobalt first to CoO and then to Co_3O_4 (reactions 1 and 2). At a temperature of 870°C, thermal reduction of Co_3O_4 to CoO occurs with a stoichiometric release of oxygen (reaction 3). The reaction stoichiometry corresponding to cobalt oxidation and thermal reduction during TPO is illustrated below.

$$Co + ½\ O_2 \rightarrow CoO \qquad (1)$$

$$3\ CoO + ½\ O_2 \rightarrow Co_3O_4 \qquad (2)$$

$$Co_3O_4 \rightarrow 3\ CoO + ½\ O_2 \qquad (3)$$

From the reaction stoichiometry, it can be deduced that the ratio of the oxygen uptake caused by reactions (1) and (2) relative to the oxygen release caused by reaction (3) should be 4. The ratio of the peak areas corresponding to oxygen uptake and oxygen release during TPO was 3.92 which confirms the reaction stoichiometry during the experiment. Appendix II contains the TPO calibration procedure and the methods of calculation.

In the case of supported cobalt catalysts, the extent of reduction may be limited due to interaction with the support or due to the formation of cobalt-support species. Following

hydrogen reduction, cobalt may be present either as zerovalent cobalt, unreduced divalent cobalt species which may be oxidized and divalent cobalt-support species which are not able to oxidized. The presence of residual trivalent cobalt species following reduction at 500°C is unlikely [Arnoldy and Moulijn, 1985; van't Blik and Prins, 1986] and therefore should not influence the TPO calculations.

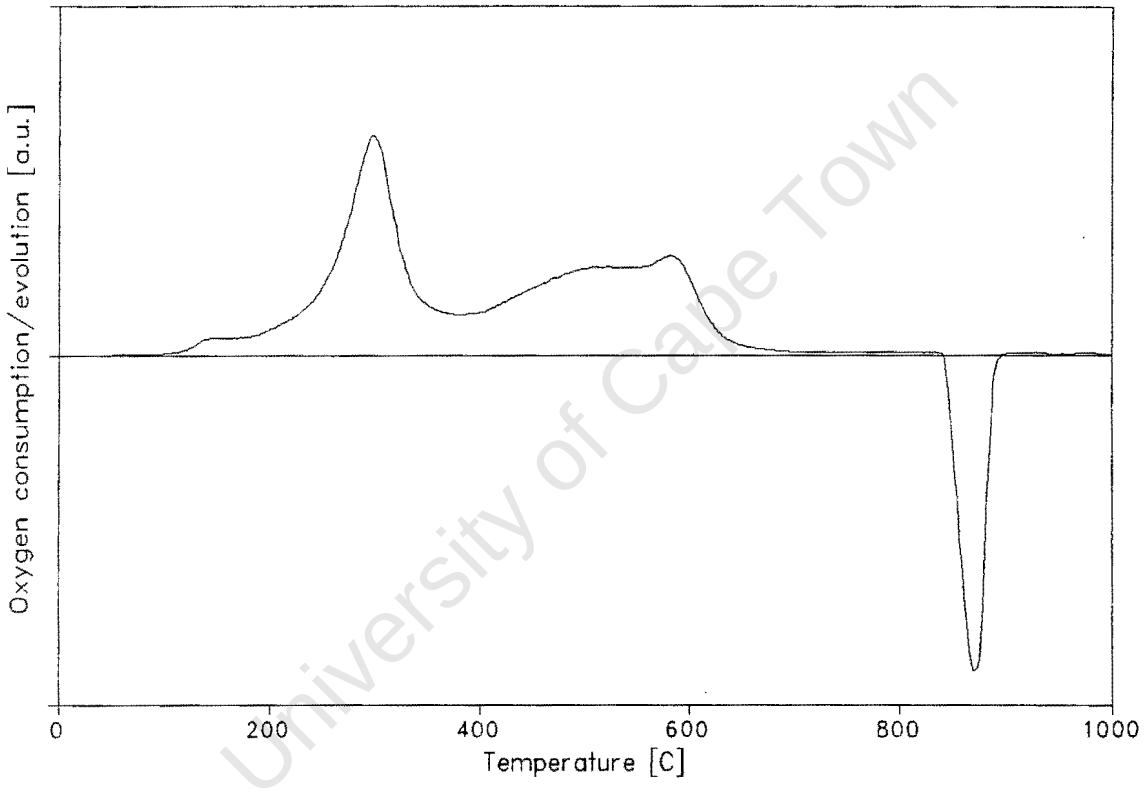

Figure 2.2. TPO spectrum of reduced cobalt
(Reducing gas = 60 ml(NTP)/min 5% H_2/N_2, reduction temperature = 500°C, oxidizing gas = 60 ml(NTP)/min 2% O_2/He, temperature programming rate = 10°C/min, $m_{cat} \approx 0.50$ g)

Depending on the extent of cobalt reduction, the ratio of the oxygen uptake peak to the oxygen release peak will range between 1 and 4. A ratio of 1 indicates that the cobalt species present after hydrogen reduction are divalent in nature and therefore the oxygen uptake is identical to the oxygen release (see reactions 2 and 3). A ratio of 4 indicates complete reduction of the supported cobalt species.

The high temperature oxygen release during TPO corresponds to the oxygen released from all trivalent species present on the catalyst (*i.e.* excluding the cobalt species which were not able to be oxidized to trivalent cobalt). Cobalt not able to be oxidized to trivalent cobalt by a temperature of 800°C is probably present as a stable cobalt-support species. Knowledge of the total cobalt content of the catalyst sample and measurement of the high temperature oxygen release therefore allows quantification of the extent of cobalt-support compound formation.

From the TPO measurements, 3 different type of cobalt species were observed. These different types of cobalt were designated in the following manner :

Zerovalent cobalt - the amount of metallic cobalt following reduction

Oxidizable divalent cobalt - the amount of residual unreduced cobalt which has not been reduced by 500°C but which can be oxidized during TPO

Non-oxidizable divalent cobalt - the amount of cobalt which cannot be reduced by 500°C and cannot be oxidized up to temperatures of 1000°C

The TPO measurements were made using the same apparatus as used for recording the TPR spectra except that a mixture of 2% O_2/He was used as the oxidizing gas and He was used as the TCD reference gas. Prior to recording the oxygen uptake during TPO, the catalyst sample (typically 0.50 g for the supported metal catalysts) was reduced using a 60 ml(NTP)/min 5% H_2/N_2 stream. The time and temperature of reduction could be varied as required and the temperature programming rate used was 10°C/min. Following catalyst reduction, the temperature was cooled to 50°C at which temperature the TCD was stabilized for at least 4 hours. Upon stabilization of the detector, the oxidizing gas (60 ml(NTP)/min 2% O_2/He) was diverted through the reactor and the temperature was raised linearly from 50 to 1000°C at 10°C/min. The reactor temperature was maintained at 1000°C for 30 minutes in order to ensure complete oxidation of the reduced metal catalyst. The oxygen uptake during TPO was calculated by measuring the oxygen concentration in the outlet

stream as a function of the oxidation temperature using a linear temperature programme and a constant inlet flowrate (the flowrate does not vary significantly due to oxygen consumption/release during TPO). Data were collected and stored by microcomputer for further processing.

2.2.1.3. Thermogravimetric differential thermal analysis

Thermogravimetric differential thermal analysis (TG-DTA) of the catalyst precursors and the spent amination catalysts was conducted using a STA 780 series Stanton Redcroft Thermal Analyzer. These measurements were used to determine the mass loss upon heating of the catalyst precursors and to calculate the coke content of the spent amination catalysts.

Typically, 25 mg samples were loaded into quartz sample holders and the temperature was raised linearly from 50 to 500°C at 10°C/min in a 30 ml(NTP)/min air stream. For the spent amination catalysts, the sample was heated to 700°C in order to ensure complete combustion of any carbonaceous material. The reference sample used was 25 mg of α-alumina. The thermal decomposition of $CuSO_4 \cdot 7H_2O$ in a 30 ml(NTP)/min N_2 stream was used to confirm the proper operation of the apparatus.

2.2.2. Adsorptive Characterization Techniques

2.2.2.1. Hydrogen chemisorption

Metal surface area determinations were performed in a conventional Pyrex glass volumetric adsorption apparatus using the Micromeritics ASAP 2000. Hydrogen was used as the adsorbate since it has been shown to yield monolayer surface coverage under appropriately selected conditions for supported cobalt [Reuel and Bartholomew, 1984], nickel [Bartholomew and Pannell, 1980] and copper catalysts [Myasaki, 1980].

Prior to recording the hydrogen uptake during chemisorption, the catalyst sample ($\approx$ 0.5 g)

was reduced in a 60 ml(NTP)/min H_2 stream. The time and temperature of reduction were adjusted as per the experimental requirements using a temperature programming rate of 10°C/min. The reduction procedure was performed *in situ* in order to avoid atmospheric degradation of the sample which might occur during transfer.

Following reduction, the sample was evacuated at 400°C for 3 hours in order to remove any residual adsorbed hydrogen or water present on the catalyst surface following the activation procedure. The total pressure following this procedure was less than 1 x 10^{-3} torr and the removal of all adsorbed species was confirmed by observing the pressure rise as a function of time. The sample was then cooled under vacuum to the adsorption temperature and the hydrogen adsorption isotherms were measured between 100 and 350 torr. To determine the reversibility of the adsorption process, the sample was evacuated for 15 mins at the temperature of adsorption and the hydrogen adsorption isotherms were remeasured. The reversibility of hydrogen adsorption was defined as the amount of hydrogen not removed by evacuation relative to the total hydrogen uptake of the catalyst. The reversibility of hydrogen adsorption is calculated using the following expression :

$$Reversibility = \frac{V_{irr}}{V_{total}} \times 100\%$$

where V_{irr} represents the amount of hydrogen not able to be removed by a 15 minute evacuation at the adsorption temperature and V_{total} represents the total hydrogen uptake of the catalyst. The reproducible behaviour of the apparatus was tested using a Pt/Al_2O_3 standard. A sample calculation for determining the metal surface area, dispersion, average crystallite diameter and the reversibility of hydrogen adsorption is attached in Appendix V.

2.2.2.2. Nitrogen B.E.T.

Nitrogen B.E.T. measurements of the inorganic oxide catalyst supports were performed using the Micromeritics ASAP 2000. These measurements were conducted in order to measure the surface area, pore volume and average pore diameter of the metal carrier materials. Prior to

measuring the nitrogen adsorption isotherms, the sample ($\approx$ 0.5 g) was evacuated at 100°C until the pressure was less than 1 x 10^{-3} torr. This procedure was followed in order to remove all adsorbed species which may affect the adsorption measurements and also to obtain the true mass of the sample. The conventional N_2 B.E.T. technique was then performed. Reproducible operation of the machine was tested periodically by measuring the nitrogen adsorption isotherms of a standard γ-Al_2O_3 supplied with the instrument.

2.2.3. Spectroscopic Characterization Techniques

2.2.3.1. X-Ray diffraction

Powder X-ray diffraction (XRD) spectra were recorded on a Philips PW 1390 diffractometer using nickel filtered Cu K_α radiation with a wavelength 1.542 Å and generated at 40 kV and 30 mA. Data were collected between 2θ values of 35 and 65° in increments of 0.05° and a scan time of 1 second was used. Application of the Scherrer line broadening equation to estimate the average metal crystallite diameter was not successful due to a low signal to noise ratio and due to the broad nature of the diffraction peaks.

2.2.3.2. Atomic absorption spectroscopy

Atomic absorption (AA) was used to determine the aluminium content in a range of SiO_2-Al_2O_3 supports of varying silicon to aluminium ratios using a Varian Spectra AA-30 spectrometer. Extraction of aluminium from the SiO_2-Al_2O_3 supports was performed by high temperature fusion of 0.5 g of the support material with 5 g of sodium peroxide (Na_2O_2) followed by dissolution in 50 ml deionized water and 20 ml concentrated hydrochloric acid. The measurements were made at a wavelength of 309.3 nm using a lamp current of 10 mA.

2.3. Reductive Amination of Ethanol

2.3.1. Experimental Apparatus

The gas phase amination of ethanol was conducted in an atmospheric, continuous flow system (Figure 2.3.). Ethanol was delivered via a temperature controlled double stage saturator ($\Delta T = 25^{\circ}C$) operated at atmospheric pressure using hydrogen fed via a Brooks Series 9650 mass flow controller as the carrier gas. Collection of ethanol in a dry-ice acetone trap at -80°C confirmed saturation of the ethanol in the hydrogen outlet stream. Ammonia was fed using a Brooks mass flow controller as a 10 wt% mixture in nitrogen. The concentration of the ammonia gas mixture was initially determined by back-titration (using a sulphuric acid trap) after which the determined gas chromatographic response factors could be used. Typical conditions used for the amination studies were a reaction temperature of 180°C, an ethanol WHSV of 1 g_{EtOH}/g_{cat}·h and an EtOH : NH_3 : H_2 : N_2 molar ratio of 1 : 2 : 8.6 : 17.6.

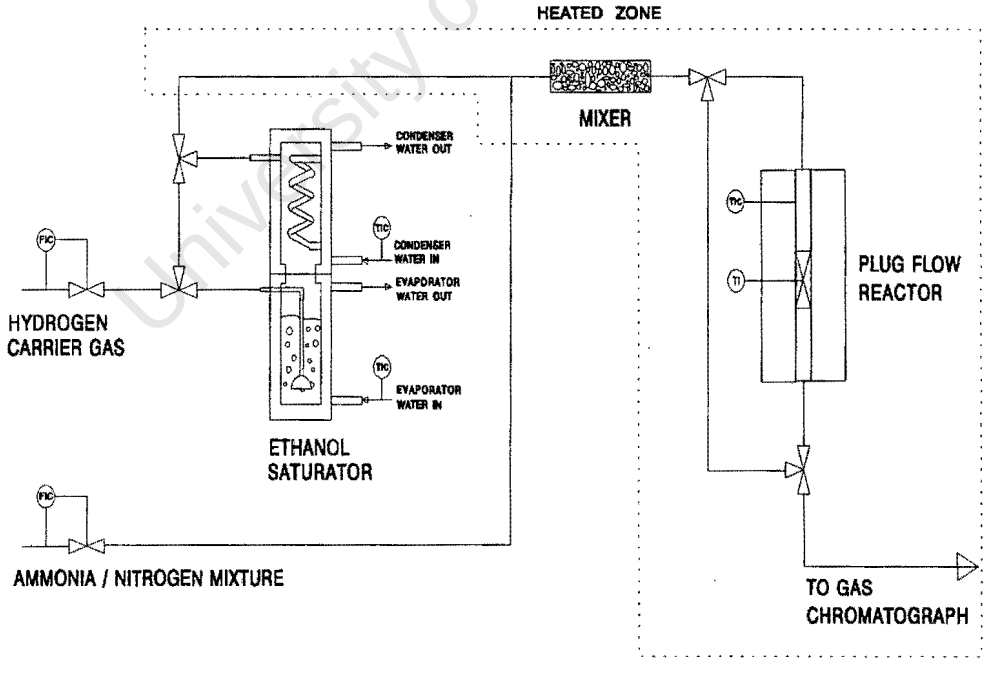

Figure 2.3. Schematic of ethanol amination apparatus

Before entry into the temperature controlled, stainless steel plug flow reactor (Figure 2.4.),

the feed was diverted through a heated glass bead mixer in order to ensure homogeneity. The catalyst was placed between glass wool plugs inside the reactor and 1 mm glass beads were used to preheat the feed mixture to the reaction temperature. Temperatures in the reactor were measured by means of a thermocouple which could be moved up and down a thermowell situated axially inside the reactor. Considerable axial temperature gradients were observed (Figure 2.5.) and a stainless steel riser was used in order to facilitate the placement of the catalyst sample in the isothermal region of the reactor. Condensation of reaction products was prevented by heating all valves and tubing to a temperature of 150°C.

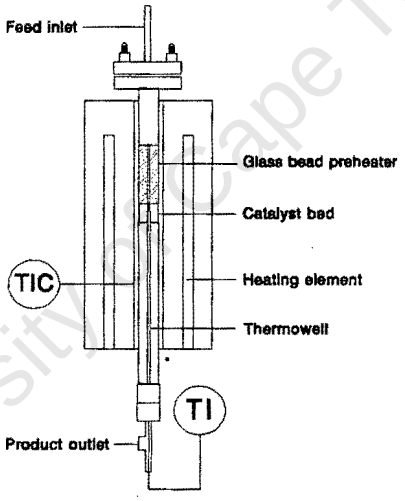

Figure 2.4. Schematic of reactor configuration used for ethanol amination (TI = temperature indication, TIC = temperature indication and control)

Sampling of the reactant and product gases was performed using a six-way valve and analysis was performed using a Varian Model 3700 gas chromatograph equipped with thermal conductivity detector. The separation was achieved using a 4m x 3mm ID glass column packed with 60/80 mesh Carbopack B / 4% Carbowax 20M / 0.8% KOH. The GC oven was ramped from 40 to 180°C at 10°C/min in order to obtain adequate elution of the reaction products. The nitrogen in the NH_3/N_2 feed gas mixture was used as an internal standard

allowing mass balances to be determined to within 5%. The mass balance calculations used are detailed in Appendix III and the data obtained from the amination studies is listed in Appendix IV.

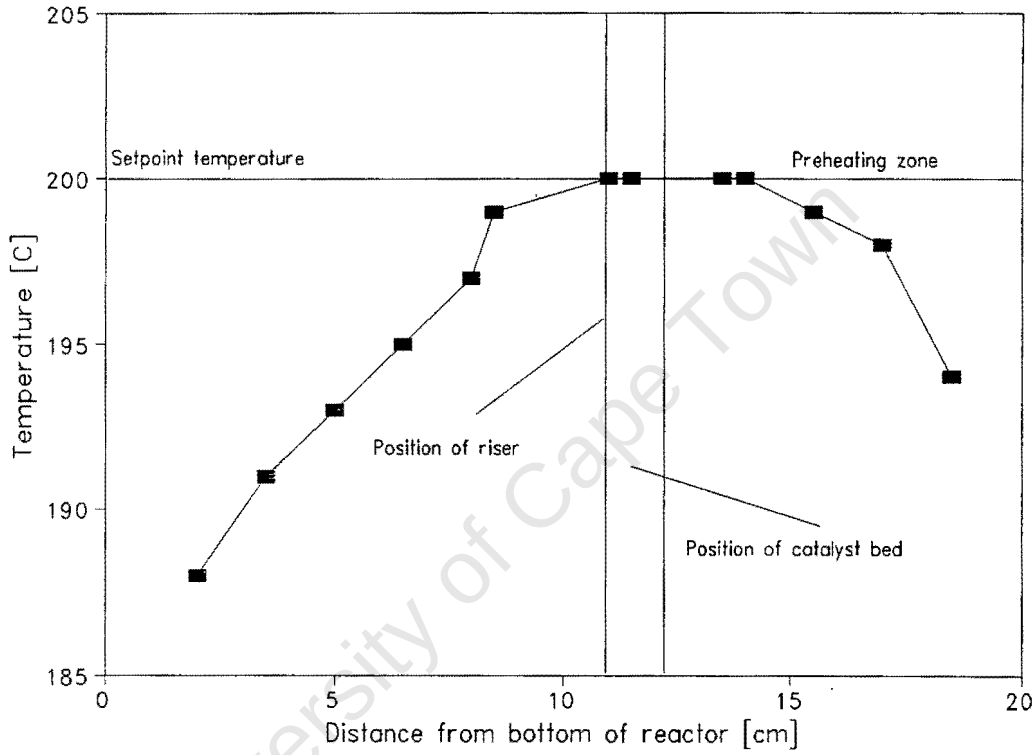

Figure 2.5. Axial temperature gradients in the amination reactor

2.3.2. Experimental Procedure

Prior to the amination experiments, the dried catalyst precursors need to be transformed into their active metallic form. This transformation may be achieved by either a calcination/reduction procedure or by simply reducing the catalyst precursor directly. Both of these procedures were tested during this study.

During the activation procedure, the catalysts undergo varying weight losses due to the decomposition of the precursor compound, the loss of adsorbed water and the reduction of

the supported metal. These weight losses were compensated for by measuring the weight loss during TG-DTA and an appropriate amount of catalyst was added such that all experiments were conducted using 1.00 g of catalyst (after calcination/reduction).

Calcination of the catalyst precursor was conducted using a 60 ml(NTP)/min stream of either air or N_2, depending on the experimental requirements. The time and temperature of calcination could be adjusted as required and a temperature programming rate of 10°C/min was used. Following the calcination step, the reactor was cooled to 100°C in the calcination gas at which stage it was replaced by the reducing gas which comprised a 60 ml(NTP)/min H_2 stream. After allowing a period of 15 minutes for the hydrogen to fully purge the system of the residual calcination gas, the reactor temperature was increased linearly from 100°C at 10°C/min. The final time and temperature of reduction were determined by the specific requirements of the experiment.

The catalyst was then cooled to 100°C in hydrogen and the flow directed through the reactor bypass via three way valves. At this point, the feed delivery system was started and allowed to stabilize. Upon stabilization of the feed delivery system (as confirmed by gas chromatographic analysis), the reactor feed stream was diverted downwards through the catalyst bed and the temperature was increased at 10°C/min up to the desired reaction temperature. Sampling of the reaction products was initiated when the reactor temperature had reached the setpoint value (approximately 10 to 15 minutes for a reaction temperature of 180°C).

The ethanol conversion and the amine selectivity was seen to change during the first 24 hours of operation due to catalyst deactivation. After this initial period of deactivation, catalyst activity and selectivity were relatively stable indicating that steady state had been achieved. Gas chromatographic samples were taken every hour (with the exception of the time in which the system was allowed to run overnight) which allowed the deactivation process to be monitored. Comparisons of the activity and selectivity of the various catalysts were based on the steady state measurements however.

2.3.3. Experimental Reproducibility

The reproducibility of the catalyst preparation and evaluation procedure is of critical importance when the experimental objective is the comparison of catalytic performance. It is thus important that both the catalyst preparation and testing procedure be reproducible. To investigate the reproducibility of the catalytic testing procedure, the ethanol conversion activity of the same batch of catalyst was measured at a reaction temperature of 180°C, an ethanol WHSV of 1 g_{EtOH}/g_{cat}·h and an EtOH : NH_3 : H_2 : N_2 molar ratio of 1 : 2 : 8.6 : 17.6. The catalyst tested was a potassium promoted, Al_2O_3 supported cobalt catalyst (0.25K-Co/Al_2O_3) which was activated by reduction in a 60 ml(NTP)/min H_2 stream at 500°C for 60 minutes. The time on stream behaviour of the 0.25K-Co/Al_2O_3 catalyst illustrated that the catalyst testing procedure was reproducible to within 2% (Figure 2.6).

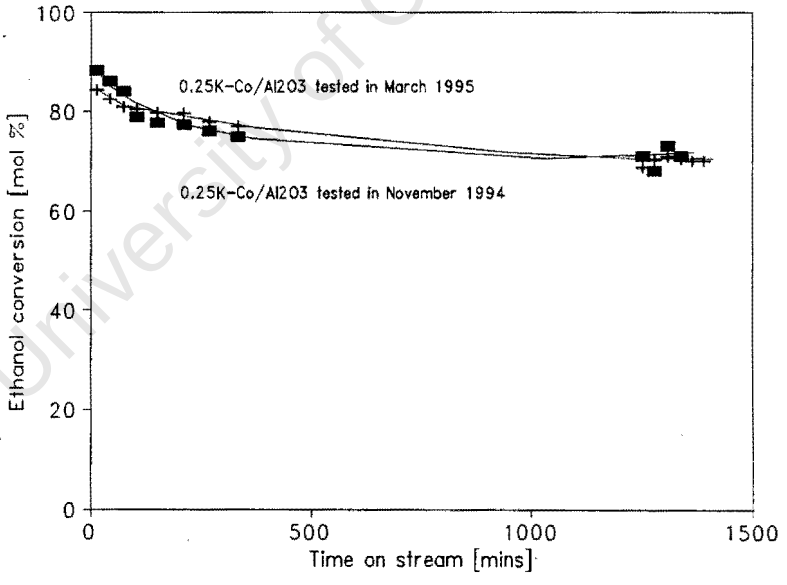

Figure 2.6. Reproducibility of catalyst testing procedure
(T = 180°C, P = 1 bar, WHSV = 1 g_{EtOH}/g_{cat}·h, EtOH : NH_3 : H_2 : N_2 = 1 : 2 : 8.6 : 17.6)

To test the reproducibility of the catalyst preparation procedure, two separate batches of an Al_2O_3 supported cobalt catalyst were formulated using identical procedures and evaluated at

a reaction temperature of 180°C, an ethanol WHSV of 1 g_{EtOH}/g_{cat}·h and an EtOH : NH_3 : H_2 : N_2 molar feed ratio of 1 : 2 : 8.6 : 17.6. The catalysts were reduced in a 60 ml(NTP)/min H_2 stream at 500°C for 60 minutes prior to testing. By comparing the time on stream activity of the two Al_2O_3 supported cobalt catalysts (Figure 2.7.), it can be seen that although the catalyst preparation procedure decreased the reproducibility of the experimental procedure, substantial differences were not obtained. As a consequence of the differences obtained during the calibration procedures, only changes in activity larger than 5% were considered to be significant.

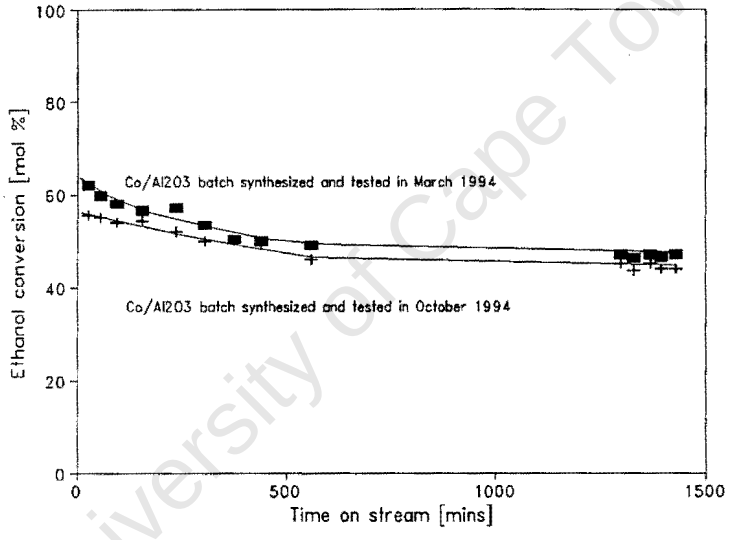

Figure 2.7. Reproducibility of catalyst preparation procedure
(T = 180°C, P = 1 bar, WHSV = 1 g_{EtOH}/g_{cat}·h, EtOH : NH_3 : H_2 : N_2 = 1 : 2 : 8.6 : 17.6)

CHAPTER 3

RESULTS

3.1. Comparison of Cobalt, Nickel and Copper Catalysts

Catalysts of very different chemical composition are reported to be effective for the reductive amination of alcohols. These catalysts include copper, platinum, nickel, cobalt, silver, iron, rhenium, palladium and ruthenium [Kirk-Othmer, 1992; Baiker and Kijenski, 1985; Klyuev and Khikedel, 1980; Nekrasova and Shuikin, 1965; Gardner and Clark, 1980]. Of these catalysts, cobalt, nickel and copper appear to be the preferred catalysts for industrial application [Gardner and Clark, 1981; Heft *et al*, 1990; Deeba, 1988; Best, 1978]. An evaluation of each of these catalysts was undertaken by investigating the influence of the feed partial pressures, the space velocity and the reaction temperature on the activity and selectivity during reductive amination. The amination performance of these catalysts was related to their physico-chemical characteristics using TPR and hydrogen chemisorption.

3.1.1. Catalyst characterization

The reducibility of the SiO_2 supported cobalt, nickel and copper catalysts was evaluated using TPR and the reduced metal surface area was measured using hydrogen chemisorption. These measurements were performed in order to base comparisons of catalytic performance on the physicochemical characteristics of the supported metal catalysts.

3.1.1.1. Temperature programmed reduction

The reduction behaviours of the SiO_2 supported cobalt, nickel and copper catalysts were measured at temperatures between 100 and 1000°C using a 60 ml(NTP)/min 5% H_2/N_2 stream as the reducing gas. The temperature programming rate used to effect the temperature changes during TPR was 10°C/min. Reduction of the corresponding bulk metal oxides Co_3O_4, NiO and CuO was used to compare the reducibility of the SiO_2 supported metal catalysts. These bulk oxides were prepared by heating the corresponding metal nitrates in a muffle furnace at 500°C for 5 hours.

The hydrogen consumption during TPR of the Co/SiO_2 catalyst and the bulk cobalt oxide

Co_3O_4 is illustrated in Figure 3.1. The TPR spectrum of the bulk cobalt oxide Co_3O_4 was characterized by two hydrogen consumption maxima occurring at 270 and 350°C. The two hydrogen consumption peaks are in accordance with the consecutive reduction of Co_3O_4 first to divalent cobalt and then to zerovalent cobalt [Viswanathan and Gopalakrishnan, 1986; Lapidus *et al*, 1991; Chen and Wang, 1993]. The stoichiometry of these reduction reactions is illustrated below.

$$Co_3O_4 + H_2 \rightarrow 3\ CoO + H_2O$$
$$CoO + H_2 \rightarrow Co + H_2O$$

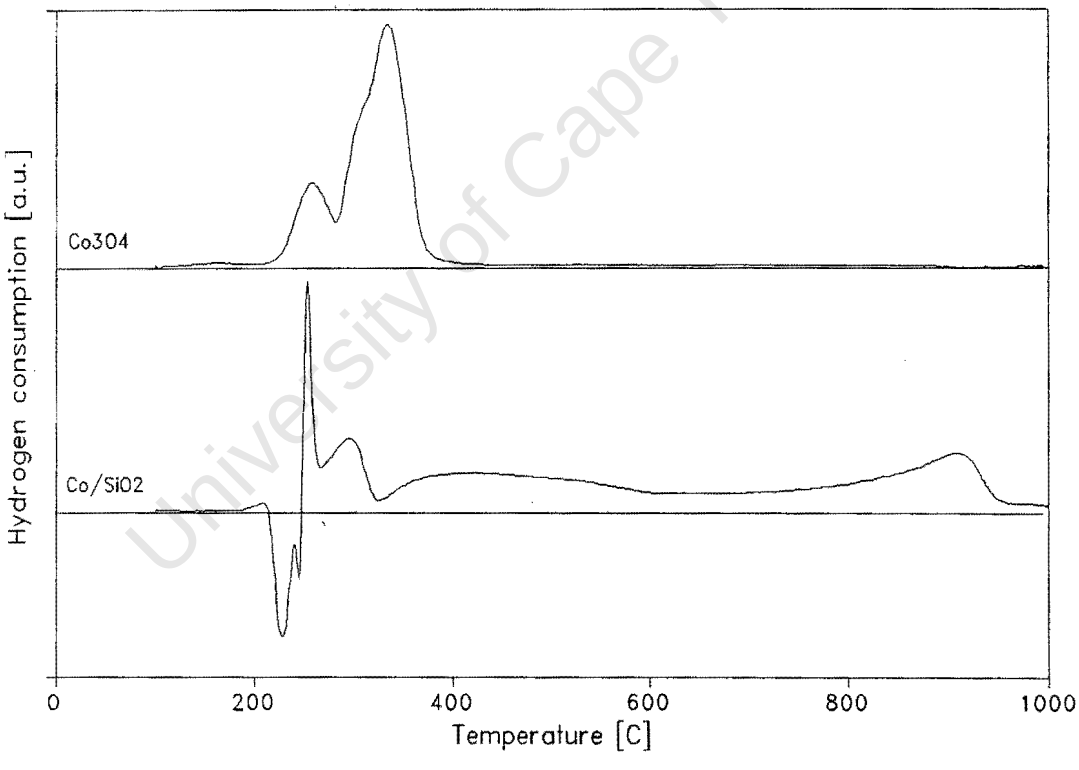

Figure 3.1. TPR spectra of Co/SiO_2 and Co_3O_4
(Reducing gas = 60 ml(NTP)/min 5% H_2/N_2, temperature programming rate = 10°C/min)

The TPR spectrum of the Co/SiO_2 catalyst showed a number of hydrogen consumption peaks which indicated the presence of a number of reducible species on the surface of the catalyst

precursor. The increased temperatures required for reduction of these species relative to the bulk unsupported cobalt oxide indicated that the presence of the SiO_2 support decreased the reducibility of the supported cobalt. The high temperature hydrogen consumption observed during TPR of the Co/SiO_2 catalyst indicates that not all cobalt present will be reduced by a temperature of 500°C. This will be expected to influence the final activity of the catalyst since only metal reduced by 500°C will be available for amination.

Measurement of the hydrogen consumption during TPR of the Co/SiO_2 catalyst yielded a hydrogen to cobalt molar ratio of 1.33. Since cobalt is present as a divalent ion in the nitrate precursor, it is likely that simultaneous reduction of the nitrate ion is responsible for the increased hydrogen consumption.

The reduction profiles of the Ni/SiO_2 catalyst and the bulk nickel oxide NiO are illustrated in Figure 3.2. The TPR spectrum of the bulk nickel oxide NiO was characterized by a single hydrogen consumption peak with a maximum at 420°C. The hydrogen consumption corresponded to the reduction of the divalent oxide to the zerovalent metal according to the following stoichiometry :

$$NiO + H_2 \rightarrow Ni + H_2O$$

In contrast to the reduction profile of nickel oxide, the TPR spectrum of the Ni/SiO_2 catalyst showed a number of peak maxima which indicated the presence of a number of reducible species in the dried catalyst precursor. These peaks may correspond to the reductive decomposition of the nitrate precursor [Bartholomew and Farrauto, 1976] and the reduction of various nickel hydrosilicate species [Gil *et al*, 1994; Coenen, 1989]. As in the instance of the Co/SiO_2 catalyst, hydrogen consumption was observed at temperatures greater than 500°C indicating that the supported nickel was not completely reduced by this temperature.

Integration of the TCD signal during TPR of the Ni/SiO_2 catalyst yielded a hydrogen to nickel molar ratio of 1.13. Since reduction of divalent nickel resulted in a H_2 : Ni molar ratio of 1, the increased hydrogen consumption is most likely caused by reduction of the nitrate

ion.

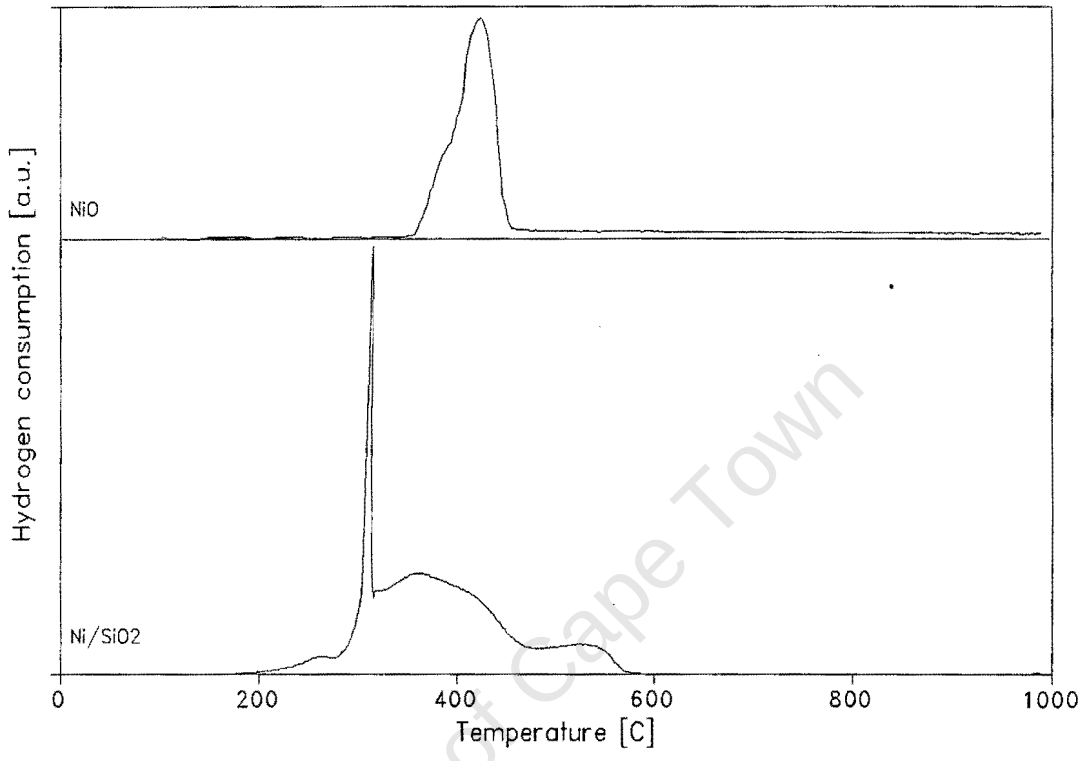

Figure 3.2. TPR spectra of Ni/SiO_2 and NiO
(Reducing gas = 60 ml(NTP)/min 5% H_2/N_2, temperature programming rate = 10°C/min)

The hydrogen consumption profiles of the SiO_2 supported copper catalyst and the bulk unsupported copper oxide CuO are illustrated in Figure 3.3. The TPR spectrum of the unsupported copper oxide CuO was characterized by a single hydrogen consumption peak at 310°C. The single hydrogen consumption peak indicated that reduction of the unsupported copper oxide occurred in a single step according to the following reaction stoichiometry :

$$CuO + H_2 \rightarrow Cu + H_2O$$

Temperature programmed reduction of the Cu/SiO_2 catalyst indicated that the copper nitrate precursor was easily reduced. The TPR spectrum showed only one hydrogen consumption peak with a maximum at 260°C which indicated that the reduction of SiO_2 supported cobalt

nitrate occurred more readily than unsupported CuO. The hydrogen to copper molar ratio during TPR was 1.37. The increased hydrogen consumption was most likely due to reduction of the nitrate ion in the copper nitrate precursor compound and the single peak during TPR suggests that copper nitrate was reduced directly to metallic copper. The absence of further hydrogen consumption peaks at higher temperatures indicates that metal-support compounds such as copper hydrosilicates [van der Grift *et al*, 1990] were not formed. Since no hydrogen consumption was observed at temperatures greater than 500°C, it is likely that the supported copper is completely reduced by this temperature.

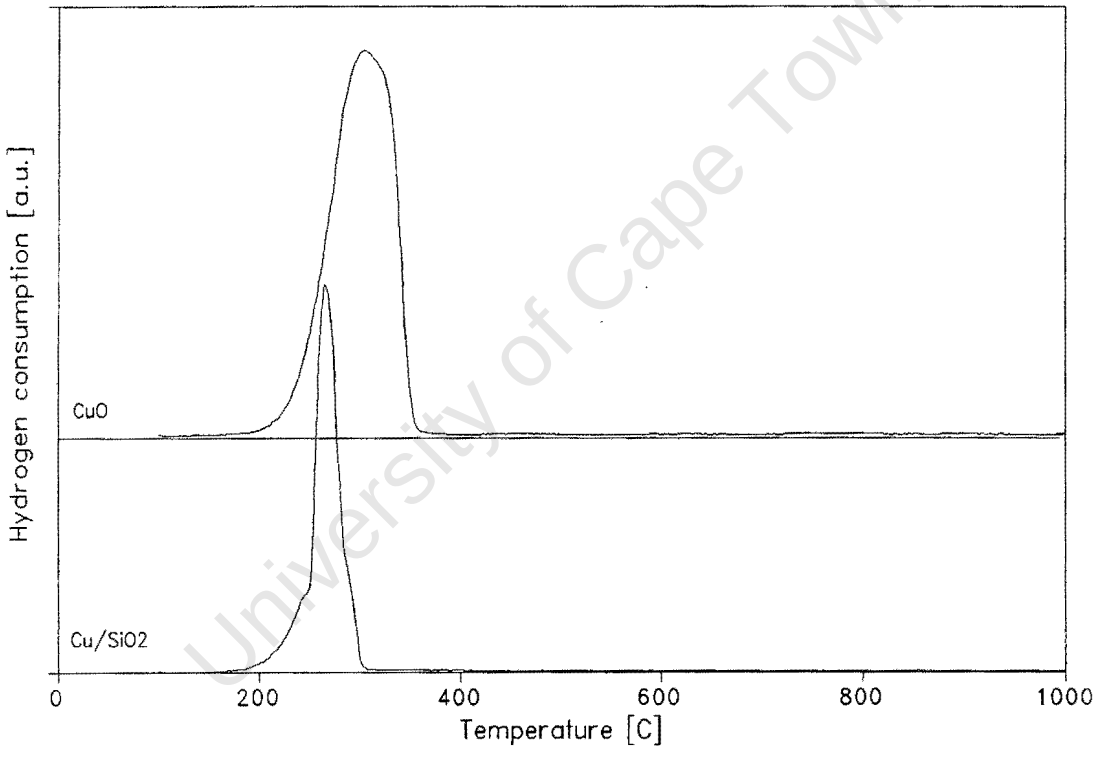

Figure 3.3. TPR spectra of Cu/SiO_2 and CuO
(Reducing gas = 60 ml(NTP)/min 5% H_2/N_2, temperature programming rate = 10°C/min)

Since the temperature of hydrogen reduction selected for activation of the catalysts used in the amination studies was 500°C, it is apparent that not all of the supported metal catalysts will be reduced completely by this temperature. By measuring the hydrogen consumption occurring at temperatures greater than 500°C, an indirect estimate of the degree of metal

reduction can be obtained. Measurement of the hydrogen consumption occurring at temperatures lower than 500°C is inaccurate due to simultaneous reduction of the nitrate ion. Using this technique, it can be seen that the extent of metal reduction decreased as the catalyst was changed from Cu/SiO_2 to Ni/SiO_2 to Co/SiO_2 (Table 3.1.).

Table 3.1. Hydrogen consumption during TPR and nitrate reduction temperatures for SiO_2 supported cobalt, nickel and copper catalysts

Catalyst	$(H_2 : Me)_{total}$ (mol : mol)	$(H_2 : Me)_{>500}$ (mol : mol)	$T_{decomposition}$ (°C)
Co/SiO_2	1.33	0.73	240
Ni/SiO_2	1.13	0.44	310
Cu/SiO_2	1.37	≈ 0	270

3.1.1.2. Hydrogen chemisorption

Hydrogen chemisorption was used to measure the metallic surface area of the cobalt, nickel and copper catalysts following hydrogen reduction at 500°C. The hydrogen adsorption isotherms were measured at 35°C for the Ni/SiO_2 and Cu/SiO_2 catalysts and at 100°C for the Co/SiO_2 catalyst. A temperature of 100°C was used when recording the metal surface area of the Co/SiO_2 catalyst due to the activated nature of hydrogen adsorption on polycrystalline cobalt [Reuel and Bartholomew, 1984]. Prior to the chemisorption measurements, the catalyst precursors were activated by reduction in a 60 ml(NTP)/min H_2 stream at 500°C for 1 hour. The reduced catalyst sample was then evacuated for 3 hours at a temperature of 400°C in order to remove any residual hydrogen remaining after the reduction process. The results of the chemisorption measurements are listed in Table 3.2.

The chemisorption results indicated that the metallic surface area decreases as the catalyst was changed from Ni/SiO_2 to Co/SiO_2 to Cu/SiO_2. The high surface area of the Ni/SiO_2

catalyst is due to the high extent of metal reduction without the loss of metal dispersion caused by crystallite agglomeration at high temperatures. The lower metal surface area obtained after reduction of the Co/SiO_2 catalyst is due to the low extents of metal reduction caused by metal-support compound formation. The Cu/SiO_2 catalyst had the lowest measured metal surface area even though reduction was complete by 500°C. The decreased metal surface of the Cu/SiO_2 catalyst can be ascribed to the sintering of copper crystallites during the reduction procedure as the dispersion of the copper catalyst was considerably lower than the dispersions obtained for the cobalt and nickel catalysts.

Table 3.2. Surface area, dispersion, diameter and reversibility of hydrogen adsorption on SiO_2 supported cobalt, nickel and copper catalysts

Catalyst	Metal Surface Area (m^2/g_{cat})	Dispersion (%)	Diameter (nm)	Reversibility (%)
Co/SiO_2	1.95	11.3	8.5	46
Ni/SiO_2	4.90	10.5	9.2	77
Cu/SiO_2	0.97	2.2	44.0	25

The reversibility of hydrogen adsorption (see Appendix V) was defined as the percentage of adsorbed hydrogen which could not be removed by evacuation at the adsorption temperature relative to the total hydrogen uptake of the metal. As such, the reversibility of adsorption can be used as an indicator of the strength of hydrogen adsorption on the metal surface. The reversibility of hydrogen adsorption decreased as the catalyst was changed from Ni/SiO_2 to Co/SiO_2 to Cu/SiO_2. This indicates that the percentage of strong hydrogen adsorption sites decreased as the metal catalyst was changed from nickel to cobalt to copper. Differences in the ratio of "strong" and "weak" adsorption sites on the different metal catalysts may alter the strength of the adsorption of certain reactants and intermediates during reaction and may alter the catalytic behaviour.

3.1.2. Catalyst deactivation behaviour

Comparison of the SiO_2 supported cobalt, nickel and copper catalysts was to be performed by measuring the activity and selectivity as a function of the reactant partial pressure, the reaction temperature and the weight hourly space velocity. In order to be able to make accurate comparisons, it was important that the activity and selectivity measurements were made at steady state. The time-on-stream behaviour of the cobalt, nickel and copper catalysts was therefore recorded at a reaction temperature of 180°C, a space velocity of 2 g_{EtOH}/g_{cat}·h and an EtOH : NH_3 : H_2 : N_2 molar ratio of 1 : 2 : 4.1 : 13.6. Figure 3.4. illustrates the time-on-stream activity of the Co/SiO_2, Ni/SiO_2 and Cu/SiO_2 catalysts. The period in which no data points were measured (*ca.* 400 to 1300 minutes) is the period in which the catalyst was left to run overnight.

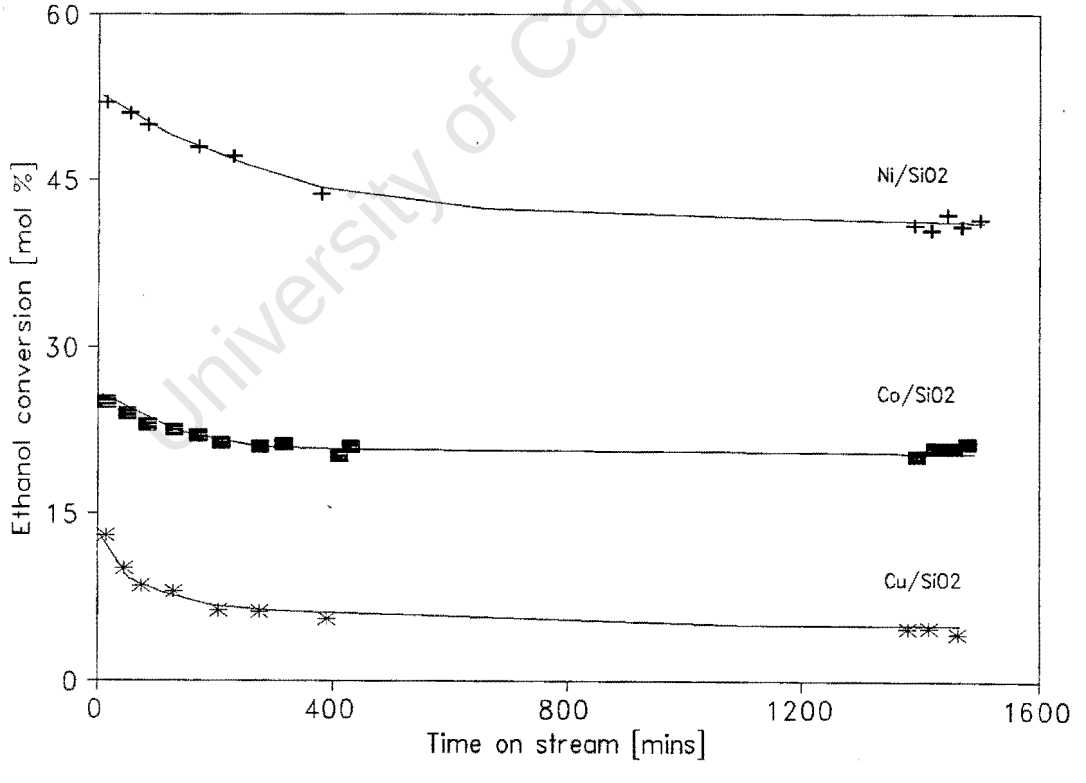

Figure 3.4. Time on stream activity of Co/SiO_2, Ni/SiO_2 and Cu/SiO_2
(T = 180°C, P = 1 bar, WHSV = 2 g_{EtOH}/g_{cat}·h, EtOH : NH_3 : H_2 : N_2 = 1 : 2 : 4.1 : 13.6)

The ethanol conversion was seen to decrease for all three catalysts as a function of time on stream. Although the decrease in ethanol conversion was relatively rapid during the first few hours of time on stream, the activity tended towards a steady state value and after a period of 24 hours, negligible loss in activity was observed. Catalyst deactivation during reductive amination has been shown to be caused by metal nitride formation, metal carbide formation, the deposition of carbonaceous material and the thermal diffusive fusion of the supported metal crystallites [Baiker and Maciejewski, 1984; Baiker *et al*, 1984; Baiker, 1981; Baiker and Richarz, 1978]. From the information available, it is not clear which of these deactivation processes is responsible for the decrease in ethanol conversion. The different rates of deactivation indicate that the influence of these deactivation pathways differs amongst the three metals tested.

The ethylamine selectivity was also seen to vary during the first 24 hours on stream. As in the case of the ethanol conversion, the product selectivity did not change significantly after this induction period. It is therefore possible that the changes in ethylamine selectivity are related to the changes in ethanol conversion. Since steady state activities and selectivities were obtained relatively quickly, a comprehensive investigation into the causes of deactivation was not pursued.

3.1.3. Influence of mass transport

In order to record true kinetic measurements, it must be confirmed that the rate of reaction is not limited by mass transfer phenomena. Mass transfer limitations may be introduced in cases where the rate of reaction is fast or where the rate of diffusion is slow. Reaction rate control by reactant and product diffusion can result in changes in both catalytic activity and in product selectivity and must therefore be avoided. Determination of the reaction regimes during reductive amination was performed by increasing the temperature of reaction at an ethanol space velocity of 2 g_{EtOH}/g_{cat}·h and an EtOH : NH_3 : H_2 : N_2 molar ratio of 1 : 2 : 4.1 : 13.6. Data were recorded over a wide range of temperatures and consequently a wide range of ethanol conversions. Figure 3.5. plots the natural logarithm of the reaction rate versus the reciprocal of the reaction temperature for the SiO_2 supported cobalt, nickel and copper catalysts.

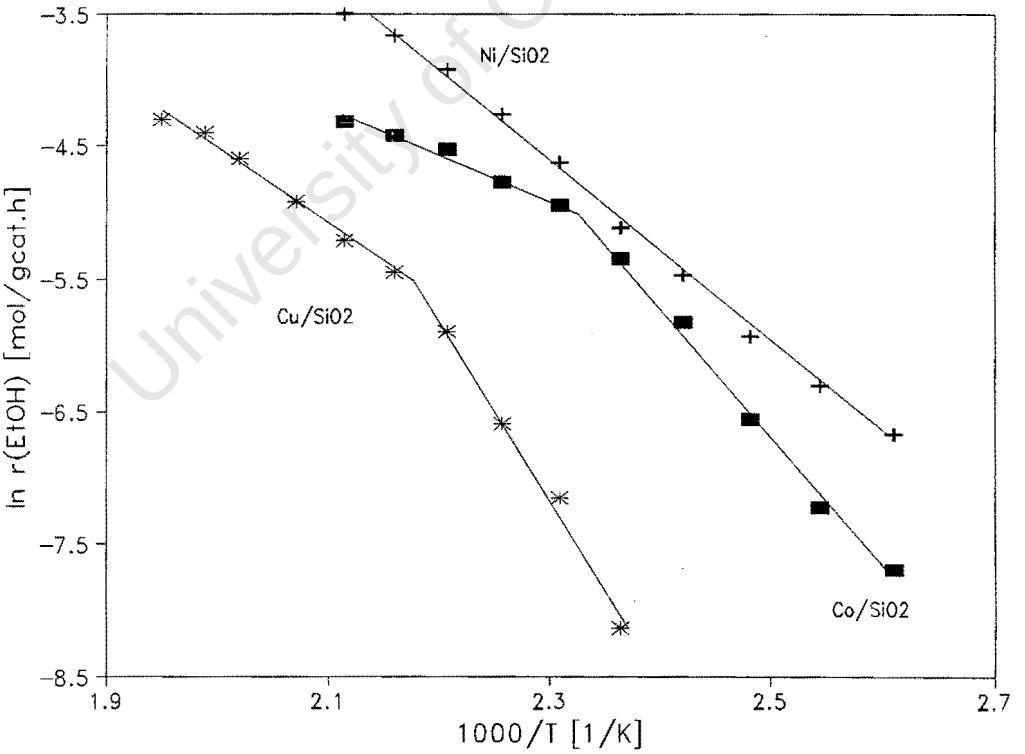

Figure 3.5. Arrhenius plots for Co/SiO_2, Ni/SiO_2 and Cu/SiO_2
(P = 1 bar, WHSV = 2 g_{EtOH}/g_{cat}·h, EtOH : NH_3 : H_2 : N_2 = 1 : 2 : 4.1 : 13.6)

The Arrhenius plots for the SiO_2 supported cobalt and copper catalysts indicate that the apparent activation energy for ethanol conversion decreases at temperatures greater than 160 and 190°C respectively. The apparent activation energy decreased from 77 to 28 kJ/mol for the Co/SiO_2 catalyst and from 88 to 44 kJ/mol for the Cu/SiO_2 catalyst. No decrease in the activation energy for ethanol conversion using the Ni/SiO_2 catalyst was observed within the temperature range investigated (100 - 200°C) and the apparent activation energy was 58 kJ/mol. The rate of ethanol conversion over the SiO_2 supported nickel catalyst is therefore not limited by either external or intrapellet diffusion.

In order to avoid diffusional restrictions it is therefore necessary to operate the SiO_2 supported cobalt and copper catalysts below temperatures of 160 and 190°C respectively. No diffusional restrictions were obtained using the Ni/SiO_2 catalyst within the temperature range investigated. Besides operating in a reaction rate controlled regime, it was also necessary that the reactor was operated in such a manner as to obtain differential conversions of the reactant ethanol. In order to ensure that the conversion of the reactant ethanol was lower than 15 % at all times, the kinetic measurements were conducted at a reaction temperature of 150°C for the Co/SiO_2 and Ni/SiO_2 catalysts and at a reaction temperature of 190°C for the Cu/SiO_2 catalyst.

3.1.4. Effect of the ethanol partial pressure

The influence of ethanol on the activity and selectivity during reductive amination was investigated between ethanol partial pressures of 1 and 7 kPa. The partial pressures of the NH_3 and H_2 feeds were kept constant at 8 and 20 kPa respectively by adjusting the flowrate of make-up N_2 such that the total flowrate was 200 ml(NTP)/min during all experiments.

Increasing the ethanol partial pressure resulted in an increase in the rate of ethanol consumption for all three catalysts investigated. The measured reaction order with respect to ethanol decreases from 0.92 to 0.64 to 0.52 as the catalyst was changed from Co/SiO_2 to Ni/SiO_2 to Cu/SiO_2. This increase in the overall rate of reductive amination with increasing ethanol partial pressure indicates that ethanol may be involved in the rate controlling step during reductive amination. Increasing the ethanol partial pressure also resulted in changes in the selectivity to individual ethylamine products during reductive amination. The influence of the ethanol partial pressure on the ethylamine selectivity of the Co/SiO_2, Ni/SiO_2 and Cu/SiO_2 catalysts is illustrated in Figures 3.6 to 3.8 respectively.

In the case of the Co/SiO_2 catalyst, the MEA selectivity first increased and then decreased, the DEA selectivity decreased and the TEA selectivity increased with increasing ethanol partial pressure (Figure 3.6.). These changes in selectivity indicate that ethanol influences the rate of formation of each individual ethylamine in a different manner. Besides changing the reactant partial pressure, changes in the degree of reactant conversion also occur upon changing the ethanol pressure. These changes in the reactant conversion may influence the ethylamine selectivity. The high DEA selectivity obtained using the Co/SiO_2 catalyst relative to the MEA selectivity indicates that the rate of formation of DEA is high, even at low ethanol conversions.

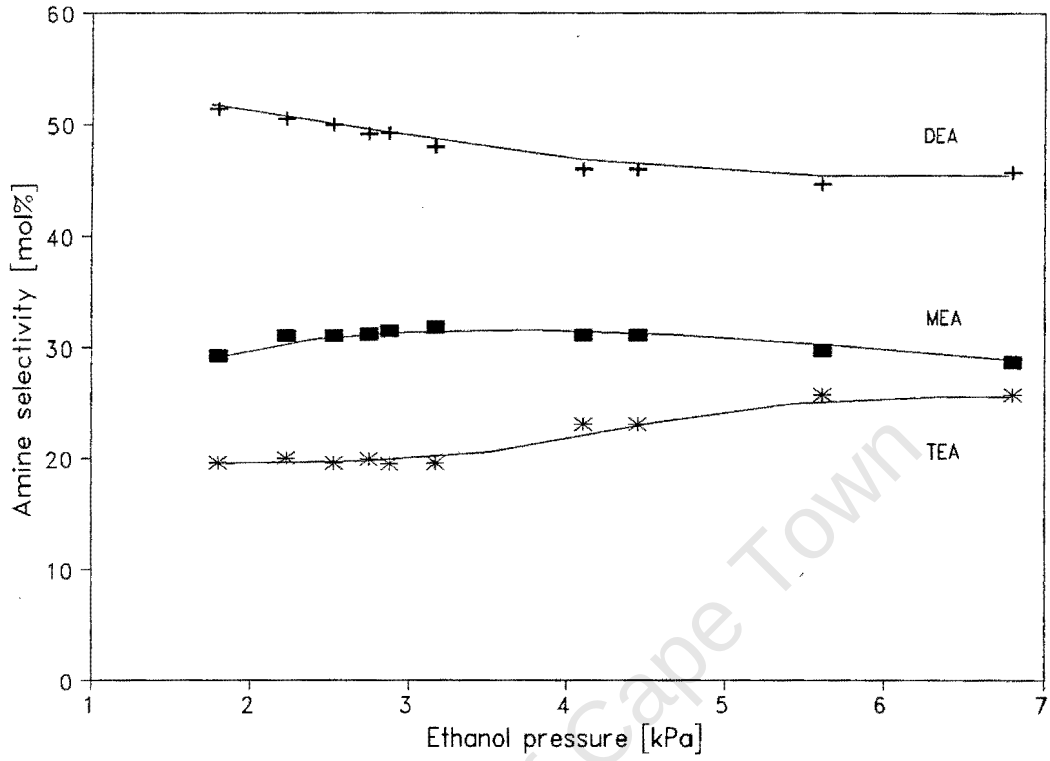

Figure 3.6. Influence of ethanol pressure on ethylamine selectivity of Co/SiO_2
(T = 150°C, P = 1 bar, p_{NH3} = 8 kPa, p_{H2} = 20 kPa, total flowrate = 200 ml(NTP)/min)

The MEA selectivity decreased and the DEA and TEA selectivities increased with increasing ethanol partial pressure over the Ni/SiO_2 catalyst (Figure 3.7.). Increasing the ethanol pressure therefore results in an increase in the degree of amine substitution during reductive amination using SiO_2 supported nickel. The increase in DEA and TEA selectivity may be caused by the increasing EtOH : NH_3 molar ratio [Baiker and Kijenski, 1985] or by the increased rate of ethanol conversion with increasing ethanol partial pressure [Sewell *et al*, 1995]. The selectivity to MEA was greater than the selectivity to DEA over the entire range of ethanol pressures investigated which indicated that the rate of conversion of MEA to DEA was lower when using the Ni/SiO_2 catalyst in comparison to the Co/SiO_2 catalyst.

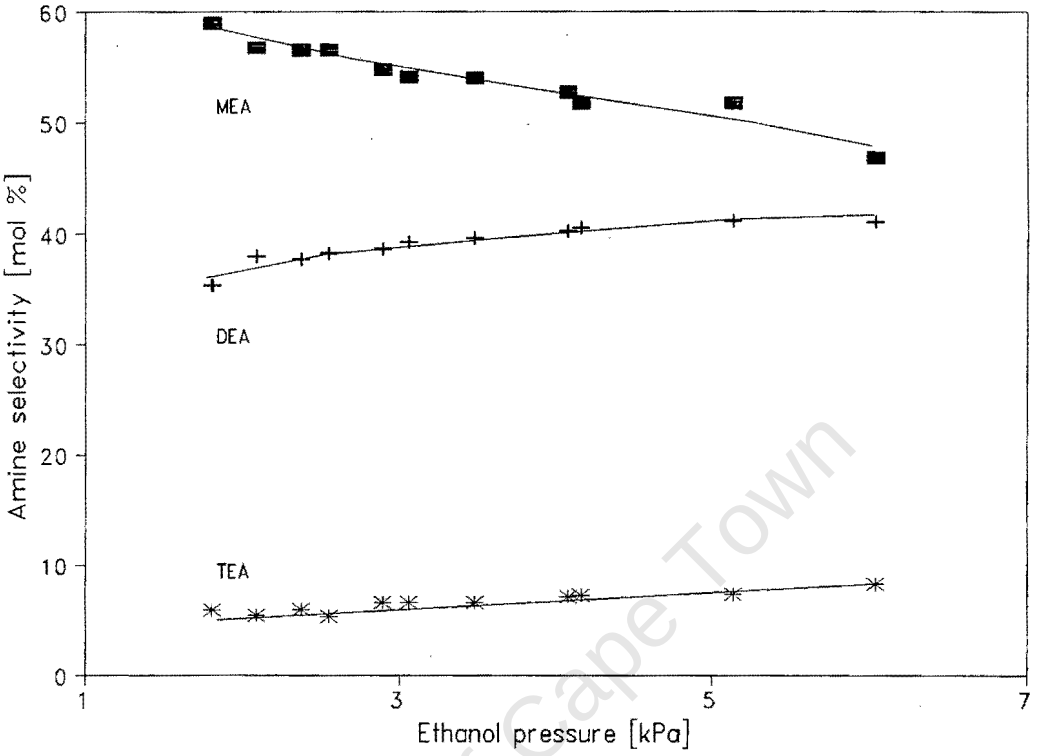

Figure 3.7. Effect of ethanol pressure on ethylamine selectivity of Ni/SiO_2
(T = 150°C, P = 1 bar, p_{NH3} = 8 kPa, p_{H2} = 20 kPa, total flowrate = 200 ml(NTP)/min)

The selectivity to individual ethylamine products differed considerably when using the Cu/SiO_2 catalyst (Figure 3.8.) when compared to the selectivities obtained with the SiO_2 supported cobalt and nickel catalysts. The selectivity to MEA first increased and then decreased, the DEA selectivity decreased and TEA selectivity remained approximately constant with increasing ethanol partial pressure. The DEA selectivity was very high and the MEA selectivity was very low which indicated that either the rate of conversion of MEA to DEA was very rapid or that the mechanism of amine formation occurred via a different pathway. Besides the formation of ethylamines, an unidentified byproduct was also formed when using the Cu/SiO_2 catalyst. The rate of formation of this byproduct species increased with increasing ethanol partial pressure which indicated that it was probably formed via a reaction involving the reactant alcohol.

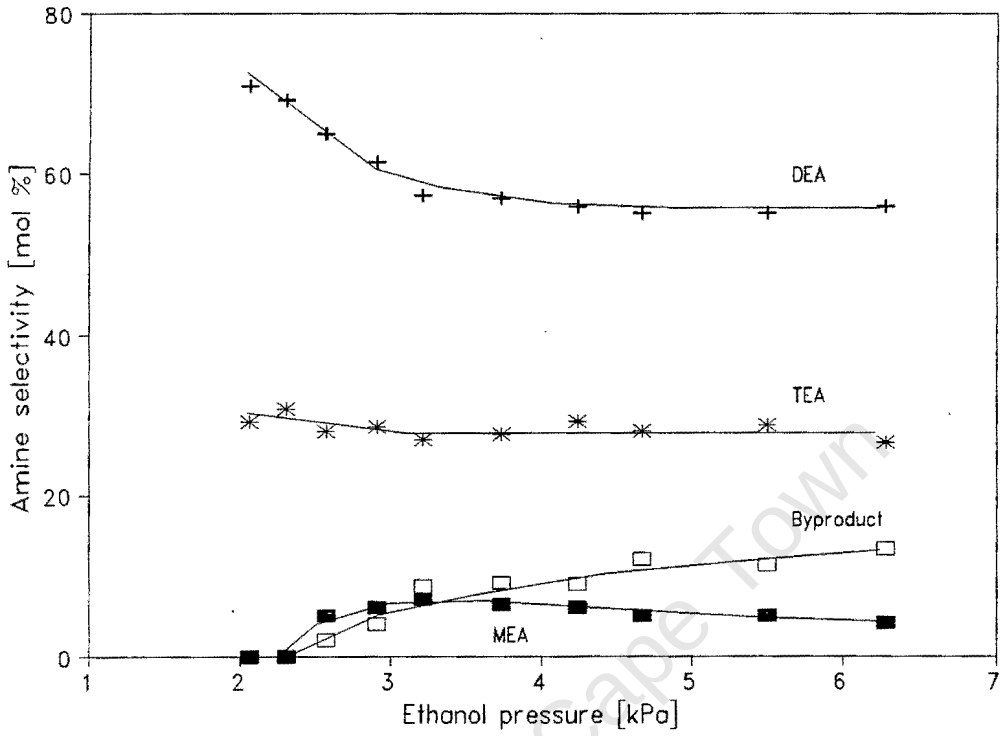

Figure 3.8. Influence of ethanol pressure on ethylamine selectivity of Cu/SiO_2
(T = 190°C, P = 1 bar, p_{NH3} = 8 kPa, p_{H2} = 20 kPa, total flowrate = 200 ml(NTP)/min)

3.1.5. Effect of the ammonia partial pressure

The influence of ammonia on the activity and selectivity of reductive amination was investigated by independently varying the ammonia pressure between 2 and 11 kPa. The partial pressures of ethanol and hydrogen were kept constant at 4 and 20 kPa respectively by adjusting the flowrate of nitrogen diluent such that the total flowrate was 200 ml(NTP)/min.

Increasing the ammonia partial pressure resulted in an increase in the rate of ethanol conversion during reductive amination for the SiO_2 supported cobalt catalyst. Using the power rate law expression, the measured reaction order with respect to ammonia was found to be 0.64. This indicates that ammonia may be involved in the step which determines the overall rate of ethanol conversion during amination over Co/SiO_2. Ammonia had little effect on the rate of ethanol conversion over the SiO_2 supported nickel and copper catalysts however and the measured reaction orders were 0.08 and -0.03 respectively.

Changing the partial pressure of ammonia in the reactor feed resulted in large changes in the ethylamine selectivity. The changes in selectivity obtained upon changing the ammonia partial pressure were greater than the changes in selectivity obtained upon changing the ethanol partial pressure. The EtOH : NH_3 molar ratio alone can therefore not be used to determine the selectivity to individual ethylamine products.

When using the Co/SiO_2 catalyst, MEA selectivity increased and TEA selectivity decreased as the ammonia pressure was increased (Figure 3.9.). The DEA selectivity first increased and then decreased with increasing ammonia pressure, with a maximum selectivity of just over 50 mol% obtained at an ammonia partial pressure of approximately 7 kPa.

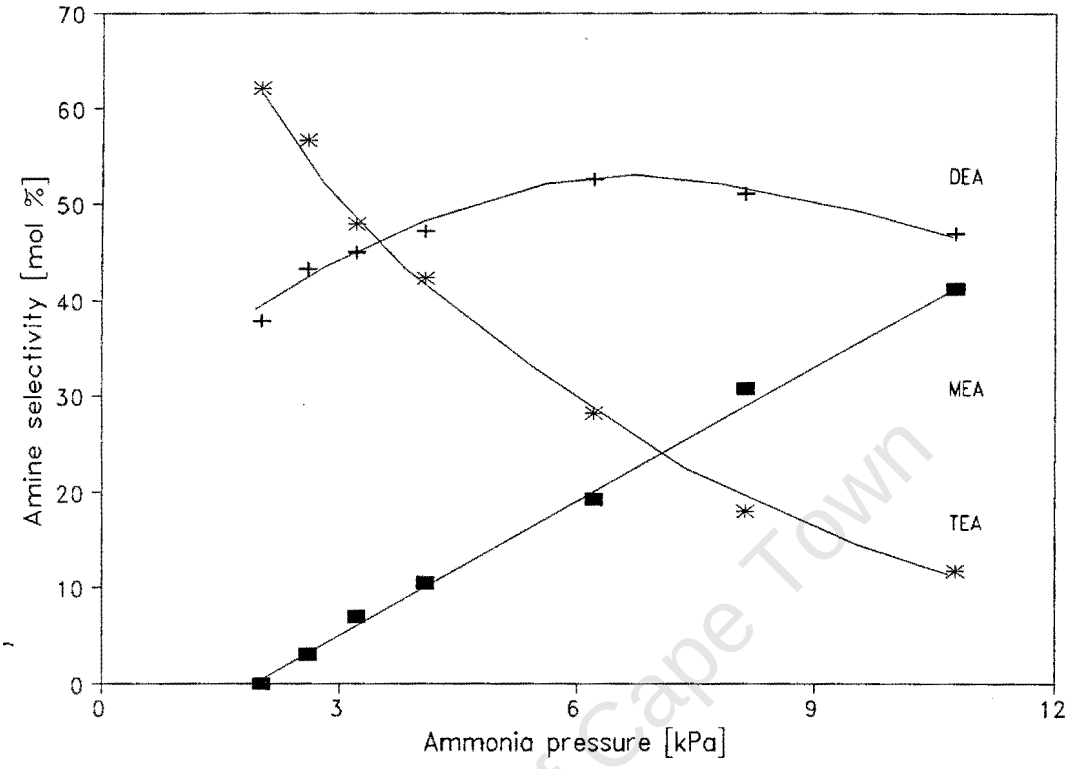

Figure 3.9. Effect of ammonia pressure on ethylamine selectivity of Co/SiO_2
(T = 150°C, P = 1 bar, p_{EtOH} = 4 kPa, p_{H2} = 20 kPa, total flowrate = 200 ml(NTP)/min)

The selectivity to MEA increased linearly with increasing ammonia partial pressure. Below ammonia pressures of 2 kPa however, no MEA was observed. This indicates that all MEA formed was converted by reaction with ethanol to form DEA. The decrease in DEA and TEA selectivities at higher ammonia pressures indicated that ammonia inhibited the formation of these species since the overall rate of ethanol conversion was seen to increase with increasing partial pressure of ammonia.

The changes in ethylamine selectivity with increasing ammonia partial pressure occurring over the Ni/SiO_2 catalyst were similar to those occurring with the Co/SiO_2 catalyst. The MEA selectivity increased, the selectivity to DEA first increased and then decreased and TEA selectivity decreased with increasing ammonia partial pressure. A maximum DEA selectivity of approximately 55% was obtained between ammonia partial pressures of 4 and 5 kPa. The increase in MEA selectivity and the decrease in TEA selectivity was more

pronounced over the Ni/SiO_2 catalyst in comparison to the Co/SiO_2 catalyst.

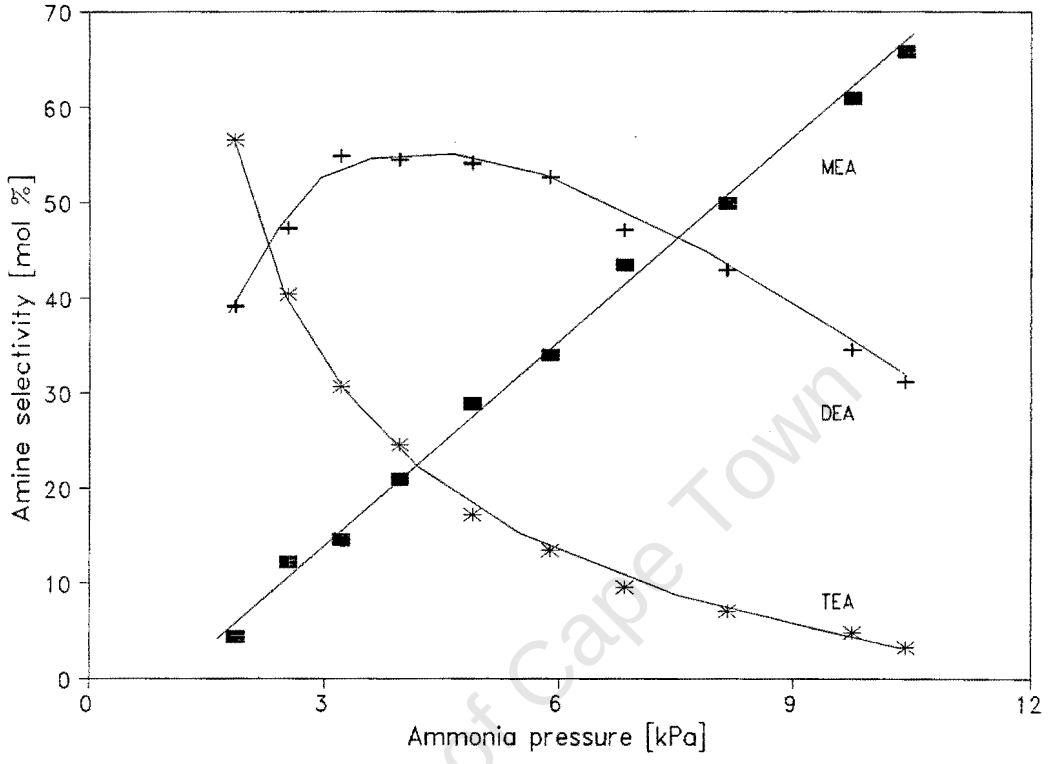

Figure 3.10. Effect of ammonia pressure on ethylamine selectivity of Ni/SiO_2
(T = 150°C, P = 1 bar, p_{EtOH} = 4 kPa, p_{H2} = 20 kPa, total flowrate = 200 ml(NTP)/min)

Increasing the ammonia pressure resulted in a decrease in MEA and TEA selectivities and an increase in the DEA selectivity of the Cu/SiO_2 catalyst (Figure 3.11.). The role of ammonia during amination using SiO_2 supported copper is therefore considerably different in comparison to the cobalt and nickel catalysts. Increasing the ammonia pressure also increased the rate of formation of the unidentified byproduct. This byproduct species may therefore also be formed via a reaction involving ammonia.

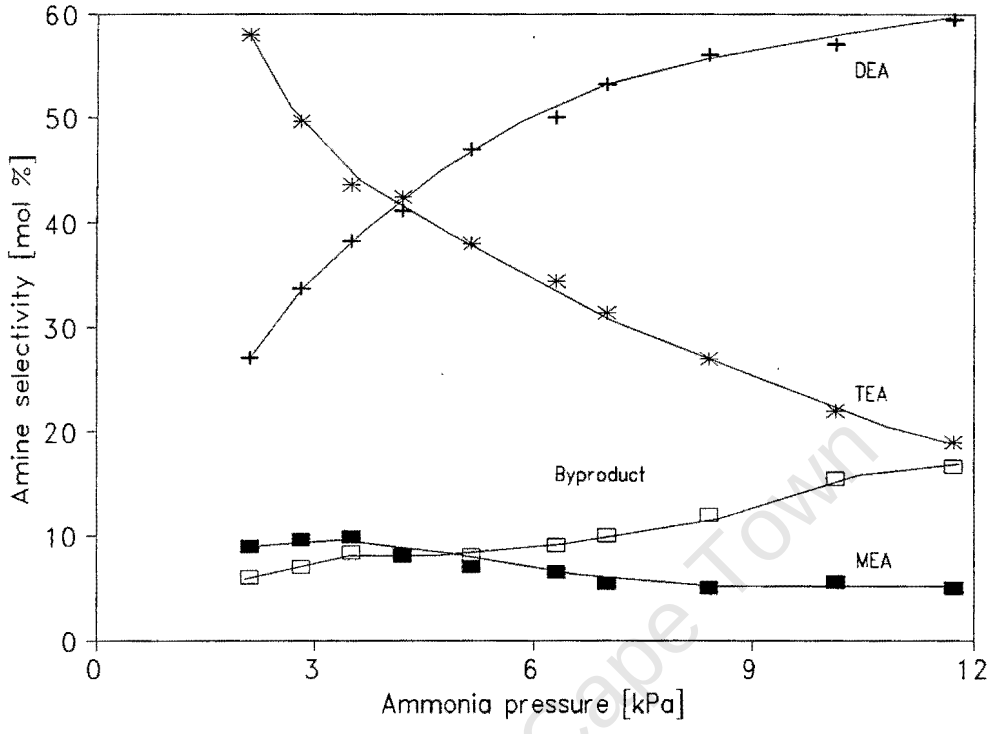

Figure 3.11. Effect of ammonia pressure on ethylamine selectivity of Cu/SiO_2
(T = 190°C, P = 1 bar, p_{EtOH} = 4 kPa, p_{H2} = 20 kPa, total flowrate = 200 ml(NTP)/min)

3.1.6. Effect of the hydrogen partial pressure

Hydrogen is neither consumed nor produced during the reductive amination reaction but it is cofed during reaction in order to prevent catalyst deactivation [Baiker *et al*, 1984]. Kinetic and mechanistic studies of the reductive amination reaction have shown however that dehydrogenation/hydrogenation steps occur during the transformation of the feed to the amine product. It can therefore be expected that the hydrogen pressure may influence both the activity and the selectivity during reductive amination. The influence of the hydrogen pressure on the reductive amination reaction was investigated by independently varying the hydrogen pressure from 8 to 20 kPa. The ethanol and ammonia partial pressures were kept constant at 2 and 8 kPa respectively by adjusting the flowrate of nitrogen diluent such that the total flowrate was 200 ml(NTP)/min.

The hydrogen pressure was shown to have markedly different influences of the activities of the three supported metal catalysts. The rate of ethanol conversion increased considerably with increasing hydrogen pressure when using the Co/SiO_2 catalyst and the measured reaction order with respect to hydrogen was 1.91. The strong dependence of the catalytic activity of Co/SiO_2 on the hydrogen pressure may indicate that hydrogen prevents catalyst deactivation caused by metal nitride formation [Baiker and Kijenski, 1985].

Hydrogen does not influence the rate of ethanol conversion of the SiO_2 supported nickel and copper catalysts significantly and the measured reaction orders with respect to the hydrogen pressure are -0.07 and 0.07 respectively. Catalyst deactivation via metal nitride formation was therefore not significant with these catalysts under the experimental operating conditions selected. Competitive adsorption of hydrogen with ethanol can also be discounted since the reaction orders were approximately zero.

Increasing the hydrogen pressure when using the Co/SiO_2 catalyst resulted in a decrease in the MEA selectivity and an increase in the selectivity to DEA and TEA (Figure 3.12.). The changes in selectivity were very large and at a hydrogen pressure of 7 kPa, only MEA was observed as a product. The changes in ethylamine selectivity were considerably greater than

the changes in selectivity obtained by simply changing the ethanol conversion. This indicates either that hydrogen is required for the series conversion of MEA to DEA and TEA or that hydrogen influences the adsorption of certain reactants or intermediates during the reductive amination reaction.

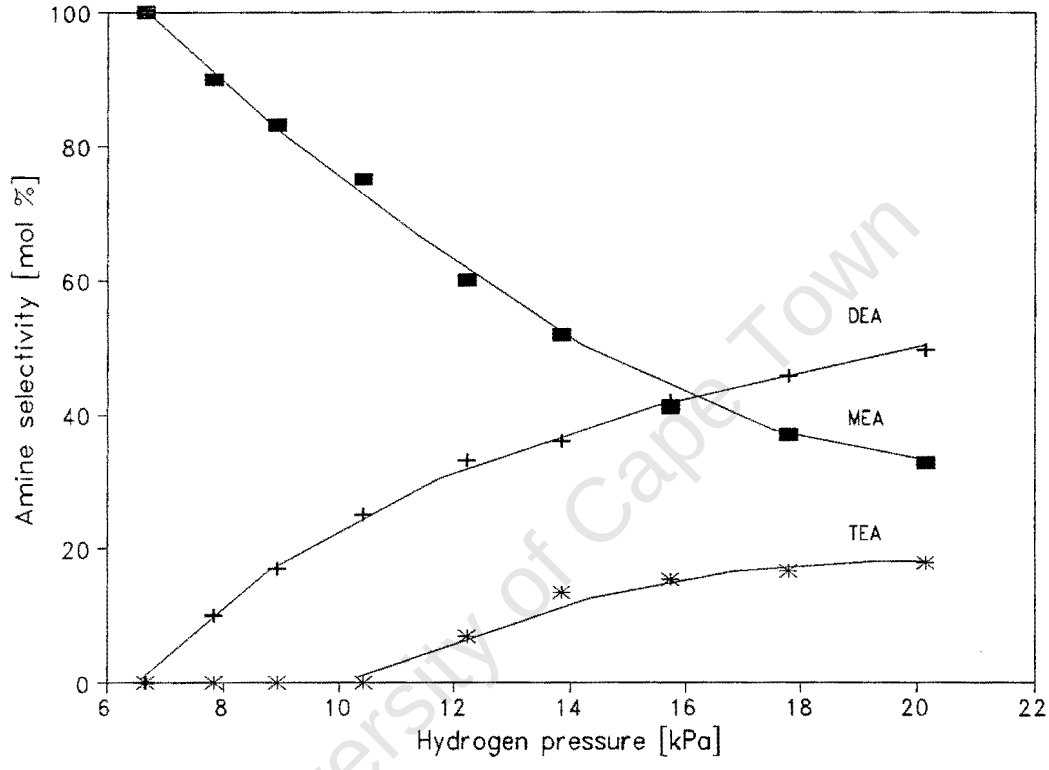

Figure 3.12. Effect of hydrogen pressure on ethylamine selectivity of Co/SiO_2
(T = 150°C, P = 1 bar, p_{EtOH} = 2 kPa, p_{NH3} = 8 kPa, total flowrate = 200 ml(NTP)/min)

Increasing the hydrogen pressure resulted in a decrease in MEA selectivity and an increase in DEA and TEA selectivities when using the Ni/SiO_2 catalyst. Although the trends measured were similar to those obtained using the Co/SiO_2 catalyst, the variations in amine selectivity were considerably smaller. The smaller changes in amine selectivity may be due to the decreased influence of the hydrogen pressure on the ethanol conversion when using the Ni/SiO_2 catalyst in comparison to the Co/SiO_2 catalyst.

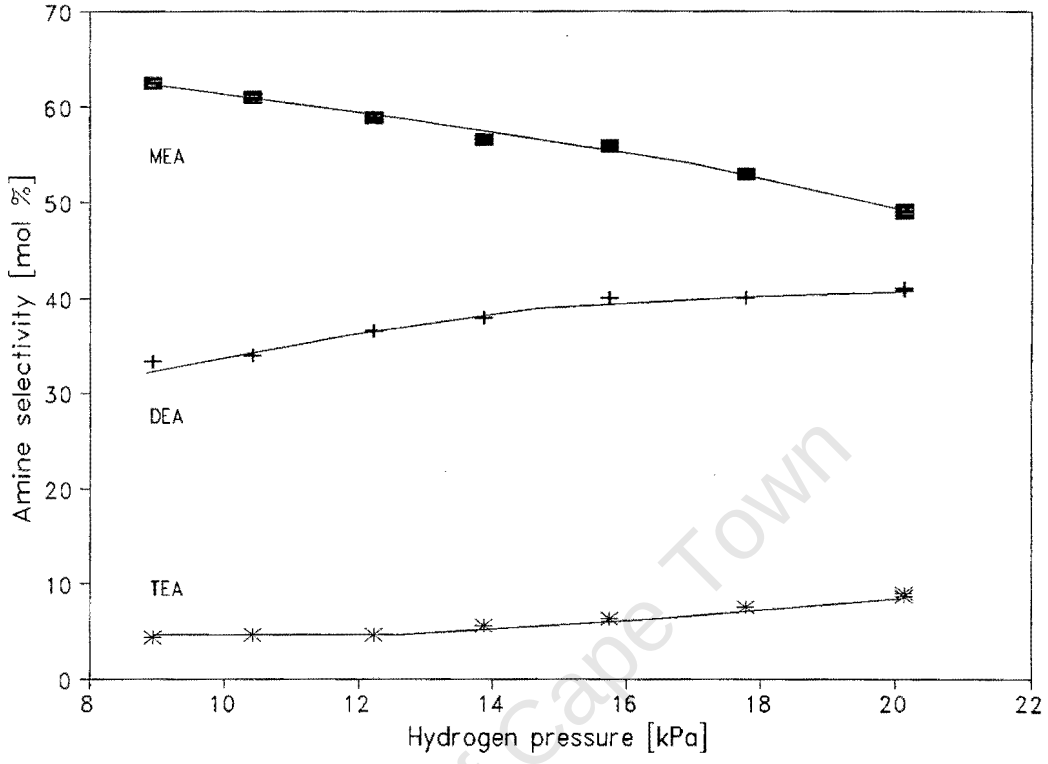

Figure 3.13. Effect of hydrogen pressure on ethylamine selectivity of Ni/SiO_2
(T = 150°C, P = 1 bar, p_{EtOH} = 2 kPa, p_{NH3} = 8 kPa, total flowrate = 200 ml(NTP)/min)

Increasing the hydrogen partial pressure during amination resulted in an increase in the selectivity to DEA and TEA of the SiO_2 supported copper catalyst (Figure 3.14.). The increased selectivity was primarily due to a decrease in byproduct selectivity with increasing hydrogen pressure. The decrease in byproduct selectivity indicates that either hydrogen inhibits side reactions during amination or that the byproduct is a dehydrogenated intermediate which is more readily hydrogenated to form the corresponding ethylamine at higher hydrogen pressures. No MEA was observed over the entire region of investigation which indicates that hydrogen does not influence the rate of formation of MEA under these specific operating conditions.

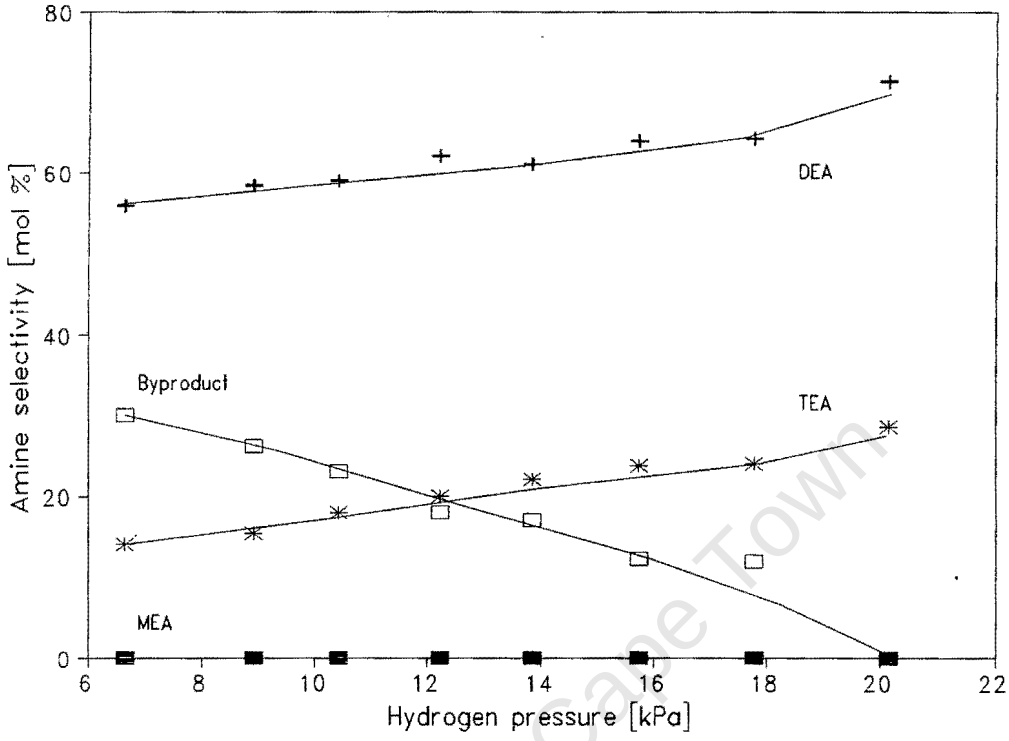

Figure 3.14. Effect of hydrogen pressure on ethylamine selectivity of Cu/SiO_2
(T = 190°C, P = 1 bar, p_{EtOH} = 2 kPa, p_{NH3} = 8 kPa, total flowrate = 200 ml(NTP)/min)

3.1.7. Influence of the space velocity

The influence of the space velocity on the activity and selectivity during reductive amination was evaluated by varying the total feedrate at a reaction temperature of 150°C for the SiO_2 supported cobalt and nickel catalysts and at 190°C for the Cu/SiO_2 catalyst. The space velocity was varied between 0.75 and 3.75 g_{EtOH}/g_{cat}·h at an EtOH : NH_3 : H_2 : N_2 molar feed ratio of 1 : 2 : 8.6 : 17.6. The influence of the space velocity on the ethanol conversion of the Co/SiO_2, Ni/SiO_2 and Cu/SiO_2 catalysts is illustrated in Figure 3.15.

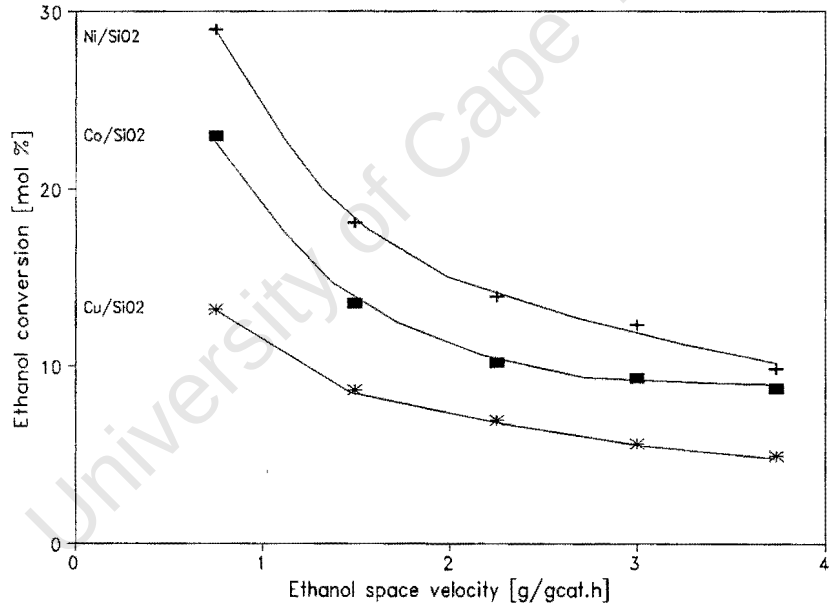

Figure 3.15. Effect of space velocity on activity of Co/SiO_2, Ni/SiO_2 and Cu/SiO_2
(P = 1 bar, EtOH : NH_3 : H_2 : N_2 = 1 : 2 : 8.6 : 17.6)

Increasing the reactant space velocity resulted in a decrease in the ethanol conversion for all three supported metal catalysts used in this study. The ethanol conversion activity decreased

as the catalyst was changed from Ni/SiO_2 to Co/SiO_2 to Cu/SiO_2 and this order did not change with changing space time. The space velocity measurements were recorded at 190°C for the SiO_2 supported copper catalyst in comparison to a temperature of 150°C for the SiO_2 supported cobalt and nickel catalysts. The low activity of Cu/SiO_2 for the reductive amination of ethanol is therefore emphasized since even though the temperature of reaction was 40°C higher, the ethanol conversion remained lower than that of the SiO_2 supported cobalt and nickel catalysts.

Increasing the space velocity resulted in an increase in the MEA selectivity and a decrease in the TEA selectivity when using the Co/SiO_2 catalyst (Figure 3.16.). The DEA selectivity did not change significantly with changing space velocity even though the reactant conversion changed considerably. The selectivity to DEA therefore appears to be insensitive to changes in the conversion of the reactant ethanol or to the residence time in the catalyst bed when using SiO_2 supported cobalt catalysts.

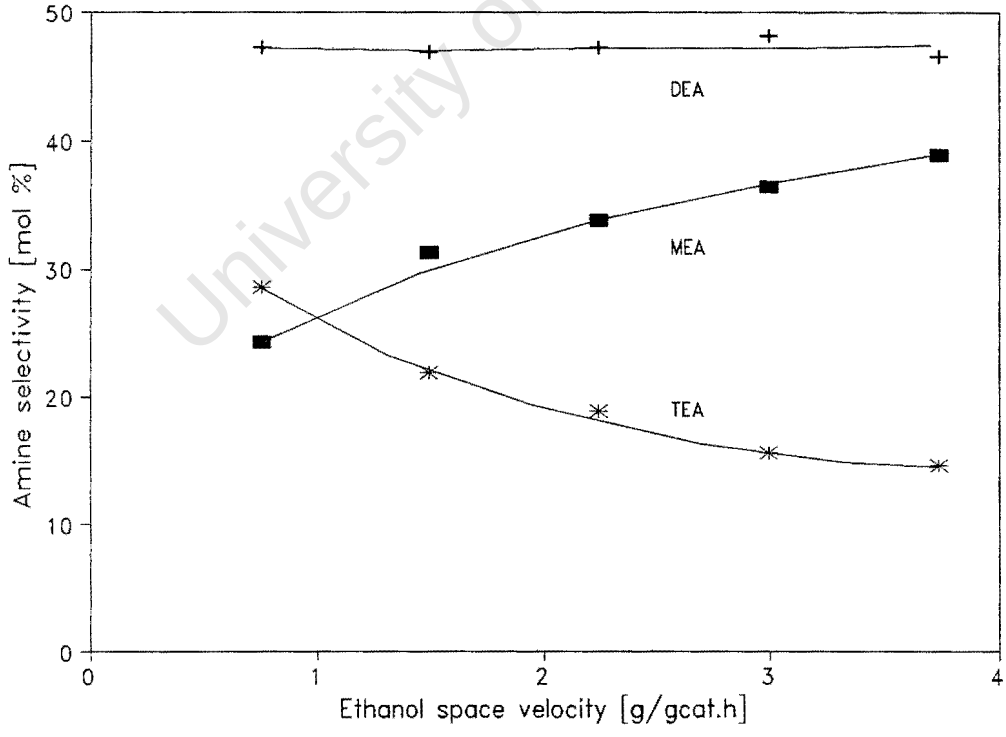

Figure 3.16. Effect of space velocity on ethylamine selectivity of Co/SiO_2
(T = 150°C, P = 1 bar, EtOH : NH_3 : H_2 : N_2 = 1 : 2 : 8.6 : 17.6)

The selectivity to individual ethylamine products was more sensitive to changes in the space velocity when using the Ni/SiO_2 catalyst in comparison to the Co/SiO_2 catalyst. When the space velocity was increased, the MEA selectivity was increased and the selectivity to DEA and TEA decreased (Figure 3.17.). This change in ethylamine selectivity may be caused either by the decreased residence times in the catalyst bed or by the decreased ethanol conversions obtained upon increasing the space velocity.

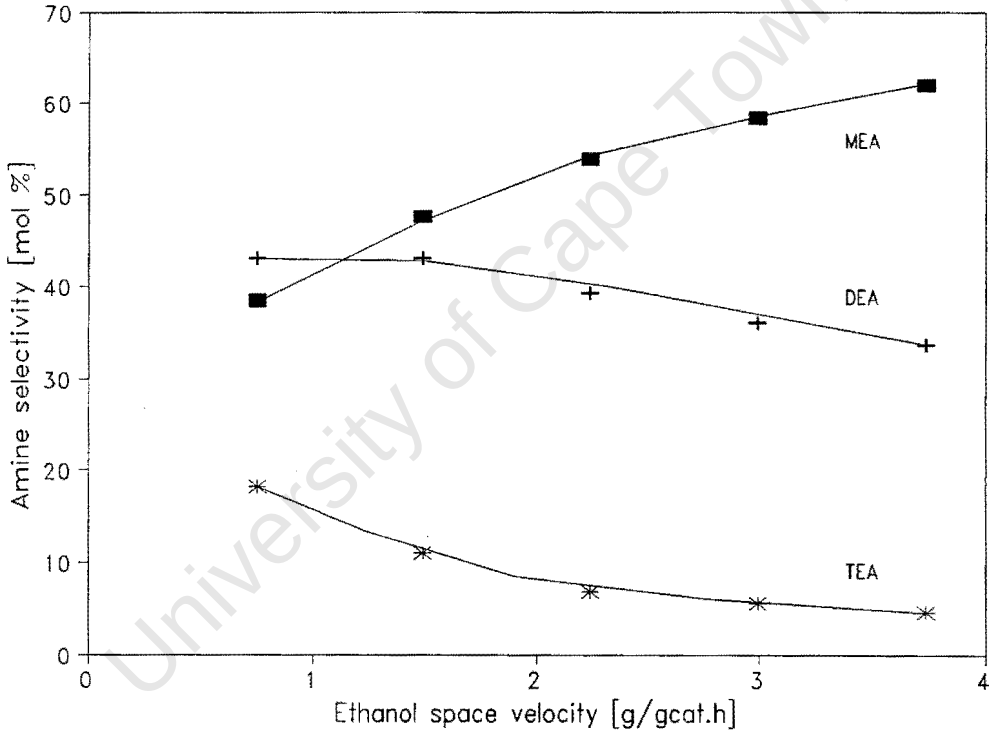

Figure 3.17. Effect of space velocity on ethylamine selectivity of Ni/SiO_2
(T = 150°C, P = 1 bar, EtOH : NH_3 : H_2 : N_2 = 1 : 2 : 8.6 : 17.6)

The space time dependence of the Cu/SiO_2 catalyst was characterized by a slight increase in MEA selectivity and a decrease in the TEA selectivity with increasing space velocity. As in the instance of the Co/SiO_2 catalyst, the DEA selectivity did not vary significantly with changes in the reactant residence time. Byproduct selectivity increased slightly with

decreasing residence time in the catalyst bed which may indicate that this species is an intermediate formed during reductive amination over SiO_2 supported copper catalysts.

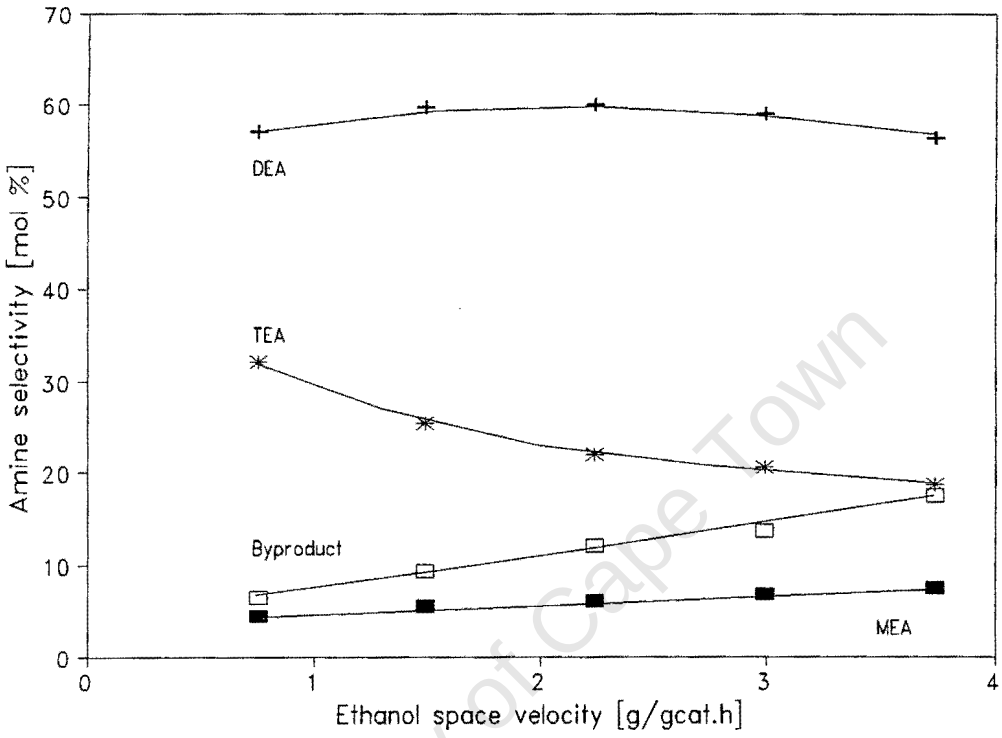

Figure 3.18. Effect of space velocity on ethylamine selectivity of Cu/SiO_2
(T = 190°C, P = 1 bar, EtOH : NH_3 : H_2 : N_2 = 1 : 2 : 8.6 : 17.6)

3.1.8. Influence of reaction temperature

The effect of the reaction temperature on the activity and selectivity of amination was investigated by varying the temperature in 5°C increments over a range of 20°C. Kinetic measurements were taken between 130 and 150°C for the Co/SiO_2 and Ni/SiO_2 catalysts and between 170 and 190°C for the Cu/SiO_2 catalyst. These temperatures were selected so that mass transfer limitations would not interfere with the measurements. The EtOH : NH_3 : H_2 : N_2 molar feed ratio was 1 : 2 : 8.6 : 17.6 and the weight hourly space velocity was 0.8 g_{EtOH}/g_{cat}·h.

As expected, the ethanol conversion activity of the supported metal catalysts increased with increasing reaction temperature (Figures 3.19 to 3.21). The increases in ethanol conversion with increasing temperature were relatively linear and only the absolute activity of the supported metal catalysts was seen to differ.

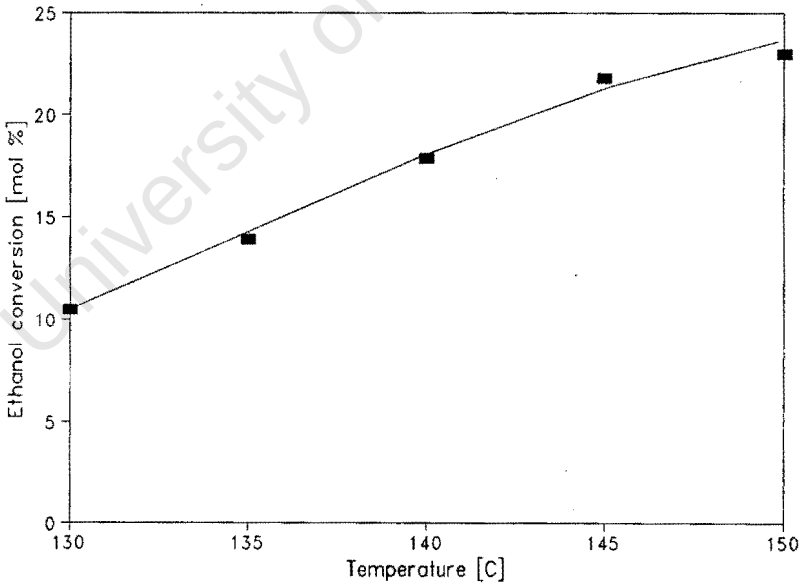

Figure 3.19. Effect of reaction temperature on the activity of Co/SiO_2
(P = 1 bar, WHSV = 0.8 g_{EtOH}/g_{cat}·h, EtOH : NH_3 : H_2 : N_2 = 1 : 2 : 8.6 : 17.6)

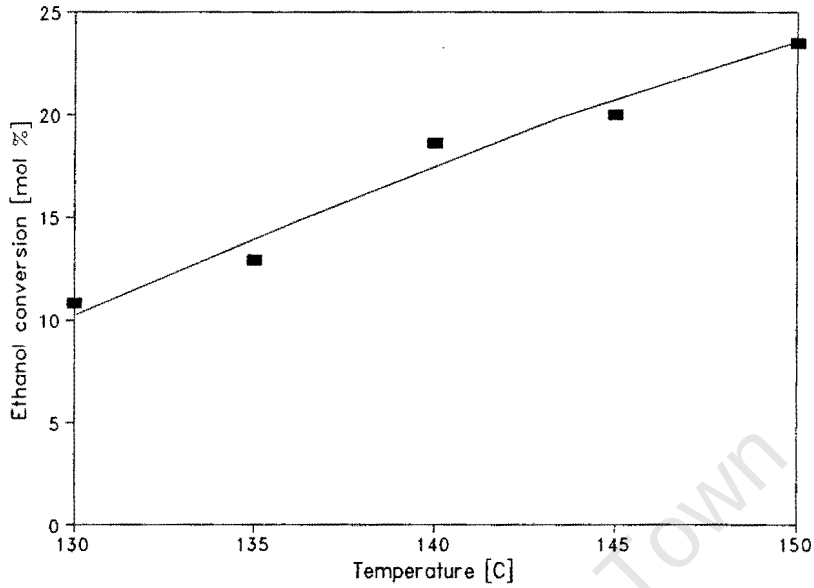

Figure 3.20. Effect of reaction temperature on the activity of Ni/SiO_2
(P = 1 bar, WHSV = 0.8 g_{EtOH}/g_{cat}·h, EtOH : NH_3 : H_2 : N_2 = 1 : 2 : 8.6 : 17.6)

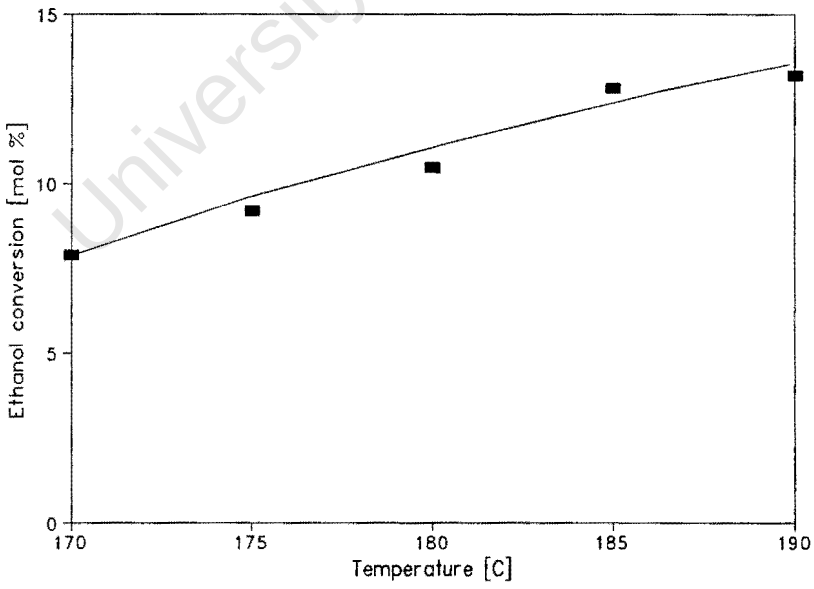

Figure 3.21. Effect of reaction temperature on the activity of Cu/SiO_2
(P = 1 bar, WHSV = 0.8 g_{EtOH}/g_{cat}·h, EtOH : NH_3 : H_2 : N_2 = 1 : 2 : 8.6 : 17.6)

The MEA selectivity decreased and the TEA selectivity increased with increasing reaction temperature using Co/SiO_2 (Figure 3.22.). The DEA selectivity only increases very slightly with increasing reaction temperature and it can be concluded that the extent of ethanol conversion does not alter the selectivity to DEA significantly when using SiO_2 supported cobalt catalysts. This may occur due to product inhibition or by the further conversion of DEA to other products at increased reaction temperatures.

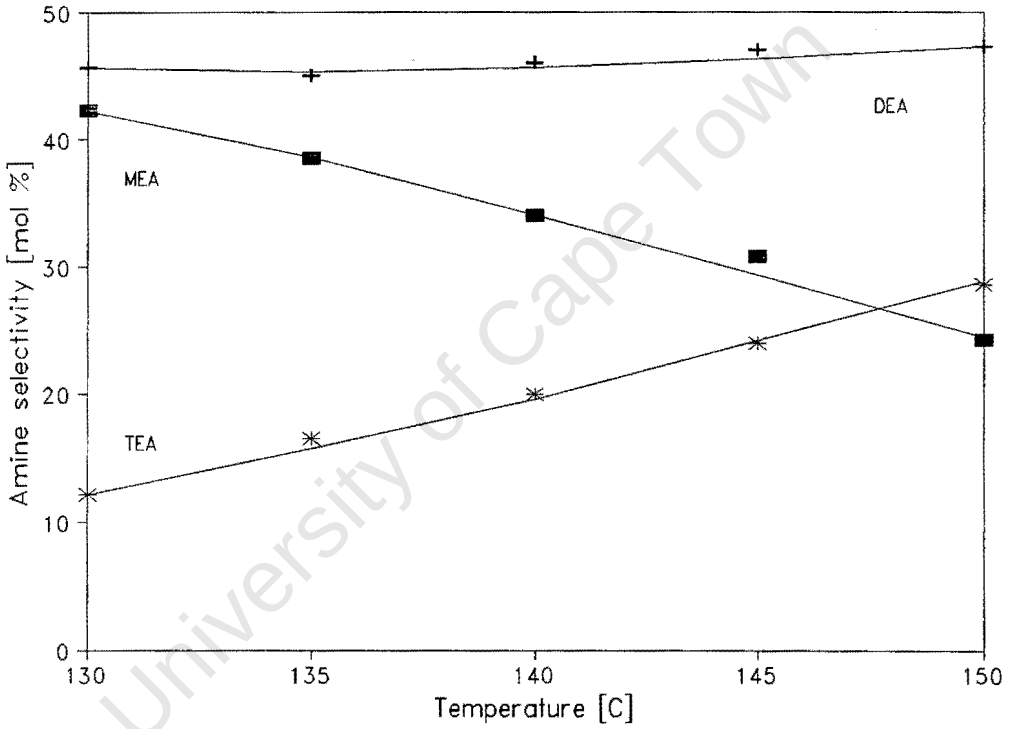

Figure 3.22. Effect of reaction temperature on ethylamine selectivity of Co/SiO_2
(P = 1 bar, WHSV = 0.8 g_{EtOH}/g_{cat}·h, EtOH : NH_3 : H_2 : N_2 = 1 : 2 : 8.6 : 17.6)

The MEA selectivity decreased and the DEA and TEA selectivities increased with increasing reaction temperature over the Ni/SiO_2 catalyst (Figure 3.23.). The change in selectivity with increasing reaction temperature therefore appears to indicate that MEA is converted by further reaction with ethanol to DEA and TEA at increased temperatures. As observed previously, the MEA selectivity was higher and DEA and TEA selectivities were lower when

using the Ni/SiO_2 catalyst in comparison to the Co/SiO_2 catalyst.

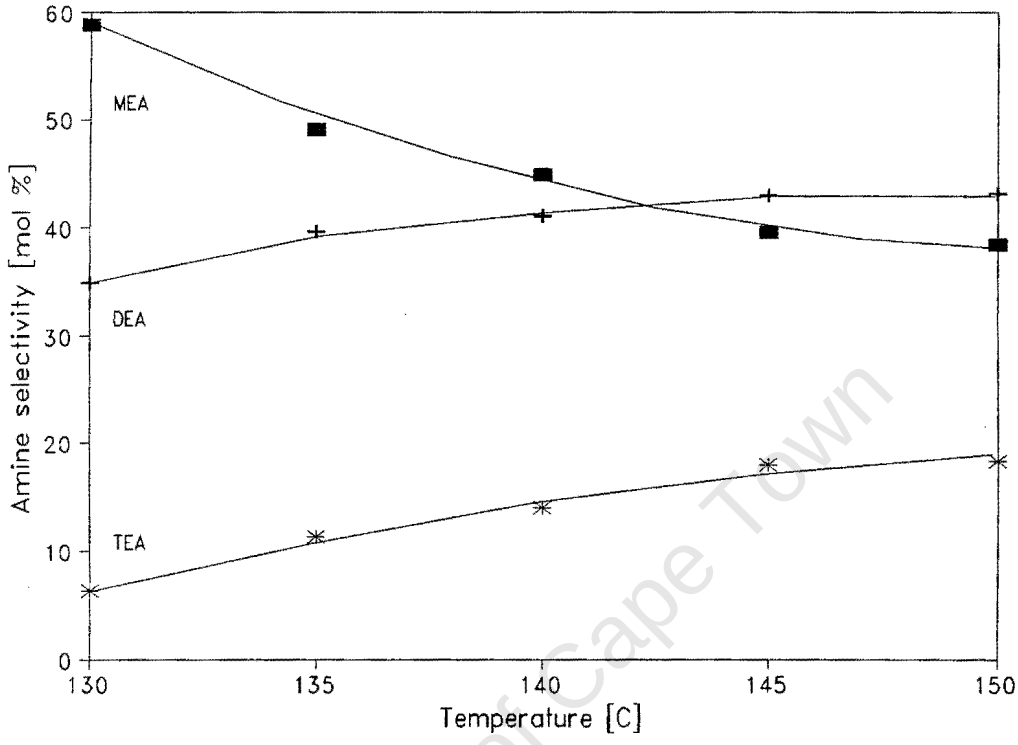

Figure 3.23. Effect of reaction temperature on ethylamine selectivity of Ni/SiO_2
(P = 1 bar, WHSV = 0.8 g_{EtOH}/g_{cat}·h, EtOH : NH_3 : H_2 : N_2 = 1 : 2 : 8.6 : 17.6)

Increasing the temperature of reductive amination using the SiO_2 supported copper catalyst resulted in a decrease in the selectivity to MEA and DEA and an increase in the selectivity to TEA (Figure 3.24.). The selectivity towards the unidentified byproduct formed by the Cu/SiO_2 catalyst increased with increasing reaction temperature. The DEA selectivity exceeded the equilibrium value of 50% (see Chapter 1.3.1.4.) thereby indicating that the rate of DEA formation was very high compared to MEA and TEA under these reaction conditions.

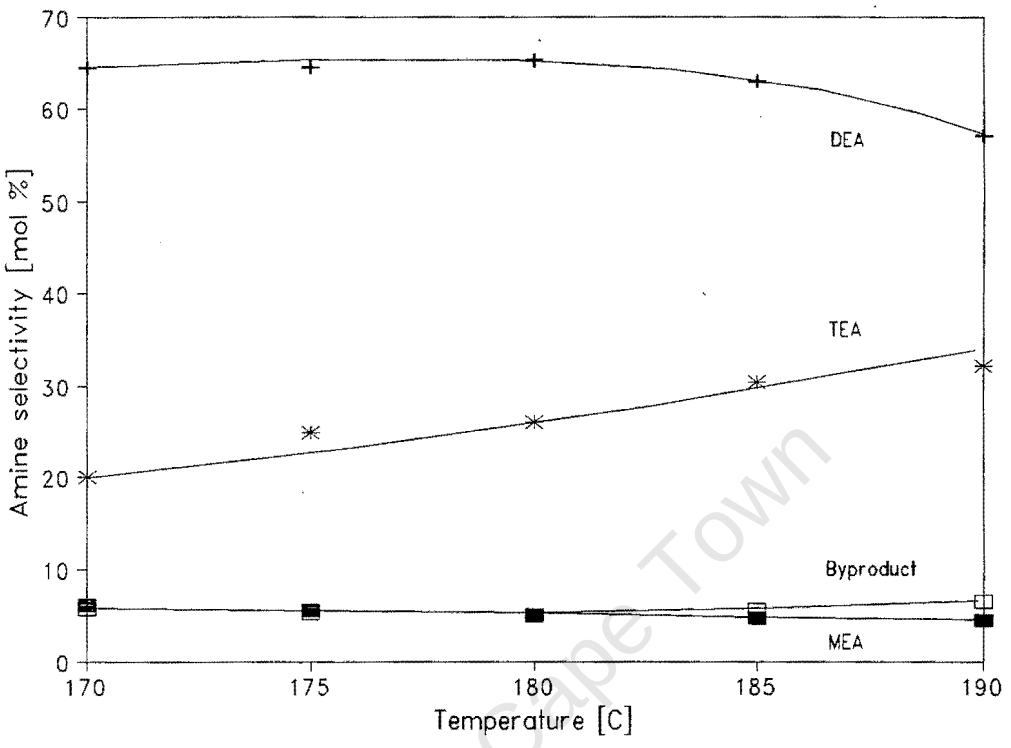

Figure 3.24. Effect of reaction temperature on ethylamine selectivity of Cu/SiO_2 (P = 1 bar, WHSV = 0.8 g_{EtOH}/g_{cat}·h, EtOH : NH_3 : H_2 : N_2 = 1 : 2 : 8.6 : 17.6)

3.2. Reductive Amination using Supported Cobalt Catalysts

The steady state ethanol conversions of the SiO_2 supported nickel, cobalt and copper catalysts were 41, 22 and 5 mol% respectively when measured at a reaction temperature of 180°C, a total pressure of 1 bar, a space velocity of 2 g_{EtOH}/g_{cat}·h and an EtOH : NH_3 : H_2 : N_2 molar feed ratio of 1 : 2 : 4.1 : 13.9 (Chapter 3.1.2.).

The decrease in ethanol conversion activity from nickel to cobalt to copper is largely caused by the decrease in the number of exposed metal atoms. The decrease in metallic surface area is caused by decreased extents of metal reduction and decreased dispersions of the metallic phase. The extent of reduction and the dispersion of metallic atoms can be optimized by adjusting the catalyst preparation and activation parameters however. In order to determine the specific activities of the three metal catalysts, the steady state ethanol conversion was measured at identical reaction conditions and compared to the number of exposed metal atoms as measured using hydrogen chemisorption. These measurements showed that the turnover frequency decreased from 0.11 to 0.09 to 0.05 molecules of ethanol converted per site per second as the metal was changed from cobalt to nickel to copper. Cobalt was therefore selected as the most promising amination catalyst as it had the highest specific activity of the metals tested.

The influence of the catalyst preparation and activation procedure on the reducibility and dispersion of supported cobalt catalysts was investigated using TPR, TPO and hydrogen chemisorption. These changes were correlated to the activity and selectivity of the metal for the reductive amination of ethanol using ammonia.

3.2.1. Catalyst Deactivation Behaviour

Catalyst deactivation during reductive amination has been shown to be caused by metal nitride formation, metal carbide formation, the deposition of carbonaceous material and the thermal diffusive fusion of the supported metal crystallites [Baiker and Maciejewski, 1984; Baiker *et al*, 1984; Baiker, 1981; Baiker and Richarz, 1978]. Deposition of carbonaceous

material and metal crystallite agglomeration will be expected to decrease the overall activity of the supported metal catalyst due to a decrease in the exposed metal surface area. Incorporation of nitrogen or carbon into the metal crystallites will be expected to alter the selectivity of the amination reaction due to changes in the electronic nature of the supported metal catalyst.

In the experiments conducted in this study, both the ethanol conversion and the selectivity to individual ethylamine products was seen to change during the first 24 hours of operation. The catalytic performance was relatively stable after this initial period however. Since steady state operation was obtained relatively quickly, a comprehensive study of the deactivation occurring during amination was not performed. Instead, experiments were designed to investigate which of the deactivation procedures as outlined in the literature was responsible for the changes in activity and selectivity with time on stream.

3.2.1.1. Time on stream behaviour

The influence of the time on stream on the catalytic activity and selectivity of the Co/SiO_2, Co/Al_2O_3 and $Co/13SiO_2$-Al_2O_3 catalysts was evaluated at a reaction temperature of 180°C, a space velocity of 1 g_{EtOH}/g_{cat}·h and an EtOH : NH_3 : H_2 : N_2 molar ratio of 1 : 2 : 8.6 : 17.6. Prior to reaction, the catalyst precursors were reduced in a 60 ml(NTP)/min H_2 stream at 500°C for 1 hour using a temperature programming rate of 10°C/min. The ethanol conversion activity of the three supported cobalt catalysts as a function of time is reported in Figure 3.25.

The ethanol conversion of all three supported cobalt catalysts decreased during the first 24 hours of operation. After an initial period of deactivation, catalyst activity remained approximately constant. The Co/SiO_2 catalyst underwent the largest decrease in ethanol conversion (18 mol%) whereas the Co/Al_2O_3 and $Co/13SiO_2$-Al_2O_3 catalysts showed similar decreases in ethanol conversion (13 mol%). Measuring the decrease in activity as a percentage of the initial activity (extrapolated to t = 0) showed a similar relative decrease in ethanol conversion for the Co/SiO_2 and Co/Al_2O_3 catalysts (22 and 21 % respectively)

however the decrease in activity was 27% for the SiO_2-Al_2O_3 supported cobalt catalyst. The type of support therefore influences the time on stream activity of the cobalt catalyst during reductive amination.

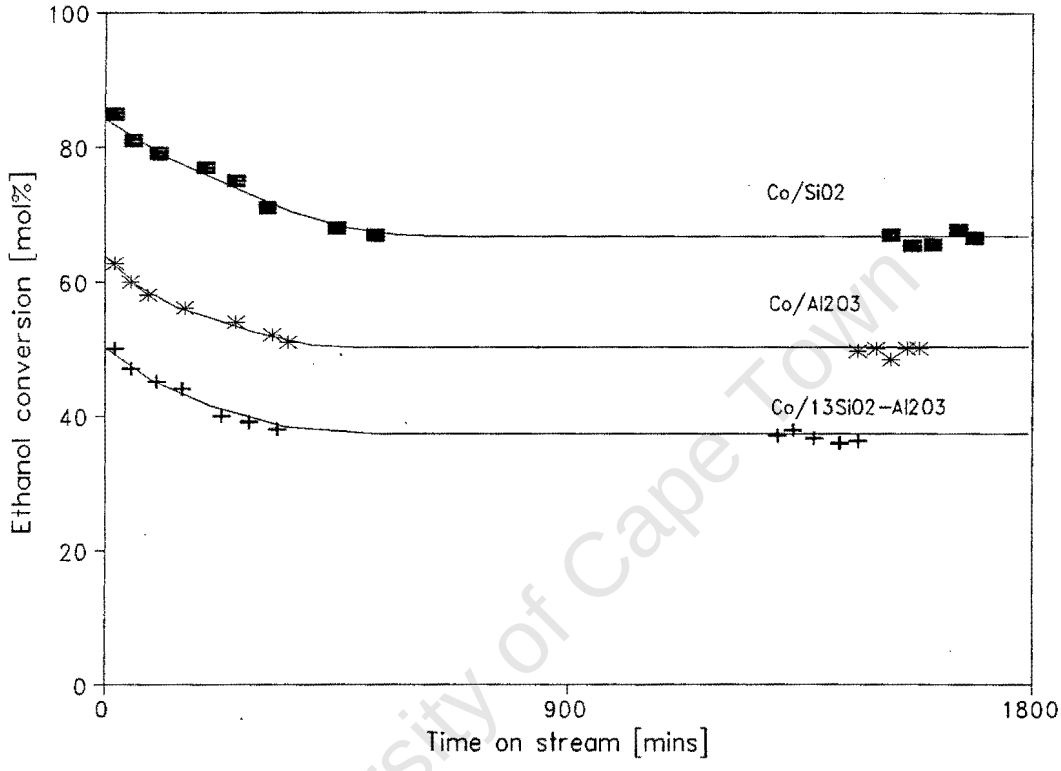

Figure 3.25. Time on stream activity of Co/SiO_2, Co/Al_2O_3, $Co/13SiO_2$-Al_2O_3
(T = 180°C, P = 1 bar, WHSV = 1 g_{EtOH}/g_{cat}·h, EtOH : NH_3 : H_2 : N_2 = 1 : 2 : 8.6 : 17.6)

The selectivity to MEA increases and the selectivity to DEA and TEA decreases with time on stream for all three catalysts tested. The change in amine selectivity occurs simultaneously with the decrease in ethanol conversion. The specific selectivity to individual ethylamine products was dependent on the type of cobalt carrier with the steady state MEA selectivity increasing and the steady state DEA and TEA selectivities decreasing as the support was changed from SiO_2 to Al_2O_3 to SiO_2-Al_2O_3.

3.2.1.2. Thermogravimetric analysis of used catalysts

Thermogravimetric analysis of the Co/SiO_2, Co/Al_2O_3 and $Co/13SiO_2$-Al_2O_3 catalysts used during the time on stream experiments was used to characterize the nature of the deposits on the catalyst surface. The catalyst samples were removed from the reactor after 24 hours of operation (*i.e.* once steady state conditions had been achieved) and therefore the weight loss during thermal analysis can be correlated to the amount of material deposited on the catalyst surface during this period. In the experiment, the mass and temperature changes of a 25 mg sample were monitored as the temperature was increased linearly from 50 to 700°C at 10°C/min in a 30 ml(NTP)/min air stream.

The TG-DTA spectrum of the spent Co/SiO_2 catalyst showed a mass loss of 4.0 wt% after oxidation in air up to 700°C (Figure 3.26). The spectrum was characterized by an endotherm at 100°C and two large exotherms occurring at 260 and 470°C respectively. The endothermic mass loss occurring at 100°C is probably due to the desorption of adsorbed water or other adsorbed compounds remaining on the catalyst surface after the amination reaction. An increase in the weight of the sample was observed between temperatures of 180 and 320°C which did not correspond to the observed exotherm. This weight increase is probably caused by the oxidation of reduced cobalt to the bulk cobalt oxide Co_3O_4 and the rate of weight increase exceeded the rate of weight loss caused by the exothermic combustion of carbonaceous material. The exothermal decrease in weight occurring at higher temperatures indicates the combustion of carbonaceous material.

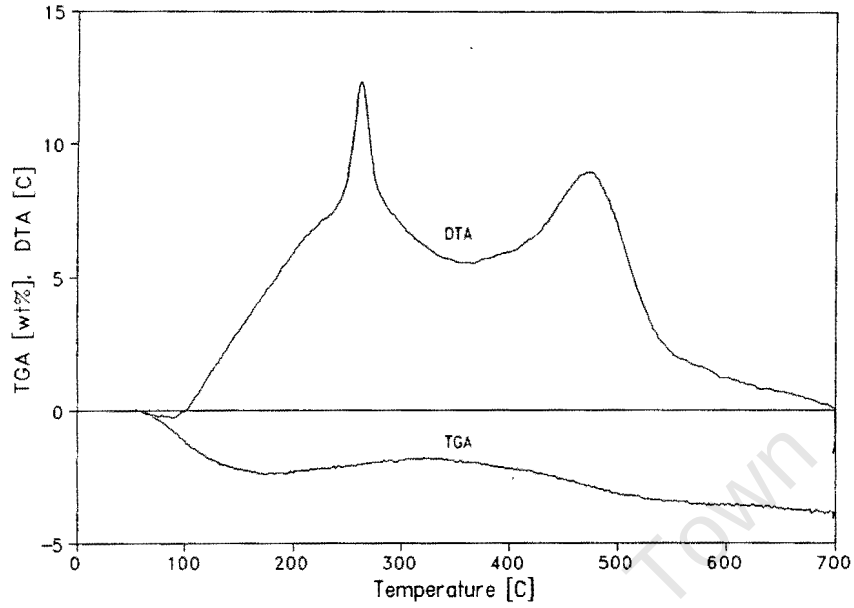

Figure 3.26. TG-DTA spectrum of used Co/SiO_2
(Oxidizing gas = 30 ml(NTP)/min air, temperature programming rate = 10°C/min, $m_{cat} \approx 25$ mg)

The Co/Al_2O_3 catalyst showed a weight loss of 6.9% following oxidation in air up to 700°C (Figure 3.27). As observed during thermogravimetric analysis of the used Co/SiO_2 catalyst, an endothermic mass loss was observed at a temperature of 100°C due to the desorption of adsorbed reaction products. Unlike the spectrum of the used Co/SiO_2 catalyst, the TG-DTA spectrum of the Co/Al_2O_3 catalyst was dominated by a single exothermic mass loss occurring at 280°C. The sharpness of this peak and the corresponding decrease in weight points towards the combustion of a particular type of surface carbon. No mass increase corresponding to the oxidation of reduced cobalt was observed. This may be due to the lower extent of metal reduction obtained using Al_2O_3 supported cobalt catalysts relative to SiO_2 supported cobalt catalysts [Lapidus *et al*, 1991].

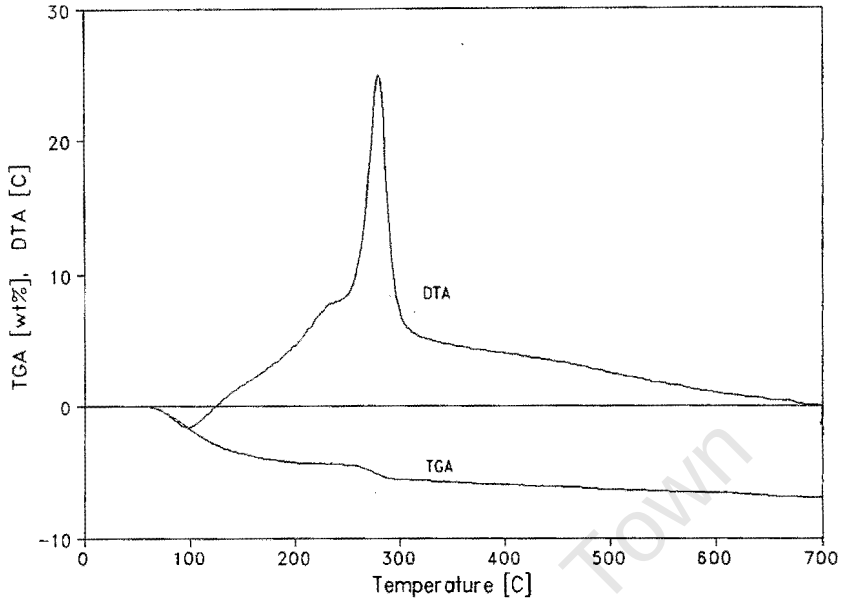

Figure 3.27. TG-DTA spectrum of used Co/Al_2O_3
(Oxidizing gas = 30 ml(NTP)/min air, temperature programming rate = 10°C/min, $m_{cat} \approx 25$ mg)

The TG-DTA spectra of the used $Co/13SiO_2$-Al_2O_3 catalyst showed a weight loss of 9.1% following oxidation in air up to a temperature of 700°C (Figure 3.28). The thermogravimetric behaviour of this sample is characterized by the endothermic loss of adsorbed water and reaction products at 100°C and the combustion of carbonaceous material deposited during reductive amination at temperatures up to 700°C. The spectrum is dominated by a sharp exotherm occurring at 350°C with a smaller exotherm appearing on the tail of the first peak. As in the TG-DTA spectra of the SiO_2 and Al_2O_3 supported cobalt catalysts, the distinct nature of the exotherm suggests that the carbonaceous deposit is of a uniform nature.

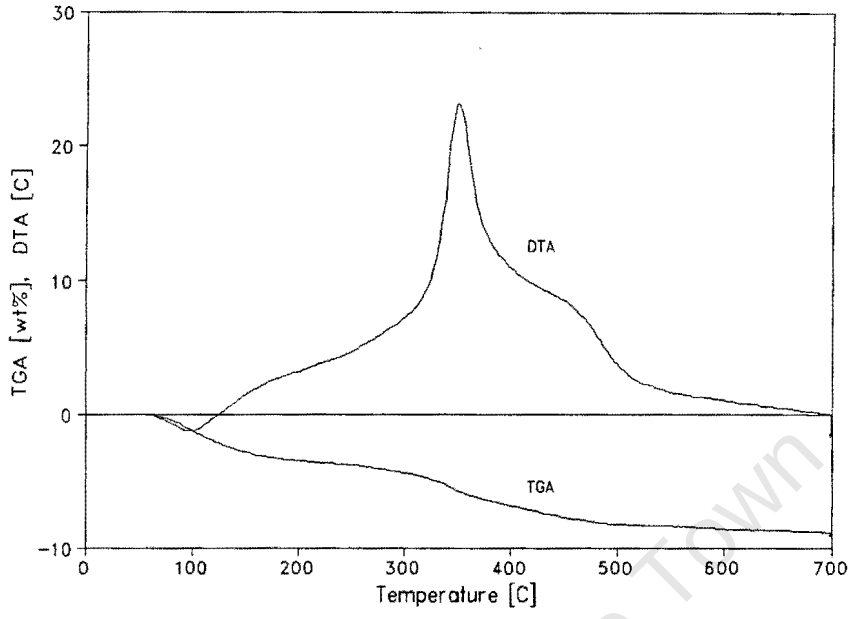

Figure 3.28. TG-DTA spectrum of used Co/SiO_2-Al_2O_3
(Oxidizing gas = 30 ml(NTP)/min air, temperature programming rate = 10°C/min, $m_{cat} \approx 25$ mg)

3.2.1.3. X-ray diffraction

XRD spectra of the calcined, reduced and used Co/SiO_2 catalyst were recorded in order to observe the crystallographic changes of the supported cobalt during catalyst activation and reaction. The semi-crystalline nature of the SiO_2 support resulted in considerable baseline "noise" (see Figure 3.29.). In combination with the relatively low metal loadings used for catalyst preparation, a low signal to noise ratio was obtained. Due to difficulties in defining the baseline, application of the Scherrer line broadening equation to calculate average particle diameters was not applied. Calcination of the Co/SiO_2 catalyst was performed in a 60 ml(NTP)/min air stream at 500°C for 1 hour using a temperature programming rate of 10°C/min. The reduced Co/SiO_2 catalyst was prepared by reduction in a 60 ml(NTP)/min H_2 stream at 500°C for 1 hour using a temperature programming rate of 10°C/min. The used Co/SiO_2 sample was that obtained from the time on stream experiments (Chapter 3.1.2.). Figure 3.29 contains the diffraction patterns obtained for the calcined, reduced and used Co/SiO_2 catalysts.

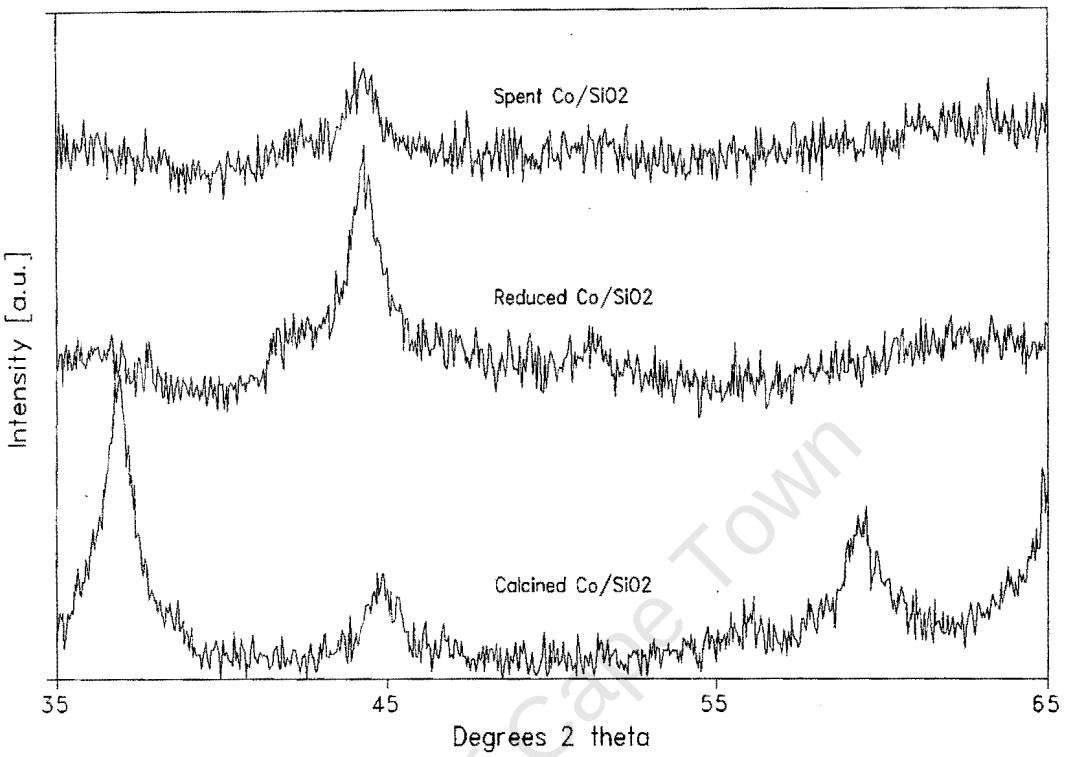

Figure 3.29. XRD spectra of calcined, reduced and used Co/SiO_2
(Calcination gas = 60 ml(NTP)/min air, calcination temperature = 500°C, reducing gas = 60 ml(NTP)/min H_2, reduction temperature = 500°C, time on stream of used catalyst = 24 hours)

The XRD spectrum of the Co/SiO_2 catalyst calcined in air at 400°C showed the characteristic spinel lines of the bulk cobalt oxide Co_3O_4 at 36.9, 44.7 and 59.6° 2θ. The cobalt nitrate precursor is therefore partially or largely transformed into the bulk metal oxide following air calcination. Following hydrogen reduction at 500°C, the diffraction peaks corresponding to Co_3O_4 were no longer present indicating that this species had been largely reduced. The reduced catalyst was characterized by a diffraction peak at 44.1° 2θ which is attributed to face centred cubic metallic cobalt (β-Co). The XRD spectrum of the Co/SiO_2 catalyst used for the reductive amination of ethanol showed a decreased intensity for the β-Co diffraction peak indicating a decrease in the crystallinity of the supported cobalt particles.

3.2.1.4. Effect of the hydrogen partial pressure

Hydrogen is included as a feed during reductive amination as it inhibits catalyst deactivation caused by the formation of metal nitrides, metal carbides and the deposition of carbonaceous material [Baiker and Maciejewski, 1984]. The influence of the partial pressure of hydrogen on the activity of Co/SiO_2 was evaluated at a reaction temperature of 180°C, a WHSV of 2 g_{EtOH}/g_{cat}·h and an EtOH : NH_3 molar ratio of 1 : 2. The hydrogen partial pressure was varied between 6 and 21 kPa and the partial pressures of ethanol and ammonia were kept constant by adjusting the flow of nitrogen diluent such that the overall flow rate was 200 ml(NTP)/min.

Decreasing the hydrogen partial pressure during reductive amination resulted in an almost linear decrease in the ethanol conversion activity of SiO_2 supported cobalt (Figure 3.30.). Increasing the hydrogen pressure to its original value of 21 kPa resulted in total restoration of the catalytic activity indicating that the deactivation was reversible. Restoration of activity occurred within 30 minutes (the time taken between gas chromatographic sampling) indicating that the reversible deactivation process occurred rapidly under the selected reaction conditions.

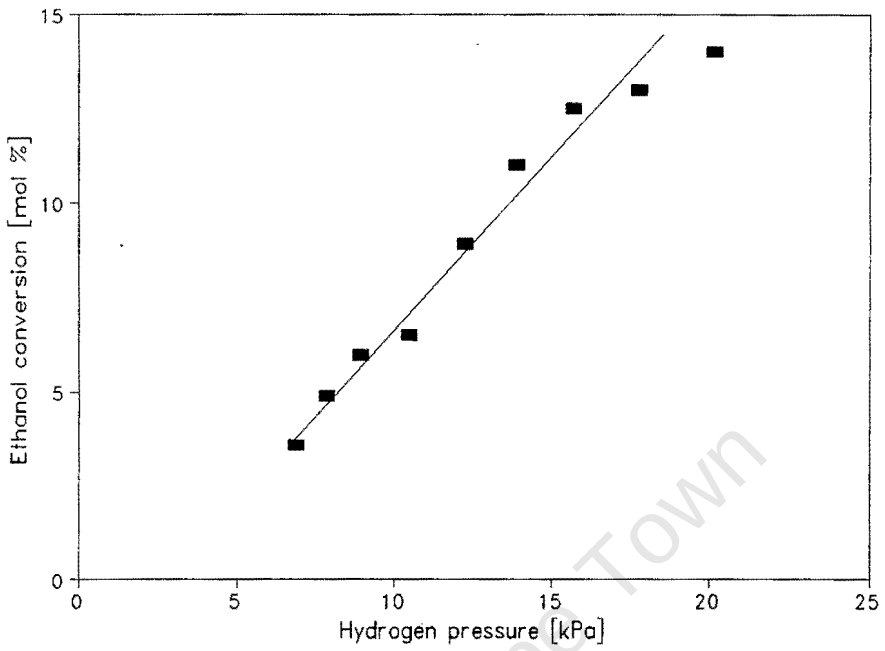

Figure 3.30. Effect of hydrogen pressure on the activity of Co/SiO_2
(T = 180°C, P = 1 bar, EtOH : NH_3 = 1 : 2, WHSV = 2 g_{EtOH}/g_{cat}·h, total flow rate = 200 ml(NTP)/min)

3.2.2. Influence of Catalyst Preparation Procedure

The reducibility as well as the dispersion of many supported metal catalysts is dependent not only on the chemical nature of the compounds involved, but also on the method of catalyst preparation. As a specific example, the final properties of supported cobalt catalysts have been shown to be dependent on the type of support [Bartholomew and Reuel, 1991] as well as on the nature of the cobalt precursor [Rosynek and Polansky, 1991; Matsuzaki *et al*, 1993]. The influence of the catalyst preparation procedure on the activity and selectivity of cobalt catalysts for the reductive amination reaction was investigated by changing the chemical nature of the support, by changing the support acidity, by changing the type of cobalt precursor and by changing the type of impregnation solvent.

3.2.2.1. Effect of the Type of Cobalt Support

It has been well established that both the activity and the selectivity of many heterogeneous catalytic reactions depends on the nature of the metal support. As a specific example, the specific activity of supported Pt used for CO hydrogenation was shown to increase 100 fold as the support was changed from SiO_2 to TiO_2 [Vannice and Twu, 1983]. Besides altering the activity, the support was also seen to influence hydrocarbon selectivity substantially. The physico-chemical characteristics of a series of SiO_2, Al_2O_3, SiO_2-Al_2O_3 and MgO supported cobalt catalysts was evaluated using TPR, TPO and hydrogen chemisorption and the catalytic activity and selectivity for the reductive amination of ethanol was evaluated.

3.2.2.1.1. Temperature programmed reduction

The TPR spectra of the SiO_2, Al_2O_3, SiO_2-Al_2O_3 and MgO supported cobalt catalysts are illustrated in Figure 3.31. The spectra represent the hydrogen consumption profiles of the dried catalyst precursors in a 60 ml(NTP)/min 5% H_2/N_2 stream as the temperature was raised linearly from 100 to 1000°C at 10°C/min.

The occurrence of multiple hydrogen consumption maxima during TPR indicated the

presence of a number of reducible species in the catalyst precursors. The most intense peak which occurs at low temperatures is due to the reductive decomposition of the cobalt nitrate precursor [Arnoldy and Moulijn, 1985; Rosynek and Polansky, 1991]. The temperature at which the reductive decomposition of the nitrate precursor occurs increased from 240 to 280 to 290 to 340°C as the support was changed from SiO_2 to Al_2O_3 to SiO_2-Al_2O_3 to MgO. The increase in the temperature required for nitrate ion reduction indicates an increase in the strength of metal precursor-support interaction which may influence the reducibility of the supported cobalt.

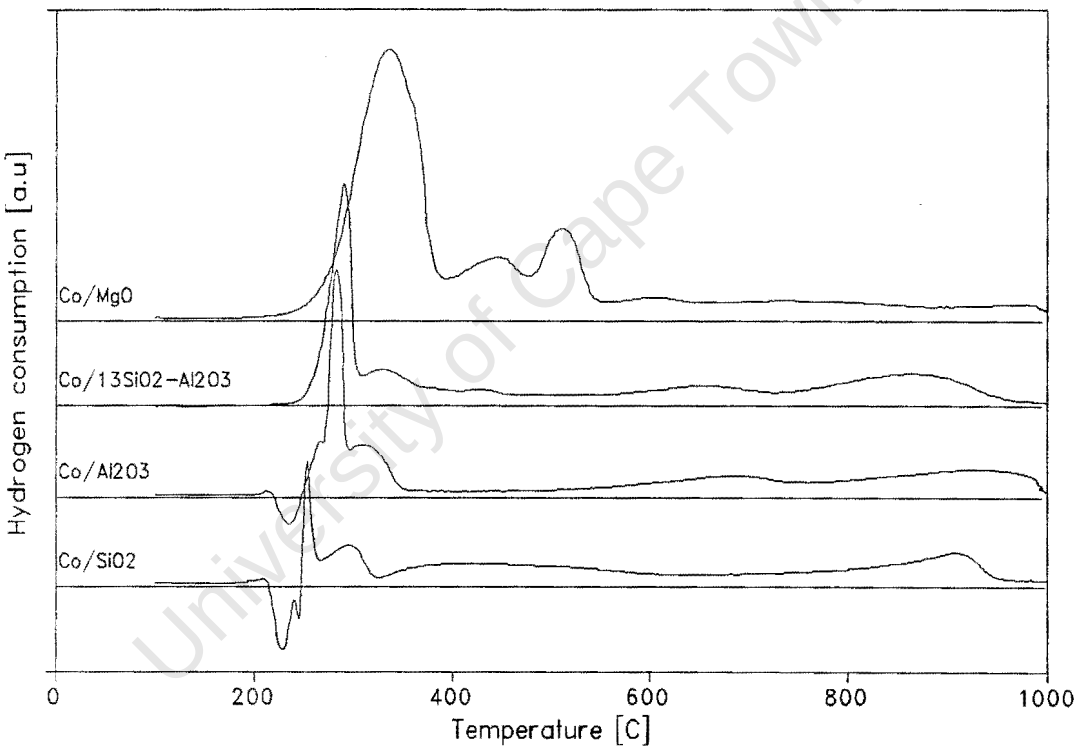

Figure 3.31. TPR spectra of SiO_2, Al_2O_3, SiO_2-Al_2O_3 and MgO supported cobalt catalysts (Reducing gas = 60 ml(NTP)/min 5% H_2/N_2, temperature programming rate = 10°C/min, $m_{cat} \approx 0.15$g)

Subsequent reduction to metallic cobalt occurs in several steps, the size and location of the peak being dependent on the type of support used. The Co/SiO_2 catalyst was characterized by a broad region of hydrogen consumption between approximately 350 and 700°C followed by a further peak of hydrogen consumption occurring at approximately 900°C. Since the bulk

cobalt oxides CoO and Co_3O_4 are reduced completely by 500°C [van't Blik and Prins, 1986], the hydrogen consumption occurring at higher temperatures is due to the reduction of cobalt species having some degree of interaction with the SiO_2 carrier. These peaks are probably caused by the reduction of surface cobalt oxides [Rosynek and Polansky, 1991] and/or cobalt silicate species [Puskas *et al*, 1992; Ming and Baker, 1995].

In the case of the Co/Al_2O_3 catalyst, two broad peaks of hydrogen consumption with maxima at approximately 700 and 950°C were observed. These regions of hydrogen consumption may be assigned to the reduction of cobalt species interacting with the Al_2O_3 support since bulk cobalt oxides are reduced at considerably lower temperatures. Arnoldy and Moulijn [1985] identified four different cobalt phases present in Al_2O_3 supported cobalt catalysts. Based on their conclusions, the cobalt species responsible for the two hydrogen consumption peaks observed at 700 and 950°C are present as surface Co^{2+} ions and as $Co_2Al_2O_4$ spinel species respectively.

The TPR spectrum of the $Co/13SiO_2$-Al_2O_3 catalyst showed the presence of two high temperature reduction maxima at approximately 600 and 800°C. Rathousky *et al* [1991] proposed that the high exothermicity of the reductive decomposition of the nitrate precursor was responsible for the strong metal-support interaction. This does not explain the strong metal-support interaction obtained for SiO_2 and Al_2O_3 supported cobalt catalysts however. Literature citings pertaining to SiO_2-Al_2O_3 supported cobalt catalysts are scarce and it may be more likely that the formation of a combination of cobalt silicate and cobalt aluminate species are responsible for the high temperature hydrogen consumption occurring with this catalyst.

The MgO supported cobalt catalyst was characterized by a number of hydrogen consumption peaks during TPR. The reduction profile of the Co/MgO catalyst varied considerably compared to the SiO_2, Al_2O_3 and SiO_2-Al_2O_3 supported cobalt catalysts and it is likely that the mechanism of precursor reduction is considerably different. The multiple hydrogen consumption maxima indicated the presence of a number of reducible species on the surface of the catalyst precursor.

Integration of the TCD signal during TPR showed that the H_2 : Co molar ratio increased from 1.33 to 1.64 to 2.07 to 3.98 as the support was changed from SiO_2 to Al_2O_3 to SiO_2-Al_2O_3 to MgO (Table 3.3). The high hydrogen consumption values indicate that simultaneous reduction of the nitrate ion was occurring during TPR. The changes in hydrogen consumption with changing metal carrier indicate a change in the mechanism of precursor reduction.

Table 3.3. Hydrogen consumption during TPR and nitrate decomposition temperature for Co/SiO_2, Co/Al_2O_3, $Co/13SiO_2$-Al_2O_3 and Co/MgO

Catalyst	$(H_2 : Co)_{total}$ (mol : mol)	$(H_2 : Co)_{>500}$ (mol : mol)	$T_{decomposition}$ (°C)
Co/SiO_2	1.33	0.73	240
Co/Al_2O_3	1.64	0.95	280
$Co/13SiO_2$-Al_2O_3	2.07	0.95	290
Co/MgO	3.98	0.87	340

Due to the complicated stoichiometry of nitrate ion reduction, an accurate measurement of the degree of reduction could not be obtained by measurement of the hydrogen consumption at temperatures below 500°C. Instead, an indirect measurement of the degree of cobalt reduction was obtained by measurement of the hydrogen consumption occurring at temperatures greater than 500°C. This hydrogen consumption represents the reduction of cobalt not reduced by 500°C. This technique requires that all cobalt is reduced by 1000°C (see Chapter 3.3.3.) and that the cobalt reduced at temperatures greater than 500°C is divalent in nature.

Measurement of the hydrogen consumption occurring at temperatures greater than 500°C showed that the H_2 : Co molar ratio increased as the cobalt carrier was changed from SiO_2 to Al_2O_3 to SiO_2-Al_2O_3. The high temperature hydrogen consumption of the Co/MgO catalyst was lower than that expected from the high temperature required for precursor decomposition, possibly indicating that the supported cobalt was not completely reduced by

a temperature of 1000°C for this catalyst.

3.2.2.1.2. Temperature programmed oxidation

The extent of reduction of supported cobalt catalysts is difficult to determine by simply measuring the hydrogen consumption during TPR because of the complicated nature of the reduction (*i.e.* besides the reduction of unknown quantities of divalent and trivalent cobalt ions, reduction of the nitrate ion may also occur). Instead, by measuring the oxygen uptake during TPO, a simple measurement of the amount of reduced metal present may be obtained. Furthermore, by measuring the oxygen release caused by the high temperature thermal reduction of trivalent cobalt to divalent cobalt, the degree of cobalt-support compound formation may be obtained. A full description of the technique is listed in Chapter 2.2.1.2. The TPO spectra of the SiO_2, Al_2O_3, SiO_2-Al_2O_3 and MgO supported cobalt catalysts are illustrated in Figure 3.32. These spectra indicate the oxygen uptake of the reduced catalysts in a 60 ml(NTP)/min 2% O_2/He stream as the temperature was increased from 50 to 1000°C at 10°C/min. Reduction of the catalyst precursors in a 60 ml(NTP)/min 5% H_2/N_2 stream was conducted at 500°C for 1 hour.

The TPO results showed that the extent of metal reduction decreased from 42 to 32 to 8 to 0 % as the metal carrier was changed from SiO_2 to SiO_2-Al_2O_3 to Al_2O_3 to MgO (Table 3.4). Although the temperature of nitrate decomposition during TPR is determined by the strength of the metal salt - support interaction, the extents of metal reduction as calculated using TPO were not correlated to this increasing strength of interaction. It can therefore be concluded that the temperature of nitrate ion reduction does not solely determine metal reducibility but that it is also a function of the chemical nature of the carrier material. No zerovalent cobalt was detected on the Co/MgO catalyst following hydrogen reduction at 500°C and it is possible that a solid solution between cobalt and magnesium oxide is formed. The hydrogen consumption occurring below 500°C during TPR of Co/MgO is therefore only caused by reduction of the nitrate ion.

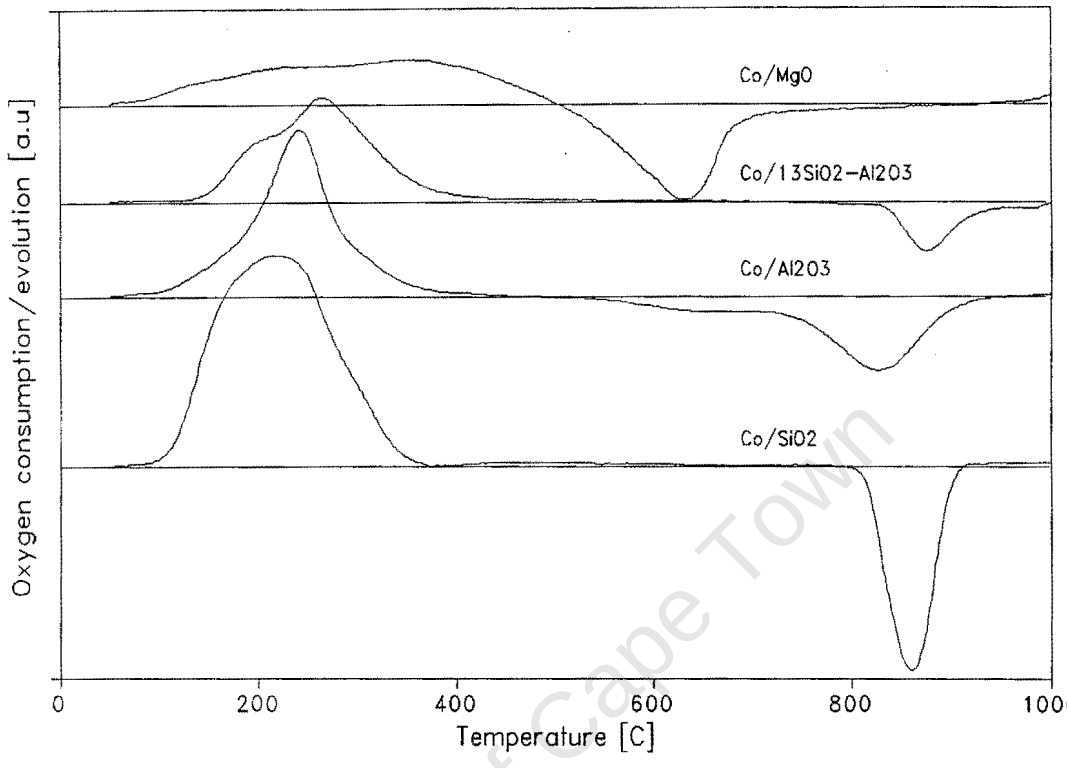

Figure 3.32. TPO spectra of SiO_2, Al_2O_3, SiO_2-Al_2O_3 and MgO supported cobalt catalysts (Reducing gas = 60 ml(NTP)/min 5% H_2/N_2, reduction temperature = 500°C, oxidizing gas = 60 ml(NTP)/min 2% O_2/He, temperature programming rate = 10°C/min, $m_{cat} \approx 0.50$ g)

The temperature of the oxygen consumption maxima corresponding to the oxidation of reduced cobalt and unreduced divalent cobalt species was seen to increase from 220 to 240 to 260 to 360°C as the support was changed from SiO_2 to Al_2O_3 to SiO_2-Al_2O_3 to MgO (Table 3.4.). The increase in the temperature of maximum oxygen uptake reflects a change in the oxygen affinity of the supported cobalt which may affect the catalytic properties of the metal. This increase in the temperature of maximum oxidation may be due to an increase in the strength of interaction between the reduced metal and the support or due to a changing chemical environment.

Table 3.4. Composition and metal oxidation temperatures during TPO for Co/SiO_2, Co/Al_2O_3, $Co/13SiO_2$-Al_2O_3 and Co/MgO

Catalyst	Zerovalent Co (mol %)	Oxidizable Co^{2+} (mol %)	Non-oxidizable Co^{2+} (mol %)	$T_{oxidation}$ (°C)
Co/SiO_2	42	29	29	220
Co/Al_2O_3	8	65	27	240
$Co/13SiO_2$-Al_2O_3	32	24	44	260
Co/MgO	≈ 0	84	16	360

3.2.2.1.3. Hydrogen chemisorption

Table 3.5. contains the results of the hydrogen chemisorption measurements performed on the SiO_2, Al_2O_3, SiO_2-Al_2O_3 and MgO supported cobalt catalysts. Hydrogen adsorption was performed at 100°C for the SiO_2 and MgO supported cobalt catalysts and at 125°C for the Al_2O_3 and SiO_2-Al_2O_3 supported catalysts due to the activated nature of hydrogen chemisorption on cobalt [Reuel and Bartholomew, 1984]. Prior to hydrogen adsorption, the catalysts were reduced in 60 ml(NTP)/min H_2 at 500°C for 1 hour and evacuated at 400°C for 3 hours to remove any residual adsorbed hydrogen.

Table 3.5. Surface area, dispersion, diameter and reversibility of hydrogen adsorption of SiO_2, Al_2O_3, SiO_2-Al_2O_3 and MgO supported cobalt catalysts

Catalyst	Surface Area (m^2/g_{cat})	Dispersion (%)	Diameter (nm)	Reversibility (%)
Co/SiO_2	1.68	8.1	12.2	39.3
Co/Al_2O_3	0.96	10.6	9.1	50.4
$Co/13SiO_2$-Al_2O_3	0.24	1.5	64.8	91.1
Co/MgO	≈0	-	-	-

The measured metal surface area decreased from 1.68 to 0.96 to 0.24 m^2/g_{cat} as the cobalt support was changed from SiO_2 to Al_2O_3 to SiO_2-Al_2O_3. The decrease in the surface area of reduced cobalt metal is a function of both the extent of reduction and the metal dispersion. The high extent of reduction obtained with the Co/SiO_2 catalyst in combination with the relatively good metal dispersion resulted in this catalyst having the highest metal surface area following hydrogen reduction at 500°C. No measurable hydrogen adsorption was recorded for the Co/MgO catalyst. This measurement is in agreement with the TPO results which showed no zerovalent cobalt species following hydrogen reduction at 500°C.

The reversibility of hydrogen adsorption on cobalt increased as the support was changed from SiO_2 to Al_2O_3 to SiO_2-Al_2O_3. The reversibility of hydrogen adsorption is an indicator of the strength of hydrogen adsorption on cobalt and increase in the reversibility of hydrogen adsorption corresponds to an increase in the concentration of strong hydrogen adsorption sites. Changes in the nature of metal active sites may alter the strength of adsorption of certain reactants and intermediates and may therefore alter the catalytic behaviour of the supported cobalt catalyst. Bartholomew and Reuel [1985] equated an increase in the reversibility of hydrogen adsorption on supported cobalt to an increase in the strength of metal-support interaction.

3.2.2.1.4. Reductive amination of ethanol

The activity and selectivity of the SiO_2, Al_2O_3, SiO_2-Al_2O_3 and MgO supported cobalt catalysts was measured at a temperature of 180°C, a space velocity of 1 g_{EtOH}/g_{cat}·h and an EtOH : NH_3 : H_2 : N_2 molar ratio of 1 : 2 : 8.6 : 17.6. Catalyst reduction was conducted at 500°C for 1 hour using a 60 ml(NTP)/min H_2 stream as the reducing gas. The time on stream activity of these catalysts is illustrated in Figure 3.33.

The activity of the supported cobalt catalysts for ethanol conversion decreased from 66 to 47 to 37 to 2 % as the support was changed from SiO_2 to Al_2O_3 to SiO_2-Al_2O_3 to MgO (Table 3.6.). Large variations in catalytic activity are therefore obtained upon changing the type of cobalt carrier. The decrease in activity can be explained by the decrease in the reduced metal

surface area as measured by hydrogen chemisorption. The low activity measured for the Co/MgO catalyst is surprising since no reduced cobalt was measured using TPO and hydrogen chemisorption. This indicates that either divalent cobalt species are active for the conversion of ethanol or that the TPO and chemisorption techniques were not sensitive enough to measure low extents of metal reduction and low metallic surface areas.

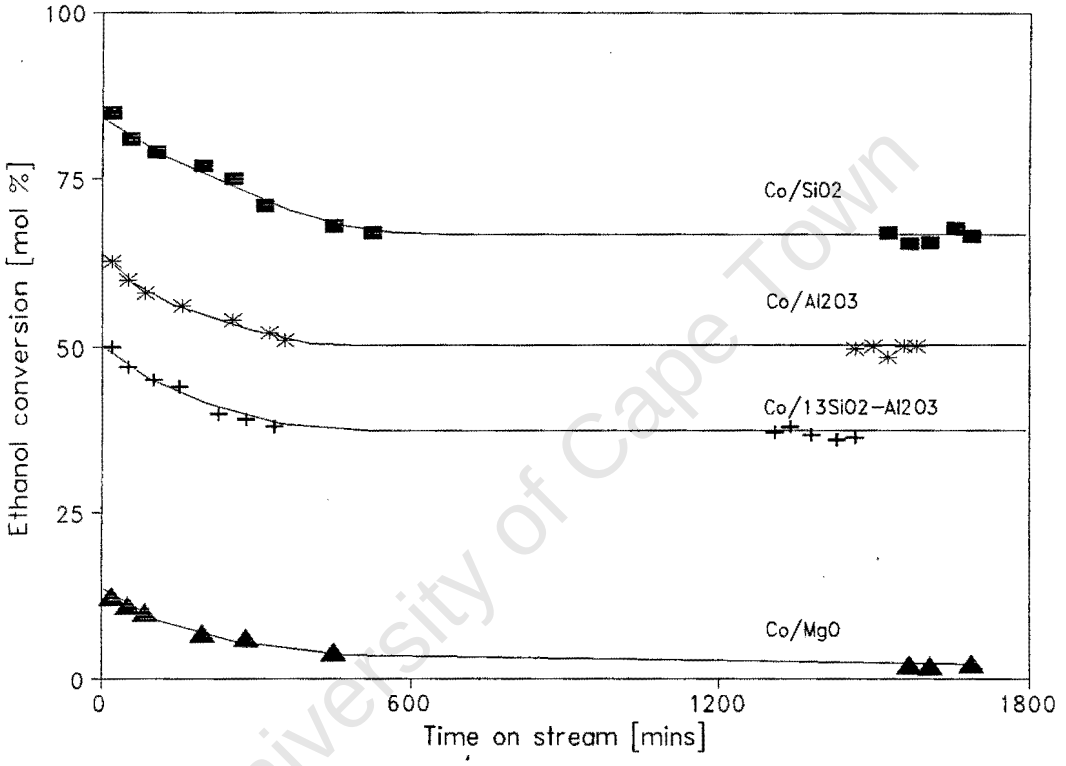

Figure 3.33. Time on stream activity of SiO_2, Al_2O_3, SiO_2-Al_2O_3 and MgO supported Co ($T = 180^{\circ}C$, $P = 1$ bar, WHSV = 1 g_{EtOH}/g_{cat}·h, EtOH : NH_3 : H_2 : N_2 = 1 : 2 : 8.6 : 17.6)

The selectivity to individual ethylamine products obtained using the SiO_2 and Al_2O_3 supported cobalt catalysts did not vary substantially under the experimental conditions used (Table 3.6.). The ethylamine selectivity varied considerably when the cobalt carrier was changed to SiO_2-Al_2O_3 however. The MEA selectivity was higher and the DEA and TEA selectivities were lower when using the Co/13SiO_2-Al_2O_3 catalyst in comparison to the SiO_2 and Al_2O_3 supported cobalt catalysts. The type of cobalt support therefore influences the ethylamine selectivity during reductive amination.

No amine product was observed when using the Co/MgO catalyst. This indicates that even though the cobalt species present on the Co/MgO catalyst were active for ethanol conversion, they do not selectively produce ethylamines under the conditions tested.

Table 3.6. Effect of cobalt support on activity and selectivity for reductive amination ($T = 180^{\circ}C$, $P = 1$ bar, WHSV = 1 g_{EtOH}/g_{cat}·h, EtOH : NH_3 : H_2 : N_2 = 1 : 2 : 8.6 : 17.6)

Catalyst	Conversion[1] (mol %)	MEA Selectivity[2] (mol %)	DEA Selectivity[2] (mol %)	TEA Selectivity[2] (mol %)
Co/SiO_2	66.2	49.5	41.1	9.4
Co/Al_2O_3	47.2	46.5	45.6	7.9
$Co/13SiO_2$-Al_2O_3	36.6	64.3	30.6	5.1
Co/MgO	1.7	-[3]	-[3]	-[3]

[1] Conversion measured at a WHSV of 1 g_{EtOH}/g_{cat}·h

[2] Selectivities interpolated to an ethanol conversion of 50%

[3] No amine product observed

3.2.2.2. Effect of Support Acidity

Isomorphous substitution of aluminium into a SiO_2 support results in the generation of an anionic framework. Countercations are required in order to maintain electronic neutrality and this results in Brönsted acidity. For every substitution by a cation of lower valency, an extra countercation is required. Consequently, acidity increases in direct proportion to the aluminium content in a SiO_2-Al_2O_3 support. In order to investigate the effect of support acidity on the reductive amination reaction, the performance of cobalt was evaluated using SiO_2-Al_2O_3 carriers of varying silicon to aluminium ratios (*i.e.* with varying acidity). The aluminium content in the SiO_2-Al_2O_3 supports was varied between 0 and 13 wt% and the corresponding catalysts were designated Co/$x$$SiO_2$-$Al_2O_3$ where x was the aluminium content of the support in wt%.

3.2.2.2.1. Temperature programmed reduction

The TPR spectra of the SiO_2-Al_2O_3 supported cobalt catalysts are illustrated in Figure 3.34. The spectra represent the hydrogen consumption behaviour of the catalyst precursors in a 60 ml(NTP)/min 5% H_2/N_2 stream as the temperature was raised linearly from 100 to 1000°C at 10°C/min.

The multiple reduction peaks occurring during TPR indicated the presence of a number of reducible cobalt species in the SiO_2-Al_2O_3 supported catalyst precursors. The reduction profiles were dominated by a sharp hydrogen consumption peak occurring at low temperatures which is due to the reductive decomposition of the cobalt nitrate precursor [Rosynek and Polansky, 1991; Arnoldy and Moulijn, 1985]. Both the size and shape of this peak vary with varying aluminium content of the SiO_2-Al_2O_3 support indicating that either the chemical composition or the acidity of the support material influences the mechanism of cobalt nitrate reduction.

A number of hydrogen consumption peaks occurring at high temperatures were observed. The broadness of the reduction peaks and the high temperature at which the reduction occurs

indicated that the hydrogen consumption was probably due to the reduction of cobalt species interacting strongly with the SiO_2-Al_2O_3 support. Reduction of bulk cobalt oxide (Co_3O_4) is characterized by a relatively sharp hydrogen consumption peak occurring at low temperatures (Figure 3.1.). The size of the high temperature hydrogen consumption peaks increased with increasing aluminium content of the SiO_2-Al_2O_3 support which indicated an increase in the extent of cobalt-support species formation.

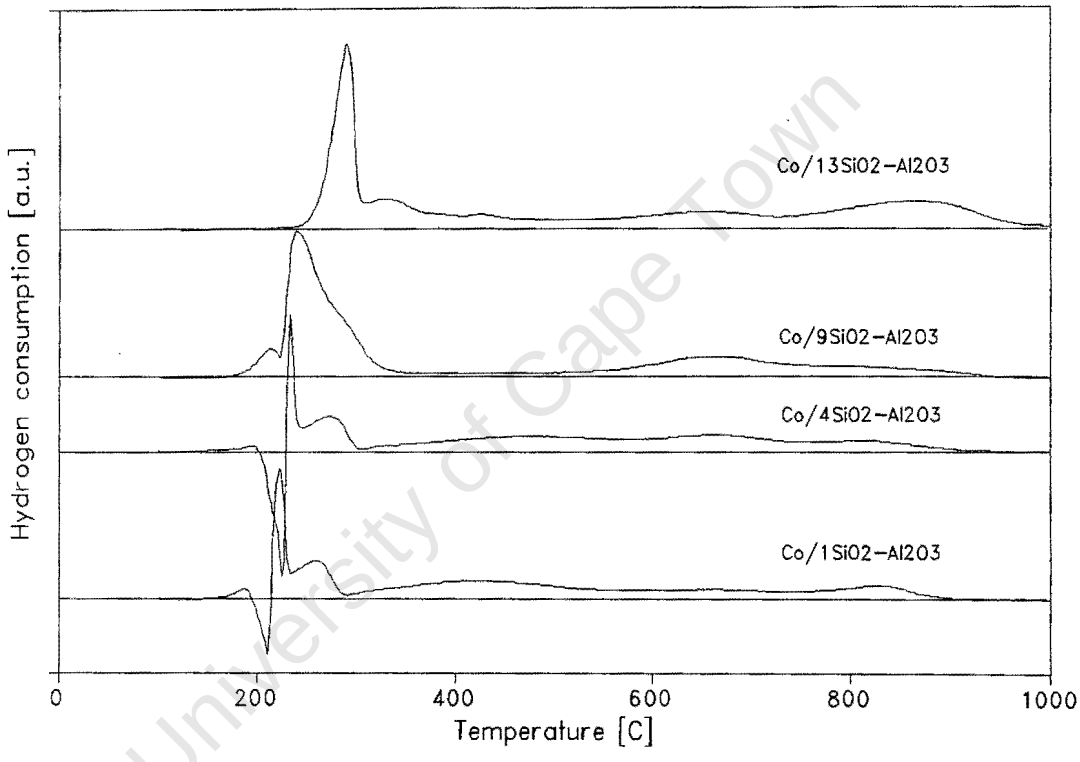

Figure 3.34. TPR spectra of SiO_2-Al_2O_3 supported cobalt catalysts
(Reducing gas = 60 ml(NTP)/min 5% H_2/N_2, temperature programming rate = 10°C/min, $m_{cat} \approx 0.15$ g)

Integration of the TCD signal resulted in molar hydrogen to cobalt ratios which varied between 1.30 and 2.07 (Table 3.7.). This indicated that simultaneous reduction of the nitrate ion was also occurring since reduction of divalent cobalt would result in a hydrogen to cobalt molar ratio of 1 and reduction of the bulk cobalt oxide Co_3O_4 would be expected to result in a hydrogen to cobalt molar ratio of 1.33. The complicated stoichiometry of nitrate reduction and the corresponding release of nitrogen oxides (which interfere with the TCD

signal) does not allow for an accurate estimate of the degree of metal reduction by measurement of the hydrogen consumption occurring prior to 500°C. An indirect estimate of the degree of metal reduction may be obtained by integration of the TCD signal occurring above 500°C since this represents the reduction of cobalt not reduced prior to 500°C.

The hydrogen consumption occurring at temperatures greater than 500°C increased from 0.57 to 0.95 mol H_2 : mol Co as the aluminium content in the SiO_2-Al_2O_3 carrier was increased from 1 to 13 wt%. Increasing the aluminium content of the carrier therefore decreases the reducibility of the supported cobalt. The temperature at which the reductive decomposition of the nitrate precursor occurs similarly increases with increasing aluminium content of the metal carrier material. An increase in the temperature required for reduction of the nitrate precursor may be interpreted as an increase in the strength of precursor-support interaction which would be expected to decrease the reducibility of the supported metal. There may therefore be a correlation between the temperature at which precursor decomposition occurs and the extent of metal reduction at 500°C.

Table 3.7. Hydrogen consumption during TPR and nitrate decomposition temperature of SiO_2-Al_2O_3 supported cobalt catalysts

Catalyst	$(H_2 : Co)_{total}$ (mol : mol)	$(H_2 : Co)_{>500}$ (mol : mol)	$T_{decomposition}$ (°C)
Co/SiO_2-$1Al_2O_3$	1.30	0.57	236
Co/SiO_2-$4Al_2O_3$	1.21	0.70	242
Co/SiO_2-$9Al_2O_3$	1.99	0.78	249
Co/SiO_2-$13Al_2O_3$	2.07	0.95	290

3.2.2.2.2. Temperature programmed oxidation

The TPO spectra of the SiO_2-Al_2O_3 supported catalysts are illustrated in Figure 3.35.

Temperature programmed oxidation was performed in a 60 ml(NTP)/min 2% O_2/He stream as the temperature was raised linearly from 50 to 1000°C at 10°C/min. Prior to TPO, the catalyst precursors were reduced in a 60 ml(NTP)/min 5% H_2/N_2 stream at 500°C for 1 hour.

Increasing the aluminium content of the SiO_2-Al_2O_3 support resulted in a decrease in both the size of the low temperature oxygen uptake and the high temperature oxygen release. The decrease in the size of the low temperature oxygen uptake corresponded to a decrease in the extent of cobalt reduction from 46 to 32 % as the aluminium content of the SiO_2-Al_2O_3 support was increased from 1 to 13 wt%. Increasing the aluminium content of the carrier material therefore decreases the reducibility of the supported cobalt.

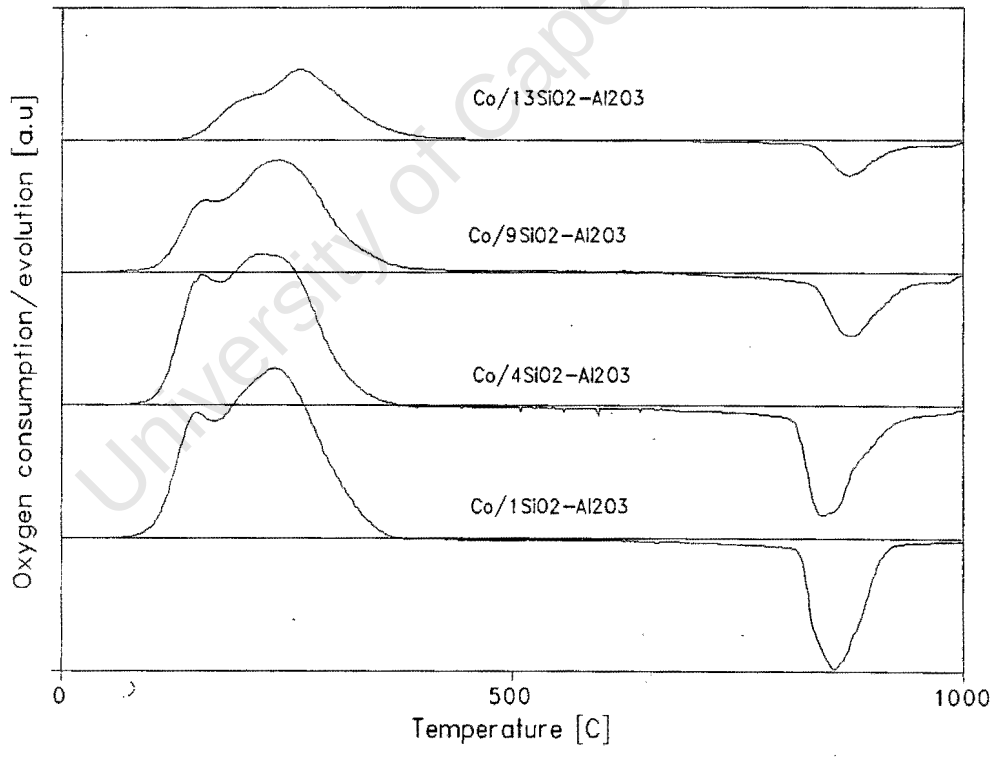

Figure 3.35. TPO spectra of SiO_2-Al_2O_3 supported cobalt catalysts
(Reducing gas = 60 ml(NTP)/min 5% H_2/N_2, reduction temperature = 500°C, oxidizing gas = 60 ml(NTP)/min 2% O_2/He, temperature programming rate = 10°C/min, $m_{cat} \approx 0.50$ g)

Increasing the aluminium content of the SiO_2-Al_2O_3 support similarly decreases the size of the high temperature peak caused by the thermal reduction of trivalent cobalt to divalent cobalt. It can therefore be deduced that increasing the aluminium content of the SiO_2-Al_2O_3 carrier increases the formation of cobalt-support species which cannot be oxidized to form trivalent cobalt species.

Table 3.8. Composition and metal oxidation temperatures during TPO for SiO_2-Al_2O_3 supported cobalt catalysts

Catalyst	Zerovalent Co (mol %)	Oxidizable Co^{2+} (mol %)	Non-oxidizable Co^{2+} (mol %)	$T_{oxidation}$ (°C)
Co/1SiO_2-Al_2O_3	46	44	10	233
Co/4SiO_2-Al_2O_3	40	40	20	213
Co/9SiO_2-Al_2O_3	35	34	31	217
Co/13SiO_2-Al_2O_3	32	24	44	260

3.2.2.2.3. Hydrogen chemisorption

The hydrogen adsorption measurements indicated considerable differences in the physical characteristics of the reduced catalysts as the aluminium content in the SiO_2-Al_2O_3 support was changed. The metal surface area decreased as the aluminium content of the carrier was increased due to decreased extents of metal reduction and due to decreased metal dispersion. The decrease in metal dispersion with increasing aluminium content of the SiO_2-Al_2O_3 support is surprising since an increase in the degree of metal-support interaction (as indicated by TPR) is expected to reduce metal mobility and therefore increase the dispersion.

The reversibility of hydrogen adsorption increased with increasing aluminium content of the metal carrier. This indicates that the percentage of weak hydrogen adsorption sites on the reduced catalyst is decreasing. The changes in the reversibility may be related to the average

particle size of the supported cobalt crystallites which may influence the particle morphology and thus the nature of the exposed adsorption sites.

Table 3.9. Surface area, dispersion, diameter and reversibility of hydrogen adsorption on SiO_2-Al_2O_3 supported cobalt catalysts

Catalyst	Surface Area (m^2/g_{cat})	Dispersion (%)	Diameter (nm)	Reversibility (%)
$Co/1SiO_2$-Al_2O_3	1.83	8.0	12.1	36.6
$Co/4SiO_2$-Al_2O_3	1.15	5.8	16.6	57.1
$Co/9SiO_2$-Al_2O_3	0.74	4.3	22.6	84.7
$Co/13SiO_2$-Al_2O_3	0.24	1.5	64.8	91.1

3.2.2.2.4. Reductive amination of ethanol

The activity and selectivity of the SiO_2-Al_2O_3 supported catalysts was measured at a temperature of 180°C, a WHSV of 1 g_{EtOH}/g_{cat}·h and an EtOH : NH_3 : H_2 : N_2 molar ratio of 1 : 2 : 8.6 : 17.6. Prior to reaction, the catalyst precursors were activated by reduction in a 60 ml(NTP)/min 5% H_2 stream at 500°C for 1 hour. The time on stream activity of these catalysts is illustrated in Figure 3.36.

The ethanol conversion activity of the SiO_2-Al_2O_3 supported cobalt catalysts decreased from 66 to 37 % as the aluminium content in the metal carrier was increased from 1 to 13 wt% (Table 3.10.). The decrease in activity corresponds to the decrease in metal reduction and the decrease in metallic surface area with increasing aluminium content of the carrier material. The time on stream behaviour of the SiO_2-Al_2O_3 supported catalysts was similar and steady state activity was achieved after approximately 24 hours. With the exception of the $Co/13SiO_2$-Al_2O_3 catalyst, increasing the acidity of the support material did not increase the rate of catalyst deactivation during amination significantly.

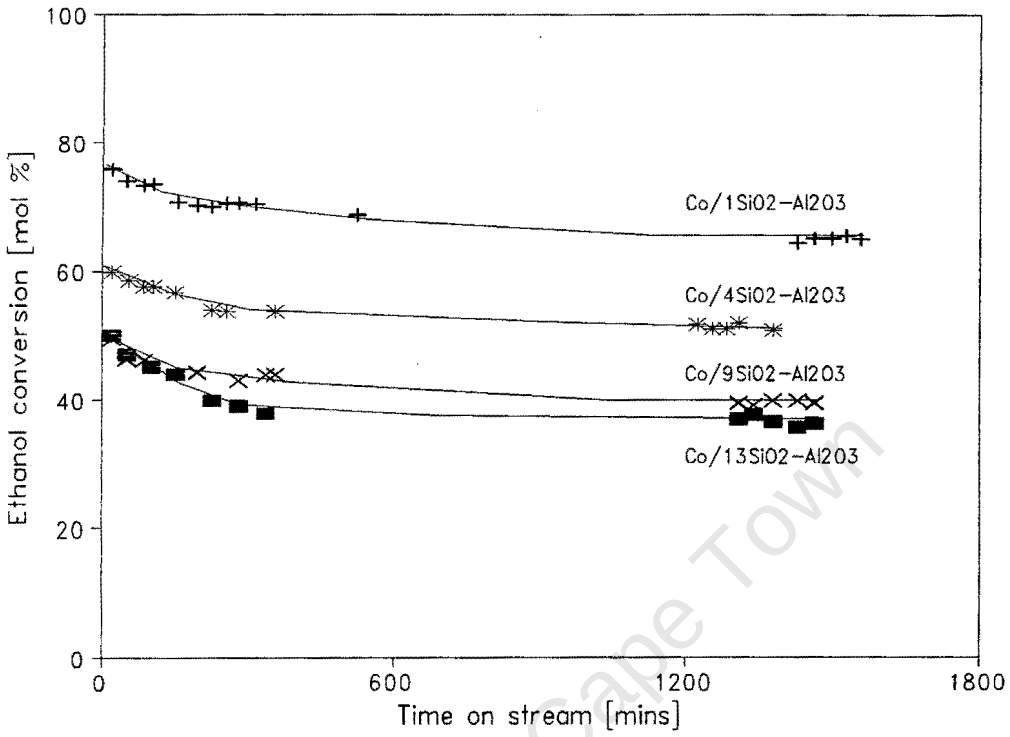

Figure 3.36. Time on stream activity of SiO_2-Al_2O_3 supported cobalt catalysts
(T = 180°C, P = 1 bar, WHSV = 1 g_{EtOH}/g_{cat}·h, EtOH : NH_3 : H_2 : N_2 = 1 : 2 : 8.6 : 17.6)

Comparison of the selectivity to individual ethylamine products at an ethanol conversion of 50 % indicated that changing the aluminium content of the SiO_2-Al_2O_3 support resulted in changes in the product distribution (Table 3.10.). The MEA selectivity increased, the DEA selectivity decreased and the TEA selectivity remained approximately constant as the aluminium content of the metal carrier was increased. These changes in selectivity are due to changes in the rates of formation of the individual amines and indicate a change in the catalytic action of the supported cobalt catalysts.

Table 3.10. Effect of support acidity on the activity and selectivity of cobalt catalysts for reductive amination

(T = 180°C, P = 1 bar, WHSV = 1 g_{EtOH}/g_{cat}·h, EtOH : NH_3 : H_2 : N_2 = 1 : 2 : 8.6 : 17.6).

Catalyst	Conversion[1] (mol %)	MEA Selectivity[2] (mol %)	DEA Selectivity[2] (mol %)	TEA Selectivity[2] (mol %)
Co/1SiO_2-Al_2O_3	65.5	50.5	41.6	7.9
Co/4SiO_2-Al_2O_3	52.4	51.1	39.5	9.4
Co/9SiO_2-Al_2O_3	41.6	52.6	37.5	9.9
Co/13SiO_2-Al_2O_3	36.6	64.3	30.6	5.1

[1] Conversion measured at a WHSV of 1 g_{EtOH}/g_{cat}·h

[2] Selectivity interpolated to an ethanol conversion of 50%

3.2.2.3. Influence of the Type of Cobalt Precursor

The identity of the metal precursor employed in catalyst synthesis can have a significant effect on the reduction properties of the supported catalyst and will therefore affect the eventual catalytic behaviour of the material. As a specific example, it has been shown that the type of cobalt precursor used during impregnation not only influences the metal reducibility but also the activity and selectivity of the metal for CO hydrogenation [Rosynek and Polansky, 1991; Matsuzaki *et al*, 1993]. The reducibility of a series of SiO_2 supported cobalt catalysts synthesized using the corresponding nitrate, sulphate, chloride and acetate salts was evaluated using TPR and the activity and selectivity for reductive amination was measured. The catalysts are referred to as Co/SiO_2, $Co(S)/SiO_2$, $Co(Cl)/SiO_2$ and $Co(A)/SiO_2$ respectively.

3.2.2.3.1. Temperature programmed reduction

The TPR spectra of the SiO_2 supported cobalt catalysts prepared using the nitrate, sulphate, chloride and acetate salts of cobalt are shown in Figure 3.37. The reduction behaviour of the catalysts was measured using a 60 ml(NTP)/min 5% H_2/N_2 stream as the reducing gas as the temperature was increased linearly from 100 to 1000°C at 10°C/min. Prior to reduction, the catalysts were calcined in a 60 ml(NTP)/min air stream at 400°C for 1 hour.

The TPR spectra showed considerable changes in the ease of metal reducibility upon changing the identity of the cobalt precursor used during impregnation. The TPR spectrum of the Co/SiO_2 catalyst prepared using the nitrate salt of cobalt showed multiple reduction peaks with maxima occurring at 290, 410 and 920°C. These peaks are due to reduction of various cobalt species formed during the impregnation and calcination steps. Hydrogen consumption occurring at temperatures greater than 500°C may be assigned to the reduction of various cobalt-silicate species [Puskas *et al*, 1992] since the bulk cobalt oxides CoO and Co_3O_4 are completely reduced by 500°C [van't Blik and Prins, 1986]. The hydrogen to cobalt molar ratio during TPR was 1.35 which indicates that the supported cobalt is present as a mixture of divalent and trivalent cobalt ions following calcination in air at 400°C (Table

3.11.). Reduction of divalent cobalt results in a H_2 : Co molar ratio of 1 and reduction of trivalent cobalt results in a H_2 : Co molar ratio of 1.5.

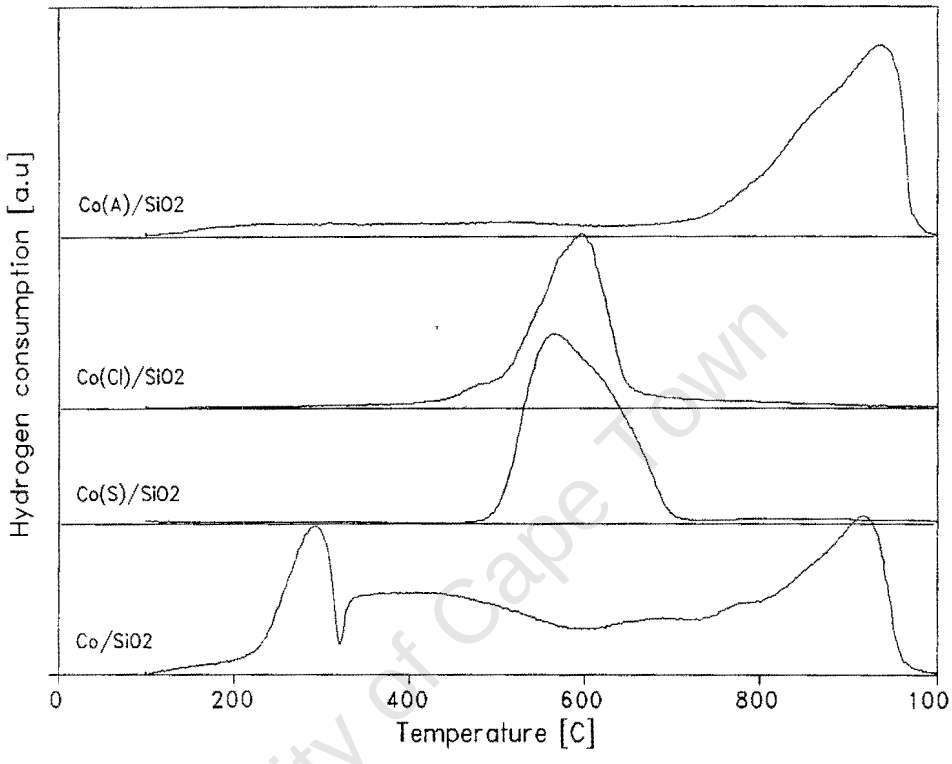

Figure 3.37. TPR spectra of Co/SiO_2, $Co(S)/SiO_2$, $Co(Cl)/SiO_2$ and $Co(A)/SiO_2$ (Calcination gas = 60 ml(NTP)/min air, calcination temperature = 400°C, reducing gas = 60 ml(NTP)/min 5% H_2/N_2, temperature programming rate = 10°C/min, $m_{cat} \approx 0.15$ g)

The TPR spectrum of the $Co(S)/SiO_2$ catalyst prepared using the sulphate salt of cobalt was characterized by a single hydrogen consumption peak occurring at 570°C. The hydrogen to cobalt molar ratio during TPR was 4.79 which is considerably higher than the hydrogen consumption required purely for cobalt reduction. The higher than expected hydrogen consumption may be explained by reduction of the cobalt sulphate precursor during TPR to form metallic cobalt, hydrogen sulphide and water. The theoretical H_2 : Co ratio for this reduction reaction is 5.

$$CoSO_4 + 5\ H_2 \rightarrow Co + H_2S + 4\ H_2O$$

The high H_2 : Co molar ratio and the characteristic smell of hydrogen sulphide during TPR indicates that the cobalt sulphate precursor did not decompose to form the bulk oxide Co_3O_4 during air calcination.

The reduction profile of the $Co(Cl)/SiO_2$ catalyst prepared using the chloride salt of cobalt was similar to that of the $Co(S)/SiO_2$ catalyst and showed a single hydrogen consumption peak with a maximum at 600°C. Rosynek and Polansky [1991] showed that the reduction of $CoCl_2$ was virtually unaffected by the presence of a SiO_2 support and occurred at approximately 540°C. It is therefore likely that the $CoCl_2$ precursor is not decomposed during air calcination and that the single peak observed during TPR is due to reduction of cobalt chloride to metallic cobalt and hydrogen chloride, *viz.*.

$$CoCl_2 + H_2 \rightarrow Co + 2\ HCl$$

The measured hydrogen to cobalt molar ratio during TPR was 1.25 which is greater than the expected stoichiometry of 1. The higher than expected hydrogen consumption may be due to hydrogen chloride formed through metal precursor reduction interfering with the measured thermal conductivity.

The TPR spectrum of the $Co(A)/SiO_2$ catalyst prepared by impregnation of the SiO_2 support with an aqueous solution of cobalt acetate showed a broad area of hydrogen consumption occurring between 200 and 800°C followed by a large hydrogen consumption peak with a maximum at 940°C. The measured hydrogen to cobalt molar ratio was 1.48 which indicates that the supported cobalt is probably present as a trivalent ion following air calcination at 400°C. The high temperature required for metal reduction indicates that the cobalt is most likely present as a cobalt silicate species since bulk cobalt oxide (Co_3O_4) is reduced completely by 500°C. The high temperature hydrogen consumption obtained for the Co/SiO_2 catalyst prepared from the nitrate precursor has a maximum at 920°C which indicates that these two cobalt silicate species are similar in nature.

Table 3.11. Hydrogen consumption during TPR and reduction peak temperatures for Co/SiO_2, $Co(S)/SiO_2$, $Co(Cl)/SiO_2$ and $Co(A)/SiO_2$

Catalyst	H_2 : Co Ratio (mol : mol)	T_{low} (°C)	T_{medium} (°C)	T_{high} (°C)
Co/SiO_2	1.35	290	410	920
$Co(S)/SiO_2$	4.79	-	570	-
$Co(Cl)/SiO_2$	1.25	-	600	-
$Co(A)/SiO_2$	1.48	-	-	940

3.2.2.2.2. Reductive amination of ethanol

The influence of the type of cobalt precursor used during catalyst preparation on the activity and selectivity during reductive amination was evaluated at a temperature of 180°C, a WHSV of 1 g_{EtOH}/g_{cat}·h and an EtOH : NH_3 : H_2 : N_2 molar ratio of 1 : 2 : 8.6 : 17.6. Activation of the catalyst precursors was performed by calcination in a 60 ml(NTP)/min air stream at 400°C for 1 hour followed by reduction in a 60 ml(NTP)/min H_2 stream at 500°C for 1 hour. Temperature programming rates of 10°C/min were used to effect the temperature changes during activation.

The TPR spectra showed considerable changes in the metal reducibility upon changing the cobalt precursor used during impregnation. Since only the metallic form of cobalt is active for reductive amination [Kirk-Othmer, 1992], it is clear that a large proportion of the supported cobalt will not be available for reaction following hydrogen reduction at 500°C. A decrease in the amount of cobalt reduced by 500°C will be expected to result in a decreased metal surface area and consequently a decrease in the activity for reductive amination. The expected activity as estimated by the amount of hydrogen consumed at temperatures lower than 500°C during TPR will thus decrease as the catalyst is changed from Co/SiO_2 to $Co(A)/SiO_2$ to $Co(Cl)/SiO_2$ to $Co(S)/SiO_2$.

A strong dependence between the activity of the supported cobalt catalysts and the identity of the cobalt precursor used during catalyst preparation was observed (Table 3.12.). The ethanol conversion activity decreased from 54 to 1 % as the catalyst was changed from Co/SiO_2 to $Co(A)/SiO_2$. The $Co(S)/SiO_2$ and $Co(Cl)/SiO_2$ catalysts exhibited no ethanol conversion activity under the conditions selected. The activity for reductive amination can therefore be correlated to the extent of metal reduction as measured using TPR.

The ethylamine selectivity varied considerably as the catalyst was changed from Co/SiO_2 to $Co(A)/SiO_2$. Higher MEA selectivities and lower DEA and TEA selectivities were obtained when the $Co(A)/SiO_2$ catalyst was used instead of the Co/SiO_2 catalyst. The differences in amine selectivity may be a consequence of the different ethanol conversions since it has been shown that the selectivity during reductive amination is dependent on the extent of reactant conversion [Sewell *et al*, 1995].

Table 3.12. Effect of cobalt precursor on the activity and selectivity of SiO_2 supported cobalt ($T = 180^{\circ}C$, $P = 1$ bar, WHSV = 1 g_{EtOH}/g_{cat}·h, EtOH : NH_3 : H_2 : N_2 = 1 : 2 : 8.6 : 17.6)

Catalyst	Conversion (mol %)	MEA Selectivity (mol %)	DEA Selectivity (mol %)	TEA Selectivity (mol %)
Co/SiO_2	54.4	44.4	42.3	12.9
$Co(S)/SiO_2$	0	-	-	-
$Co(Cl)/SiO_2$	0	-	-	-
$Co(A)/SiO_2$	1.0	73.1	26.9	0

3.2.2.4. Influence of the Type of Impregnation Solvent

Changing the identity of the cobalt precursor during preparation of Co/SiO_2 catalysts resulted in large differences in the ethanol conversion activity during reductive amination (Chapter 3.2.2.3.). These differences are caused by the formation of cobalt-silicate species which are not easily reduced to metallic cobalt by 500°C (the temperature used for reduction during the amination studies). Upon dissolution of the cobalt precursor in the impregnating solution, the cobalt ion will be either partially or fully solvated. The degree of solvation and the degree of interaction of the associated anions with the dissolved cobalt will affect the electronic state of the cobalt ion in solution and therefore its reactivity towards the support material. Changing the nature of the solvent of impregnation will therefore be expected to alter the environment of dissolved cobalt ions and thus its reactivity towards the carrier material.

The effect of the solvent of impregnation on the reducibility and activity of SiO_2 supported cobalt catalysts was investigated using a series of protonic solvents and one aprotonic solvent. The protonic solvents used were water, methanol, ethanol and propanol and the corresponding catalysts were named Co/SiO_2, $Co(Me)/SiO_2$, $Co(Et)/SiO_2$ and $Co(Pr)/SiO_2$ respectively. The aprotonic solvent used was dimethylsulphone and the resultant catalyst was named $Co(DMSO)/SiO_2$. The nitrate salt of cobalt was used as the metal precursor compound largely because this material showed the greatest solubility in a range of solvents.

3.2.2.4.1. Temperature programmed reduction

The influence of the type of impregnation solvent on the reducibility of SiO_2 supported cobalt is illustrated in Figure 3.38. The reducing gas during TPR was 60 ml(NTP)/min 5% H_2/N_2 and the temperature program used comprised a linear temperature ramp between 100 and 1000°C at 10°C/min. Prior to TPR, the catalyst precursors were calcined in a 60 ml(NTP)/min air stream at 400°C for 1 hour.

The TPR spectra of the SiO_2 supported cobalt catalysts prepared using water, methanol and ethanol as solvents did not show large differences in either the metal reducibility or the

profile of metal reduction. Accordingly, the temperatures at which the hydrogen consumption maxima were observed were approximately similar. Changing the solvent from water to methanol to ethanol is therefore not expected to alter the degree of metal reduction of the supported cobalt catalysts significantly.

Changing the solvent of impregnation to propanol resulted in an increase in the hydrogen consumption attributed to reduction of cobalt-silicate species. The increase in hydrogen consumption occurring at temperatures greater than 500°C corresponds to a decreased extent of metal reduction. This decrease in metal reducibility is accompanied by a decrease in the temperature at which the first hydrogen consumption peak occurs and an increase in the temperature at which reduction of cobalt-silicate species occurs.

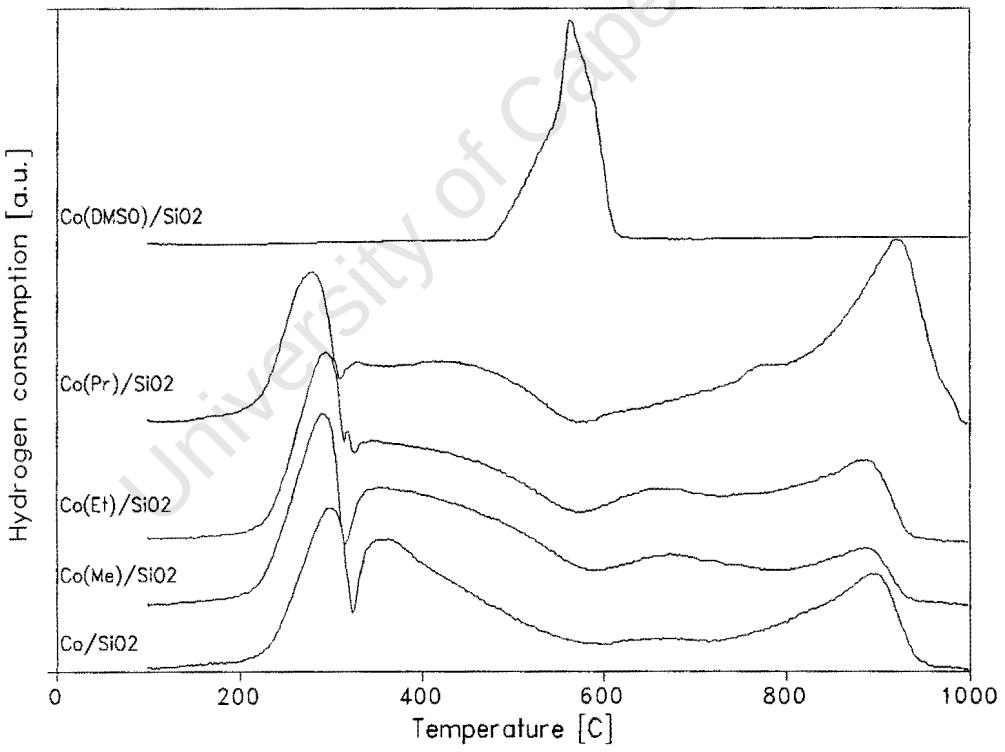

Figure 3.38. Influence of impregnation solvent on TPR spectra SiO_2 supported cobalt (Calcination gas = 60 ml(NTP)/min air, calcination temperature = 400°C, reducing gas = 60 ml(NTP)/min 5% H_2/N_2, temperature programming rate = 10°C/min, $m_{cat} \approx 0.15$g)

Measurement of the hydrogen consumption during TPR showed that the H_2 : Co molar ratios

decreased with decreasing polarity of the impregnation solvent, *i.e.* from water to methanol to ethanol to propanol (Table 3.13.). The decrease in the measured hydrogen consumption indicates that the supported cobalt becomes more divalent in nature with decreasing polarity of the impregnation solvent.

The TPR spectrum of the cobalt catalyst prepared using the aprotonic solvent DMSO was characterized by a single hydrogen consumption peak with a maximum at 560°C. The hydrogen consumption occurred at a temperature higher than that required for reduction of the bulk cobalt oxides CoO and Co_3O_4 and the high H_2 : Co ratio of 3.28 indicates that species other than cobalt are also reduced. The higher than expected hydrogen consumption could be due to reduction of the solvent DMSO molecules. Since DMSO is a strong chelating agent, it is possible that solvent molecules replace the water ligands associated with the cobalt ion during the impregnation step. It is the reduction of this compound that is responsible for the increased hydrogen consumption. This idea is substantiated by the occurrence of only one hydrogen consumption peak during TPR (which indicates the reduction of a single species) and by the absence of cobalt-silicate formation (strong chelation of the cobalt ion would be expected to prevent interaction with the carrier material to form cobalt-silicate species).

Table 3.13. Hydrogen consumption during TPR and reduction peak temperatures for SiO_2 supported cobalt catalysts prepared using different impregnation solvents

Catalyst	H_2 : Co ratio (mol : mol)	T_{low} (°C)	T_{high} (°C)
Co/SiO_2	1.15	300	890
$Co(Me)/SiO_2$	1.14	290	890
$Co(Et)/SiO_2$	1.14	290	880
$Co(Pr)/SiO_2$	1.07	270	920
$Co(DMSO)/SiO_2$	3.28	-	-

3.2.2.4.2. Reductive amination of ethanol

The influence of the solvent of impregnation on the activity and selectivity of SiO_2 supported cobalt for the reductive amination of ethanol was measured at a reaction temperature of 180°C, a WHSV of 1 g_{EtOH}/g_{cat}·h and an EtOH : NH_3 : H_2 : N_2 molar ratio of 1 : 2 : 8.6 : 17.6. Catalyst activation consisted of precalcination in a 60 ml(NTP)/min air stream at 400°C for 1 hour followed by reduction in a 60 ml(NTP)/min H_2 stream at 500°C for 1 hour. The temperature programming rates used during activation were 10°C/min. The time on stream activity of the catalysts is illustrated in Figure 3.39.

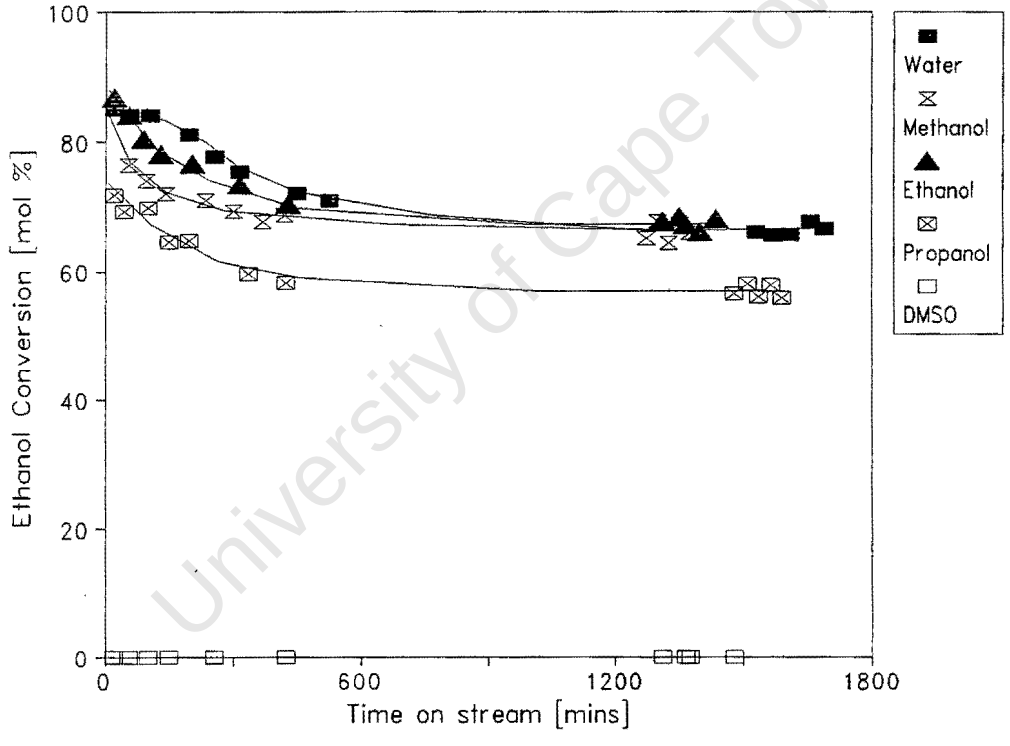

Figure 3.39. Effect of the solvent on the time on stream activity of SiO_2 supported cobalt (T = 180°C, P = 1 bar, WHSV = 1 g_{EtOH}/g_{cat}·h, EtOH : NH_3 : H_2 : N_2 = 1 : 2 : 8.6 : 17.6)

The SiO_2 supported cobalt catalysts prepared using water, methanol and ethanol as solvents showed similar ethanol conversions once steady state activity had been obtained. The deactivation profiles of the three catalysts were slightly different however. The similarity in

ethanol conversion activity therefore corresponds to the similarity in cobalt reducibility as determined using TPR. Changing the solvent of impregnation to propanol resulted in a decrease in the ethanol conversion activity of the SiO_2 supported cobalt catalyst. The decrease in activity is probably due to the decrease in the extent of metal reduction which is caused by increased cobalt-silicate formation. The Co(DMSO)/SiO_2 catalyst showed no ethanol conversion activity under the conditions selected, in agreement with the TPR measurements.

The selectivity to ethylamine products did not vary significantly as the impregnation solvent was changed (Table 3.14.). Even though the Co(Pr)/SiO_2 catalyst had a lower ethanol conversion activity than the catalysts prepared using water, methanol and ethanol as solvents, the selectivity to amine product was similar when compared at the same conversion. This indicates that the presence of cobalt-silicate compounds (which result in a lower extent of reduction and therefore the lower activity of the Co(Pr)/SiO_2 catalyst) do not alter the selectivity during reductive amination. In other words, cobalt silicate species are inactive for the reductive amination reaction. Since the Co(DMSO)/SiO_2 catalyst exhibited no activity under the experimental conditions used, the selectivity to ethylamine products could not be determined.

Table 3.14. Effect of impregnation solvent an activity and selectivity for reductive amination ($T = 180^{\circ}C$, $P = 1$ bar, WHSV = 1 g_{EtOH}/g_{cat}·h, EtOH : NH_3 : H_2 : N_2 = 1 : 2 : 8.6 : 17.6)

Catalyst	Conversion[1] (mol %)	MEA Selectivity[2] (mol %)	DEA Selectivity[2] (mol %)	TEA Selectivity[2] (mol %)
Co/SiO_2	66.2	38.8	46.7	14.5
Co(Me)/SiO_2	66.2	34.6	47.5	17.9
Co(Et)/SiO_2	66.5	35.6	48.2	16.2
Co(Pr)/SiO_2	58.5	36.2	48.7	15.1
Co(DMSO)/SiO_2	0	-	-	-

[1] Conversion measured at a WHSV of 1 g_{EtOH}/g_{cat}·h

[2] Selectivities interpolated to an ethanol conversion of 66%

3.2.3. Effect of Catalyst Activation Procedure

The specific type of activation procedure can result in considerable changes to the final characteristics of a supported metal catalyst. As a specific example, changes in the temperature and medium of activation can result in changes in the metallic dispersion [Foger, 1985] and the reducibility of the supported metal [LoJacono *et al*, 1971]. Since the extent of reduction in combination with the metallic dispersion determines the total number of exposed metal atoms, it is clear that the activation procedure is of paramount importance in the formulation of an efficient catalyst. The influence of the time and temperature of hydrogen reduction as well as the temperature and type of atmosphere during calcination on the activity and selectivity of supported cobalt was evaluated.

3.2.3.1. Effect of Reduction Temperature

The temperature of catalyst reduction is a critical parameter in determining the final catalytic activity of a supported metal since it is this parameter which most widely affects the extent of metal reduction. Although increasing the temperature of hydrogen reduction results in an increase in the extent of metal reduction with a resultant increase in the metallic surface area available for catalytic reaction, too high a reduction temperature results in surface area losses due to the thermal diffusive fusion of metal crystallites which effectively reduces the active metallic surface area. There thus exists an optimum temperature for which the active metallic surface area is maximized.

Because of the agglomeration of metal crystallites at high temperatures, changes in the surface characteristics of the exposed metal atoms may occur. These effects may prove to be important in the instance where a reaction is sensitive to the particular catalytic site available. Changes in catalytic selectivity must therefore be balanced with changes in catalytic activity in order to optimize catalytic productivity. The influence of the temperature of hydrogen reduction on the extent of metal reduction of Co/Al_2O_3 was measured using TPO and the effect on the activity and selectivity of the catalyst for the reductive amination of ethanol was evaluated.

3.2.3.1.1. Temperature programmed oxidation

Figure 3.40. illustrates the TPO spectra of the Co/Al_2O_3 catalysts in which the temperature of hydrogen reduction was varied. The spectra represent the oxidation profiles of the Al_2O_3 supported cobalt catalysts in a 60 ml(NTP)/min 2% O_2/He stream as the temperature was increased from 100 to 1000°C at 10°C/min. Prior reduction of the catalyst sample was performed using a 60 ml(NTP)/min 5% H_2/N_2 stream. The temperature of hydrogen reduction was varied between 300 and 600°C and the time of reduction was 1 hour.

Increasing the temperature of hydrogen reduction of the Co/Al_2O_3 catalyst from 300 to 600°C resulted in an increase in the size of the oxygen uptake peak occurring at low temperatures. This corresponding increase in the extent of metal reduction is from 1 to 27% (Table 3.15.). The increased extents of cobalt reduction are accompanied by a decrease in the level of residual unreduced divalent cobalt species.

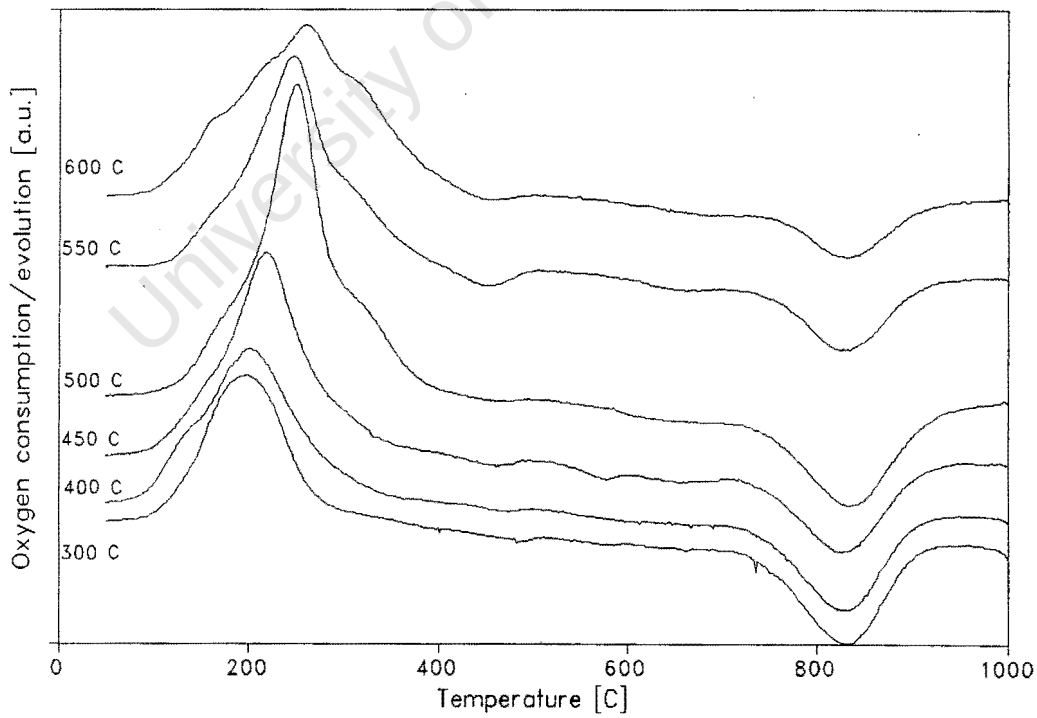

Figure 3.40. TPO spectra of Co/Al_2O_3 catalysts reduced at different temperatures (Reducing gas = 60 ml(NTP)/min 5% H_2/N_2, reduction time = 1 hour, oxidizing gas = 60 ml(NTP)/min 2% O_2/He, temperature programming rate = 10°C/min, $m_{cat} \approx 0.50$ g)

The concentration of non-oxidizable divalent cobalt species first decreased and then increased with increasing temperature of hydrogen reduction. Increasing the temperature of catalyst activation up to 450°C therefore appears to enable the reduction of stable cobalt-alumina support species. The increase in the formation of stable cobalt-support species at higher reduction temperatures may be caused by the increased diffusion of metal ions into the Al_2O_3 lattice where they are not easily reduced.

Table 3.15. Composition and metal oxidation temperatures during TPO of Co/Al_2O_3 catalysts reduced at different temperatures

Reduction Temperature	Zerovalent Co (mol %)	Oxidizable Co^{2+} (mol %)	Non-oxidizable Co^{2+} (mol %)	$T_{oxidation}$ (°C)
300°C	1	72	27	190
400°C	4	70	26	200
450°C	6	79	15	220
500°C	8	65	27	240
550°C	15	53	32	240
600°C	27	25	48	260

The temperature at which maximum oxygen uptake was observed increased with increasing temperature of hydrogen reduction. Since unsupported cobalt metal showed a maximum oxygen uptake at a temperature of 298°C (Figure 2.2.), it appears that the supported cobalt is becoming more similar in nature to its unsupported counterpart. Increasing the reduction temperature results in increased metal mobility which leads to larger metal crystallites. If the temperature of maximum oxygen uptake was influenced by the rate of oxygen diffusion through the metal particle during the TPO experiment, an increase in the metal particle size would result in an increase in the temperature of maximum oxygen uptake. Since the average

particle size of the unsupported cobalt crystallites is expected to be large, this increase in the temperature of maximum oxygen uptake could be related to the increased metal particle sizes obtained with increasing reduction temperatures.

3.2.3.2.2. Hydrogen chemisorption

The adsorption isotherms of the Co/Al_2O_3 catalysts were measured at 125°C due to the activated nature of hydrogen adsorption on cobalt [Reuel and Bartholomew, 1984]. Prior to adsorption, the catalysts were reduced in a 60 ml(NTP)/min H_2 stream after which they were evacuated at 400°C for 3 hours in order to remove all residual adsorbed species. The time of hydrogen reduction was 1 hour and the temperature of reduction was adjusted as per the experimental requirements.

The chemisorption measurements indicate that the reduced metal surface area first increases and then decreases with increasing temperature of hydrogen reduction (Table 3.16.). The highest metal surface area was obtained at a reduction temperature of 500°C. The optimum in the surface area of reduced cobalt can be ascribed to the counteractive processes of increased metal reduction and increased metal sintering. Increasing the reduction temperature increases the extent of metal reduction therefore increasing the number of cobalt atoms available for adsorption. The increased temperature of activation also results in increased metal mobility which results in larger crystallites and consequently decreased surface areas. The decrease in metal dispersion is accompanied by an increase in the average diameter of the supported metal crystallites.

Table 3.16. Surface area, dispersion, diameter and reversibility of hydrogen adsorption of Co/Al_2O_3 catalysts reduced at different temperatures

Reduction Temperature	Surface Area (m^2/g_{cat})	Dispersion (%)	Diameter (nm)	Reversibility (%)
300°C	0.13	25.9	3.7	82
400°C	0.33	14.9	7.3	66
450°C	0.51	16.3	5.9	54
500°C	0.59	14.7	6.7	51
550°C	0.42	5.7	16.8	57
600°C	0.38	2.9	33.7	48

The reversibility of hydrogen adsorption on the Al_2O_3 supported cobalt decreased with increasing temperature of hydrogen reduction, *i.e.* the percentage of weak hydrogen adsorption sites increases with increasing temperature of hydrogen reduction. The decrease in the reversibility of hydrogen adsorption on the supported cobalt indicates a change in the surface coordination of the supported metal crystallites and could possibly be related to the changes in particle size occurring with increasing temperature of hydrogen reduction.

3.2.2.3.3. Reductive amination of ethanol

The influence of the reduction temperature on the activity and selectivity of Al_2O_3 supported cobalt was evaluated at a reaction temperature of 180°C, a WHSV of 1 g_{EtOH}/g_{cat}·h and an EtOH : NH_3 : H_2 : N_2 molar ratio of 1 : 2 : 8.6 : 17.6. Prior to amination, the catalyst precursor was reduced in a 60 ml(NTP)/min stream of H_2 at the specified reduction temperature for 1 hour. The steady state activity of the Co/Al_2O_3 catalysts as a function of the reduction temperature is reported in Figure 3.41.

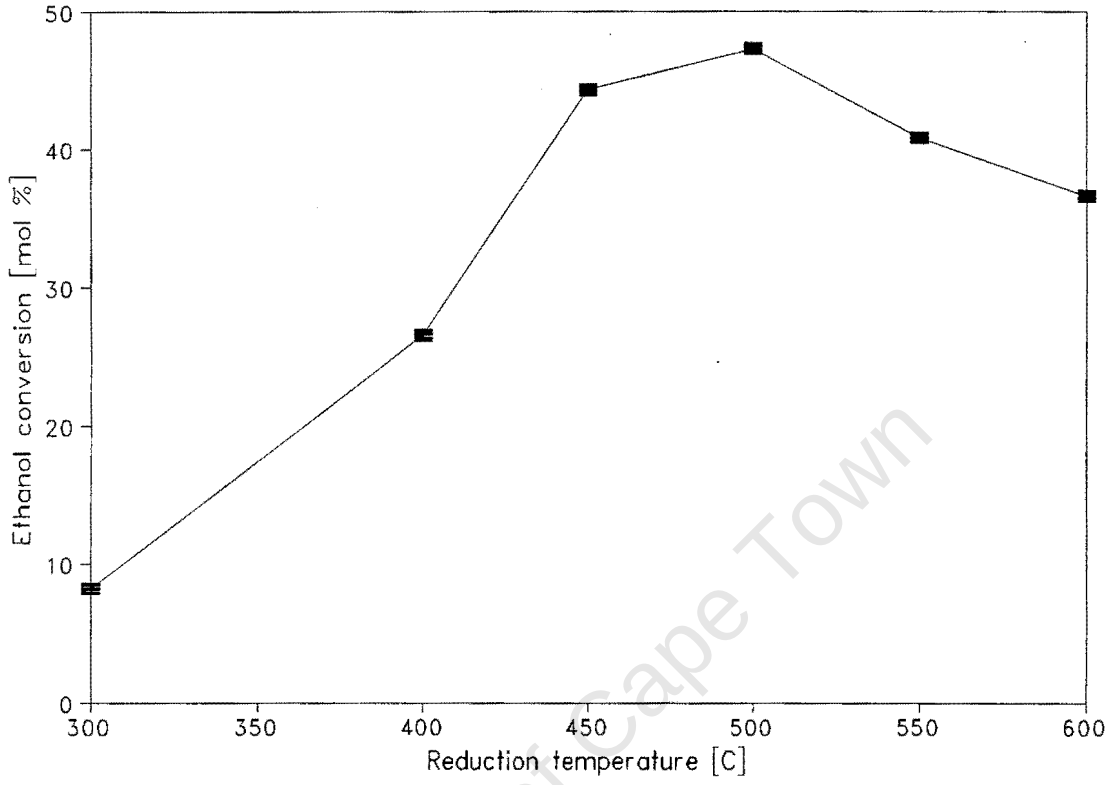

Figure 3.41. Steady state activity of Co/Al_2O_3 as a function of the reduction temperature ($T = 180^{\circ}C$, $P = 1$ bar, WHSV = 1 g_{EtOH}/g_{cat}·h, EtOH : NH_3 : H_2 : N_2 = 1 : 2 : 8.6 : 17.6)

The activity of Al_2O_3 supported cobalt for the conversion of ethanol first increased and then decreased with increasing temperature of hydrogen reduction. The measured activity was in accordance with the metallic surface areas measured using hydrogen chemisorption. This indicates that the conversion of ethanol is proportional to the number of cobalt atoms available for reactant adsorption.

The selectivity to individual ethylamine products varied significantly with changes in the temperature of hydrogen reduction (Figure 3.42.). The MEA selectivity first decreased and then increased and the DEA and TEA selectivities first increased and then decreased with increasing temperature of hydrogen reduction. The respective maxima and minima correspond roughly with the temperature at which maximum ethanol conversion activity is obtained. The temperature of hydrogen reduction therefore results in a change in the nature of the supported cobalt catalyst which results in changes in ethylamine selectivity.

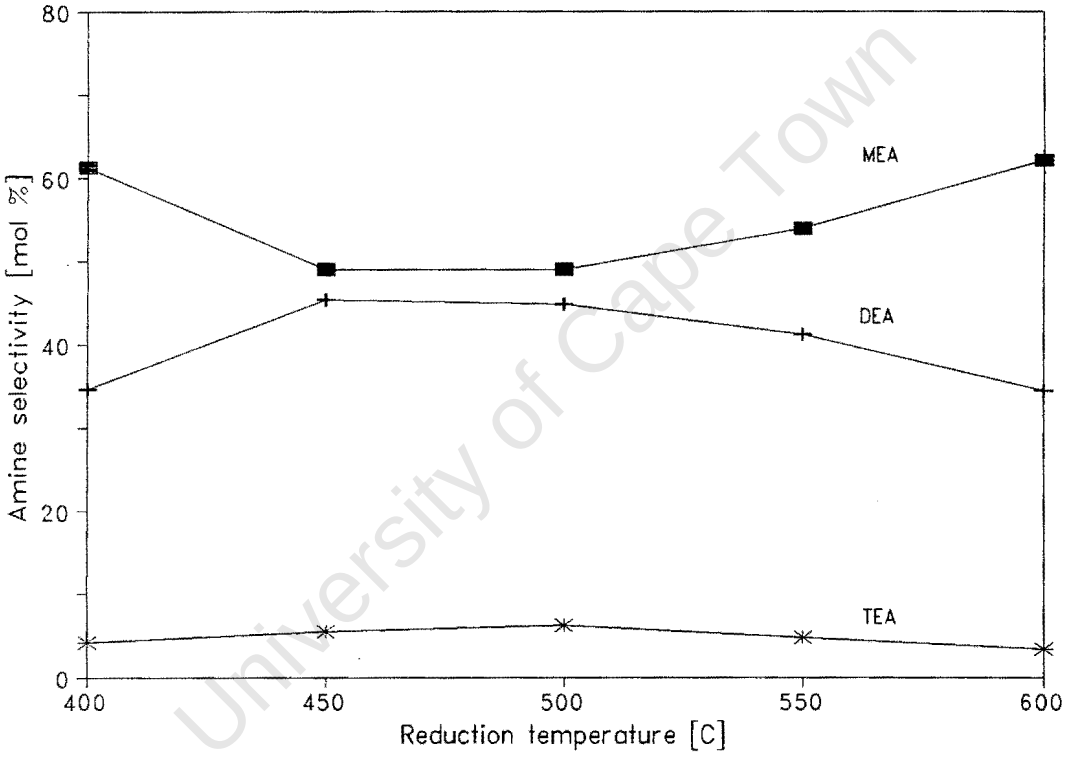

Figure 3.42. Effect of reduction temperature on ethylamine selectivity of Co/Al_2O_3
(T = 180°C, P = 1 bar, EtOH : NH_3 : H_2 : N_2 = 1 : 2 : 8.6 : 17.6, ethanol conversion = 50%)

Table 3.17. Effect of reduction temperature on the activity and selectivity of Co/Al_2O_3

Reduction Temperature	Conversion[1] (mol %)	MEA Selectivity[2] (mol %)	DEA Selectivity[2] (mol %)	TEA Selectivity[2] (mol) %
300°C	8.2	-[3]	-[3]	-[3]
400°C	26.6	61.3	34.6	4.1
450°C	44.3	49	45.4	5.6
500°C	47.2	49	44.8	6.3
550°C	40.8	54	41.2	4.8
600°C	36.6	62.1	34.5	3.4

[1] Ethanol conversion measured at a WHSV of 1 g_{EtOH}/g_{cat}·h

[2] Selectivities interpolated to an ethanol conversion of 35%

[3] Activity too low for valid comparison

3.2.3.2. Effect of Reduction Time

The time of hydrogen reduction is an important parameter in the activation of metallic catalysts since if the reduction process is slow, an increase in the time of reduction will result in increased extents of metal reduction. In the case of oxide reduction, an increase in the extent of reduction will change the ratio of reduced metal to unreduced metal oxide in the activated catalyst. The presence of unreduced metal oxide will affect the bulk electronic properties of the metal crystallite and therefore its catalytic properties. The object of this experiment was to investigate the effect of the time of hydrogen reduction on the reducibility and the catalytic properties of Al_2O_3 supported cobalt.

3.2.3.2.1. Temperature programmed oxidation

The TPO spectra of the Al_2O_3 supported cobalt catalysts were measured between 50 and 1000°C using a 60 ml(NTP)/min 2% O_2/He mixture as the oxidizing agent. Prior to recording the TPO spectra, the catalyst precursors were reduced in a 60 ml(NTP)/min stream of 5% H_2/N_2 at 500°C for periods ranging between 1 and 20 hours. The TPO spectra are illustrated in Figure 3.43.

Increasing the time of hydrogen reduction of Al_2O_3 supported cobalt catalysts resulted in an increase in the size of the low temperature oxygen uptake peak and a decrease in the area of the high temperature oxygen release. The increase in the size of the low temperature oxygen uptake corresponded to an increase in the extent of cobalt reduction from 18 to 40% as the reduction time at 500°C was increased from 1 to 20 hours (Table 3.18.). The decrease in the high temperature oxygen release with increasing reduction time corresponds to an increase in the formation of non-oxidizable Co^{2+} species. It therefore appears that by increasing the time of high temperature reduction, oxidizable Co^{2+} can either be reduced to zerovalent cobalt or transformed into stable cobalt-alumina species, *i.e.* there is a competing reaction between the reduction reaction which forms metallic cobalt and diffusion of cobalt ions into the Al_2O_3 lattice to form cobalt-alumina spinel species.

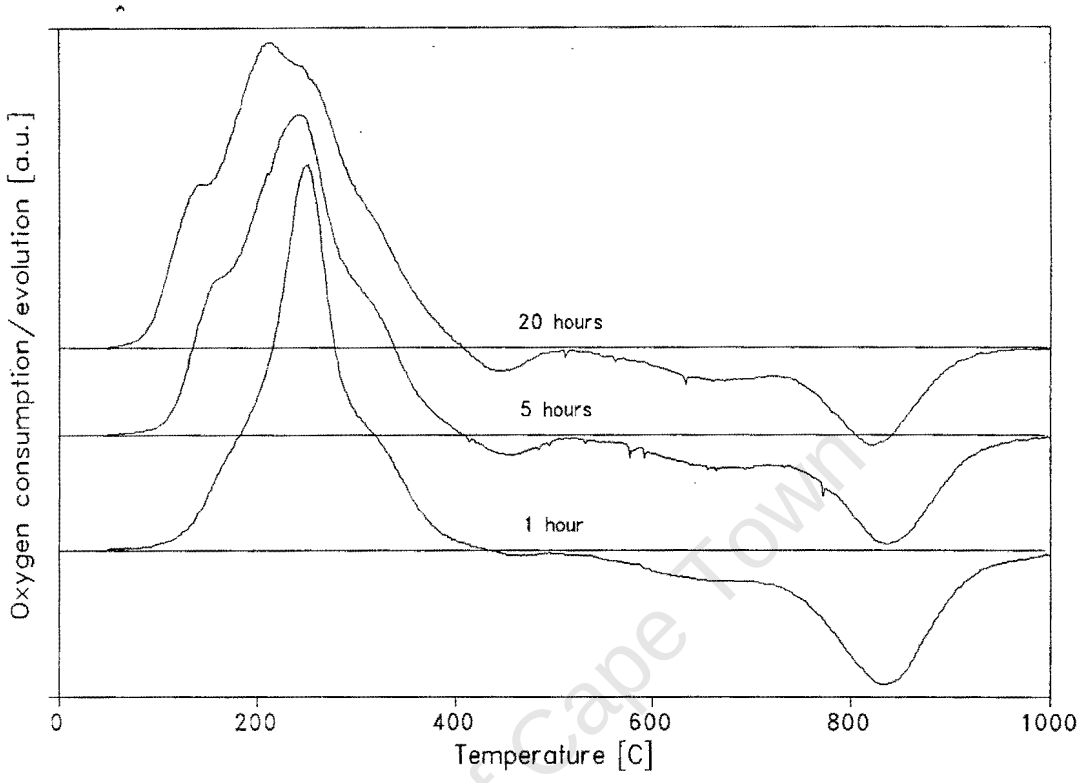

Figure 3.43. Effect of reduction time on TPO spectra of Co/Al_2O_3
(Reducing gas = 60 ml(NTP)/min 5% H_2/N_2, reduction temperature = 500°C, oxidizing gas = 60 ml(NTP)/min 2% O_2/He, temperature programming rate = 10°C/min, $m_{cat} \approx 0.50$ g)

The temperature at which maximum oxygen uptake was observed decreased as the reduction time at 500°C was increased. Since the average crystallite diameter of the supported cobalt crystallites increases with increasing reduction time (see Chapter 3.2.3.2.2.), it is evident that the changes in the temperature of maximum oxygen uptake are not caused by diffusion limitations. These changes may be caused by a change in the degree of interaction of the cobalt crystallites with the Al_2O_3 support or by a change in the chemical environment of the metal particles.

Table 3.18. Composition and metal oxidation temperatures during TPO of Co/Al_2O_3 catalysts reduced for different times at 500°C

Reduction Time	Zerovalent Co (mol %)	Oxidizable Co^{2+} (mol %)	Non-oxidizable Co^{2+} (mol %)	$T_{oxidation}$ (°C)
1 hour	18.1	70.7	11.2	250
5 hours	29.4	57.5	13.1	240
20 hours	39.5	37.6	22.9	210

3.2.3.2.2. Hydrogen chemisorption

The surface areas of the reduced Co/Al_2O_3 catalysts were calculated by measuring the hydrogen adsorption isotherms at 125°C. The catalysts were activated by reduction in a 60 ml(NTP)/min H_2 stream at 500°C for periods ranging between 1 and 20 hours. Following reduction, the catalysts were evacuated at 400°C for 3 hours in order to remove any adsorbed species remaining on the catalyst surface after the reduction process. Table 3.19. summarizes the results of the chemisorption measurements.

Table 3.19. Surface area, dispersion, diameter and reversibility of hydrogen adsorption on Co/Al_2O_3 catalysts reduced at 500°C for different times

Reduction Time	Surface Area (m^2/g_{cat})	Dispersion (%)	Diameter (nm)	Reversibility (%)
1 hour	0.59	6.5	14.7	50
5 hours	0.69	4.7	20.5	66
20 hours	0.79	4.0	24.1	58

The chemisorption results indicated that increasing the time of hydrogen reduction at 500°C

resulted in an increase in the exposed metal surface area of Al_2O_3 supported cobalt catalysts. The increase in the number of exposed metal atoms with increasing the time of reduction was caused by the increased extents of metal reduction. The increase in the metal surface area was not directly proportional to the increase in the extent of metal reduction however because of the increased amount of metal crystallite agglomeration with increasing reduction time. The reversibility of hydrogen adsorption first increased and then decreased with increasing time of hydrogen reduction. No direct relationship between the time of hydrogen reduction at 500°C and the reversibility of hydrogen adsorption was therefore obtained.

3.2.3.2.3. Reductive amination of ethanol

The effect of the time of hydrogen reduction on the performance of Al_2O_3 supported cobalt on the activity and selectivity during reductive amination was investigated at a temperature of 180°C, a WHSV of 1 g_{EtOH}/g_{cat}·h and an EtOH : NH_3 : H_2 : N_2 molar ratio of 1 : 2 : 8.6 : 17.6. Prior to the evaluation of the catalytic performance of the Co/Al_2O_3 catalyst, the catalyst precursor was reduced in a 60 ml(NTP)/min H_2 stream at 500°C for times ranging between 1 and 20 hours. The effect of the time of hydrogen reduction on the time on stream activity of Co/Al_2O_3 is illustrated in Figure 3.44.

Increasing the time of hydrogen reduction at 500°C from 1 to 5 to 20 hours resulted in an increase in the initial ethanol conversion of the Co/Al_2O_3 catalyst from 65 to 72 to 81%. The initial activity (*i.e.* the activity extrapolated to t = 0) corresponded to the increase in the metal surface area as measured using hydrogen chemisorption. This relationship is not valid at steady state since the Co/Al_2O_3 catalyst reduced for 5 hours did not deactivate to the same extent as the catalysts reduced for 1 and 20 hours respectively. The Co/Al_2O_3 catalyst reduced for 5 hours at 500°C therefore appears to be less susceptible to deactivation.

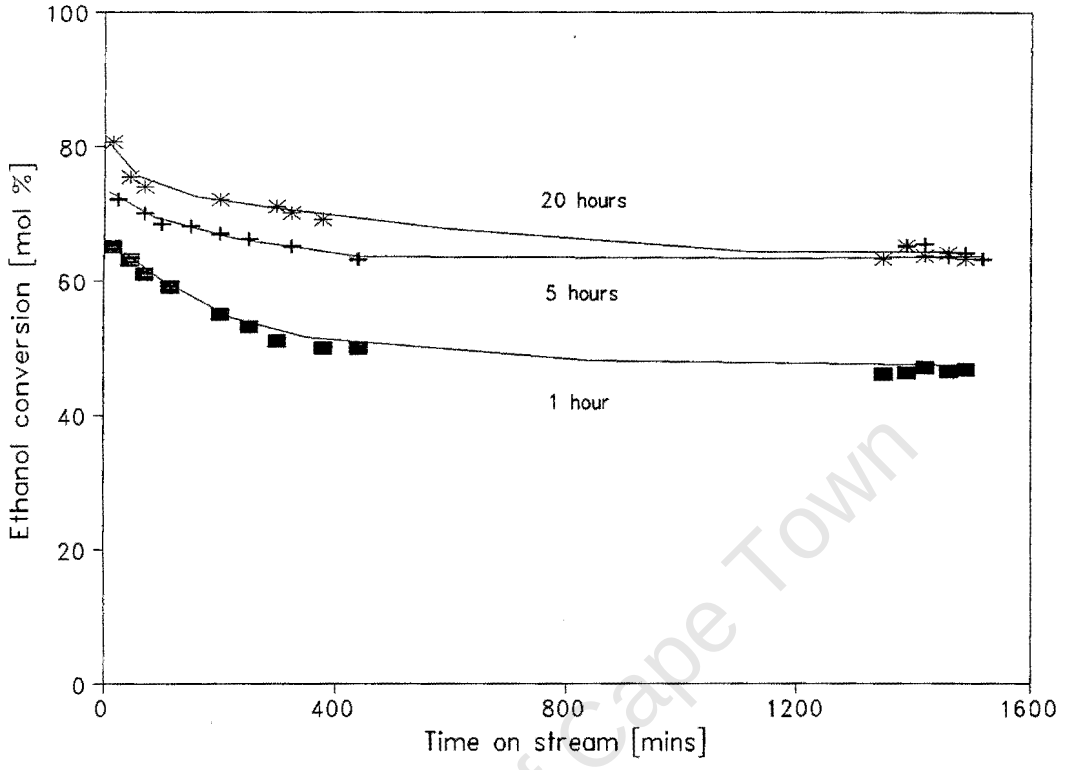

Figure 3.44. Effect of reduction time on the time on stream activity of Co/Al_2O_3
(T = 180°C, P = 1 bar, WHSV = 1 g_{EtOH}/g_{cat}·h, EtOH : NH_3 : H_2 : N_2 = 1 : 2 : 8.6 : 17.6)

The selectivity to individual ethylamine products changed with changing time of hydrogen reduction at 500°C (Table 3.20.). The MEA and TEA selectivities decreased and the DEA selectivity increased with increasing time of hydrogen reduction. These changes in selectivity are due to changes in the nature of the supported cobalt catalyst since the selectivities are compared at the same ethanol conversion.

Table 3.20. Effect of the reduction time on the activity and selectivity of Co/Al_2O_3
(T = 180°C, P = 1 bar, WHSV = 1 g_{EtOH}/g_{cat}·h, EtOH : NH_3 : H_2 : N_2 = 1 : 2 : 8.6 : 17.6)

Reduction time	Conversion[1] (mol %)	MEA Selectivity[2] (mol %)	DEA Selectivity[2] (mol %)	TEA Selectivity[2] (mol %)
1 hour	47.2	46.4	45.7	7.9
5 hours	64.5	43.3	49.2	7.5
20 hours	65.8	42.6	50.1	7.3

[1] Conversion measured at a WHSV of 1 g_{EtOH}/g_{cat}·h
[2] Selectivities interpolated to an ethanol conversion of 50%

3.2.3.3. Effect of the Calcination Atmosphere

Catalyst calcination is a thermal pretreatment procedure which serves to decompose the metal precursor material to the bulk oxide. This procedure can result in changes in both the dispersion and the reducibility of supported metal catalysts. In general, the metal dispersion is determined by the degree of interaction between the precursor compound and the support material and by the temperature of activation. The mobility of certain metal species has been shown to vary with the nature of the pretreatment gas however which can result in changes in metallic dispersion. The formation of difficult to reduce metal-support species may also be affected by the chemical nature of the calcination gas. The formation of difficult to reduce nickel-alumina spinels was more pronounced when Ni/Al_2O_3 catalysts were thermally activated using N_2 instead of air, therefore resulting in lower extents of metal reduction [LoJacono *et al*, 1971]. The effect of the calcination atmosphere on the activity and selectivity of Co/SiO_2 catalysts was investigated using air and N_2 as calcination media and the performance of these catalysts was compared to a catalyst reduced directly following drying (*i.e.* without prior calcination).

3.2.3.3.1. Temperature programmed reduction

The TPR spectra of the Co/SiO_2 catalysts in which the calcination gas was varied are illustrated in Figure 3.45. The spectra represent the hydrogen uptake of the catalyst samples in a 60 ml(NTP)/min 5% H_2/N_2 stream as the temperature was increased linearly from 100 to 1000°C at 10°C. The calcined catalysts were activated in a 60 ml(NTP)/min stream of either air or N_2 at 400°C for 1 hour using a temperature programming rate of 10°C/min.

The TPR spectra indicated significant changes in the reduction profile of the Co/SiO_2 catalyst following calcination. Most notably, the sharp hydrogen consumption peak corresponding to the reductive decomposition of the nitrate precursor was no longer present. Thermal activation at 400°C therefore decomposes the cobalt nitrate precursor. The reduction profiles of the air and N_2 calcined catalysts were very similar however which indicates that the decomposition of the nitrate precursor is not significantly affected by the chemical nature of

the calcination medium.

Measurement of the hydrogen consumption during TPR confirms the removal of the nitrate ion by calcination at 400°C using air or N_2 (Table 3.21.). Direct reduction of the Co/SiO_2 catalyst without prior calcination results in a measured H_2 : Co molar ratio of 1.88. Reduction of divalent cobalt results in a H_2 : Co molar ratio of 1 and reduction of trivalent cobalt results in a H_2 : Co molar ratio of 1.5. The increased hydrogen consumption can therefore be ascribed to reduction of the nitrate ion. The H_2 : Co molar ratios of the Co/SiO_2 catalysts calcined in air and nitrogen were 1.33 and 1.31 respectively which indicates the reduction of a mixture of divalent and trivalent cobalt species.

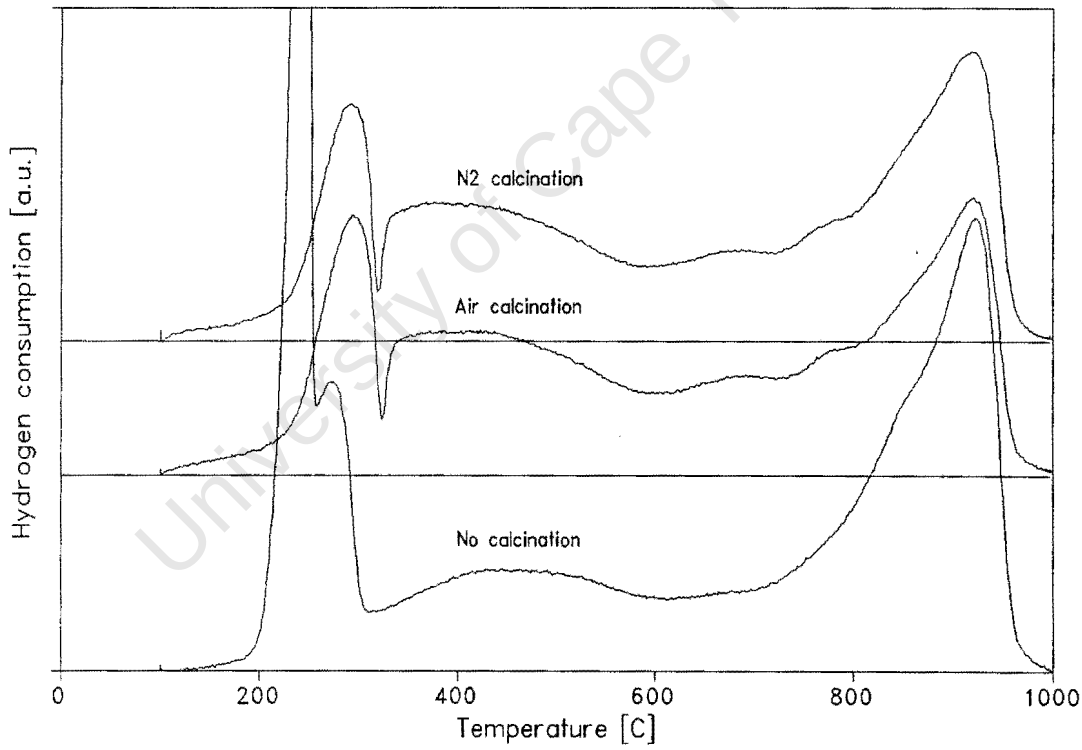

Figure 3.45. Effect of calcination medium on TPR spectra of Co/SiO_2
(Calcination gas = 60 ml(NTP)/min air or N_2, calcination temperature = 400°C, reducing gas = 60 ml(NTP)/min 5% H_2/N_2, temperature programming rate = 10°C/min, $m_{cat} \approx 0.15$ g)

Besides changing the hydrogen consumption during TPR, precalcination resulted in a change

in the reducibility of the supported cobalt. The extent of metal reduction (as measured by the hydrogen consumption occurring at temperatures greater than 500°C) was increased by precalcination of the Co/SiO_2 catalyst principally due to a decrease in the high temperature hydrogen consumption attributed to cobalt-silicate reduction. The extent of metal reduction for both the air and N_2 calcined catalysts was similar. This indicates that the decreased cobalt-silicate formation was probably due to thermal pretreatment alone since the two calcination gases differed considerably with regards to their chemical properties.

Table 3.21. Effect of calcination medium on hydrogen consumption of SiO_2 supported cobalt

Calcination atmosphere	$(H_2 : Co)_{total}$ (mol : mol)	$(H_2 : Co)_{>500}$ (mol : mol)
No calcination	1.88	1.00
Air calcination	1.33	0.79
N_2 calcination	1.31	0.80

3.2.3.3.2. Reductive amination of ethanol

The influence of the calcination atmosphere on the activity and selectivity of Co/SiO_2 was evaluated at a temperature of 180°C, a WHSV of 1 g_{EtOH}/g_{cat}·h and an EtOH : NH_3 : H_2 : N_2 molar ratio of 1 : 2 : 8.6 : 17.6. Catalyst activation consisted of calcination in a 60 ml(NTP)/min stream of either air or N_2 at 400°C for 1 hour followed by reduction in a 60 ml(NTP)/min H_2 stream at 500°C for 1 hour. The time on stream activity of these catalysts is illustrated in Figure 3.46.

Direct reduction of the Co/SiO_2 catalyst resulted in the most active amination catalyst even though the extent of metal reduction as measured using TPR was lower than the precalcined catalysts. The activities of the air and N_2 calcined catalysts were very similar as expected from the similar reduction profiles obtained during TPR. The decreased activity of the

precalcined catalysts is probably due to increased metal crystallite sintering occurring during the calcination procedure.

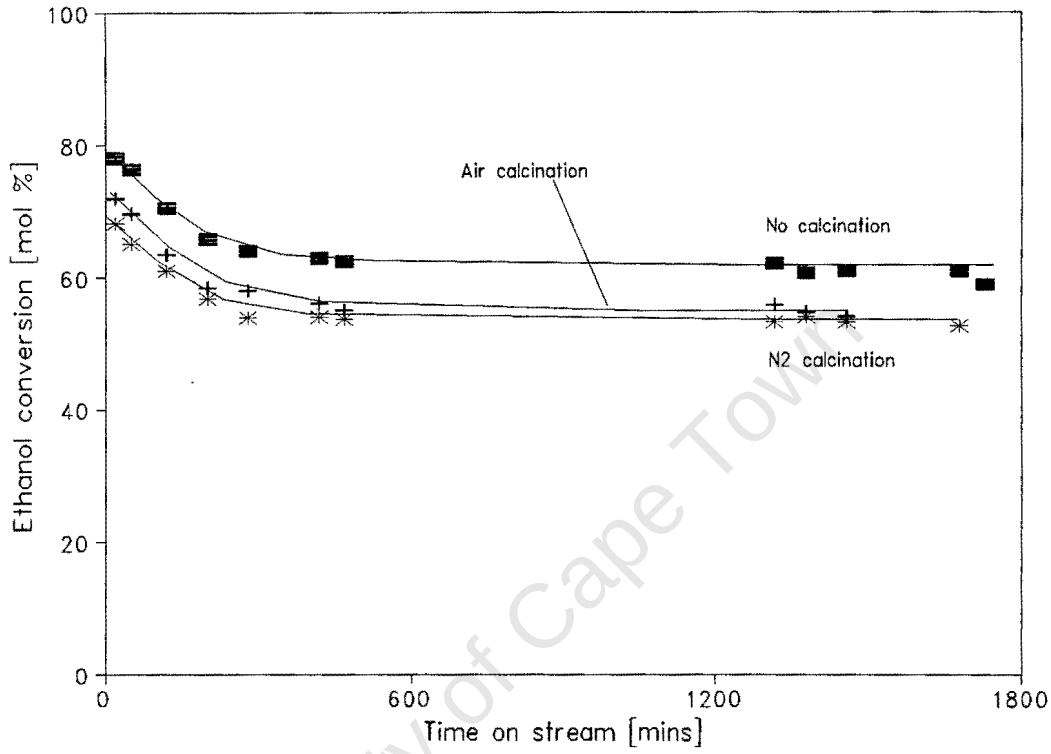

Figure 3.46. Effect of calcination on the time on stream behaviour of Co/SiO_2
(T = 180°C, P = 1 bar, WHSV = 1 g_{EtOH}/g_{cat}·h, EtOH : NH_3 : H_2 : N_2 = 1 : 2 : 8.6 : 17.6)

A change in the calcination gas from air to N_2 changes the selectivity to individual ethylamine products even though the activity for ethanol conversion is nearly identical (Table 3.22.). The selectivity to MEA was lower and the selectivity to DEA and TEA was higher when using the N_2 calcined catalyst instead of the air calcined catalyst. Accurate comparison between the selectivity of the precalcined catalysts and the catalyst reduced directly cannot be made since the selectivity measurements were recorded at different ethanol conversions. From the data available, it appears that the selectivity to individual ethylamine products obtained using the Co/SiO_2 catalyst which was reduced without prior calcination is similar to the selectivities obtained with the air calcined catalyst.

Table 3.22. Effect of the calcination atmosphere on the activity and selectivity of Co/SiO_2 ($T = 180^{\circ}C$, $P = 1$ bar, WHSV = 1 g_{EtOH}/g_{cat}·h, EtOH : NH_3 : H_2 : N_2 = 1 : 2 : 8.6 : 17.6)

Calcination gas	Conversion (mol %)	MEA Selectivity (mol %)	DEA Selectivity (mol %)	TEA Selectivity (mol %)
None	60.4	41.9	43.6	14.1
Air	54.9	42.1	43.1	14.4
N_2	53.2	36.9	43.5	18.9

3.2.3.4. Effect of the Calcination Temperature

Increasing the calcination temperature can alter the physical and catalytic properties of a supported metal catalyst considerably. For example, by increasing the temperature of catalyst calcination in a series of Al_2O_3 supported catalysts a number of different cobalt species were obtained [Arnoldy and Moulijn, 1985]. The reducibility of the cobalt and therefore the amount of metal available for reaction in the final catalyst formulation therefore depends considerably on the temperature of precalcination. Whereas the reducibility of Co/Al_2O_3 catalysts generally decreases with increasing temperature of calcination due to the formation of cobalt-alumina surface spinels [Arnoldy and Moulijn, 1985; LoJacono *et al*, 1971], the reducibility of Co/SiO_2 catalysts is increased with increasing temperature of precalcination [Rosynek and Polansky, 1991]. It is therefore possible that an optimum calcination temperature exists such that metal reducibility is increased whilst not sacrificing metal dispersion which is decreased by high temperature pretreatment. This experiment outlines the influence of the calcination temperature on the metal reducibility as well as the activity and selectivity of Co/SiO_2 catalysts for the reductive amination reaction.

3.2.3.4.1. Temperature programmed reduction

The TPR spectra of the Co/SiO_2 catalysts in which the temperature of air calcination was changed are illustrated in Figure 3.47. The spectra represent the hydrogen consumption profiles of the catalyst samples in a 60 ml(NTP)/min 5% H_2/N_2 stream upon increasing the temperature from 100 to 1000°C at 10°C/min. Calcination of the catalyst samples was performed using a 60 ml(NTP)/min air stream at the specified calcination temperature of either 400 or 600°C for 1 hour.

Calcination of the Co/SiO_2 catalyst at 400 or 600°C resulted in the total decomposition of the nitrate precursor so that the sharp hydrogen consumption peak corresponding to reduction of the nitrate ion was no longer observed. Accordingly, the measured H_2 : Co ratios of the catalysts calcined at 400 and 600°C were 1.33 which is characteristic of the reduction of a mixture of divalent and trivalent cobalt species (Table 3.23.). Measurement of the hydrogen

consumption occurring at temperatures greater than 500°C indicated that the extent of metal reduction at 500°C increased with increasing temperature of air calcination.

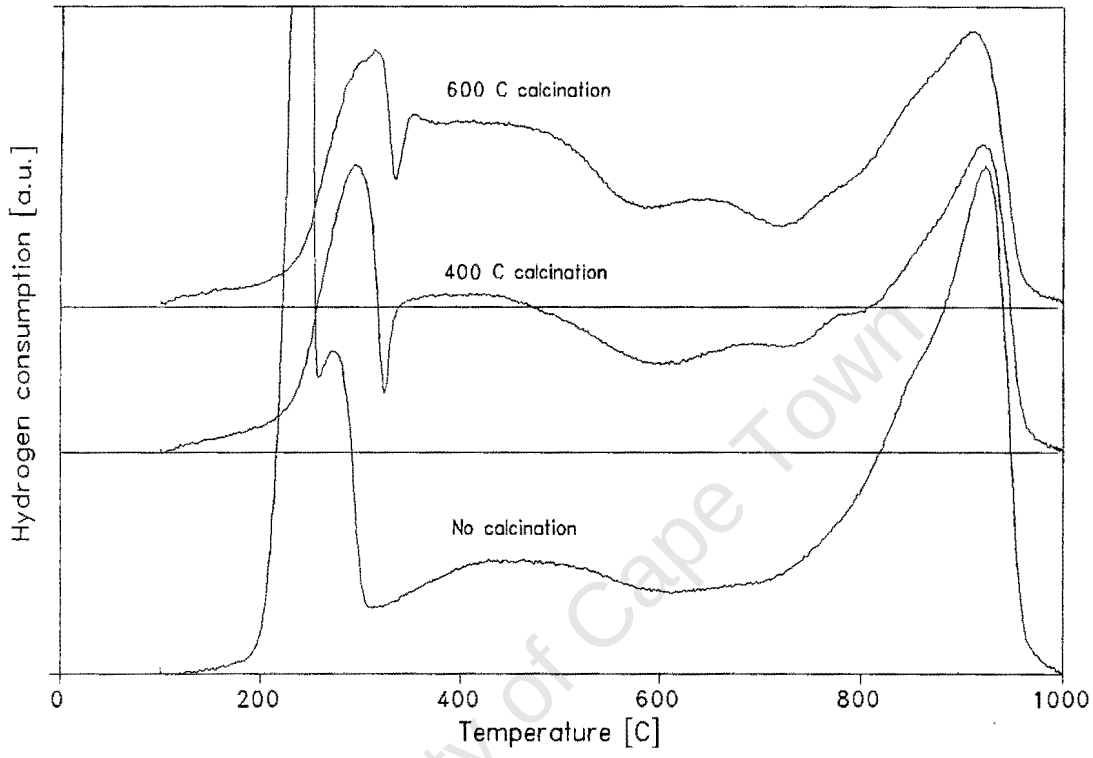

Figure 3.47. Effect of calcination temperature on TPR spectra of Co/SiO_2 catalysts (Calcination gas = 60 ml(NTP)/min air, reducing gas = 60 ml(NTP)/min 5% H_2/N_2, temperature programming rate = 10°C/min, $m_{cat} \approx 0.15$ g).

Table 3.23. Hydrogen consumption during TPR and reduction peak temperatures of Co/SiO_2 catalysts calcined at different temperatures

Calcination temperature	$(H_2 : Co)_{total}$ (mol : mol)	$(H_2 : Co)_{>500}$ (mol : mol)
No calcination	1.88	1.00
400°C	1.33	0.79
600°C	1.33	0.75

3.2.3.4.2. Reductive amination of ethanol

The effect of the calcination temperature on the activity and selectivity of Co/SiO_2 was measured at a temperature of 180°C, a WHSV of 1 g_{EtOH}/g_{cat}·h and an EtOH : NH_3 : H_2 : N_2 = 1 : 2 : 8.6 : 17.6. Catalyst activation comprised calcination in a 60 ml(NTP)/min air stream at either 400 or 600° for 1 hour followed by reduction in a 60 ml(NTP)/min 5% H_2/N_2 stream at 500°C for 1 hour. The time on stream activity of these catalysts is illustrated in Figure 3.48.

Increasing the temperature of air calcination decreased the ethanol conversion activity of SiO_2 supported cobalt catalysts. The decrease in activity is probably caused by increasing metal particle agglomeration with increasing temperature of the calcination step since the TPR results showed that increasing the calcination temperature increased the extent of metal reduction by 500°C.

Comparison of the selectivity to individual ethylamine products indicated that the degree of amine substitution decreased with increasing temperature of air calcination, *i.e.* the MEA selectivity increased and the DEA and TEA selectivities decreased (Table 3.24.). It is possible however that the differences in amine selectivity are caused by the fact that the measurements were recorded at different conversions of the reactant ethanol since increasing the ethanol conversion increases the degree of amine substitution [Sewell *et al*, 1995].

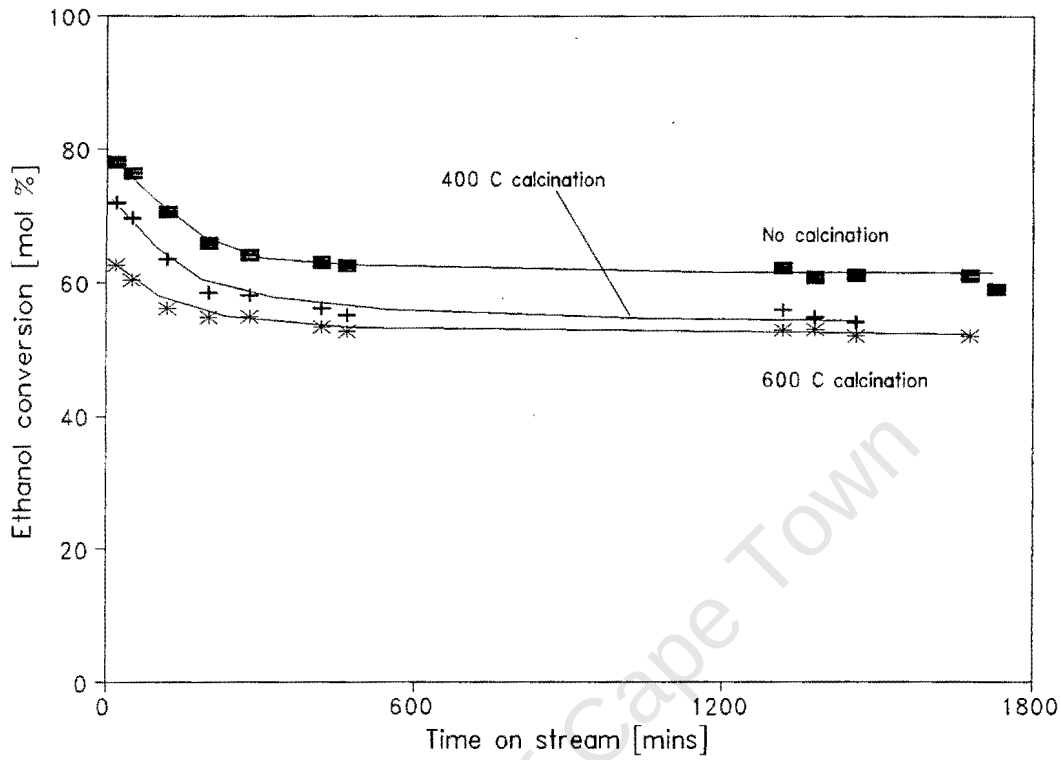

Figure 3.48. Influence of the precalcination temperature on the time on stream activity of Co/SiO_2 (T = 180°C, P = 1 bar, WHSV = 1 g_{EtOH}/g_{cat}·h, EtOH : NH_3 : H_2 : N_2 = 1 : 2 : 8.6 : 17.6).

Table 3.24. Effect of the calcination temperature on the activity and selectivity of Co/SiO_2 (T = 180°C, P = 1 bar, WHSV = 1 g_{EtOH}/g_{cat}·h, EtOH : NH_3 : H_2 : N_2 = 1 : 2 : 8.6 : 17.6)

Calcination temperature	Conversion (mol %)	MEA Selectivity (mol %)	DEA Selectivity (mol %)	TEA Selectivity (mol %)
No calcination	60.4	41.9	43.6	14.1
400°C calcination	54.9	42.1	43.1	14.4
600°C calcination	52.3	44.4	42.2	12.9

3.3. TPR Study of Co/SiO_2 catalysts

It is well known that several kinds of cobalt species are formed during the preparation of SiO_2 supported cobalt catalysts [Ming and Baker, 1995; Matsuzaki *et al*, 1993; Rosynek and Polansky, 1991; Lapidus *et al*, 1991; van't Blik *et al*, 1986; Puskas *et al*, 1992; Bessell, 1993]. The type and amount of these various cobalt-support species depends on the starting salt, the metal loading and the preparation procedure. Although the formation of these cobalt-silicate species which are difficult to reduce results in a loss of the active metallic component, it has been proposed that these species act as anchors for the reduced metal crystallites therefore inhibiting agglomeration [van't Blik *et al*, 1986].

A number of studies have been conducted which have investigated the effect of the catalyst preparation and activation steps on the reducibility of SiO_2 supported cobalt catalysts [Rosynek and Polansky, 1991; Puskas *et al*, 1992; Ming and Baker, 1995]. These studies have not been exhaustive and the nature and formation of cobalt-silicate compounds has not been comprehensively elucidated. The object of this investigation was therefore to vary systematically the preparation and activation conditions of a series of Co/SiO_2 catalysts and thereby evaluate the formation of these cobalt-silicate species. Temperature programmed reduction (TPR) was used as a tool to characterize and quantify the various cobalt species in the Co/SiO_2 catalysts.

3.3.1. Effect of Drying Conditions

The influence of the drying conditions on the formation of cobalt silicate species was investigated by varying the time of drying between 1 and 48 hours at temperatures ranging from 60 to 150°C. The TPR spectra illustrate the hydrogen consumption profiles of the Co/SiO_2 catalysts following calcination in a 60 ml(NTP)/min N_2 stream at 400°C for 60 mins.

The reduction profiles of the Co/SiO_2 catalysts in which the time and temperature of drying were varied are characterized by 4 main regions of hydrogen consumption. These different

regions of hydrogen consumption correspond to the reduction of different cobalt species formed during the catalyst preparation and activation steps. In order to facilitate analysis of the hydrogen consumption during TPR, the spectra were subdivided into 4 separate regions. Peaks I, II, III and IV represent the hydrogen consumption occurring between 200 and 330°C, 330 and 600°C, 600 - 800°C and 800 - 1000°C respectively.

Increasing the time of drying at 60°C from 1 to 48 hours did not result in any significant changes in the TPR profile of the Co/SiO_2 catalysts (Figure 3.49.). Measurement of the hydrogen consumption by integration of the TCD signal indicates that the contribution of Peak IV increases slightly and the relative hydrogen consumption occurring in Peaks I and II decreases slightly with increasing drying time. These differences are small and are probably within the error of measurement of the TPR apparatus.

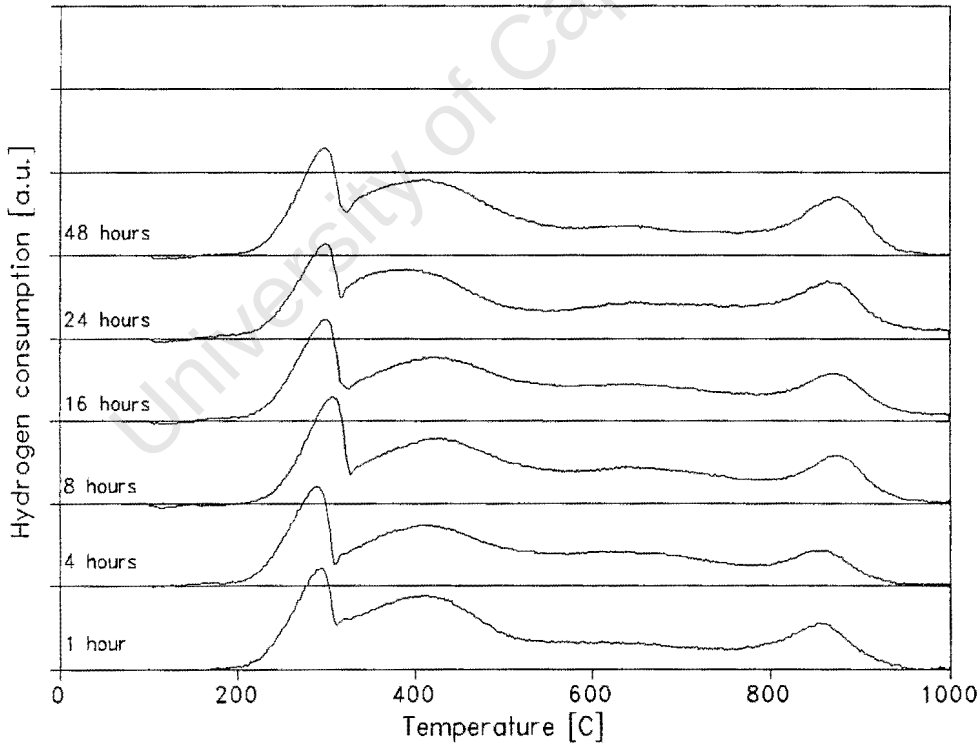

Figure 3.49. TPR spectra of Co/SiO_2 catalysts dried at 60°C for different times
(Reducing gas = 60 ml(NTP)/min 5% H_2/N_2, temperature programming rate = 10°C/min, $m_{cat} \approx 0.15$ g)

Measurement of the total hydrogen consumption occurring during TPR of the Co/SiO_2 catalysts dried at 60°C showed that the H_2 : Co ratio varied from 0.98 to 1.26 (Table 3.25). No direct relationship was observed between the overall hydrogen consumption and the time of drying at 60°C however. For the Co/SiO_2 catalyst dried at 60°C for 1 hour, the measured weight loss during TPR was 53% which indicated that a considerable portion of the impregnation solvent had remained in the catalyst precursor following the drying stage. The weight loss occurring during TPR decreased with increasing drying times which was caused by increased removal of the impregnation solvent during the drying stage.

The TPR spectra of the Co/SiO_2 catalysts in which the time of drying at 90°C was varied show similar reduction profiles to the catalysts dried at 60°C (Figure 3.50.). At increased drying times, however, the size of the hydrogen consumption peak occurring at temperatures greater than 800°C decreased slightly. The decrease in the high temperature hydrogen consumption with increased drying time at 90°C indicates that the formation of cobalt-silicate species is decreased.

The measured H_2 : Co ratio varied between 1.08 and 1.26 with hydrogen consumption increasing slightly with increasing drying time at 90°C. Although the overall hydrogen consumption increased slightly and the size of the high temperature peak decreased slightly with increasing drying time at 90°C, large differences in the TPR spectra were not observed.

Table 3.25. Effect of drying conditions on the hydrogen consumption during TPR of Co/SiO_2

Drying conditions	Peak 1 (mol %)	Peak 2 (mol %)	Peak 3 (mol %)	Peak 4 (mol %)	H_2 : Co ratio (mol H_2/mol Co)	E.O.R. [1] (mol %)
60°C - 1 hour	22.7	47.1	16.4	13.7	1.03	69.8
60°C - 4 hours	22.7	42.9	20.2	14.3	1.26	65.6
60°C - 8 hours	19.5	43.7	21.2	15.6	1.07	63.2
60°C - 16 hours	20.3	42.6	21.1	16	1.05	62.9
60°C - 24 hours	19.3	39.9	21.5	19.3	0.98	59.2
60°C - 48 hours	21.1	45	16.4	17.5	1.18	66.1
90°C - 1 hour	15.6	51.6	15.6	17.2	1.05	67.2
90°C - 4 hours	21.1	48.8	15	15.1	1.08	69.9
90°C - 8 hours	22.8	45.5	19.7	12	1.22	68.3
90°C - 16 hours	22	39.1	28.2	10.7	1.15	61.1
90°C - 24 hours	20.6	42.4	24.7	12.3	1.26	63.0
90°C - 48 hours	21	41.8	23.2	14.1	1.25	62.8
120°C - 1 hour	20.5	50.9	15.9	12.6	1.17	71.4
120°C - 4 hours	21.4	45.5	17.5	15.5	1.16	66.9
120°C - 8 hours	21.2	47.1	16.4	15.3	1.01	68.3
120°C - 16 hours	24.1	49.4	15.2	11.3	1.16	73.5
120°C - 24 hours	21	54.7	13.8	10.6	1.03	75.7
120°C - 48 hours	25.1	51.6	17	6.2	1.31	76.7
150°C - 1 hour	21.3	44.9	21.5	12.2	1.12	66.2
150°C - 4 hours	17.4	47.9	20.9	13.7	1.12	65.3
150°C - 8 hours	22.9	57.3	15.5	4.3	1.11	80.2
150°C - 16 hours	20.9	49.7	20.3	9.1	1.19	70.6
150°C - 24 hours	27.2	52.9	16.1	3.8	1.23	80.1
150°C - 48 hours	24.6	57.3	15.8	2.3	1.22	81.9

[1] Extent of reduction as estimated by measuring the hydrogen consumption at temperatures below 500°C

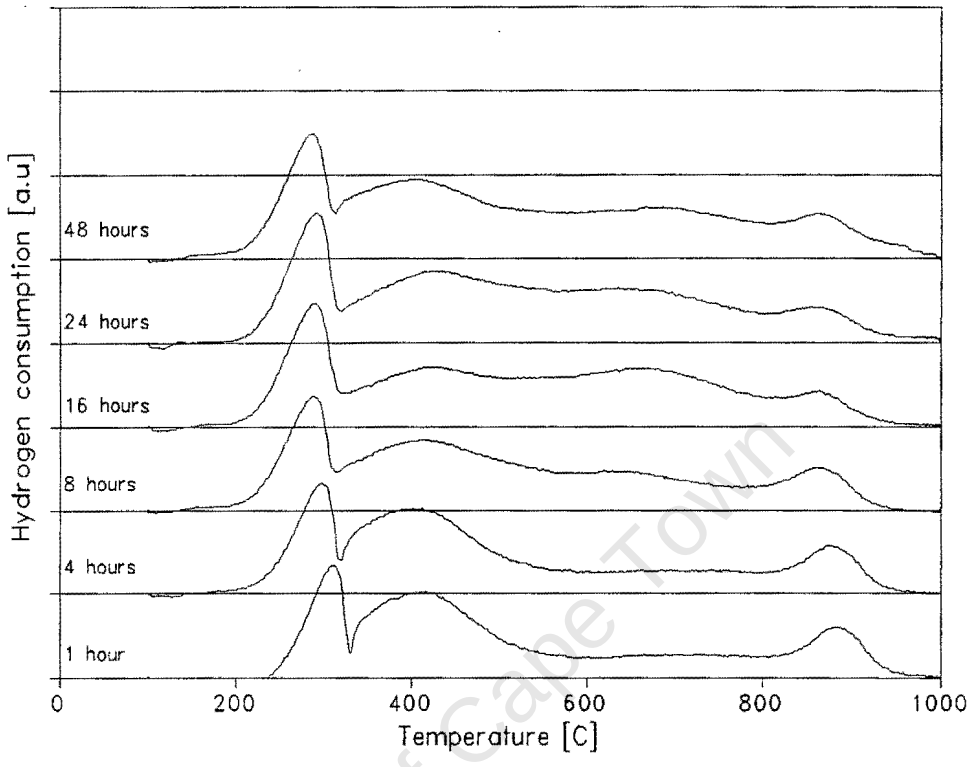

Figure 3.50. TPR spectra of Co/SiO_2 catalysts dried at 90°C for different times
(Reducing gas = 60 ml(NTP)/min 5% H_2/N_2, temperature programming rate = 10°C/min, $m_{cat} \approx 0.15$ g)

Increasing the time of drying at 120°C resulted in more pronounced changes in the TPR spectra of the Co/SiO_2 catalysts in comparison to the catalysts dried at 60 and 90°C (Figure 3.51.). The high temperature hydrogen consumption (Peak IV) decreased strongly with increasing drying time, especially in the instance of the Co/SiO_2 catalyst dried at 120°C for 48 hours. The overall hydrogen consumption does not however show any distinct pattern with increasing time of drying.

Besides showing a decrease in the size of the high temperature hydrogen consumption peaks, a change in the colour of the catalyst precursor was also observed. Regions of black were observed amongst the purple-pink catalyst precursor. Since the bulk cobalt oxide Co_3O_4 is black in colour, it appears that Co_3O_4 is formed during drying at 120°C.

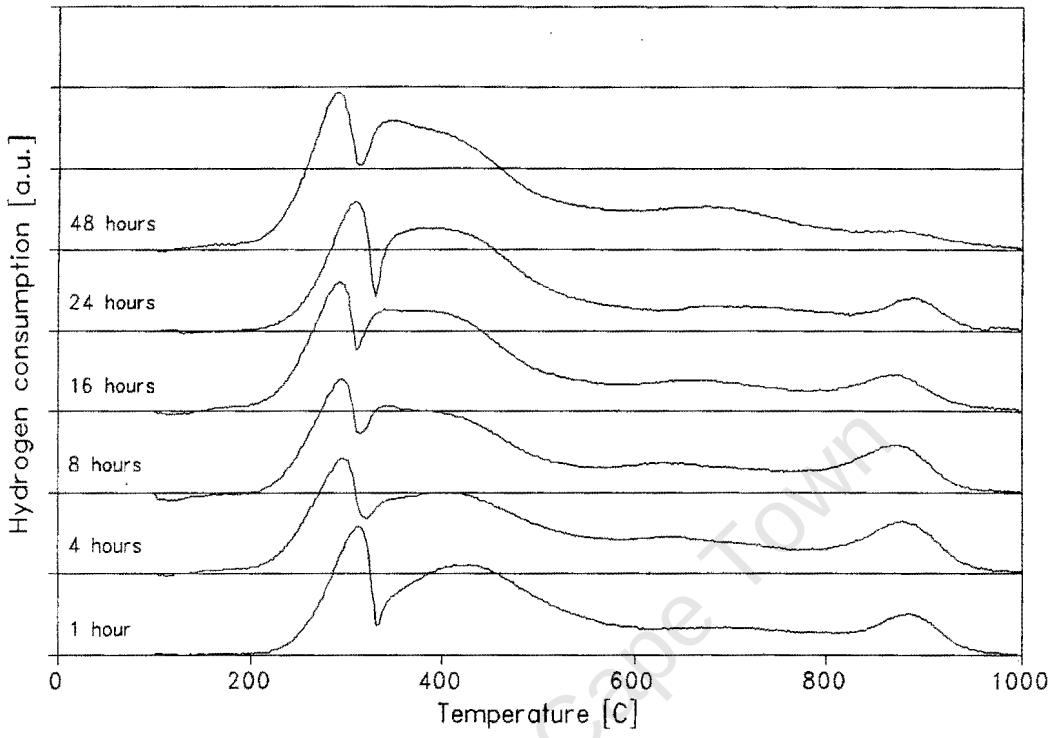

Figure 3.51. TPR spectra of Co/SiO_2 catalysts dried at 120°C for different times
(Reducing gas = 60 ml(NTP)/min 5% H_2/N_2, temperature programming rate = 10°C/min, $m_{cat} \approx 0.15$ g)

The influence of the time of drying at 150°C was considerably more pronounced than for the catalysts dried at lower temperatures and increased drying times resulted in considerable decreases in the high temperature hydrogen consumption. At drying times greater than 24 hours, the high temperature hydrogen consumption (Peak IV) is not observed and the TPR spectrum is characterized by only 3 hydrogen consumption maxima. Following the drying procedure, the catalyst precursor was predominantly black which indicates considerable formation of Co_3O_4.

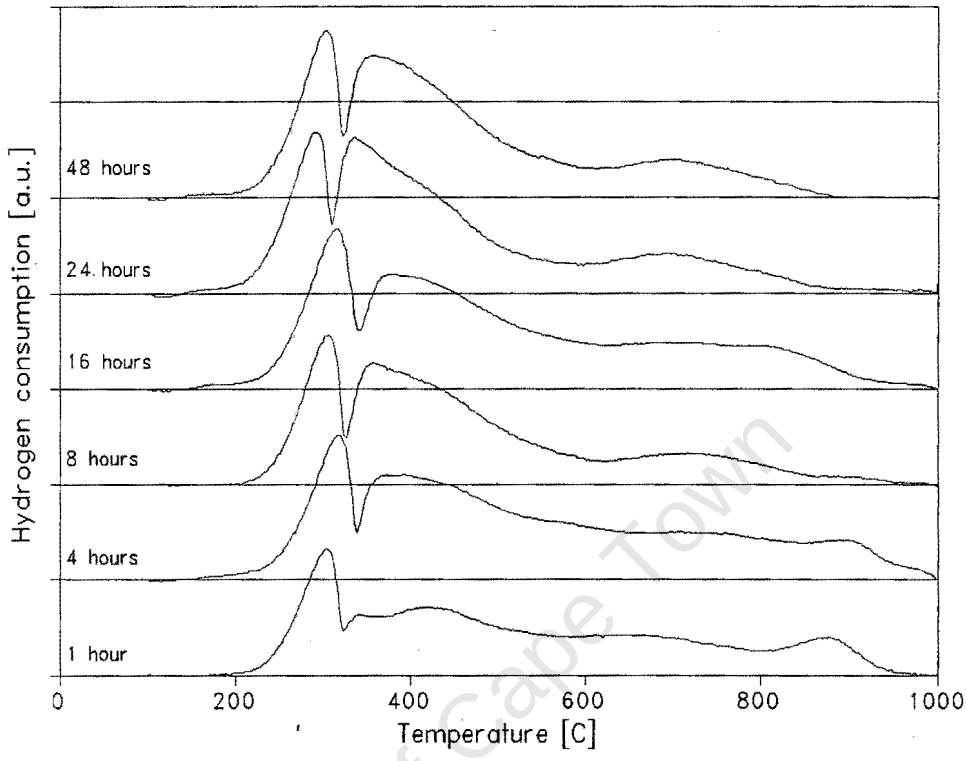

Figure 3.52. TPR spectra of Co/SiO_2 catalysts dried at 150°C for different times
(Reducing gas = 60 ml(NTP)/min 5% H_2/N_2, temperature programming rate = 10°C/min, $m_{cat} \approx 0.15$ g)

Although considerable scatter was observed, several general trends may be observed upon changing the drying conditions during catalyst preparation (Table 3.25.). With the exception of the Co/SiO_2 catalysts dried at 60°C, the relative contributions of peaks 1 and 2 increased with increasing drying time and increasing drying temperature whereas the reverse behaviour was observed for peaks 3 and 4. This indicates that the reducibility of the SiO_2 supported cobalt catalysts is increased, predominantly due to the destruction of the species which are responsible for the high temperature hydrogen consumption during TPR. The changes in metal reducibility cannot however be directly correlated to the total hydrogen consumption during TPR.

3.3.2. Effect of Catalyst Calcination

Catalyst calcination consists of a thermal pretreatment aimed at decomposing the metal precursor to form the metal oxide. Other phenomena which may occur during this thermal preactivation step may include changes in the metallic dispersion and the formation of metal-support compounds [Haberlandt, 1990]. Increasing the temperature of calcination results in decreased extents of metal reduction in the instance of Co/Al_2O_3 catalysts [Chin and Hercules, 1982] due to the formation of cobalt-alumina surface spinels. On the other hand, the extent of metal reduction of SiO_2 supported cobalt catalysts was seen to increase following thermal preactivation in air at 500°C [Rosynek and Polansky, 1991]. Since increasing metal reduction will correspond to an increase in the amount of cobalt available for the metal-catalysed amination reaction, this study was conducted in order to determine the influence of the calcination procedure on the reducibility of SiO_2 supported cobalt.

3.3.2.1. Effect of the calcination temperature

The influence of the temperature of calcination on the reducibility of Co/SiO_2 catalysts was investigated using TPR. Calcination of the catalyst precursors was performed using a 60 ml(NTP)/min N_2 stream and the final temperature of calcination was varied from 100 to 1000°C. The temperature programming rate during precalcination was 10°C/min and the time of calcination at the final temperature was 1 hour. The TPR spectra represent the hydrogen consumption profiles of the Co/SiO_2 catalyst in a 60 ml(NTP)/min 5% H_2/N_2 stream as the temperature was raised linearly from 100 to 1000°C/min at 10°C/min.

Considerable changes in the TPR spectra were observed upon increasing the calcination temperature and a number of discernable hydrogen consumption peaks were observed. Unlike the experiments in which the time and temperature of drying were varied, six different regions of hydrogen consumption were identified. These different regions were separated according to the temperature at which the maximum in the hydrogen uptake occurs. Peaks I to VI correspond to the hydrogen consumption peaks occurring between 180 and 240°C, 270 and 330°C, 350 and 390°C, 450 and 520°C, 650 and 780°C and 880 and 990°C

respectively. The different temperatures of the peak maxima in combination with the broad nature of some of the hydrogen consumption peaks complicate the integration procedure. The hydrogen consumption attributed to the different regions was therefore measured by integration between the local minima in the TPR curve.

For low calcination temperatures, the TPR spectra of the Co/SiO_2 catalysts exhibit a sharp hydrogen consumption peak occurring at temperatures between 180 and 240°C (Figure 3.53.). The contribution of this peak decreased with increasing calcination temperature and no hydrogen uptake corresponding to Peak I was observed following calcination at 400°C. It can therefore be concluded that the source of this hydrogen consumption can be removed by calcination in nitrogen at 400°C. The overall H_2 : Co molar ratio decreased from 2.22 to 1.25 as the calcination temperature was increased from 200 to 400°C (Table 3.26.). Since the reduction of the bulk cobalt oxide Co_3O_4 results in a hydrogen to cobalt molar ratio of 1.33 and reduction of divalent cobalt results in a hydrogen to cobalt ratio of 1.00, it is clear that the increased hydrogen consumption is due to the reduction of a species other than cobalt. Peak I can therefore be ascribed to reductive decomposition of the nitrate ion.

The hydrogen consumption attributed to Peak II remained approximately constant up to calcination temperatures of 700°C after which it decreased rapidly. The species responsible for this hydrogen uptake is therefore transformed by preactivation at temperatures greater than 700°C. The temperature at which the peak maximum occurs increased from 270 to 350°C as the calcination temperature was increased from 200 to 700°C. This may indicate that the degree of interaction with the SiO_2 carrier increases with increasing calcination temperature or that the average size of the supported cobalt particles is increasing. An increase in the diameter of supported metal crystallites can result in an increase in the temperature at which maximum hydrogen uptake occurs because of diffusional restrictions [Hurst *et al*, 1982].

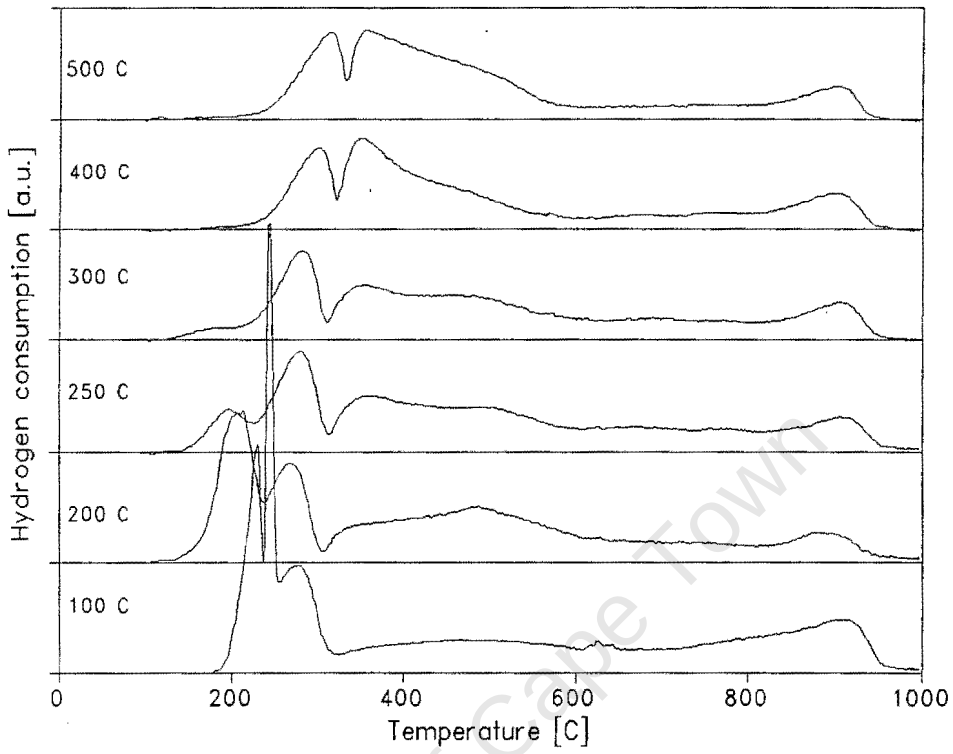

Figure 3.53. Influence of calcination temperature on TPR spectrum of Co/SiO_2
(Calcination gas = 60 ml(NTP)/min N_2, reducing gas = 60 ml(NTP)/min 5% H_2/N_2, temperature programming rate = 10°C/min, $m_{cat} \approx 0.15$ g)

At calcination temperatures greater than 700°C, considerable changes to the reduction profiles of the Co/SiO_2 catalysts were observed (Figure 3.54.). The low temperature hydrogen consumption attributed to Peaks I, II and III is decreased considerably and the contribution of Peaks IV, V and VI is increased. The increase in the contribution of the high temperature hydrogen consumption indicates that the reducibility of the supported cobalt decreases as the calcination temperature is raised above 700°C. High temperature calcination of Co/SiO_2 therefore appears to promote the formation of difficult to reduce cobalt-support species.

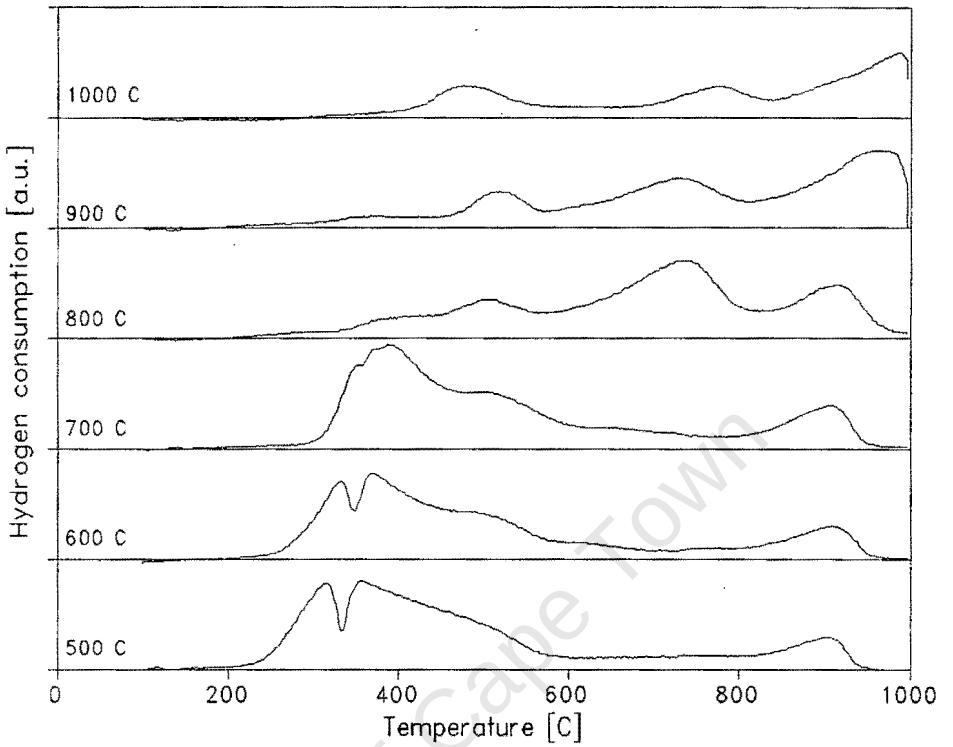

Figure 3.54. Influence of calcination temperature on TPR spectrum of Co/SiO_2
(Calcination gas = 60 ml(NTP)/min N_2, reducing gas = 60 ml(NTP)/min 5% H_2/N_2, temperature programming rate = 10°C/min, $m_{cat} \approx 0.15$ g)

Measurement of the hydrogen consumption during TPR showed that the calcination temperature affected the reducibility of the supported cobalt considerably (Table 3.26.). The contribution of Peaks II and III first increased and then decreased with increasing calcination temperature. Since these peaks represent cobalt species which can be reduced at temperatures lower than 500°C, it can be seen that the reducibility of the Co/SiO_2 catalyst first increases and then decreases with increasing calcination temperature. In contrast, the contribution of Peak VI (which represents cobalt species that cannot be reduced by 500°C) first decreases and then increases with increasing calcination temperature.

Table 3.26. Effect of calcination temperature on the hydrogen consumption during TPR

Calcination temperature	Peak 1 (%)	Peak 2 (%)	Peak 3 (%)	Peak 4 (%)	Peak 5 (%)	Peak 6 (%)	H_2 : Co ratio (mol H_2/mol Co)
100°C	28.5	11.9	0	22.7	17.4	19.5	2.04
200°C	18.9	11.9	7.3	23.5	9.6	28.8	2.22
250°C	7.2	17.8	22.4	16.3	18.7	17.6	1.76
300°C	2.0	21.3	20.8	21.7	23.6	10.6	1.29
400°C	0	20.2	30.8	19.3	16.6	13.1	1.25
500°C	0	21.4	30.8	26.6	13.2	8.0	1.16
600°C	0	18.4	26.3	18.1	17.1	20.1	1.47
700°C	0	13.5	34.6	22.4	9.7	19.8	1.47
800°C	0	1.4	6.0	17.1	46.6	28.8	1.36
900°C	0	0.9	4.8	12.9	31.0	50.4	1.36
1000°C	0	0	18.6	6.3	16.2	58.9	1.02

3.3.2.2. Effect of the calcination medium

Decomposition of the cobalt nitrate precursor during catalyst calcination results in the release of the nitrogen oxides NO and NO_2 which are stronger oxidizing agents than molecular oxygen [Arnoldy and Moulijn, 1985]. In a typical calcination procedure, these nitrogen oxides will be continuously removed by the calcination gas and therefore their oxidizing ability will be diminished.

In this experiment, the influence of the chemical nature of the calcination gas on the reducibility of the Co/SiO_2 catalyst was investigated by calcining the catalyst in an inert gas stream (nitrogen) and in an oxidizing gas stream (air). The flowrate of the calcination gas was 60 ml(NTP)/min and the temperature programme consisted of heating the catalyst sample

to 400°C at 10°C/min. To investigate the influence of the nitrogen oxide concentration on the reducibility of the supported cobalt, the catalyst was heated to the final calcination temperature of 400°C in a nitrogen atmosphere but without gas flow. The residual nitrogen oxides were removed following the calcination procedure using a 60 ml(NTP)/min N_2 stream. The hydrogen uptake of these catalysts was measured in a 60 ml(NTP)/min 5% H_2/N_2 stream as the temperature was raised linearly from 100 to 1000°C at 10°C/min.

The TPR spectra of the Co/SiO_2 catalysts calcined in air and nitrogen at 400°C show similar reduction profiles (Figure 3.55.). The similarity of the hydrogen uptake behaviour of these catalysts indicates that the chemical nature of the calcination gas does not affect the reducibility of the supported cobalt significantly. In contrast, the TPR spectrum of the Co/SiO_2 catalyst heated to 400°C without gas flow was characterized by only two hydrogen consumption peaks occurring at 320 and 360°C. The reduction behaviour of this catalyst is similar to that of the bulk unsupported cobalt oxide Co_3O_4 (Figure 3.1.). The reducibility of SiO_2 supported cobalt catalysts is therefore influenced by the concentration of the nitrogen oxides released during decomposition of the cobalt nitrate precursor.

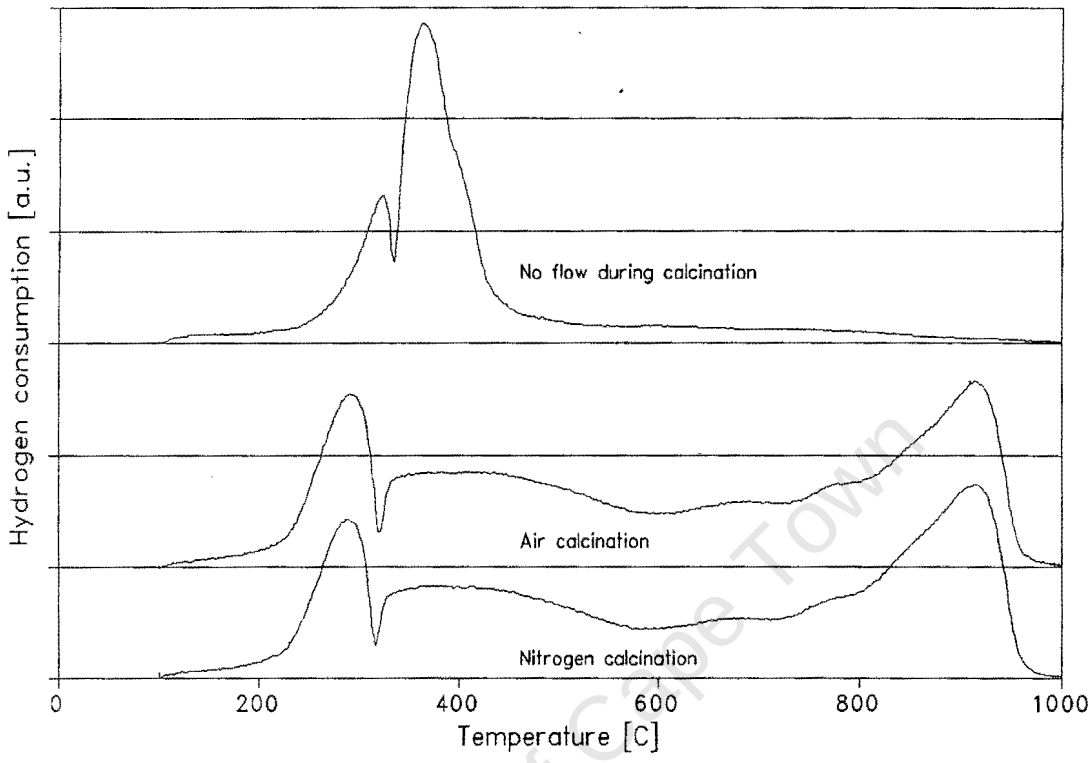

Figure 3.55. Influence of the calcination medium on the TPR spectrum of Co/SiO_2
(Reducing gas = 60 ml(NTP)/min 5% H_2/N_2, temperature programming rate = 10°C/min, $m_{cat} \approx 0.15$ g)

3.3.3. Extent of Reduction of Co/SiO_2 Catalysts

In the experiments conducted in this study, the hydrogen to cobalt molar ratio during TPR was seen to vary between 1 and 1.3 mol H_2 per mol Co. Since reduction of divalent cobalt species results in a H_2 : Co molar ratio of 1 and reduction of the cobalt oxide Co_3O_4 results in a H_2 : Co ratio of 1.33, it was not clear whether these differences in hydrogen consumption were caused by different reduction stoichiometries or by incomplete reduction of the supported cobalt. To determine whether the cobalt was completely reduced during the TPR experiments, a combined reduction/oxidation cycle was performed.

In the experiment, the Co/SiO_2 catalyst was initially calcined at 400°C using a 60 ml(NTP)/min N_2 stream. This calcination procedure was used in order to ensure complete

decomposition of the cobalt nitrate precursor (see Chapter 3.2.2.1.). After catalyst calcination, the sample was reduced in a 60 ml(NTP)/min 5% H_2/N_2 stream as the temperature was raised linearly from 100 to 1000°C at 10°C/min. The reduced catalyst sample was cooled to 50°C in a 60 ml(NTP)/min N_2 stream and then the extent of reduction was determined using TPO. The TPO procedure involved heating the reduced catalyst sample in a 60 ml(NTP)/min 2% O_2/He stream from 50 to 1000°C at 10°C. The oxidized catalyst sample was then cooled to 100°C in a 60 ml(NTP)/min He stream after which the TPR/TPO cycle was repeated.

The TPR spectrum of the Co/SiO_2 catalyst calcined at 400°C is characterized by four main regions of hydrogen consumption (Figure 3.56.). The reduction behaviour of this catalyst is consistent with previous findings (Chapter 3.2.2.1.). Measurement of the hydrogen consumption during TPR showed that 1.19 moles of hydrogen were consumed for every mole of cobalt present in the sample (Table 3.27.). The measured hydrogen consumption is therefore greater than that expected for the reduction of divalent cobalt species and less than that expected for the reduction of trivalent cobalt species.

The TPO spectrum of the reduced Co/SiO_2 catalyst was characterized by a low temperature peak of oxygen consumption (which is caused by cobalt oxidation) and a high temperature peak of oxygen release (which is caused by the thermal reduction of Co_3O_4 to 3 CoO). Measurement of the oxygen consumption during TPO resulted in an O_2 : Co molar ratio of 0.65. Since complete oxidation of zerovalent cobalt to the bulk cobalt oxide Co_3O_4 would result in an O_2 : Co molar ratio of 0.67, it can be seen that the extent of cobalt reduction is essentially complete by 1000°C.

Measurement of the oxygen release caused by the high temperature thermal reduction of Co_3O_4 to divalent cobalt resulted in an O_2 : Co molar ratio of 0.17. This value is identical to that expected from the stoichiometry of the thermal reduction reaction indicating that all of the cobalt present in the catalyst sample had been completely oxidized to Co_3O_4. Following the TPO experiment, the catalyst was a purple-pink colour. Since Co_3O_4 is black in colour and CoO is grey-black in colour, it can be deduced that the supported cobalt has reacted with

the SiO_2 carrier to form a cobalt-silicate species which is characterized by a purple-pink colour.

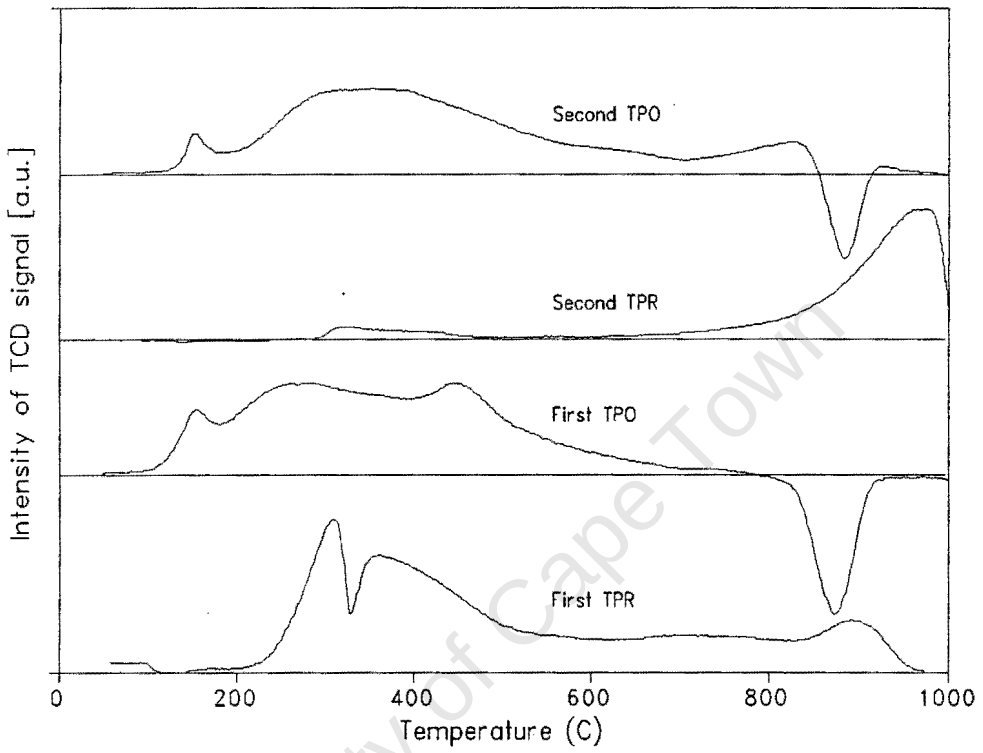

Figure 3.56. Reduction/oxidation behaviour of Co/SiO_2
(Calcination gas = 60 ml(NTP)/min N_2, calcination temperature = 400°C, reducing gas = 60 ml(NTP)/min 5% H_2/N_2, oxidizing gas = 60 ml(NTP)/min 2% O_2/He, temperature programming rate = 10°C/min, $m_{cat} \approx 0.30$ g)

Reduction of the Co/SiO_2 catalyst following TPO resulted in a small hydrogen consumption peak between temperatures of 300 and 500°C. The major portion of the hydrogen consumed during TPR however occurs between temperatures of 800 and 1000°C. The measured H_2 : Co molar ratio during TPR of the Co/SiO_2 catalyst oxidized up to a temperature of 1000°C was 1.00. This is characteristic of the reduction of divalent cobalt and is consistent with the observation that trivalent cobalt species are thermally reduced to divalent cobalt species at temperatures greater than 800°C.

Subsequent oxidation of the Co/SiO_2 catalyst following TPR resulted in a similar TPO

spectrum as obtained during the first measurement. The oxygen consumption was shifted towards higher temperatures however and the size of the peak occurring at 450°C was diminished. The repeated high temperature treatment may result in large cobalt crystallites and the rate of oxidation of these crystallites may be limited by the rate of oxygen diffusion within the crystallite. Since the TPO procedure is a dynamic process, this limitation by the rate of diffusion will appear as an upward shift in temperature.

The measured oxygen uptake during the second TPO was slightly lower than that obtained during the first oxidation and the O_2 : Co molar ratio was 0.61. Although this would indicate that the extent of reduction is lower in the second instance, it is possible that this decrease was caused by the poor separation of the oxygen uptake and oxygen release peaks at high temperatures.

Table 3.27. Hydrogen consumption during TPR and oxygen consumption during TPO of Co/SiO_2

Experiment	H_2 : Co ratio (mol H_2 : mol Co)	O_2 : Co ratio (mol O_2 : mol Co)
First reduction	1.19	
First oxidation		0.65
Second reduction	1.00	
Second oxidation		0.61

3.3.4. Influence of the Silica Surface Area

An increase in the surface area of the metal carrier will result in a larger interface through which the supported metal and the carrier material can interact. This greater degree of interaction between metal and carrier may be expected to result in an increase in the likelihood of metal-support reaction. In the case of SiO_2 supported cobalt catalysts, Puskas *et al* [1992] stated that the formation of cobalt silicates was favoured by high surface area silica supports. To investigate the influence of the support surface area on the reducibility of supported cobalt, four different silicas with different surface areas were tested. The physical characteristics of these silica supports are listed in Table 2.2. The surface areas of the SiO_2 supports were 300, 480, 675 and 750 m^2/g and the corresponding TPR spectra are illustrated in Figure 3.57.

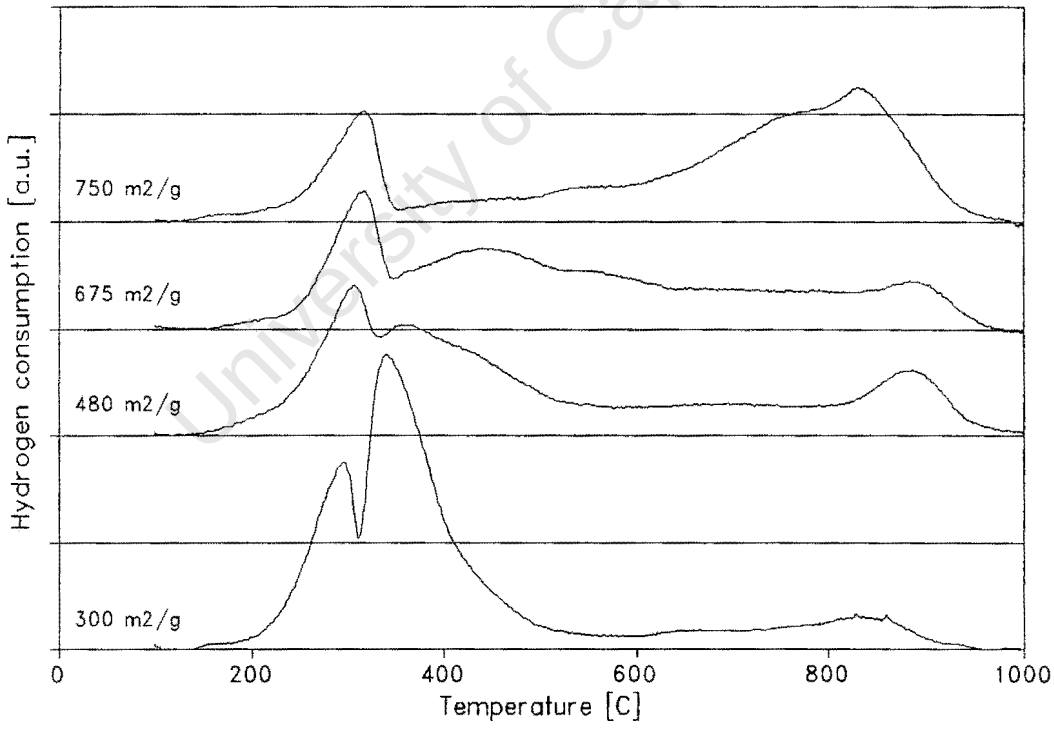

Figure 3.57. Effect of silica source on the reducibility of Co/SiO_2 catalysts
(Calcination gas = 60 ml(NTP)/min N_2, calcination temperature = 400°C, reducing gas = 60 ml(NTP)/min 5% H_2/N_2, temperature programming rate = 10°C/min, $m_{cat} \approx 0.15$ g)

The TPR spectra of the SiO_2 supported cobalt catalysts in which the carrier surface area was varied were characterized by four general hydrogen consumption regions. Peak I corresponds to the hydrogen consumption occurring between 150 and 350°C, Peak II between 350 and 500°C, Peak III between 500 and 800°C and Peak IV between 800 and 1000°C. Increasing the surface area of the SiO_2 support resulted in a decrease in the size of Peak II and an increase in the size of Peaks III and IV (Table 3.28.). The contribution of Peak I towards the total hydrogen consumption during TPR was not significantly affected by the surface area of the silica support. The increase in the contribution of cobalt species which can only be reduced at high temperatures (Peaks III and IV) indicates that increasing the surface area of the SiO_2 carrier decreases the reducibility of the supported cobalt. No correlation with respect to the total hydrogen consumption during TPR could be obtained however.

Table 3.28. Influence of the support surface area on the hydrogen consumption during TPR of Co/SiO_2

SiO_2 surface area (m^2/g)	Peak I (mol %)	Peak II (mol %)	Peak III (mol %)	Peak IV (mol %)	H_2 : Co (mol : mol)
300	24	60	8	8	1.27
480	27	38	19	16	1.18
675	24	32	34	10	1.10
750	19	15	37	29	1.17

3.3.5. Effect of the Impregnation Solvent

It has been shown that the nature of the cobalt precursor during impregnation influences the reducibility of SiO_2 supported cobalt catalysts significantly [Rosynek and Polansky, 1991; Matsuzaki *et al*, 1993]. These changes in reducibility could possibly be caused by changes in the coordination (and therefore the reactivity) of the cobalt ions in solution and will

therefore be expected to be influenced by the nature of the impregnation solvent. Accordingly, some authors have used organic solvents in order to prepare highly dispersed metal catalysts [Reuel and Bartholomew, 1984; Babb and White, 1986]. In this study, the influence of the solvent of impregnation on the reducibility of Co/SiO_2 catalysts was evaluated using TPR.

Using water, methanol or ethanol as the impregnation solvent resulted in similar TPR profiles (Figure 3.58.). In contrast, considerable changes in the TPR spectra of the Co/SiO_2 catalysts were observed when either n-propanol or n-butanol are used as impregnation solvents. In particular, an increase in the size of the hydrogen consumption peak occurring at temperatures greater than 800°C was observed. The increase in the size of this high temperature hydrogen consumption peak corresponds to a decrease in the reducibility of the supported cobalt.

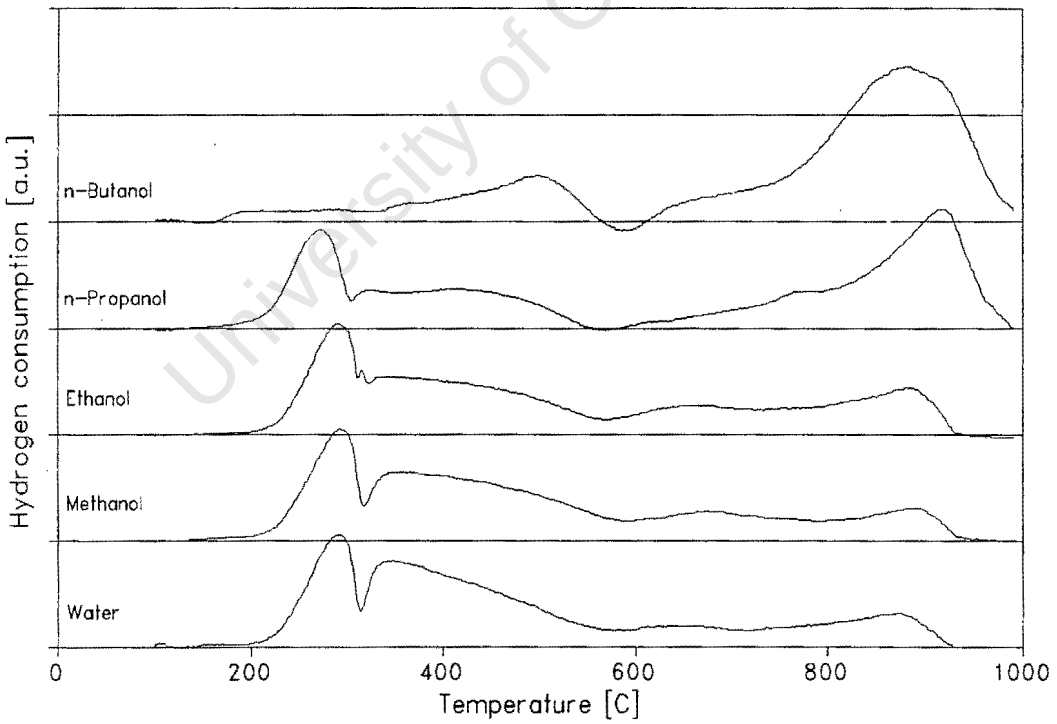

Figure 3.58. Influence of the impregnation solvent of the reducibility of Co/SiO_2 (Calcination gas = 60 ml(NTP)/min 5% N_2, calcination temperature = 400°C, reducing gas = 60 ml(NTP)/min 5% H_2/N_2, temperature programming rate = 10°C/min, $m_{cat} \approx 0.15$ g)

Although using THF as a solvent did not result in significant changes to the TPR profile in comparison to water, considerable changes in the reduction behaviour were observed when using DMSO as a solvent (Figure 3.59.). With this catalyst, the TPR spectrum was dominated by a single hydrogen consumption peak occurring at a temperature of approximately 550°C. The H_2 : Co molar ratio during TPR of the Co/SiO_2 catalyst prepared using DMSO as an impregnation solvent was 3.2 which indicates the reduction of species other than cobalt. Since DMSO is a strong chelating agent, it is possible that it replaces water as a ligand thus turning the cobalt-aquo complex into a cobalt-DMSO complex. This complex is apparently not destroyed by calcination in nitrogen at 400°C and the reduction of residual DMSO molecules is probably responsible for the increased hydrogen consumption during TPR.

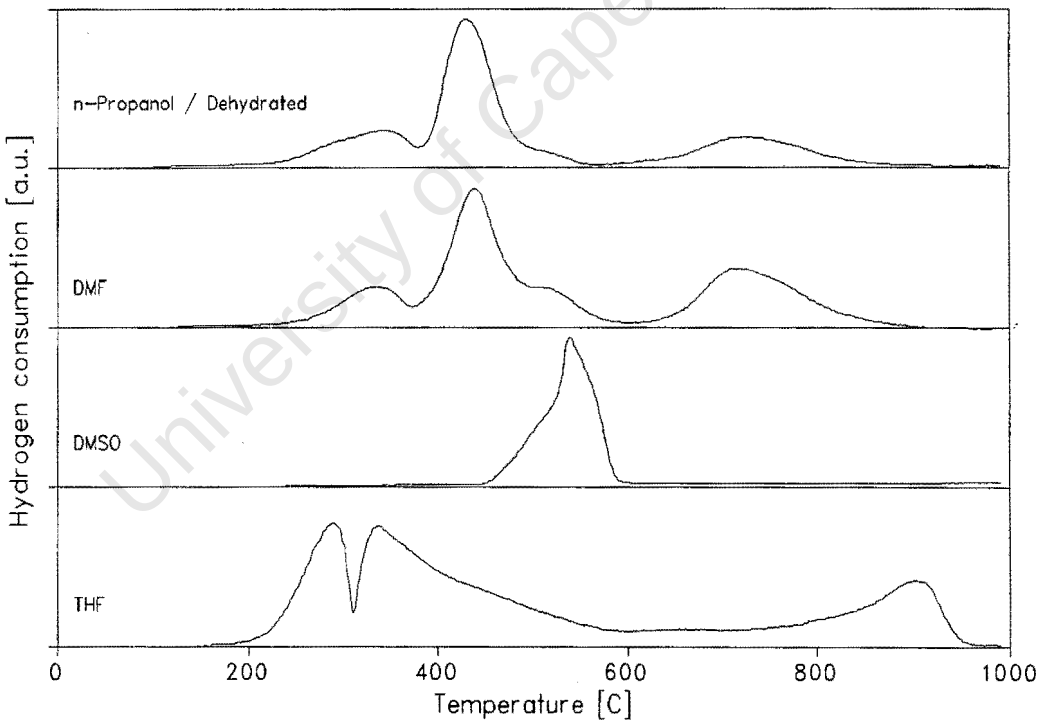

Figure 3.59. Influence of the impregnation solvent on the reducibility of Co/SiO_2 (Calcination gas = 60 ml(NTP)/min N_2, calcination temperature = 400°C, reducing gas = 60 ml(NTP)/min 5% H_2/N_2, temperature programming rate = 10°C/min, $m_{cat} \approx 0.15$ g)

Using DMF as a solvent also resulted in considerable changes in the TPR spectrum and

hydrogen consumption peaks were observed at 300, 450 and 700°C. In contrast to the catalysts prepared using water or alcohols as impregnation solvents, no hydrogen consumption was observed at temperatures greater than 800°C. This indicates that the use of DMF as a solvent inhibits the formation of the cobalt silicate species which are responsible for the high temperature hydrogen consumption during TPR.

In order to investigate the influence of the water ligand in the cobalt complex on the reducibility of the Co/SiO_2 catalyst, an attempt was made to remove the crystal water present in the cobalt nitrate precursor $Co(NO_3)_2 \cdot 6\ H_2O$. By measuring the mass loss of a sample of cobalt nitrate heated at 100°C for 3 hours, it was determined that 90% of the crystal water had been removed. An appropriate amount of this dehydrated cobalt nitrate precursor was dissolved in propanol and the resulting solution was impregnated into the SiO_2 support. The TPR spectrum of the resulting catalyst was considerably different to the catalyst prepared using the hydrated cobalt nitrate precursor but was remarkably similar to the catalyst prepared using DMF as a solvent. It is therefore evident that the crystal water associated with the cobalt ion during impregnation influences the reducibility of Co/SiO_2 catalysts.

CHAPTER 4

DISCUSSION

4.1. Comparison of Silica Supported Cobalt, Nickel and Copper

In literature, cobalt [Deeba, 1988; Heft *et al*, 1990; Fowlkes and de Pinillos, 1979], nickel [Gardner and Clark, 1981; Best, 1978; Fowlkes and de Pinillos, 1979] and copper [Baiker, 1981; Baiker and Richarz, 1977] have been suggested to be efficient catalysts for the reductive amination of alcohols using ammonia. In order to characterize the ability of each metal to catalyze this reaction, the efficiency of the exposed metal atoms should be compared on the basis of a mechanically based kinetic expression. Therefore, both the catalyst characteristics and their amination kinetics need to be compared.

4.1.1. Catalyst characterization

Significant variations in both the reducibility as well as the dispersion of the SiO_2 supported cobalt, nickel and copper catalysts were observed using TPR and hydrogen chemisorption. These differences can be ascribed to different degrees of interaction of the metal precursor compounds with the support.

The TPR spectrum of the Co/SiO_2 catalyst showed the presence of a number of reducible species in the catalyst precursor. The most intense hydrogen consumption peak occurring at low temperatures was ascribed to the reduction of the cobalt nitrate precursor which is not decomposed during catalyst drying [Rosynek and Polansky, 1991; Lapidus *et al*, 1991]. Following this peak are a number of further hydrogen consumption peaks which are most probably caused by the reduction of various cobalt oxide and cobalt-silicate species [Puskas *et al*, 1992; Ming and Baker, 1995]. The strong interaction between cobalt and the silica support results in incomplete reduction by activation in hydrogen at 500°C. As a consequence, a significant proportion of cobalt atoms is unavailable for reaction since only zero-valent cobalt is active for the reductive amination reaction under these conditions (Chapter 4.2.3.).

The TPR spectrum of the Ni/SiO_2 catalyst was dominated by an intense hydrogen consumption peak at approximately 310°C. Occurring concurrently with this hydrogen

consumption was a slight upward deviation in the linear temperature ramp of the TPR program which indicated that this reduction reaction is exothermic. Due to the sharp nature of this hydrogen consumption peak and since the reduction of nickel nitrate using hydrogen is an exothermic process [Bartholomew and Farrauto, 1976], it is likely that this hydrogen consumption is caused by the reductive decomposition of the nickel nitrate precursor. Further hydrogen consumption is most likely caused by the reduction of nickel oxide and nickel silicate species [Gil *et al*, 1994; Coenen, 1989]. As in the instance of the Co/SiO_2 catalyst, hydrogen consumption was observed at temperatures greater than 500°C indicating that the SiO_2 supported nickel catalyst was not completely reduced by the time this temperature was reached.

The TPR spectrum of the Cu/SiO_2 catalyst indicated that the copper nitrate precursor was easily reduced and occurred at a temperature 50°C lower than that of the bulk unsupported oxide. The low temperature required for reduction of this catalyst resulted in complete reduction of the copper nitrate precursor to metallic copper by the time a temperature of 500°C was reached. The absence of further high temperature hydrogen consumption peaks indicates that copper hydrosilicate species are probably not formed [van der Grift *et al*, 1990].

Measurement of the hydrogen uptake during chemisorption showed that the reduced metallic surface area decreased as the metal catalyst was changed from nickel to cobalt to copper. The discrepancy between the extent of reduction as measured using TPR and the metal surface area as measured using hydrogen chemisorption can be ascribed to metal particle agglomeration. Considerable particle agglomeration on the Cu/SiO_2 catalyst during hydrogen reduction resulted in this catalyst having the lowest metal surface area in spite of the fact that this catalyst had the highest extent of reduction. The high extent of agglomeration on this catalyst points toward a low degree of interaction between the reduced metal particles and the carrier material. It has been postulated that metal-silicate species act as "anchors" for the reduced metal crystallites during reduction [van't Blik *et al*, 1986; Coenen, 1989]. These "anchors" decrease the mobility of the metal crystallites thereby decreasing agglomeration. The absence of copper silicate formation (as shown by TPR) may explain the low dispersion

consumption was a slight upward deviation in the linear temperature ramp of the TPR program which indicated that this reduction reaction is exothermic. Due to the sharp nature of this hydrogen consumption peak and since the reduction of nickel nitrate using hydrogen is an exothermic process [Bartholomew and Farrauto, 1976], it is likely that this hydrogen consumption is caused by the reductive decomposition of the nickel nitrate precursor. Further hydrogen consumption is most likely caused by the reduction of nickel oxide and nickel silicate species [Gil *et al*, 1994; Coenen, 1989]. As in the instance of the Co/SiO_2 catalyst, hydrogen consumption was observed at temperatures greater than 500°C indicating that the SiO_2 supported nickel catalyst was not completely reduced by the time this temperature was reached.

The TPR spectrum of the Cu/SiO_2 catalyst indicated that the copper nitrate precursor was easily reduced and occurred at a temperature 50°C lower than that of the bulk unsupported oxide. The low temperature required for reduction of this catalyst resulted in complete reduction of the copper nitrate precursor to metallic copper by the time a temperature of 500°C was reached. The absence of further high temperature hydrogen consumption peaks indicates that copper hydrosilicate species are probably not formed [van der Grift *et al*, 1990].

Measurement of the hydrogen uptake during chemisorption showed that the reduced metallic surface area decreased as the metal catalyst was changed from nickel to cobalt to copper. The discrepancy between the extent of reduction as measured using TPR and the metal surface area as measured using hydrogen chemisorption can be ascribed to metal particle agglomeration. Considerable particle agglomeration on the Cu/SiO_2 catalyst during hydrogen reduction resulted in this catalyst having the lowest metal surface area in spite of the fact that this catalyst had the highest extent of reduction. The high extent of agglomeration on this catalyst points toward a low degree of interaction between the reduced metal particles and the carrier material. It has been postulated that metal-silicate species act as "anchors" for the reduced metal crystallites during reduction [van't Blik *et al*, 1986; Coenen, 1989]. These "anchors" decrease the mobility of the metal crystallites thereby decreasing agglomeration. The absence of copper silicate formation (as shown by TPR) may explain the low dispersion

of the Cu/SiO_2 catalyst in comparison to the SiO_2 supported cobalt and nickel catalysts.

Besides the differences in metal surface area, changes in the strength of hydrogen adsorption were also observed. The reversibility of hydrogen adsorption decreased as the catalyst was changed from nickel to cobalt to copper indicating that the ratio of "strong" adsorption sites relative to "weak" adsorption sites decreases as the metal catalyst is changed in the same order. These changes in the type of site may influence the strength of adsorption of certain reactants and intermediates during reaction and could possibly influence the amination behaviour of the different catalysts.

4.1.2. Amination behaviour of silica supported cobalt, nickel and copper

4.1.2.1. Time on stream behaviour

Different extents of catalyst deactivation were observed during the first 24 hours of operation. The deactivation processes resulting in a decrease in the conversion of the reactant alcohol have been shown to be caused by metal nitride formation, metal carbide formation, the deposition of carbonaceous material and the thermal diffusive fusion of the supported metal crystallites [Baiker and Maciejewski, 1984; Baiker *et al*, 1984; Baiker, 1981; Baiker and Richarz, 1978]. By simply monitoring the time on stream behaviour of these catalysts, it could not be clearly elucidated which of these processes was directly responsible for the decrease in activity.

With copper catalysts, only nitride formation has been observed to contribute towards catalyst deactivation [Baiker *et al*, 1984]. Since a relatively high hydrogen pressure of 22 kPa was used in this experiment and since the formation of copper nitride is known to be prevented by the presence of hydrogen in the feed stream [Baiker *et al*, 1984; Baiker and Kijenski, 1985], it is unlikely that the decrease in ethanol conversion is due to the incorporation of nitrogen into the copper lattice. Decreased activity caused by metal crystallite agglomeration is also unlikely since this process was found to be insignificant for SiO_2 supported copper catalysts during reductive amination [Baiker and Richarz, 1978]. By inference, it therefore

appears that the deactivation occurring is due to the deposition of carbonaceous material.

As with copper, nickel and cobalt can also interact with ammonia to form nitrides which are inactive for the reductive amination reaction [Baiker *et al*, 1984; Baiker, 1981]. Hydrogen was shown to prevent the incorporation of nitrogen into the metal lattices under typical amination conditions and also inhibited the deposition of carbonaceous material [Baiker *et al*, 1984]. By changing the hydrogen pressure during amination, the activity of the SiO_2 supported nickel catalyst was largely unaffected (Chapter 3.1.2.5.) indicating that nickel nitride formation was not significant. A decrease in activity caused by metal particle agglomeration is also unlikely since in comparison to the high temperature of reduction (500°C), it is unlikely that the supported nickel crystallites will sinter at the low temperatures used for the reductive amination reaction ($\approx$ 180°C). The decrease in the ethanol conversion activity of the Ni/SiO_2 catalyst with time on stream might therefore be ascribed to site coverage by carbon deposition.

By changing the hydrogen pressure during amination over Co/SiO_2, it was found that the ethanol conversion was directly proportional to the hydrogen pressure (Chapter 3.1.2.5.). Since hydrogen has been reported to have no influence on the rate of reductive amination [Kliger *et al*, 1975; Baiker *et al*, 1983], it appears that the changes in the reaction rate are caused by a modification of the catalyst surface. It has been shown previously that the reaction between gas phase ammonia and cobalt to form cobalt nitride (which is inactive for the reductive amination reaction) is feasible under typical amination conditions [Baiker *et al*, 1984].

$$3\ Co + NH_3 \rightleftarrows Co_3N + 1.5\ H_2$$

If this reaction were at equilibrium under the conditions used in this study, then it is clear that the number of cobalt atoms (and therefore the total activity) would be directly proportional to the hydrogen partial pressure. The sharp decrease in activity with decreasing hydrogen pressure therefore appears to be caused by cobalt nitride formation. The changes in activity upon changing the hydrogen pressure occurred within 30 minutes (the time

between sampling) which indicates that the equilibrium between cobalt and cobalt nitride is readily established. Therefore, even though some catalyst deactivation is occurring due to the formation of cobalt nitride, this cannot explain the observed deactivation which occurs during the first 5 hours on stream. It therefore appears likely that the deposition of carbonaceous material is also responsible for the decrease in activity with time on stream of the Co/SiO_2 catalyst.

By comparing the steady state activities to the reduced metallic surface area as measured by hydrogen chemisorption, an estimation of the turnover frequency of the three supported metals was obtained. The activity for ethanol conversion decreased from 0.11 to 0.09 to 0.05 molecules of ethanol converted per active site per second as the metal was changed from cobalt to nickel to copper. Although the increased activity of the cobalt catalyst relative to the nickel catalyst is consistent with the findings of Gardner and Clark [1981] and Fowlkes and de Pinillos [1979], these researchers measured the overall and not the specific activity of these metal catalysts. The actual turnover numbers are probably higher than the values reported above since the steady state activity measurements were compared to the surface areas of the freshly reduced catalysts. A more accurate measurement of the turnover frequency could be obtained by measuring the metallic surface area of the catalyst at the time at which the activity measurements were obtained.

4.1.2.2. Mechanism of reductive amination

The stoichiometry during reductive amination can be described by a set of series reactions in which the hydrogen atoms of the ammonia molecule are sequentially substituted by the alkyl groups of the reactant alcohol (reactions [1] to [3]). From the reaction stoichiometry it can be seen that MEA is formed via the reaction between ethanol and ammonia and DEA and TEA are formed via the reaction of ethanol with MEA and DEA respectively.

$$C_2H_5OH + NH_3 \rightleftarrows C_2H_5NH_2 + H_2O \qquad [1]$$

$$C_2H_5OH + C_2H_5NH_2 \rightleftarrows (C_2H_5)_2NH + H_2O \qquad [2]$$

$$C_2H_5OH + (C_2H_5)_2NH \rightleftarrows (C_2H_5)_3N + H_2O \qquad [3]$$

In order to obtain an indication of the reaction pathway over the SiO_2 supported cobalt, nickel and copper catalysts during reductive amination, the ethylamine selectivity was plotted as a function of the ethanol conversion. In the case of the Co/SiO_2 catalyst, an increase in the ethanol conversion resulted in a decrease in the MEA selectivity, an increase in the TEA selectivity and the selectivity to DEA first increased and then decreased (Figure 4.1.). At low ethanol conversions, the MEA selectivity tends towards 100% which indicates that this species is the primary product formed during reductive amination over Co/SiO_2. This is in agreement with the series reaction mechanism as illustrated above. Since MEA is required for the formation of DEA via the reaction with ethanol, an increase in the DEA selectivity is observed upon increasing the ethanol conversion (and thus the MEA concentration). At an ethanol conversion of approximately 5%, the DEA selectivity passes through a maximum and then decreases slowly. The decrease in the DEA selectivity is caused by an increase in the rate of TEA formation which is formed via the reaction of DEA and ethanol. The high DEA selectivities obtained at low ethanol conversions indicate that the rate of reaction [2] between MEA and ethanol is rapid relative to the rate of reaction [1] between ethanol and ammonia over the Co/SiO_2 catalyst.

increased surface coverage of ethanol would be expected to result in an increase in the rate of formation of all three ethylamines. The lower DEA and TEA selectivities obtained over the Ni/SiO_2 catalyst compared to the Co/SiO_2 catalyst may indicate a higher surface coverage of ammonia on nickel as opposed to cobalt (which inhibits DEA and TEA formation).

Plotting the ethylamine selectivity as a function of the ethanol conversion over the Cu/SiO_2 catalyst shows that the amination behaviour of the copper catalyst is considerably different to that of the cobalt and nickel catalysts (Figure 4.3.).

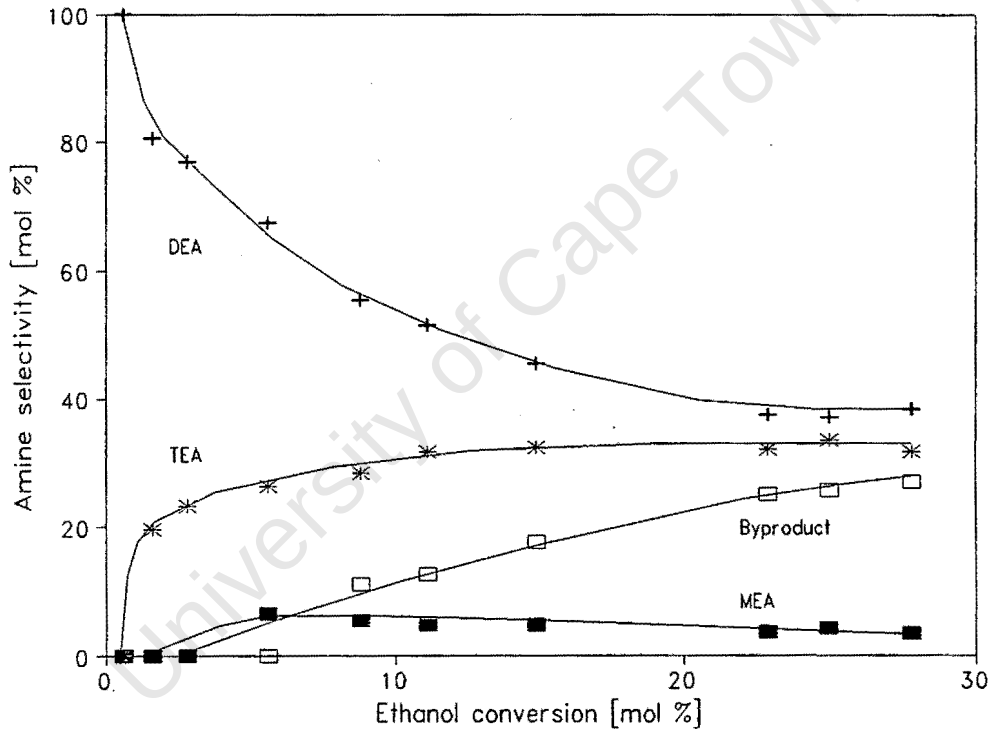

Figure 4.3. Effect of the ethanol conversion on the ethylamine selectivity over Cu/SiO_2 (P = 1 bar, WHSV = 2 g_{EtOH}/g_{cat}·h, EtOH : NH_3 : H_2 : N_2 = 1 : 2 : 4.1 : 13.6)

Instead of MEA appearing as a primary product, DEA is obtained at selectivities of 100% at low ethanol conversions. To form DEA directly as a primary product would require the reaction between two ethanol molecules and an ammonia molecule. Since a trimolecular reaction is highly unlikely, it appears that the rate of reaction [2] is large compared to the

rate of reaction [1] (*i.e.* the majority of the MEA formed is rapidly converted to form DEA). The reaction pathway of the Cu/SiO_2 catalyst can therefore be described by that of a typical series reaction in which the rate of MEA conversion to form DEA is rapid. The low MEA concentrations at low ethanol conversions resulted in this species not being detected by the gas chromatograph and is responsible for the apparent increase in MEA selectivity with increasing ethanol conversion.

The increase in TEA selectivity with increasing ethanol conversion is caused by the increase in the concentration of DEA which reacts with ethanol to form this species. Besides MEA, DEA and TEA, an unidentified byproduct was also obtained when using the Cu/SiO_2 catalyst. By simply varying the ethanol conversion, it was not clear whether this byproduct species was a reaction intermediate or whether it was formed as the product of a side reaction occurring on the copper catalyst. The possible identity of this byproduct will be discussed in further detail in Chapter 4.1.2.6.

4.1.2.3. Activity of SiO_2 supported cobalt, nickel and copper catalysts

In previous studies, it has been shown that the rate determining step during the amination of ethanol using ammonia [Kryukov *et al*, 1967], 1,6-hexanediol with dimethylamine [Vultier *et al*, 1987], 1-methoxypropan-2-ol with ammonia [Bassili and Baiker, 1991] and octanol or dodecanol with monomethylamine [Baiker *et al*, 1983] was the abstraction of the α-hydrogen from the reactant alcohol. Ammonia is not involved in the reaction resulting in alcohol dehydrogenation and should therefore not influence the overall rate of ethanol consumption (besides the possibility of a slight decrease in the rate of ethanol consumption due to competitive adsorption).

In the case of the Co/SiO_2 catalyst, positive reaction orders were obtained with respect to both the ethanol and the ammonia partial pressures. If the rate controlling step during amination over the Co/SiO_2 catalyst was the rate of alcohol dehydrogenation, then an increase in the ammonia partial pressure would not result in an increase in the rate of alcohol conversion. Since this is not observed, it must be concluded that the rate determining step

over silica supported cobalt catalysts is different to that proposed in literature. The positive reaction orders obtained with respect to the ethanol and ammonia partial pressures may indicate that the rate determining step involves the surface reaction between adsorbed ethanol and ammonia species. The increase in the rate of ethanol consumption over the Co/SiO_2 catalyst with increasing hydrogen partial pressure was ascribed to the destruction of cobalt nitride species which are inactive for the reductive amination reaction (Chapter 4.1.2.1.). Furthermore, if the rate of ethanol dehydrogenation was the rate controlling step, increasing the hydrogen partial pressure would be expected to decrease the rate of ethanol consumption.

In the case of the SiO_2 supported nickel and copper catalysts, an increase in the rate of ethanol consumption was observed when the partial pressure of the ethanol feed was increased. The increase in the rate of reaction with increasing ethanol partial pressure indicates that ethanol is involved in the rate controlling step over these metal catalysts. On the other hand, changing the partial pressure of the ammonia and hydrogen feeds did not influence the overall rate of ethanol consumption significantly. Since increasing the ammonia partial pressure does not result in an increase in the overall rate of reaction, it can be deduced that either ammonia is not involved in the rate controlling step or that the increase in the reaction rate is counterbalanced by an inhibition by ammonia (*i.e.* competitive adsorption). The negligible influence of hydrogen on the overall rate of ethanol consumption is consistent with previous findings [Smeykal, 1936; Heft *et al*, 1990] and also indicates that catalyst deactivation via metal nitride formation [Baiker and Maciejewski, 1984] is not significant under the conditions used in this study.

4.1.2.4. Ethylamine selectivity of Co/SiO_2

Changing the partial pressures of the ethanol, ammonia and hydrogen feeds resulted in considerable changes in the ethylamine selectivity of the Co/SiO_2 catalyst. These changes in selectivity could not be directly related to the ethanol conversion as would be expected for a simple series reaction. From this it can be deduced that either the reaction pathway cannot be described by a series reaction mechanism or that competitive adsorption phenomena are important during the reductive amination of ethanol over Co/SiO_2 catalysts.

Increasing the ammonia partial pressure resulted in an increase in the MEA selectivity, a decrease in the TEA selectivity and the DEA selectivity first increased and then decreased. An increase in the ethanol conversion with increasing ammonia partial pressure was also observed. From the series nature of the amination reaction over Co/SiO_2 (Chapter 4.1.2.2.), this may be expected to result in a decrease in the MEA selectivity and an increase in the DEA and TEA selectivities. Because this is not observed, it can be deduced that ammonia inhibits the formation of DEA and TEA, thereby resulting in decreased selectivities. If the decreased selectivities were caused by an inhibition of ethanol adsorption by ammonia, then an increase in the rate of ethanol consumption would not be observed. The decrease in the selectivity to DEA and TEA with increasing ammonia partial pressure therefore indicates that ammonia inhibits the readsorption of MEA and DEA (which are required for the formation of DEA and TEA respectively). This selective inhibition indicates that the adsorption of ammonia and product ethylamines on cobalt may be site sensitive (*i.e.* ammonia inhibits the readsorption and reaction of product ethylamines but not ethanol). If simple competitive adsorption was responsible for the decrease in DEA and TEA selectivity, then a decrease in the rate of ethanol conversion would also be expected.

Increasing the ethanol partial pressure did not result in large changes in the ethylamine selectivity of the Co/SiO_2 catalyst. This may be expected since ethanol is directly involved in the reactions to form MEA, DEA and TEA and an increase in the surface coverage of ethanol would be expected to result in a similar increase in the rates of each reaction. Increasing the ethanol partial pressure increases the rate of ethanol consumption which, according to the series nature of the amination reaction over Co/SiO_2 (Figure 4.1.), results in a slight decrease in the DEA selectivity and an increase in the TEA selectivity. The slight decrease in the DEA selectivity and the slight increase in the TEA selectivity with increasing ethanol partial pressure may therefore be caused by the increase in the rate of ethanol consumption.

Considerable changes in the ethylamine selectivity were observed upon changing the hydrogen pressure over the Co/SiO_2 catalyst. Increasing the hydrogen partial pressure resulted in a decrease in the MEA selectivity whereas the DEA and TEA selectivities were

increased. These changes in selectivity are surprising since the main role of hydrogen during reductive amination has been reported to be simply to prevent catalyst deactivation [Baiker and Kijenski, 1985; Baiker *et al*, 1984]. Decreasing the hydrogen partial pressure resulted in a large decrease in the ethanol consumption rate of the Co/SiO_2 catalyst due to the formation of cobalt nitride which is inactive for the reductive amination reaction. It was shown previously that a decrease in the ethanol conversion resulted in similar selectivity behaviour (Figure 4.1.). By plotting the MEA selectivity as a function of the ethanol conversion for the experiments in which the hydrogen pressure was varied and the experiments in which the ethanol conversion was varied at constant hydrogen partial pressure (Figure 4.4.), it can be seen that hydrogen directly influences the ethylamine selectivity of the Co/SiO_2 catalyst. Similar differences in the DEA and TEA selectivities with changing hydrogen pressure were also observed.

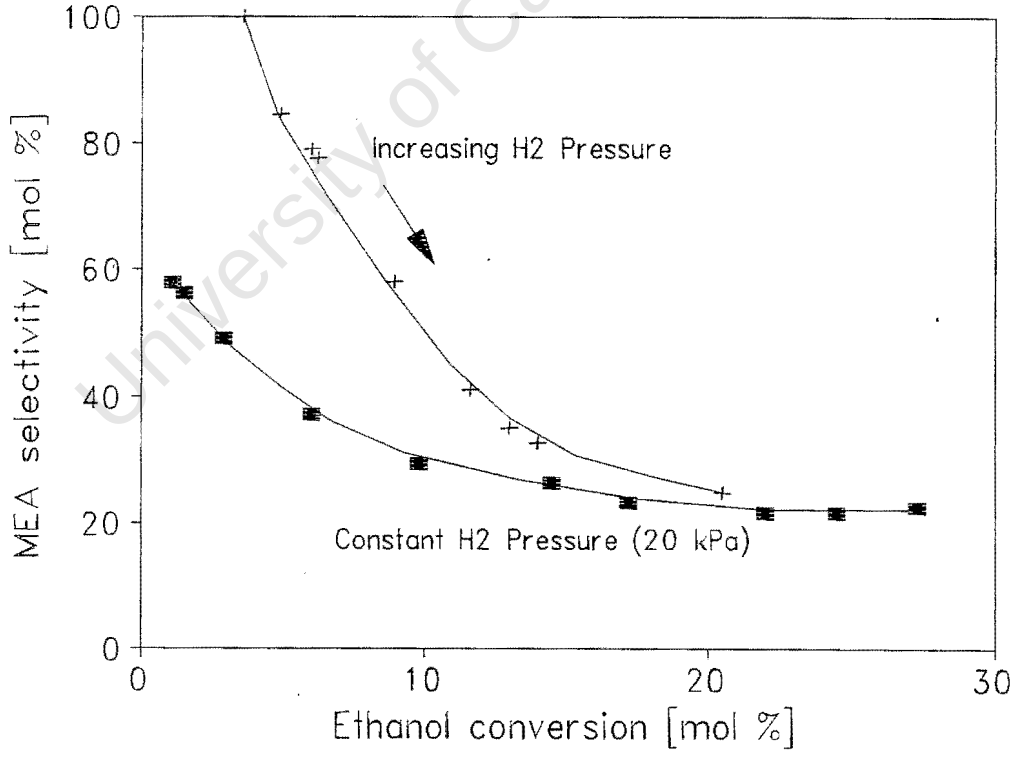

Figure 4.4. Influence of the hydrogen pressure on the MEA selectivity of Co/SiO_2
(P = 1 bar, WHSV = 1 g_{EtOH}/g_{cat}·h, EtOH : NH_3 : = 1 : 2)

If the adsorption of ammonia on cobalt occurs dissociatively via the abstraction of one or more hydrogen atoms, an increase in the hydrogen partial pressure would be expected to decrease the surface concentration of adsorbed ammonia species. The decreased surface coverage by ammonia would decrease the likelihood of reaction between adsorbed ammonia and ethanol which would result in decreased MEA selectivities. Also, a decrease in the surface coverage of ammonia would be expected to decrease the inhibition of DEA and TEA formation (as observed upon changing the ammonia partial pressure) thereby resulting in increased DEA and TEA selectivities. The changes in ethylamine selectivity upon changing the hydrogen pressure can therefore be described by changes in the surface coverage of ammonia.

If the adsorption of ethanol on cobalt occurred via the abstraction of hydrogen atoms, then an increase in the hydrogen partial pressure would be expected to decrease the surface coverage of ethanol resulting in lower conversions. This is not observed experimentally and an increase in the hydrogen pressure results in an increase in the rate of ethanol consumption. Furthermore, since ethanol is directly involved in the reactions forming MEA, DEA and TEA, little effect on the overall selectivity with changing ethanol surface coverages would be expected.

4.1.2.5. Ethylamine selectivity of Ni/SiO_2

By changing the partial pressures of the ethanol, ammonia and hydrogen feeds, considerable changes in the ethylamine selectivity of the Ni/SiO_2 catalyst were observed. Increasing the ammonia partial pressure resulted in an increase in the MEA selectivity, a decrease in the TEA selectivity and the selectivity to DEA first increased and then decreased. Since the overall rate of ethanol consumption over the Ni/SiO_2 catalyst was not significantly affected by increasing the ammonia partial pressure, it can be seen that the decrease in the rate of DEA and TEA formation is caused by an inhibition of MEA and DEA readsorption respectively (which react with ethanol to form DEA and TEA). This selective inhibition is similar to that observed when changing the ammonia partial pressure over the Co/SiO_2

catalyst. The fact that increased ammonia partial pressures do not decrease the overall rate of ethanol conversion may indicate that ethanol is more strongly adsorbed than ammonia on nickel (*i.e.* ethanol cannot be displaced by ammonia) or that an increase in the rate of ethanol consumption is counterbalanced by the inhibition of ethanol adsorption by ammonia.

Increasing the ethanol partial pressure resulted in a decrease in the selectivity to MEA and an increase in the selectivities to DEA and TEA when using the Ni/SiO_2 catalyst. This indicates that the rates of DEA and TEA formation are increased to a greater extent with increasing ethanol partial pressure in comparison to the rate of MEA formation. If the rate controlling step during reductive amination was the rate of ethanol dehydrogenation, then the rates of formation of MEA, DEA and TEA would be directly proportional to the ethanol partial pressure (*i.e.* rate $\propto P_{EtOH}$). This would not alter the selectivity during reductive amination and consequently it can be deduced that the rate of ethylamine formation over Ni/SiO_2 is not controlled by the rate of alcohol dehydrogenation. Because of the series nature of the reductive amination reaction over the nickel catalyst, an increase in the rate of reactant consumption is expected to result in a decrease in the MEA selectivity and an increase in the selectivity to DEA and TEA. The changes in ethylamine selectivity observed upon changing the ethanol partial pressure over the Ni/SiO_2 catalyst can therefore be ascribed to the increased rate of reactant consumption.

Increasing the hydrogen partial pressure resulted in a decrease in the selectivity to MEA and an increase in the selectivities to DEA and TEA when using the Ni/SiO_2 catalyst. The changes in ethylamine selectivity upon changing the hydrogen pressure were not as pronounced when using the Ni/SiO_2 catalyst compared to the Co/SiO_2 catalyst, primarily due to the fact that the ethanol conversion was not influenced by the hydrogen pressure over the nickel catalyst (*i.e.* catalyst deactivation via nickel nitride formation was not significant). Since the ethanol conversion remains constant, the change in selectivity with increasing hydrogen partial pressure represents a decrease in the rate of ammonia consumption. These changes in the rate of ammonia consumption with changing hydrogen partial pressure can be explained by assuming that ammonia adsorbs dissociatively on nickel via the abstraction of one or more hydrogen atoms. Increasing the hydrogen partial pressure will therefore result

in a decreased surface coverage of ammonia which in turn will result in decreased MEA formation and a decreased inhibition of DEA and TEA formation. If the increased DEA and TEA selectivities were caused by an increase in the rate of hydrogenation of the reaction intermediates leading to DEA and TEA, then an increase in the rate of ethanol consumption would be expected. Since this is not observed, it appears that it is more likely that hydrogen alters the adsorption equilibria of ammonia of nickel which results in the observed selectivity changes.

4.1.2.6. Ethylamine selectivity of Cu/SiO_2

The selectivity behaviour of the SiO_2 supported copper catalyst is considerably different to that of the SiO_2 supported cobalt and nickel catalysts. In particular, the MEA selectivity is much lower and the DEA selectivity is much higher when using the copper catalyst in comparison to the nickel and copper catalysts. The low MEA selectivity is caused by the rapid conversion of MEA to DEA and as a consequence, DEA behaves as a primary product during reductive amination over Cu/SiO_2. If DEA was the primary product formed during reductive amination over Cu/SiO_2, then a trimolecular reaction between two ethanol molecules and an ammonia molecule would be required. Since this is unlikely, it can be deduced that MEA is rapidly converted to form DEA.

Increasing the ammonia partial pressure resulted in an increase in the selectivity to DEA and a decrease in the selectivity to TEA. The MEA selectivity was very low and did not change significantly with changing ammonia pressure. The increased rate of DEA formation can be ascribed to a greater rate of MEA formation via the reaction between ethanol and ammonia at higher ammonia partial pressures. The increased rate of MEA formation results in an increased rate of DEA formation and is observed as an increase in the selectivity. The increase in the surface coverage of ammonia at increased ammonia pressures inhibits the readsorption and reaction of DEA thereby resulting in a decrease in the TEA selectivity. It is unlikely that ammonia inhibits the adsorption of ethanol (which is required for TEA formation) since the overall rate of reductive amination over Cu/SiO_2 is not influenced significantly by the ammonia partial pressure.

Increasing the ethanol partial pressure resulted in a decrease in the DEA selectivity and a slight increase in the TEA selectivity. The MEA selectivity was low and no clear trend could be identified. The selectivity behaviour obtained upon changing the ethanol partial pressure was similar to that in which the ethanol conversion was changed (Figure 4.3.). The changes in ethylamine selectivity are therefore probably caused by changes in the ethanol conversion with changes in the ethanol partial pressure during amination over the Cu/SiO_2 catalyst.

By increasing the hydrogen partial pressure over the Cu/SiO_2 catalyst, the rate of byproduct formation was decreased and the rate of DEA and TEA formation was increased. Since this unidentified byproduct was not observed at higher hydrogen partial pressures, it can be deduced that either hydrogen inhibits the formation of this species or that this species is a reaction intermediate which can be hydrogenated to form either DEA or TEA. By increasing the ethanol and ammonia partial pressures, an increase in the rate of byproduct formation was observed which indicates that this species is probably formed via the reaction between these two species. If hydrogen inhibited the formation of this byproduct species, then a decrease in the overall rate of ethanol conversion would be expected. Since this is not observed and since the rates of DEA and TEA formation are increased with increasing hydrogen pressure, it appears that this unidentified byproduct is a dehydrogenated reaction intermediate which is converted to form DEA and TEA at higher hydrogen pressures.

4.1.3. Modelling of the Amination Behaviour of Cobalt, Nickel and Copper Catalysts

In the previous section, it was shown that the reaction pathway during reductive amination using cobalt, nickel and copper catalysts can be described by a series reaction in which the hydrogen atoms of the ammonia molecule are sequentially substituted by alkyl groups of the reactant alcohol. From the overall stoichiometry of reactions [1] to [3] (see Chapter 4.1.2.2.), the following simple mass action equations can be derived, *viz* :

$$r_1 = k_1 C_{EtOH} C_{NH3} - k'_1 C_{MEA} C_{H2O}$$
$$r_2 = k_2 C_{EtOH} C_{MEA} - k'_2 C_{DEA} C_{H2O}$$
$$r_3 = k_3 C_{EtOH} C_{DEA} - k'_3 C_{TEA} C_{H2O}$$

where r_i represents the rate of reaction in mmol/g_{cat}·h. These mass action equations result in the following description of the rate of formation of the individual ethylamine products.

$$r_{MEA} = r_1 - r_2$$
$$r_{DEA} = r_2 - r_3$$
$$r_{TEA} = r_3$$

The kinetic evaluation of the reaction data obtained for the cobalt, nickel and copper catalysts was structured using the mass action equations listed above (*i.e.* the rates of MEA, DEA and TEA formation were modelled).

4.1.3.1. Kinetic Evaluation of Co/SiO_2

From the mass action equations listed above, it is clear that the hydrogen partial pressure should have no influence on the rate of formation of the individual ethylamine products. By varying the hydrogen partial pressure during reductive amination using Co/SiO_2, a large variation in both the activity and selectivity of reductive amination was observed (see Chapter 3.1.6.) which indicates that hydrogen does in fact influence the rate of ethylamine formation.

Simple mass action equations are therefore inadequate in describing the amination performance of SiO_2 supported cobalt catalysts.

The large variation in catalytic activity upon changing the hydrogen partial pressure may be due to the formation of cobalt nitride species. Cobalt nitride is inactive for the reductive amination reaction [Baiker and Maciejewski, 1984] and is formed by the direct interaction between ammonia and the metal surface via the following reaction [Baiker and Kijenski, 1985] :

$$3\ Co + NH_3 \rightleftarrows Co_3N + 1.5\ H_2$$

In an instance where the above reaction to form cobalt nitride is at equilibrium under amination conditions, the number of exposed cobalt atoms (and therefore the total activity of the supported catalyst) may be estimated by the following expression :

$$N_{Co} = k \times \frac{P_{H_2}^{1.5}}{P_{NH_3}}$$

By decreasing the partial pressure of hydrogen from 20 to 6 kPa at a constant ammonia partial pressure of 8 kPa, a considerable decrease in the activity of the Co/SiO_2 catalyst was observed. Similarly, above ammonia partial pressures of 8 kPa (at a hydrogen pressure of 20 kPa), the rate of ethanol conversion decreases. Cobalt nitride formation therefore appears to be significant for supported cobalt catalysts when the H_2 : NH_3 ratio during amination is less than 20 : 8 or 2.5.

By increasing the ammonia partial pressure during reductive amination, considerable selectivity changes are observed which correspond to changes in the rates of reactions [1] to [3] (as listed in Chapter 4.1.2.2.). The rate of MEA formation increases, DEA formation first increases and then decreases and TEA formation decreases with increasing ammonia partial pressure (Chapter 3.1.5.). Description of the amination behaviour of the Co/SiO_2 catalyst using the simple mass action equations listed previously cannot account for these

phenomena since although an increase in the ammonia pressure would result in an increase in the rate of MEA formation, this would in turn result in an increase in the rates of DEA and TEA formation (because of the series nature of the amination reaction). Since this is not observed, a more complicated kinetic expression is required.

According to the Langmuir-Hinshelwood formulations, the rate of a fluid-solid catalytic reaction can be determined by either the rate of reactant adsorption, surface reaction or product desorption (in the absence of heat and mass transfer limitations). With the Co/SiO_2 catalyst, the rate of reaction [1] between ethanol and ammonia (which is not directly measured but may be evaluated from the experimental data as $r_1 = r_{MEA} + r_{DEA} + r_{TEA}$) increases with increasing partial pressures of the ethanol and ammonia reactants. The resulting kinetic expression must therefore describe the increase in the rate of this reaction with increasing partial pressures of the ethanol and ammonia feeds. If the rate of ethanol adsorption is the slowest step during reaction [1], the following Langmuir-Hinshelwood expression can be derived :

$$r_1 = k_a C_m \times \frac{C_{EtOH} - \frac{1}{K_a}\frac{C_{MEA} C_{H_2O}}{C_{NH_3}}}{1 + \frac{K_{EtOH}}{K_a}\frac{C_{MEA} C_{H_2O}}{C_{NH_3}} + K_{NH_3} C_{NH_3} + \Sigma K_{Amines} C_{Amines} + K_{H_2O} C_{H_2O}}$$

Although this Langmuir-Hinshelwood expression can describe the increase in the rate of reaction [1] with increasing ethanol partial pressure, no direct relationship with respect to the ammonia pressure is present in this expression and the model can therefore not describe the increase in the rate of this reaction with increasing ammonia pressure. In a similar manner, a Langmuir-Hinshelwood expression derived for a case where the rate of ammonia adsorption is the rate controlling step does not adequately describe the increase in the rate of reaction [1] with increasing ethanol partial pressure. Reaction rate control by the rate of reactant adsorption is therefore not the rate determining step for reaction [1]. The strong inhibition of DEA and TEA formation at increased ammonia pressures points towards a facile adsorption of ammonia on the cobalt catalyst which would further indicate that it is unlikely that the rate of ammonia adsorption is the rate controlling step.

By assuming that the rate of surface reaction between ethanol and ammonia is the rate controlling step for reaction [1], the following Langmuir-Hinshelwood expression can be formulated :

$$r_1 = k_s\, C_m\, K_{EtOH}\, K_{NH_3} \times \frac{C_{EtOH}\, C_{NH_3} - \frac{1}{K_s}\, C_{MEA}\, C_{H_2O}}{(1 + K_{EtOH}C_{EtOH} + K_{NH_3}C_{NH_3} + \Sigma K_{Amines}C_{Amines} + K_{H_2O}C_{H_2O})^2}$$

From the nature of this expression, it can be seen that an increase in the partial pressure of either the ethanol or the ammonia reactants will result in an increase in the rate of reaction [1]. This behaviour is consistent with the experimental results. As the partial pressures of the reactants increase, an increase in the contribution of the adsorption terms can describe the decrease in the rate of this reaction at higher reactant partial pressures. This kinetic expression can therefore describe the changes occurring upon changing the partial pressures of the reactants during amination.

The third possible rate controlling step could be that of product desorption. If MEA was strongly adsorbed, the adsorption and surface reaction steps would be equilibrated and the rate of reaction [1] could be described by the following expression :

$$r_1 = k_d\, C_m\, K \times \frac{\frac{C_{EtOH}\, C_{NH_3}}{C_{H_2O}} - \frac{1}{K_d}\, C_{MEA}}{1 + K_{EtOH}C_{EtOH} + K_{NH_3}C_{NH_3} + K_{MEA}K_d\frac{C_{EtOH}C_{NH_3}}{C_{H_2O}} + K_{H_2O}C_{H_2O}}$$

Positive reaction orders with respect to the ethanol and ammonia pressures are obtained using this kinetic formulation which is in agreement with the experimental measurements. The inverse relationship with respect to the water partial pressure results in the predicted rate being too high at low reactant partial pressures and too low at high reactant partial pressures however. Furthermore, if the rate of MEA desorption was low, it would be likely that the MEA would be converted to further amine products such as DEA and TEA thereby resulting in low MEA selectivities. At high ammonia partial pressures, the rate of MEA formation is high. The experimental measurements are therefore contrary to the model predictions

indicating that the rate of MEA desorption does not control the rate of reaction [1].

If the water formed via the reaction between ethanol and ammonia was strongly adsorbed, a similar kinetic expression can be obtained with the exception that the MEA and H_2O terms would be exchanged. At low partial pressures of ammonia, the rate of MEA formation is very low which results in a low MEA partial pressure. Because of the inverse relationship between ammonia and MEA in the kinetic expression, a very high rate would be predicted by the model which is contrary to the experimental evidence. The desorption of water can therefore be excluded as the rate controlling step for reaction [1]. Based on the experimental evidence, it can be deduced that the most promising kinetic expression describing the rate of reaction [1] is a case where the rate of surface reaction between adsorbed ethanol and ammonia is the controlling step.

The rate of reaction [2] (which can be evaluated from the experimental measurements as $r_2 = r_{DEA} + r_{TEA}$) increases with increasing ethanol partial pressure but remains approximately constant between ammonia partial pressures of 2 to 8 kPa. Above ammonia partial pressures of 8 kPa the rate of the reaction between ethanol and MEA decreases, probably due to catalyst deactivation caused by cobalt nitride formation (*i.e.* H_2 : NH_3 ratio less than 2.5). Since the rate of the reaction between ethanol and MEA increases with increasing ethanol partial pressures, it is likely that the rate is controlled by a step involving the ethanol reactant, *i.e.* either the adsorption of ethanol or the surface reaction between ethanol and MEA is the rate controlling step for reaction [2].

Increasing the ammonia pressure increases the rate of MEA formation which results in a higher concentration of MEA. An increase in the concentration of MEA would be expected to result in an increase in the rate of the reaction between ethanol and MEA if the rate of surface reaction between these species was the controlling step. The fact that the rate of the reaction between ethanol and MEA does not increase with increasing ammonia partial pressure indicates that it is unlikely that the rate of surface reaction between ethanol and MEA controls the rate of reaction [2] over Co/SiO_2. The behaviour of reaction [2] can be best described by a kinetic expression in which the rate of ethanol adsorption is the

controlling step. This expression can account for the increase in the rate of reaction with increasing ethanol pressure and the adsorption terms can account for the decrease in the rate of this reaction at high ammonia partial pressures.

The rate of reaction [3] (which can be evaluated from the experimental measurements as $r_3 = r_{TEA}$) increases with increasing ethanol partial pressure but decreases with increasing ammonia pressure. The increase in the rate of the reaction between ethanol and DEA with increasing ethanol pressure indicates that ethanol is involved in the controlling step during this reaction. It is therefore likely that the rate controlling step for reaction [3] is either that of ethanol adsorption or the surface reaction between ethanol and DEA.

Since the rate of DEA formation (and therefore the concentration) first increases and then decreases with increasing ammonia pressure, a kinetic expression formulated for an instance where the rate of surface reaction between ethanol and DEA was the controlling step would predict that the rate of TEA formation would first increase and then decrease with increasing ammonia partial pressure. The experimental measurements indicate that the rate of reaction [3] decreases with increasing ammonia pressure which indicates that the rate of surface reaction between adsorbed ethanol and DEA is not the controlling step for this reaction. If the rate of ethanol adsorption was the rate controlling step for reaction [3], the resulting kinetic expression would predict an increase in the rate of reaction with increasing ethanol pressure and the adsorption terms could account for the decrease in the rate of this reaction with increasing ammonia pressure. A kinetic expression in which the rate of ethanol adsorption is the controlling step therefore best describes the behaviour of this reaction.

From the experimental observations, kinetic expressions based on the Langmuir-Hinshelwood formulation were proposed and evaluated. The rate controlling step for reaction [1] was selected as the surface reaction between ethanol and ammonia whereas the rate of ethanol adsorption was selected as the rate controlling step for reactions [2] and [3]. Adsorption terms for the ethanol and ammonia reactants were included to account for the decrease in the rates of reactions [1] to [3] at increased reactant partial pressures.

The influence of the hydrogen partial pressure was not included in the model due to the formation of cobalt nitride species. Two distinct regimes are obtained which require two separate models. The model which accounts for the formation of cobalt nitride species will need to relate the number of metal sites (C_m) and therefore the total catalytic activity to the hydrogen and ammonia partial pressures as discussed earlier. Since the ammonia partial pressure data was recorded in a regime essentially void of cobalt nitride formation whereas the hydrogen partial pressure data was recorded in a regime in which cobalt nitride formation was significant, a disparity in the model was obtained when including the hydrogen partial pressure data.

The kinetic expressions obtained from the regression procedure for reactions [1] to [3] are illustrated below. The rate r_i represents the rate of amine formation in $mmol/g_{cat}{\cdot}h$ and the pressures P_i represent the pressures of the reactants and products in kPa.

$$r_1 = \frac{1.746\ P_{EtOH}\ P_{NH_3}}{(1 + 0.225 P_{EtOH} + 0.205 P_{NH_3})^2}$$

$$r_2 = \frac{2.502\ [\ P_{EtOH} - 0.061\ P_{DEA}\ P_{H_2O} / P_{MEA}\ ]}{1 + 0.225 P_{EtOH} + 0.205 P_{NH_3}}$$

$$r_3 = \frac{0.913\ P_{EtOH}}{1 + 0.225 P_{EtOH} + 0.205 P_{NH_3}}$$

The kinetic expressions obtained from the regression procedure indicated that the rate of the reverse reactions was negligible. This may be expected from the differential mode of

4.1.3.2. Kinetic Evaluation of Ni/SiO_2

By plotting the ethylamine selectivity as a function of the ethanol conversion, it was seen that the amination behaviour of the Ni/SiO_2 catalyst could be described by a series reaction mechanism (Figure 4.2.). Modelling of the reductive amination reaction using the Ni/SiO_2 catalyst was therefore based on the assumption of a series reaction mechanism.

An increase in the rate of the reaction [1] between ethanol and ammonia was observed upon increasing the partial pressures of the ethanol and ammonia reactants. If the rate of ethanol adsorption was the rate controlling step for reaction [1], an increase in the ammonia partial pressure would not be expected to increase the rate of this reaction. Similarly, if the rate of ammonia adsorption was the rate controlling step for this reaction, increasing the ethanol partial pressure would not be expected to increase the overall rate of reaction [1]. Rate control by the rate of reactant adsorption does therefore not explain the experimental observations.

If the rate of surface reaction was the controlling step, an increase in the rate of the reaction between ethanol and ammonia would be expected upon increasing the partial pressures of these species. This is observed experimentally and a kinetic model in which the surface reaction between ethanol and ammonia is the controlling step can be used to explain the amination behaviour of the Ni/SiO_2 catalyst. At high ammonia pressures however, the rate of reaction [1] only increases marginally with increasing ammonia partial pressure. Since the selectivity to MEA is increased at increased ammonia partial pressures, it is possible that the increased concentration of MEA results in an increase in the rate of the reverse reaction thereby decreasing the overall rate of reaction [1].

If the rate of MEA desorption was the controlling step for reaction [1], the Langmuir-Hinshelwood kinetic expression would predict a decrease in the rate of reaction [1] with increasing partial pressures of the ethanol and ammonia reactants. Since the rate of reaction [1] increases with increasing reactant partial pressure, it can be concluded that the rate of MEA desorption is not the controlling step for the reaction between ethanol and ammonia

using a SiO_2 supported nickel catalyst. This conclusion is further supported by the high MEA selectivities obtained during amination. If MEA were strongly adsorbed, it is likely that it would be converted via the reaction with ethanol to form DEA which would result in low selectivities. This is contrary to the experimental measurements. If the rate of desorption of water was the rate controlling step, a similar kinetic expression would be obtained in which the rate of reaction [1] decreases with increasing reactant partial pressures. The rate of product desorption does therefore not control the rate of the reaction between ethanol and ammonia over a Ni/SiO_2 catalyst.

The rate of reaction [2] between ethanol and MEA increases with increasing ethanol partial pressure and first increases and then decreases with increasing ammonia partial pressure. If the rate of the reaction between ethanol and MEA was controlled by the adsorption of ethanol, only an increase in the ethanol partial pressure would be expected to result in an increase in the rate of this reaction. The increase in the rate of this reaction at low ammonia partial pressures can therefore not be described by a kinetic expression in which the rate of ethanol adsorption is the controlling step. If the rate of reaction [2] was controlled by the rate of surface reaction between ethanol and MEA, the increase in the MEA concentration with increasing ammonia partial pressure could explain the initial increase in the rate of reaction [2] at low ammonia pressures. The decrease in the rate of this reaction at higher ammonia pressures can be explained by adsorption phenomena, *i.e.* ammonia inhibits the readsorption of MEA at higher pressures thereby lowering the rate of reaction [2]. Reaction rate control by the rate of MEA adsorption can be excluded since increasing the ammonia partial pressure (which results in increased MEA concentrations) results in a decrease in the rate of reaction [2].

If the rate of product desorption was the controlling step for reaction [2], an increase in the gas phase concentration of DEA or water would be expected to result in a decrease in the rate of the reaction between ethanol and MEA. No decrease in the rate of reaction [2] with increasing ethanol partial pressure (and therefore increasing DEA and water concentrations) is observed indicating that the rate of product desorption is not the controlling step for this reaction. The relatively high DEA selectivities obtained over the Ni/SiO_2 catalyst are not

characteristic of a case where DEA is strongly adsorbed.

The rate of reaction [3] between ethanol and DEA increases with increasing ethanol partial pressure but decreases with increasing ammonia partial pressure. The increase in the rate of this reaction with increasing ethanol partial pressure indicates that ethanol is involved in the rate determining step, *i.e.* either the rate of ethanol adsorption or the rate of surface reaction between adsorbed ethanol and DEA is the rate controlling step for reaction [3].

The behaviour of this reaction can be described by a kinetic expression in which the rate of surface reaction between adsorbed ethanol and DEA is the rate controlling step. Increasing the ethanol partial pressure results in an increase in the surface concentration of ethanol which results in an increase in the rate and increasing the ammonia pressure decreases the DEA concentration which results in a decrease in the rate.

The Langmuir-Hinshelwood expressions developed to describe the amination behaviour of the Ni/SiO_2 catalyst upon changing the ethanol and ammonia partial pressures do not explain the changes occurring upon changing the hydrogen partial pressure. It was seen that an increase in the hydrogen partial pressure resulted in a decrease in the rate of reaction [1] and an increase in the rates of reactions [2] and [3]. If the changes in reaction rate upon changing the hydrogen pressure were simply due to the competitive adsorption of hydrogen, a similar decrease in the rates of each reaction would be expected. This is not observed experimentally and therefore the role of hydrogen during amination is more complicated than simply to prevent catalyst deactivation by nickel nitride formation [Baiker and Maciejewski, 1984].

The hydrogen partial pressure does not influence the rate of ethanol conversion significantly and it is therefore unlikely that hydrogen influences the adsorption or reaction of ethanol during amination. The decrease in MEA selectivity and the increase in the selectivity to DEA and TEA with increasing hydrogen pressure represents a decrease in the rate of ammonia consumption and consequently it can be deduced that hydrogen inhibits the adsorption and/or reaction of ammonia. Inhibition of ammonia adsorption/reaction would result in a decrease in the rate of reaction [1] between ethanol and ammonia. The decrease in the surface

concentration of ammonia would also result in a decreased inhibition of MEA and DEA readsorption which would be expected to result in an increase in the rates of reactions [2] and [3].

If hydrogen transfer processes are involved in the adsorption of ammonia on metallic nickel, a dependency of the surface coverage of ammonia species on the hydrogen pressure can be obtained. Depending on the degree of ammonia dehydrogenation, a number of surface reactions are possible. The successive abstraction of hydrogen atoms from an ammonia molecule is illustrated below (where ✳ represents a nickel active site).

$$NH_3 + ✳ \rightleftarrows NH_3✳$$
$$NH_3✳ + ✳ \rightleftarrows NH_2✳ + H✳$$
$$NH_2✳ + ✳ \rightleftarrows NH✳ + H✳$$
$$NH✳ + ✳ \rightleftarrows N✳ + H✳$$
$$2\,H✳ \rightleftarrows H_2 + 2✳$$

If ammonia adsorbs with the loss of hydrogen, the equilibrium concentration of adsorbed ammonia species would be inversely proportional to the hydrogen partial pressure. The order of this hydrogen dependency will vary depending on the degree of dehydrogenation and can range from 0 in the case of simple adsorption to 1.5 in the case where the adsorbed ammonia molecule is completely dehydrogenated. The surface concentration of ammonia as a function of the hydrogen partial pressure may be expressed by the following relationship.

$$\theta_{NH_{3-x}} \propto \frac{P_{NH_3}}{P_{H_2}^{x/2}}$$

where x represents the number of hydrogen atoms which have been removed from the adsorbed ammonia molecule.

From the experimental results, a Langmuir-Hinshelwood kinetic model was developed in which the rates of reactions [1] to [3] were controlled by the rate of surface reaction. In this

model, the surface concentration of ammonia was expressed as a function of the hydrogen partial pressure according to the assumption that ammonia adsorbs with the loss of hydrogen on nickel. In order to determine the extent to which the ammonia molecule was dehydrogenated during amination over the Ni/SiO_2 catalyst, the order with respect to the hydrogen pressure was varied from 0 to 1.5 in increments of 0.5. The best correlation was taken to represent the degree of hydrogen abstraction of the ammonia molecule during reductive amination. This approach does not preclude that ammonia cannot however exist in a number of dehydrogenated states (*i.e.* NH_3, NH_2, NH and N-species).

Direct regression of the Langmuir-Hinshelwood kinetic expressions derived for reactions [1] to [3] did not result in a satisfactory correlation, primarily due to the adsorption term. The rate of reaction [1] as predicted by the model was too low and the rates of reactions [2] and [3] were too high. Modification of the kinetic expression describing reaction [1] such that the adsorption term was not raised to the power 2 resulted in a good description of the experimental data (Figures 4.8. to 4.10.).

The kinetic expressions for reactions [1] to [3] are listed below along with the rate and adsorption constants obtained from the non-linear regression. The rate r_i represents the rate of amine formation in $mmol/g_{cat}{\cdot}h$ and the pressure P_i represents the partial pressures of the reactants and products in kPa.

$$r_1 = \frac{83.15\ P_{EtOH}\ [\ P_{NH_3}/P_{H_2}^{0.5}\ ]}{1 + 2.54\ P_{EtOH} + 58.3\ [\ P_{NH_3}/P_{H_2}^{0.5}\ ]}$$

$$r_2 = \frac{30700\ P_{EtOH}\ P_{MEA}}{(1 + 2.54\ P_{EtOH} + 58.3\ [\ P_{NH_3}/P_{H_2}^{0.5}\ ]\ )^2}$$

$$r_3 = \frac{4194\ P_{EtOH}\ P_{DEA}}{(1 + 2.54\ P_{EtOH} + 58.3\ [\ P_{NH_3}/P_{H_2}^{0.5}\ ])^2}$$

Although modification of the kinetic model by altering the adsorption term for reaction [1] resulted in a much better prediction of the experimentally measured results, it is inconsistent with Langmuir-Hinshelwood theory. In order to obtain a Langmuir-Hinshelwood kinetic expression in which the denominator is raised to the power 1, the rate of reaction must be controlled by either reactant adsorption or product desorption. The experimental results show clearly that this is not the case. Alternatively, an adsorption term raised to the power 1 may be obtained when the reaction between ethanol and ammonia occurs via an Eley-Rideal mechanism in which there is reaction between a gas phase molecule and an adsorbed species.

If reaction [1] were to occur between an adsorbed ethanol species and a gas phase ammonia molecule, it would be likely that the surface concentration of adsorbed ammonia species is low. The inhibition of reactions [2] and [3] at high ammonia pressures indicate that a significant amount of ammonia does adsorb on the nickel surface which is contrary to the assumption of the reaction between gas phase ammonia with adsorbed ethanol. If a gas phase ethanol species were to react with an adsorbed ammonia species, it would be expected that the surface concentration of adsorbed ethanol would be low. Since the rates of reactions [2] and [3] are well described by a kinetic expression formulated for a case in which the rate of surface reaction is controlling, it is unlikely that the surface concentration of ethanol would be very low during amination. Therefore, although an Eley-Rideal mechanism can be used to describe the amination behaviour of Ni/SiO_2, it is not consistent with the behaviour observed for reactions [2] and [3] over the Ni/SiO_2 catalyst. It is therefore clear that the mechanism of reductive amination is considerably more complicated than that used for formulation of the kinetic expression in this study.

As in the instance of the Co/SiO_2 catalysts, the rate of the reverse reactions was not significant under the reaction conditions used. This may be expected since the reaction is

kinetically controlled at the low conversions used in this study. Also, the thermodynamic calculations indicate that at equilibrium, almost total conversion of the reactant alcohol is obtained (Chapter 1.3.). If total reactant conversion is obtained at equilibrium, it is to be expected that the reverse reactions would only become significant at high ethanol conversions.

The best correlation was obtained when the hydrogen pressure term was raised to the power 0.5, corresponding to the abstraction of 1 hydrogen atom from the ammonia molecule. The ammonia molecule is therefore most likely present as a NH_2 species on the nickel surface during reductive amination on nickel catalysts. It is possible that other forms of adsorbed ammonia such as NH_3, NH and N species are also present during reaction however.

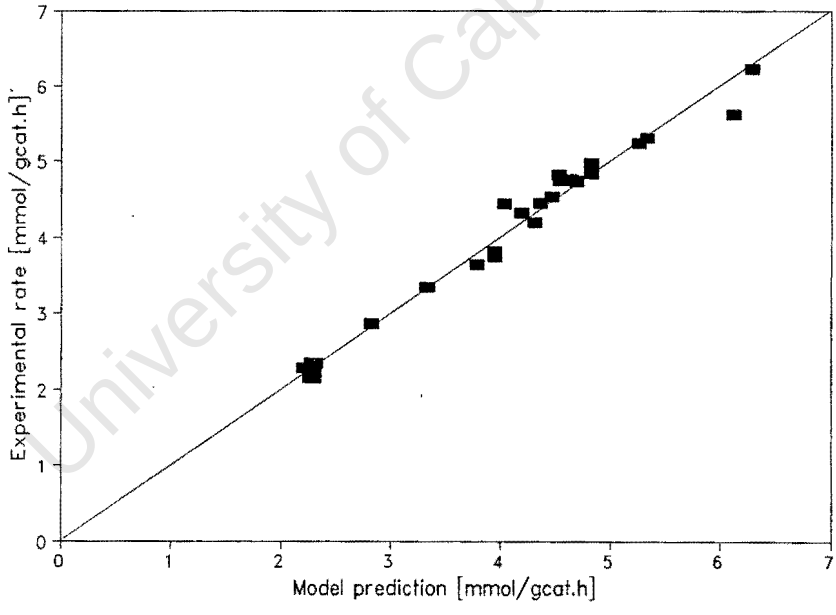

Figure 4.8. Model prediction versus experimental data for rate of reaction [1] (EtOH + NH_3 ⇄ MEA + H_2O)

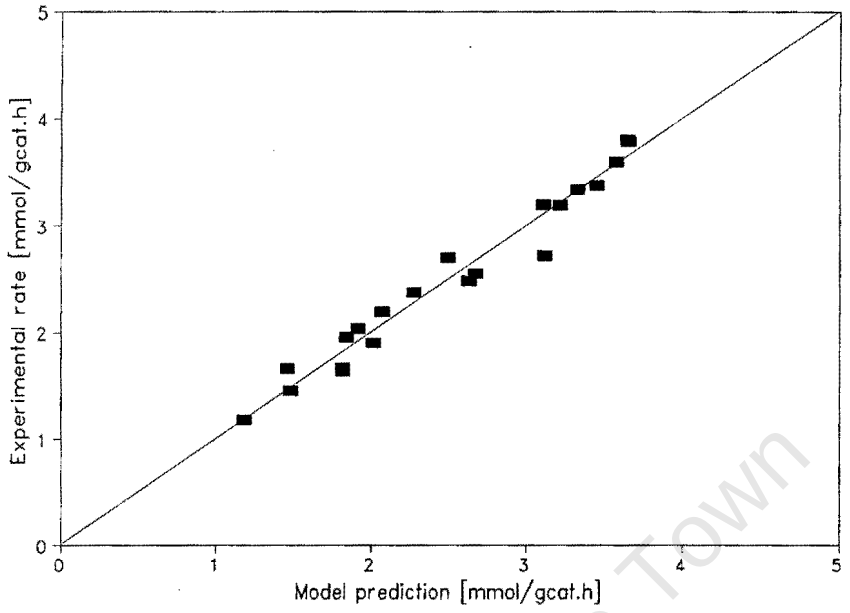

Figure 4.9. Model prediction versus experimental data for rate of reaction [2] (EtOH + MEA ⇄ DEA + H_2O)

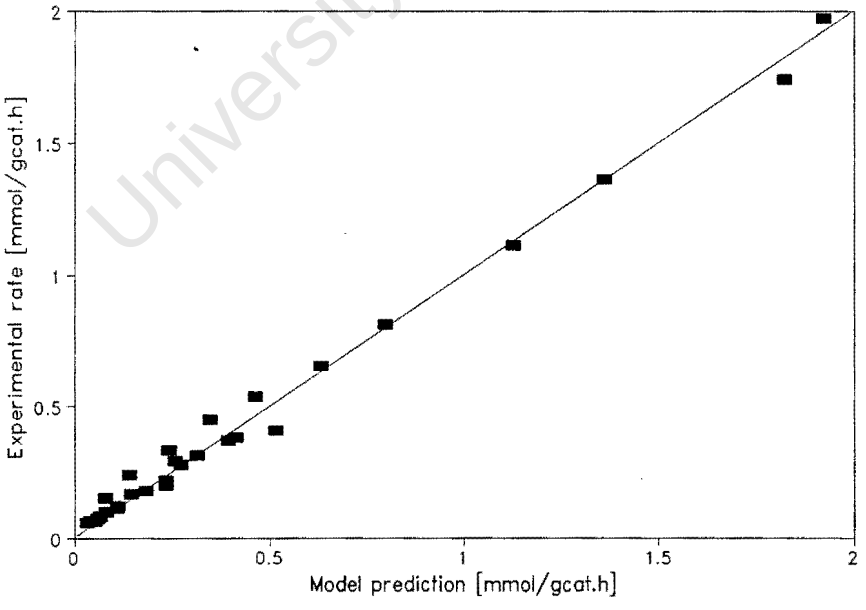

Figure 4.10. Model prediction versus experimental data for rate of reaction [3] (EtOH + DEA ⇄ TEA + H_2O)

4.1.3.3. Kinetic Evaluation of Cu/SiO_2

By plotting the ethylamine selectivity as a function of the ethanol conversion, it was observed that the amination behaviour of SiO_2 supported copper was considerably different to that of either the cobalt or nickel catalysts (Figure 4.3.). Instead of MEA appearing as a primary product, DEA was obtained at selectivities of 100% at low reactant conversions. In spite of this, the amination behaviour of the Cu/SiO_2 catalyst could be described in terms of a series reaction mechanism in which the rate of conversion of MEA to DEA was rapid.

Since the rate of MEA formation is very low during the reductive amination of ethanol over Cu/SiO_2, it is clear that the rate of reaction [1] between ethanol and ammonia and the rate of reaction [2] between ethanol and MEA are similar. Consequently, the kinetic expressions describing these two reactions will be similar. From the experimental results, it was seen that the rates of reactions [1] and [2] increased with increasing ethanol pressure but decreased with increasing ammonia partial pressure. If the rate of ethanol adsorption was the rate controlling step for these two reactions, then an increase in the rate of formation with increasing ethanol partial pressure would be expected. This is in agreement with the experimental observations. The decrease in the rate of these reactions with increasing ammonia partial pressure can be explained by adsorption phenomena.

If reaction [1] between ethanol and ammonia was controlled by either the rate of ammonia adsorption or the rate of surface reaction, an increase in the rate of formation of MEA would be expected with increasing partial pressures of ammonia. Since this is not observed experimentally, it can be deduced that these steps are not rate controlling during amination over SiO_2 supported copper catalysts. The low MEA selectivities point towards strong adsorption of MEA on SiO_2 supported copper catalysts from which it may be expected that the rate of product desorption would be the controlling step. A kinetic expression in which the rate of reaction [1] is controlled by the rate of MEA desorption cannot adequately describe the observed behaviour of this catalyst however. In instances when the MEA concentration is too low to be measured (*e.g.* as during the experiments in which the hydrogen pressure was varied), this specific kinetic formulation will predict a negative rate

of MEA formation (since $r_{MEA} = r_1 - r_2$).

If the rate of reaction [2] between ethanol and MEA was controlled by either the rate of MEA adsorption or the rate of surface reaction, the resulting kinetic expression could not adequately describe the catalytic behaviour of the Cu/SiO_2 catalyst since the MEA concentration is not always measurable. Reaction rate control by the rate of product desorption is also unlikely due to the high DEA selectivities obtained over this catalyst. The most promising kinetic expression describing reactions [1] and [2] therefore appears to be that of a case where the rate is controlled by the rate of ethanol adsorption.

The rate of reaction [3] between ethanol and DEA increases with increasing ethanol pressure but decreases with increasing ammonia pressure. Since the rate of reaction [3] increases with increasing ethanol partial pressure, it can be deduced that ethanol is involved in the rate controlling step. The possible rate controlling steps involving ethanol are the adsorption of this species or the surface reaction between ethanol and DEA to form TEA. Both of these rate limiting steps are consistent with the experimental measurements and the decrease in the rates of these reactions with increasing ammonia pressure can be described by adsorption phenomena.

From the experimental evidence, it could be deduced that the most probable rate controlling step for reactions [1] and [2] was that of ethanol adsorption. The rate of TEA formation (*i.e.* reaction [3]) could be described by a kinetic expression derived for a case where either the rate of ethanol adsorption or the rate of surface reaction between ethanol and DEA was the rate determining step. Non-linear regression of the experimental data indicated that reaction [3] was best described for a case in which the rate determining step was that of surface reaction. Although a better correlation was obtained in this manner, it cannot be concluded that this is the actual rate determining step.

As in the instance of the Ni/SiO_2 catalyst, Langmuir-Hinshelwood kinetic expressions have been developed which describe the behaviour of the Cu/SiO_2 catalyst upon changing the ammonia and ethanol partial pressures. These expressions cannot however describe the

changes occurring upon changing the hydrogen partial pressure. The rates of reactions [1] to [3] were seen to increase with increasing hydrogen pressure which indicated that either hydrogen was directly involved in the rate determining step over Cu/SiO_2 or that hydrogen altered the nature of the copper surface (*i.e.* the total number of active sites available for reaction was changed). If hydrogen was directly involved in the rate controlling step over Cu/SiO_2, the positive reaction orders with respect to both the ethanol and hydrogen partial pressures would not be expected (*i.e.* the reaction between ethanol and hydrogen would not result in an ethylamine product). The changes in catalytic activity therefore appear to be linked to changes in the nature of the copper surface.

If the changes in catalytic activity with changing hydrogen partial pressure are caused by changes in the number of active copper sites, then it may be expected that hydrogen either reacts chemically with the copper catalyst to regenerate the site or that hydrogen displaces strongly adsorbed species which act as a site poison. Regeneration of an active copper site by reaction with hydrogen may indicate that an equilibrium relationship between copper and copper nitride or copper and copper oxide species exists during amination. The reaction to form copper nitride and copper oxide may occur via the following reactions :

$$3\ Cu + NH_3 \rightleftarrows Cu_3N + 1.5\ H_2$$
$$2\ Cu + H_2O \rightleftarrows Cu_2O + H_2$$

If these reactions were responsible for the changes in activity, then the following dependency of the total number of copper active sites for the reaction to form copper nitride and the reaction to form copper oxide would be obtained :

$$N_{Cu} \propto \frac{P_{H_2}^{1.5}}{P_{NH_3}}$$

$$N_{Cu} \propto \frac{P_{H_2}}{P_{H_2O}}$$

The resulting kinetic expressions could not adequately describe the amination behaviour of Cu/SiO_2 therefore indicating that a modification of the catalyst surface via these mechanisms is unlikely. Furthermore, under the hydrogen rich conditions used in this study, it is not expected that these reactions will occur to any significant extent. By simply making the number of active copper sites directly proportional to the hydrogen pressure (*i.e.* $N_{Cu} \propto P_{H2}$), a good correlation between the model predictions and the experimentally measured rates was obtained (Figures 4.11. to 4.13.). The direct relationship between the hydrogen pressure and the number of exposed sites points towards the establishment of an equilibrium relationship during amination over Cu/SiO_2 catalysts. This equilibrium may be due to the removal of strongly adsorbed species from the copper surface by hydrogen thereby making an extra site available. This is illustrated in the following example where A represents the strongly adsorbed molecule.

$$Cu{\cdot}A_{(ads)} + H_{2\,(g)} \rightleftarrows Cu{\cdot}H_{2\,(ads)} + A_{(g)}$$

The role of hydrogen during amination over Cu/SiO_2 is therefore complicated and may be related either to intricacies in the reaction mechanism or to modifications of the nature of the catalyst surface.

The kinetic expressions obtained from the non-linear regression for reactions [1] to [3] are listed below. The rate r_i represents the rate of amine formation in $mmol/g_{cat}{\cdot}h$ and the pressure P_i represents the partial pressure of the reactants or products in kPa.

$$r_1 = 0.790\ P_{H_2}\ \frac{P_{EtOH}}{1 + 0.783P_{EtOH} + 0.161P_{NH_3}}$$

$$r_2 = 0.740\ P_{H_2}\ \frac{P_{EtOH}}{1 + 0.783P_{EtOH} + 0.161P_{NH_3}}$$

$$r_3 = 65.0\ P_{H_2}\ \frac{P_{EtOH}\ P_{DEA}}{(1 + 0.783P_{EtOH} + 0.161P_{NH_3})^2}$$

From these kinetic expressions, it can be seen that the adsorption term for ethanol is greater than ammonia. This would point towards a greater surface concentration of ethanol relative to ammonia and may explain the high DEA and TEA selectivities obtained using Cu/SiO_2 catalyst in comparison to the SiO_2 supported cobalt and nickel catalysts.

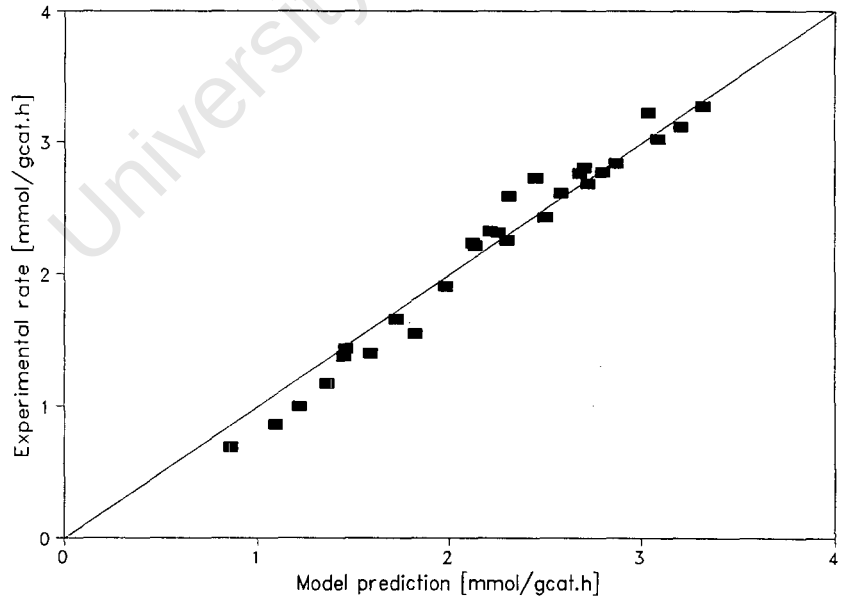

Figure 4.11. Model prediction versus experimental data for the rate reaction 1 ($EtOH + NH_3 \rightleftarrows MEA + H_2O$)

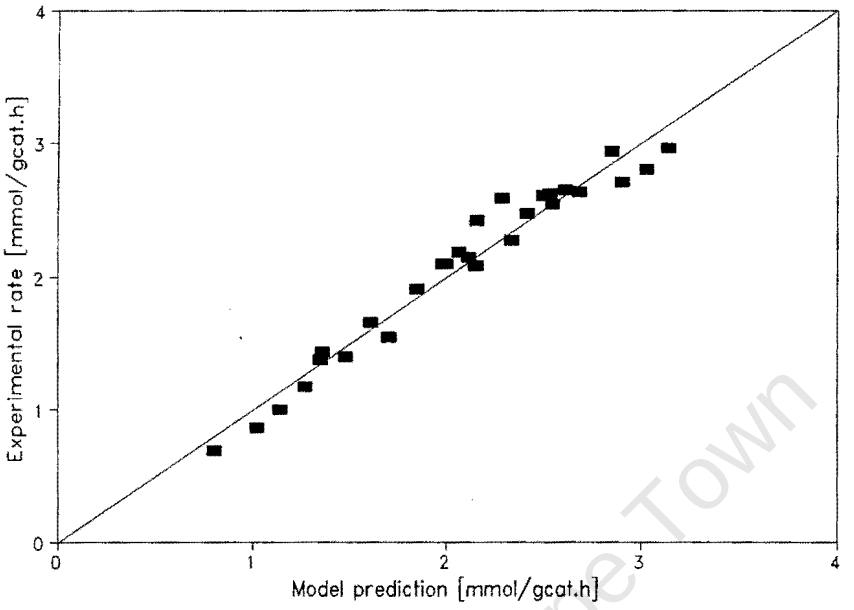

Figure 4.12. Model prediction versus experimental data for the rate of reaction [2] (EtOH + MEA ⇄ DEA + H_2O)

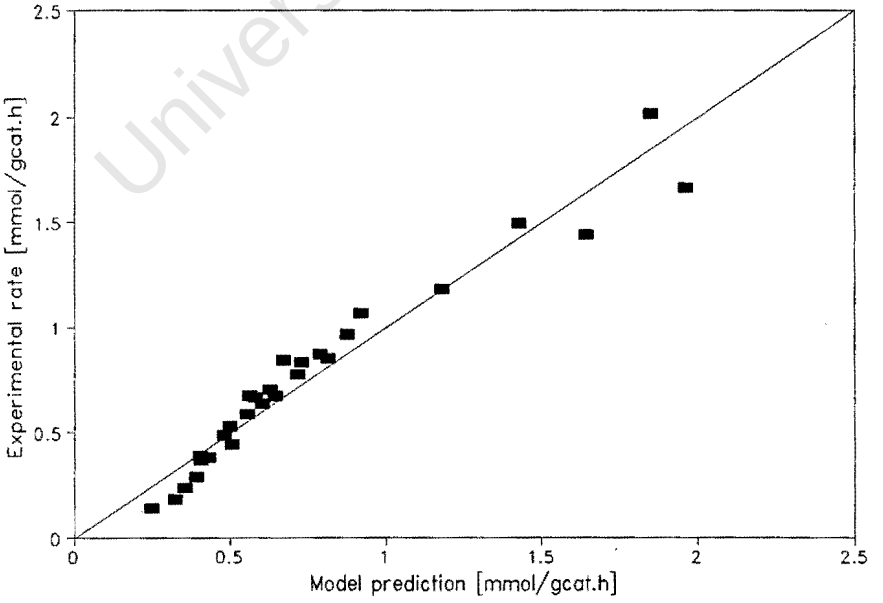

Figure 4.13. Model prediction versus experimental data for the rate of reaction [3] (EtOH + DEA ⇄ TEA + H_2O)

4.3.4. Critical Evaluation of Kinetic Modelling

In order to obtain a mechanistic description of the reductive amination behaviour of the SiO_2 supported cobalt, nickel and copper catalysts, kinetic models based on the Langmuir-Hinshelwood formulation [Hinshelwood, 1940] were developed and evaluated. Simple Langmuir-Hinshelwood models could not adequately describe the amination behaviour of these metal catalysts however. Although adjustments made to the kinetic expressions resulted in a better prediction of the experimental data, these adjustments were not justified in terms of the Langmuir-Hinshelwood assumptions. It is therefore clear that either the Langmuir-Hinshelwood formulation is not sufficient in describing the amination behaviour of these metal catalysts or that the proposed reaction mechanism was too simple.

In the case of the SiO_2 supported cobalt catalyst, a Langmuir-Hinshelwood expression was developed which described the behaviour of this catalyst upon changing the ethanol and ammonia partial pressures. It was found however that the incorporation of nitrogen into the cobalt lattice resulted in a decrease in activity due to the formation of cobalt nitride species which are inactive for the reductive amination reaction. These cobalt nitride species were only observed below a certain H_2 : NH_3 ratio and as a consequence of the conditions used during the kinetic evaluations, two separate reaction regimes were obtained. In the one regime, cobalt nitride formation was not observed and, in the other regime, an equilibrium between cobalt metal and cobalt nitride formation was obtained. As a result of the cobalt nitride formation observed during the hydrogen partial pressure experiments, the model which described the changes in reaction rate upon changing the ethanol and ammonia pressures could not account for the decrease in activity caused by nitride formation.

In the case of the Ni/SiO_2 catalyst, a set of Langmuir-Hinshelwood kinetic expressions were developed in which the rate of surface reaction was the rate controlling step for the formation of MEA, DEA and TEA. Direct application of this model did not result in an adequate description of the amination behaviour of the nickel catalyst due to the adsorption terms in

the denominator of the kinetic expressions. The best fit obtained for this catalyst was when it was assumed that the reaction between ethanol and ammonia to form MEA occurred via an Eley-Rideal step (*i.e.* reaction between a gas phase molecule and an adsorbed molecule). Although this model resulted in a good prediction of the amination behaviour of the nickel catalyst, it is unlikely that an Eley-Rideal mechanism occurs during reaction since the experimental evidence indicates that both ethanol and ammonia are able to be adsorbed on the nickel surface.

The Langmuir-Hinshelwood kinetic expressions developed for the Cu/SiO_2 catalyst described the amination behaviour of this catalyst when the ammonia and ethanol pressures were changed. The influence of hydrogen was not clearly identified however and it was not determined whether hydrogen was directly involved in the rate controlling steps for ethylamine formation or whether hydrogen influenced the nature of the copper surface. A more thorough investigation into the influence of hydrogen on the rate of ethylamine formation over copper catalysts is therefore required.

Besides differences in the overall activities of the three metal catalysts, considerable differences in ethylamine selectivity were also observed. The degree of amine substitution was seen to increase as the metal catalyst was changed from nickel to cobalt to copper (*i.e.* the MEA selectivity decreased and the DEA and TEA selectivities increased). It was seen that ammonia had the greatest influence on the selectivity during amination and that an increase in the ammonia partial pressure (and therefore the surface coverage) resulted in a decrease in the degree of amine substitution. The changes in ethylamine selectivity between the three metal catalysts may therefore be dependent on the surface coverage of ammonia on the three different metals. By comparing the relative adsorption constants for ethanol and ammonia, it was seen that K_{NH3} / K_{EtOH} decreased as the metal catalyst was changed from nickel to cobalt to copper (the relative ratio of the adsorption constants was used since the absolute values were dependent on the type of model selected). The decrease in this ratio would indicate that the relative surface concentration of ammonia decreases and the relative surface concentration of ethanol increases as the metal catalyst is changed in the same order. From this observation, it may be expected that the degree of amine substitution would

increase from nickel to cobalt to copper, in agreement with the experimental observations.

These differences in selectivity (and the relative ratio of the adsorption constants) may be related to the reversibility of hydrogen adsorption as measured using hydrogen chemisorption. A decrease in the reversibility (and therefore the percentage of strong adsorption sites) was observed as the metal was changed from nickel to cobalt to copper. If ammonia was preferentially adsorbed on "strong" adsorption sites, the decrease in the reversibility of hydrogen adsorption would result in a decrease in the surface coverage of ammonia. This would result in an increase in the degree of amine substitution as was observed experimentally.

Although an attempt was made to develop mechanistically based kinetic expressions which describe the amination behaviour of the SiO_2 supported cobalt, nickel and copper catalysts, a number of problems were encountered. Further investigation is therefore required to be able to describe the amination behaviour of cobalt, nickel and copper catalysts from a mechanistic viewpoint.

4.2. Reductive Amination using Supported Cobalt Catalysts

4.2.1. Characterization

4.2.1.1. Reducibility of supported cobalt

The occurrence of multiple hydrogen consumption peaks during TPR indicates the presence of a number of reducible cobalt species in the catalyst precursor. In comparison, the TPR spectrum of bulk unsupported Co_3O_4 (Figure 3.1.) shows only two hydrogen consumption maxima which correspond to the sequential reduction of this species first to the divalent oxide CoO and then to zerovalent cobalt [van't Blik and Prins, 1986].

The most intense peak in the TPR spectrum of the Co/SiO_2 catalyst corresponds to the reductive decomposition of the cobalt nitrate precursor [Rosynek and Polansky, 1991; Arnoldy and Moulijn, 1985]. Mass spectroscopic analysis of the effluent gas during this event showed that the decomposition of the cobalt precursor is accompanied by the evolution of the nitrogen oxides NO_2, NO and N_2O. Depending on the temperature of the TCD cell, NO_2 can dimerize to form N_2O_4 which has a higher thermal conductivity than hydrogen [Feliciani, 1934]. This may be responsible for the negative peak sometimes occurring prior to the peak ascribed to reductive decomposition.

Subsequent reduction to metallic cobalt occurs in several steps, the size and location of each peak being dependent on the type of support used. In general, hydrogen consumption occurring at temperatures greater than 500°C can be ascribed to the reduction of cobalt species interacting strongly with the metal carrier since bulk unsupported cobalt oxide is reduced completely by temperatures of 500°C [van't Blik and Prins, 1986]. In the instance of SiO_2 supported cobalt catalysts, these high temperature hydrogen consumption peaks have been ascribed to the reduction of surface cobalt oxide ($CoSiO_x$) species [Rosynek and Polansky, 1991] and various cobalt silicates [Puskas *et al*, 1992; Ming and Baker, 1995]. In the case of Al_2O_3 supported catalysts, 4 distinct regions of hydrogen consumption were identified and ascribed to the reduction of various cobalt phases [Arnoldy and Moulijn,

1985]. Phase I was assigned to Co_3O_4 reduction, Phase II was assigned to the reduction of surface Co^{3+} ions in a proposed stoichiometry of $Co_3Al_2O_6$, Phase III was assigned to the reduction of surface Co^{2+} ions and Phase IV was ascribed to the reduction of subsurface Co^{2+} ions present as the cobalt aluminate spinel structure $CoAl_2O_4$. The distinction between the different phases was based on the temperature range over which the hydrogen consumption was observed. All four types of cobalt species were observed during TPR of the Al_2O_3 supported cobalt catalysts prepared during this study.

Literature reports with respect to the characterization of SiO_2-Al_2O_3 supported catalysts are scarce. Rathousky *et al* [1991] proposed that the high exothermicity of the reductive decomposition of the cobalt nitrate precursor resulted in a high local overheating which was responsible for the strong interaction between the supported cobalt and the SiO_2-Al_2O_3 carrier. This was not observed in the instance of the SiO_2 and Al_2O_3 supported cobalt catalysts however and therefore it is more likely that the high temperature hydrogen consumption occurring with these catalysts is due to the reduction of various cobalt silicate and cobalt aluminate species. The possibility of interaction of cobalt ions with SiO_2-Al_2O_3 supports is also expected to be increased due to the possibility of ion exchange of cobalt ions with support protons. The degree of this ion exchange would be expected to increase with increasing aluminium content of the SiO_2-Al_2O_3 support which results in an increase in the Brönsted acidity of the carrier. The TPR spectra of the SiO_2-Al_2O_3 supported cobalt catalysts showed an increase in the size of the hydrogen consumption peak occurring between temperatures of 600 to 700°C as the aluminium concentration of the carrier material was increased. It is therefore possible that the hydrogen consumption occurring in this region is due to the reduction of cobalt ions which have been exchanged for support protons during the impregnation process (since the Brönsted acidity is proportional to the aluminium content of the SiO_2-Al_2O_3 carrier).

By plotting the extent of reduction versus the aluminium content of the carrier material, it can be seen that the metal reducibility decreases as the aluminium content of the support is increased (Figure 4.14.). The exception to this case is the Co/SiO_2 catalyst (not shown in the illustration due to the logarithmic scale) which shows a slightly lower extent of reduction in

comparison to the Co/1SiO_2-Al_2O_3 catalyst (42% as opposed to 46%). This deviation is within the levels of experimental error of the TPO technique and it is likely that the extents of reduction of these two catalysts are similar, as would be expected from the similar nature of the carrier material. The reducibility of supported cobalt catalysts prepared by incipient wetness impregnation therefore appears to be largely determined by the chemical nature of the support material.

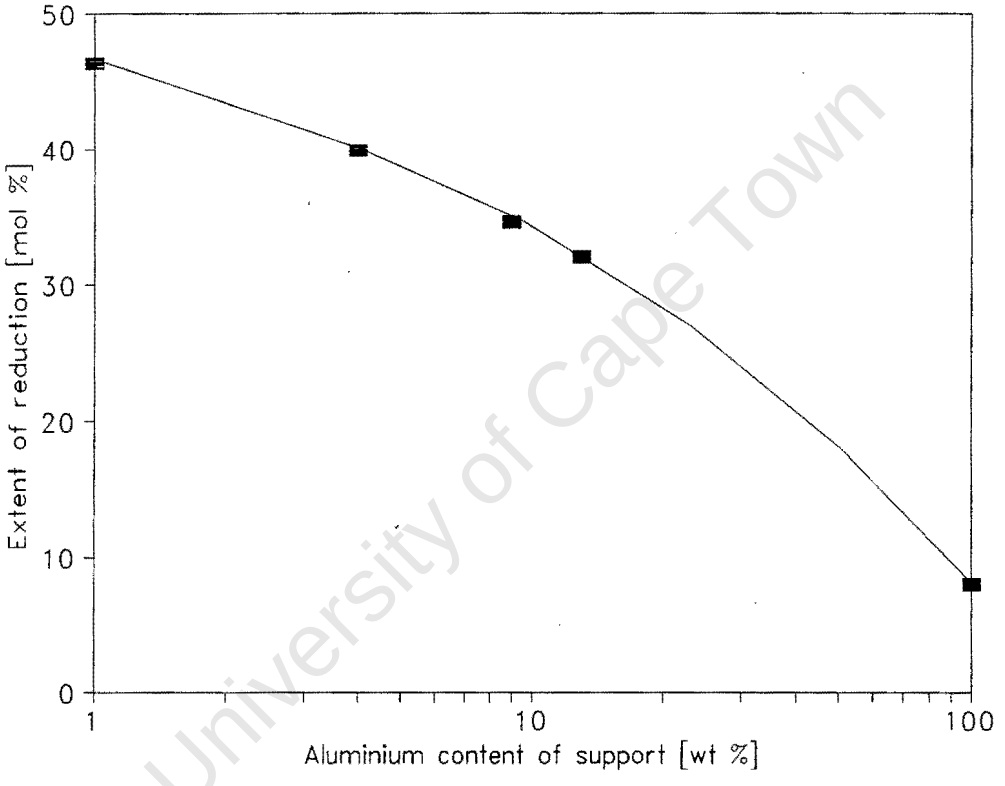

Figure 4.14. Effect of the aluminium content of the support on the extent of reduction

The temperature at which the reductive decomposition of the nitrate precursor occurs (*i.e.* the first peak in the TPR spectrum) varies as the type of metal carrier is changed. An increase in the temperature at which precursor decomposition occurs indicates that the support material stabilizes the precursor compound against reduction and may be envisaged as an increase in the degree of interaction between the cobalt precursor and the carrier material. By changing the metal carrier from SiO_2 to Al_2O_3, an increase in the temperature of reductive decomposition of the nitrate ion from 240 to 280°C was observed. Increasing

the aluminium content of the SiO_2-Al_2O_3 supports from 1 to 4 to 9 to 13 wt% resulted in an increase in the temperature of reductive decomposition from 235 to 240 to 250 to 290°C. Although there is some scatter (*e.g.* the Co/13SiO_2-Al_2O_3 catalyst which is characterized by a very high decomposition temperature), the temperature at which the reductive decomposition of the nitrate ion occurs increases with increasing aluminium content of the carrier material. There therefore appears to be a correlation between the temperature of precursor decomposition and the reducibility of the supported cobalt catalysts used in this study.

The influence of the temperature of hydrogen reduction on the type of cobalt species present on Al_2O_3 supported cobalt catalysts is illustrated in Figure 4.15. Three general types of cobalt species are expected following reduction of a supported cobalt catalyst, *viz.* zerovalent cobalt, divalent oxidizable cobalt and divalent non-oxidizable cobalt. The presence of residual unreduced trivalent cobalt species following reduction is unlikely [Arnoldy and Moulijn, 1985]. Non-oxidizable cobalt species are those cobalt atoms which cannot be oxidized to form trivalent cobalt oxide. This indicates that these species are probably stable cobalt-alumina spinels such as $CoAl_2O_4$ [Arnoldy and Moulijn, 1985; Chin and Hercules, 1982]. Oxidizable divalent cobalt species are probably present as surface cobalt species which are in intimate contact with the oxidizing atmosphere during TPO.

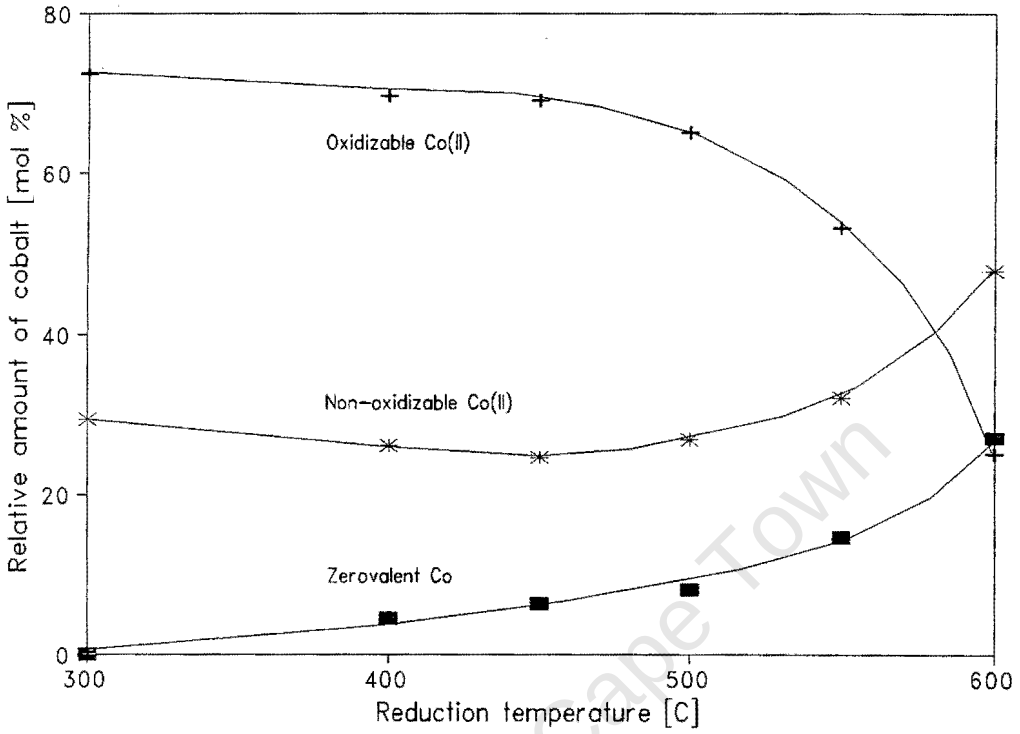

Figure 4.15. Effect of the reduction temperature on the type of cobalt species on Co/Al_2O_3

As expected, increasing the temperature of hydrogen reduction of the Co/Al_2O_3 catalyst resulted in an increase in the extent of metal reduction (*i.e.* the amount of zerovalent Co after reduction). The concentration of oxidizable Co^{2+} species decreased with increasing reduction temperature whereas the concentration of non-oxidizable Co^{2+} species remained approximately constant up to reduction temperatures of 500°C after which it increased. The increase in the extent of reduction to zerovalent cobalt therefore appears to be due to the reduction of the oxidizable cobalt species. This observation is in agreement with the oxidation behaviour of these cobalt species (*i.e.* if certain Co^{2+} species cannot be oxidized at temperatures of up to 1000°C, it is unlikely that they will be reduced before a cobalt species which can be oxidized at lower temperatures). At reduction temperatures greater than 500°C, an increase in the concentration of non-oxidizable Co^{2+} species was observed. It therefore appears that there is a competition between the reduction of oxidizable Co^{2+} species and the

transformation of these oxidizable divalent cobalt ions into non-oxidizable Co^{2+} species. The increased formation of stable, non-oxidizable cobalt species at increased temperatures of activation may be expected due to the increased mobility of the metal ions with increasing temperature. It is possible that the increased diffusivity of the cobalt atoms at elevated temperatures leads to the incorporation of these atoms into the Al_2O_3 support.

Similar behaviour was observed for the Al_2O_3 supported cobalt catalysts in which the time of hydrogen reduction at 500°C was varied. Although increased reduction times resulted in an increase in the degree of reduction to zerovalent cobalt, an increase in the concentration of non-oxidizable cobalt species is also observed. The competitive reactions between the reduction to form zerovalent cobalt and the transformation to form non-oxidizable cobalt species indicates that the extent of reduction on Co/Al_2O_3 catalysts has a finite limit which depends on both the reduction time and the reduction temperature.

4.2.1.2. Surface area of cobalt catalysts

The total number of exposed cobalt atoms differed considerably upon changing the type of metal carrier. These differences were caused by changes in the reducibility of the supported metal as well as the stability of the supported metal towards agglomeration which leads to surface area losses. The metallic surface areas of the Co/SiO_2 and $Co/1SiO_2$-Al_2O_3 catalysts were approximately similar. This may be expected from the similar extents of reduction as measured by TPO and the similarity in the chemical nature of the support material, which should result in similar dispersions.

Upon increasing the aluminium content of the SiO_2-Al_2O_3 carrier, a decrease in the reduced metallic surface area was observed. This decrease can be ascribed to both the decreased extents of reduction as well as the increase in metal crystallite agglomeration. The metallic dispersion of the Al_2O_3 supported cobalt catalyst was found to be higher than that of the SiO_2 supported cobalt catalyst however so that the dispersion cannot be simply correlated to the chemical nature of the support material. The high metallic dispersion obtained for the Al_2O_3 supported cobalt catalysts in combination with the low extent of metal reduction results in

a catalyst with a metal surface area lower than that of the SiO_2 supported catalyst but higher than that of the $Co/9SiO_2$-Al_2O_3 and $Co/13SiO_2$-Al_2O_3 supported catalysts.

Although increasing the reduction temperature of the Co/Al_2O_3 catalysts resulted in an increase in the extent of metal reduction, the number of exposed cobalt atoms first increased and then decreased with increasing temperature of hydrogen reduction. The decrease in metal surface area at higher reduction temperatures was due to increased metal agglomeration which resulted in an effective decrease in the exposed surface area of the metal crystallites. The increased mobility of cobalt atoms at temperatures greater than 500°C is in agreement with the TPO measurements which showed greater incorporation of cobalt ions into stable support lattice sites at higher temperatures.

Increasing the time of hydrogen reduction at 500°C resulted in an increase in the number of exposed metal atoms. The increase in metallic surface area was largely due to the increased extents of reduction of the supported cobalt since there was also an increase in the extent of metal crystallite agglomeration with increasing time of high temperature reduction. The agglomeration of cobalt crystallites with increasing reduction time was not as pronounced as the increases in particle agglomeration observed upon increasing the reduction temperature.

4.2.2. Catalyst Deactivation during Amination

The catalytic amination of alcohols [Baiker and Richarz, 1978; Ono and Ishida, 1981; Baiker *et al*, 1983] and the disproportionation of amines [Pommersheim and Coull, 1971; Volf *et al*, 1973] using supported metal catalysts is usually carried out in the presence of hydrogen. Although hydrogen is neither consumed nor produced during reaction, a severe decrease in activity is observed when hydrogen is not present. The decrease in activity is ascribed to metal nitride formation, the formation of metal carbide and carbonaceous deposits and the thermal diffusive fusion of supported metal crystallites. Metal particle agglomeration was only found to be significant in the instance of low surface area carriers such as kaolin ($S_{B.E.T.} \approx 40\ m^2/g$) [Baiker and Richarz, 1978] and therefore should not contribute significantly to catalyst deactivation during the amination experiments conducted in this work (the surface

areas of the SiO_2, Al_2O_3 and SiO_2-Al_2O_3 supports used were 289, 209 and 516 m^2/g respectively).

The supported cobalt catalysts used in this investigation showed a decline in the ethanol conversion activity during the first 24 hours of time on stream. After this initial period of rapid deactivation, activity was relatively stable with time on stream indicating that the processes leading to catalyst deactivation were no longer significant (*i.e.* very slow) or that the processes were in equilibrium. The overall deactivation profiles of the various supported cobalt catalysts were similar however, indicating that the manner of deactivation was probably of a similar nature.

Thermogravimetric analysis of the used cobalt catalysts indicated the presence of carbonaceous material on the surface of the catalyst following amination. The amount of carbonaceous material as estimated by the weight loss during oxidation increases as the cobalt carrier was changed from SiO_2 to Al_2O_3 to SiO_2-Al_2O_3. Although the increase in carbon deposition corresponded to a decrease in the ethanol conversion activity of the supported cobalt catalysts, it is unlikely that the extent of carbon deposition alone determines the final activity of the catalyst. Similar activity trends are observed if the ethanol conversion activity is extrapolated to zero time (where no carbon deposition is obtained) and therefore it is more likely that the activity of the catalyst is determined by the number of exposed metal atoms as well as the extent of carbon deposition.

The weight loss during oxidation of the used Co/SiO_2-Al_2O_3 catalyst up to 700°C was 9%. This weight loss was due to the loss of adsorbed reaction products and due to the combustion of carbonaceous residues. The actual weight loss due to the abovementioned events is larger than the value actually measured since simultaneous cobalt oxidation will result in an increase in the sample mass during TG-DTA (2.5 wt% increase assuming complete oxidation of all zerovalent cobalt to Co_3O_4). Assuming that the observed weight loss (9%) is simply due to the oxidation of residual carbon, it can be seen that the carbon to cobalt ratio on the used Co/SiO_2-Al_2O_3 catalyst is 3.7 mol C/mol Co. Since the decrease in ethanol conversion with time on stream is only 27% of the original value, it is clear that the majority of the deposited

carbon is present on the support. Unless spillover of carbon and/or carbonaceous residues onto the support occurs during reductive amination, it can be concluded that catalyst deactivation is at least to some extent caused by side reactions occurring on the support material. The increased acidity of the SiO_2-Al_2O_3 support in comparison to the SiO_2 and Al_2O_3 supports may be the cause of the increased carbon deposition on this catalyst during amination. Heft *et al* [1990] have shown that the use of a neutral support material resulted in fewer byproducts during the reductive amination of ethanol using supported cobalt catalysts.

X-ray diffraction of the used Co/SiO_2 catalyst showed a decrease in the crystallinity of the supported cobalt crystallites following amination. The crystalline structure of the reduced cobalt particles is therefore perturbed during amination indicating the incorporation of foreign material into the metal particles. Both cobalt carbide formation and cobalt nitride formation have been observed during amination reactions using supported cobalt catalysts [Baiker *et al*, 1984] and incorporation of either carbon or nitrogen into the cobalt crystal lattice would result in a decrease in the crystallinity as measured using XRD. It cannot be concluded directly from the XRD measurements whether the decreased crystallinity was caused by carbiding or nitriding of the cobalt catalyst.

The TG-DTA spectra of the SiO_2, Al_2O_3 and SiO_2-Al_2O_3 supported cobalt catalysts used for the reductive amination of ethanol were characterized by reasonably sharp exotherms at 262, 279 and 349 °C respectively. The sharpness of the peak and the large exotherm corresponding to this event (*ca.* 25 °C for the 25 mg samples of the spent Co/Al_2O_3 and Co/SiO_2-Al_2O_3 catalysts) points towards the combustion of a singular carbon species. The incorporation of carbon into the cobalt crystallites during amination to form cobalt carbides could explain the decrease in crystallinity of the supported cobalt crystallites following amination (as observed during XRD).

Decreasing the hydrogen pressure resulted in an almost linear decrease in the ethanol conversion of SiO_2 supported cobalt (Figure 4.16.). This either indicates that hydrogen is directly involved in the rate determining step over Co/SiO_2 or that hydrogen prevents the

deactivation of the cobalt surface via nitride formation.

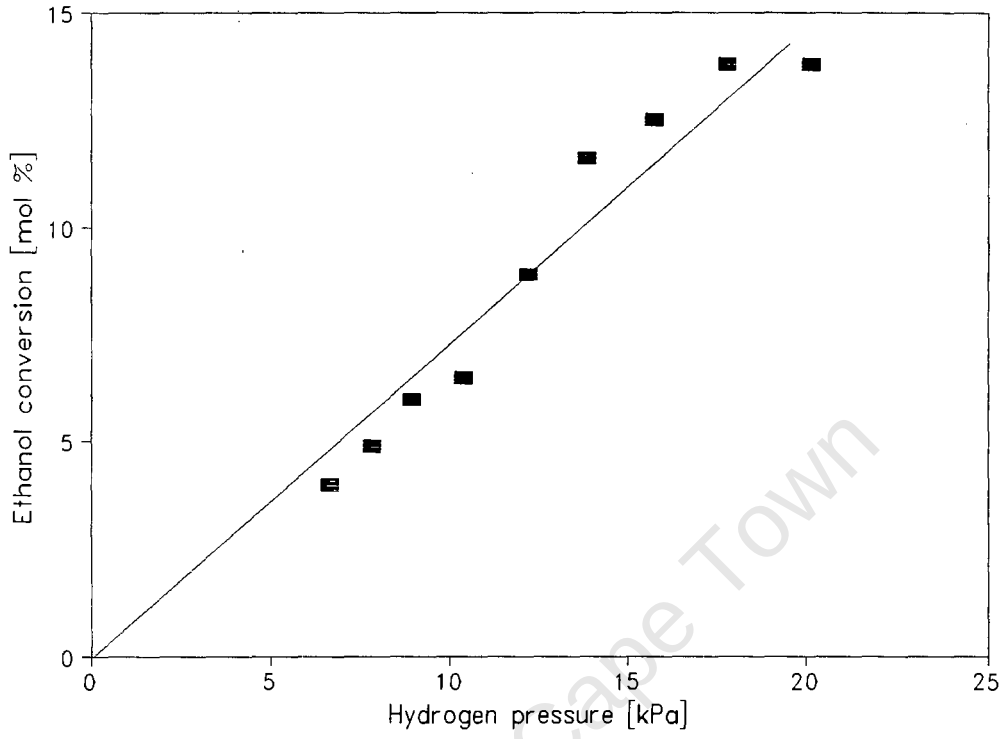

Figure 4.16. Influence of hydrogen on activity of Co/SiO_2

From the kinetic evaluation of the amination behaviour of Co/SiO_2 (Chapter 4.1.3.1.), it was seen that this decrease in activity was most probably caused by cobalt nitride formation and not due to a change in the rate of the controlling step. The incorporation of nitrogen into the cobalt lattice upon nitride formation may explain the decrease in crystallinity as observed using XRD.

Gas chromatographic sampling during reductive amination was conducted every 30 minutes. The decrease in activity upon changing the hydrogen pressure was seen to occur within 30 minutes since consecutive samples resulted in the same activity and selectivity measurements. From this is can be deduced that the time taken for the reaction to form cobalt nitride to reach equilibrium is less than 30 minutes. The deactivation which occurs during the first 24 hours of operation cannot therefore not be attributed to metal nitride formation alone. For

this reason, the decrease in activity with time on stream is ascribed to the deposition of carbonaceous material which results in site coverage.

The selectivity to MEA increased and the selectivity to DEA and TEA decreased during the first 24 hours of operation. The selectivity to individual ethylamines was constant once the ethanol conversion reached a steady state value and it is likely that the changes in amine selectivity were caused by the changes in reactant conversion with time on stream. A decrease in the degree of amine substitution was observed as the ethanol conversion was decreased during reductive amination [Sewell *et al*, 1995; Baiker and Kijenski, 1985]. Incorporation of nitrogen into the cobalt crystallites during metal nitride formation is expected to result in a change in the electronic nature of the cobalt which in turn will affect the selectivity during reaction. Since nitride formation occurs within the first 30 minutes of operation, this cannot be used to explain the changes in selectivity with time on stream.

4.2.3. Activity of supported cobalt catalysts

By changing the nature of the cobalt support, considerable changes in the activity of the supported cobalt for the reductive amination reaction were observed. Differences in the ethanol conversion activity of the supported cobalt catalysts was also observed upon varying the time and temperature of hydrogen reduction. The large differences in activity can be ascribed to changes in the reducibility of the supported cobalt and the changes in the dispersion of the metallic phase over the oxide support. By plotting the reduced metal surface area versus the ethanol conversion, a relatively linear plot is obtained (Figure 4.17.).

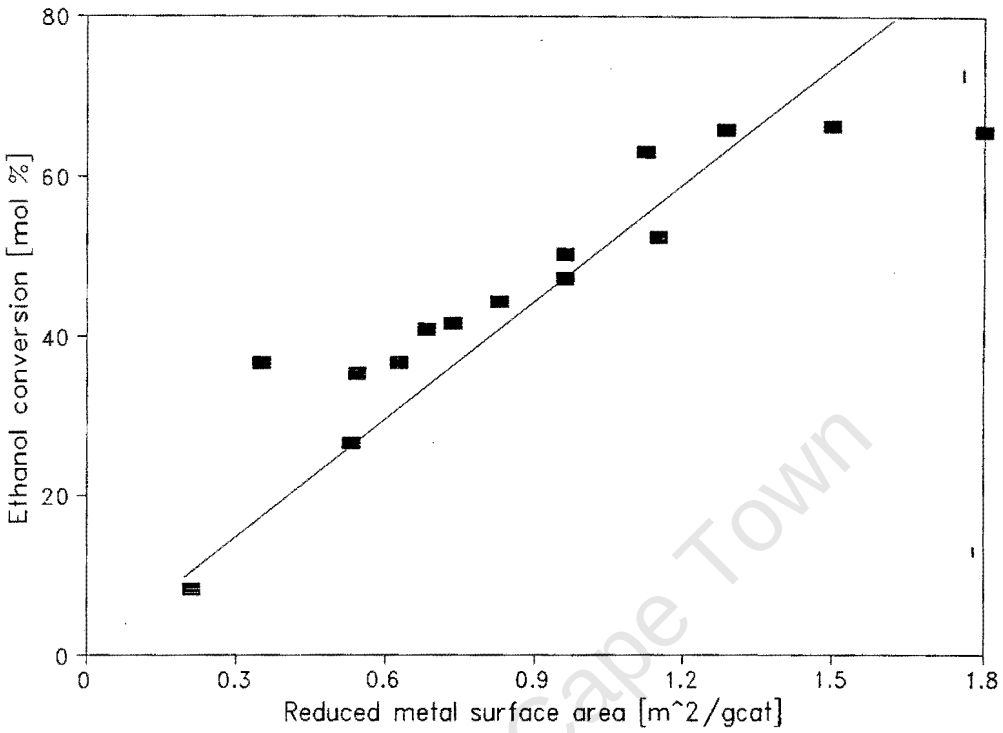

Figure 4.17. Ethanol conversion versus reduced metal surface area of cobalt catalysts
(T = 180°C, P = 1 bar, WHSV = 1 g_{EtOH}/g_{cat}·h, EtOH : NH_3 : H_2 : N_2 = 1 : 2 : 8.6 : 17.6)

The linear nature of this plot indicates that the activity of supported cobalt catalysts is proportional to the number of exposed cobalt atoms. No correlation between the amount of oxidizable or non-oxidizable Co^{2+} species and the total activity during amination could be obtained, indicating that these species do not contribute significantly towards the total ethanol conversion activity of supported cobalt catalysts. Similarly, no correlation between the metallic dispersion and the specific activity of the supported cobalt catalysts was obtained which indicates that the conversion of ethanol is not a structure sensitive reaction (*i.e.* it is not affected by particle size or morphology). The low activity of the Co/MgO catalyst in which no reduced metal was measured using both TPO and chemisorption confirms that unreduced cobalt species do not contribute significantly to the overall activity of supported cobalt catalysts.

4.2.4. Selectivity of supported cobalt catalysts

The selectivity to individual ethylamine products was seen to change substantially upon changing the type of cobalt support. The selectivity of MEA increased and the selectivity to DEA and TEA decreased as the support was changed from SiO_2 to Al_2O_3 to SiO_2-Al_2O_3. Changes in the specific ethylamine selectivity were also observed upon changing the time and temperature of hydrogen reduction. Since the amination behaviour of cobalt can be modelled as a series reaction (see Chapter 4.1.2.2.) and since the selectivity measurements were made at the same ethanol conversion, it is apparent that the type of preparation and activation procedure alters the specific selectivity of the supported cobalt.

If the reduced cobalt metal and the residual unreduced cobalt species are intimately mixed following hydrogen reduction, it may be expected that the electron deficient unreduced cobalt species might alter the electronic nature of the supported cobalt crystallites. A change in the electronic nature of the supported cobalt would be expected to alter the specific selectivity of the metal. No correlation between the extent of metal reduction and the selectivity of supported cobalt during amination could be obtained indicating that any influence of residual unreduced cobalt species is small. As a specific example, the extent of cobalt reduction was seen to increase with increasing reduction time and with increasing reduction temperature. The selectivity to MEA first decreased and then increased with increasing reduction temperature and decreased with increasing reduction time. The increase in MEA selectivity at high reduction temperatures would therefore not be expected if a decrease in MEA selectivity corresponded to an increase in the extent of reduction. A similar argument can be applied to the DEA and TEA selectivities which show the reverse behaviour in comparison to the MEA selectivity.

If the reactions occurring on the surface of the supported cobalt catalyst were structure specific (*i.e.* the rates of certain reactions are influenced by the type and geometry of the active site), a change in the specific selectivity with changes in metal particle size would be expected. No correlation between the average crystallite diameter (calculated indirectly using chemisorption) and the selectivity during reductive amination could be obtained. The

reactions occurring on the supported cobalt catalysts are therefore not influenced by the physical structure of the metal crystallites. As a specific example, the average crystallite diameter increased with increasing reduction time and with increasing reduction temperature. The MEA selectivity first decreased and then increased with increasing reduction temperature and decreased with increasing reduction time. No direct correlation between the particle size and the specific selectivity was evident from these measurements.

Distinct trends were observed when the specific ethylamine selectivity was plotted as a function of the reduced metallic surface area (Figure 4.18.). The MEA selectivity decreased and the selectivity to DEA and TEA increased as the metal surface area was increased. A correlation therefore exists between the specific selectivity during amination and the number of exposed metal atoms.

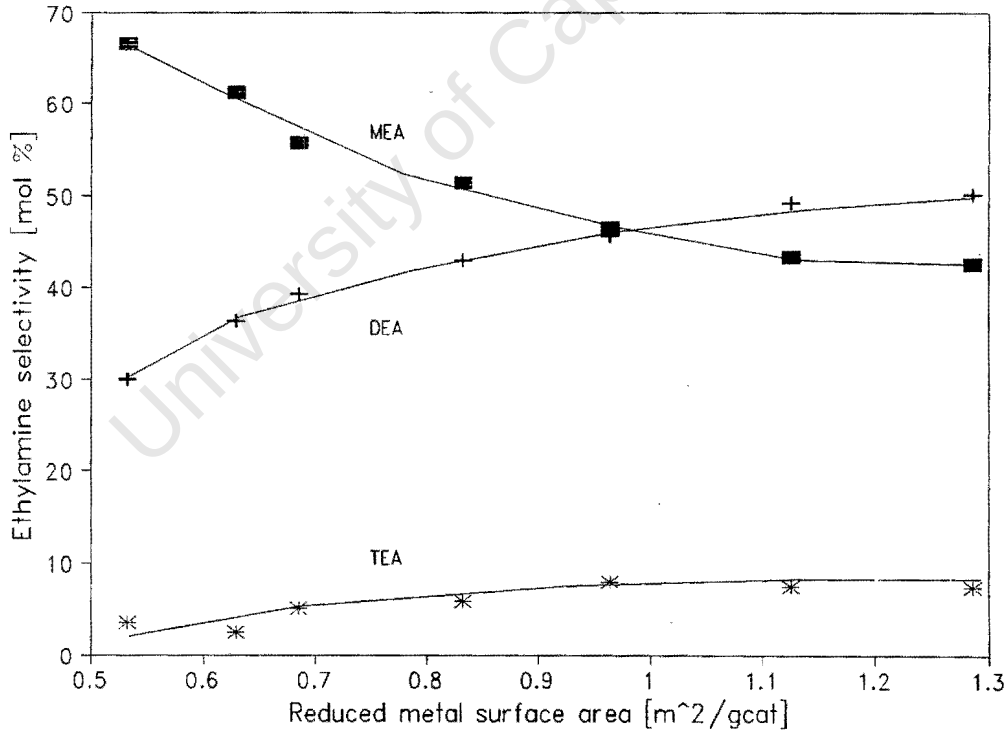

Figure 4.18. Specific ethylamine selectivity as a function of the metal surface area (T = 180°C, P = 1 bar, EtOH : NH_3 : H_2 : N_2 = 1 : 2 : 8.6 : 17.6, ethanol conversion = 50%)

Since the specific activity for the conversion of ethanol is not affected by the metal surface area (Figure 4.17.), this indicates that the relative rate of ammonia consumption decreases with increasing metal surface area. The nature of the cobalt active sites is therefore changed as the metal surface area increases which results in a change in the rate of ammonia consumption. These changes were found to be independent of the extent of metal reduction and the average particle size. The only parameter which was found to correlate to changes in the metal surface area was the strength of hydrogen adsorption as measured using chemisorption (Figure 4.19.). The strength of hydrogen adsorption was defined as the amount of strongly adsorbed hydrogen relative to the total hydrogen uptake during chemisorption, where strongly adsorbed hydrogen was taken as that hydrogen which was not removed by a 15 minute evacuation at the temperature of adsorption. The strength of hydrogen adsorption was calculated using the following relationship :

$$Strength\ of\ adsorption = \frac{V_{irr}}{V_{total}} \times 100\%$$

where V_{irr} is the amount of hydrogen not removed by a 15 minutes evacuation at the temperature of adsorption and V_{total} is the total hydrogen uptake of the freshly reduced metal catalyst.

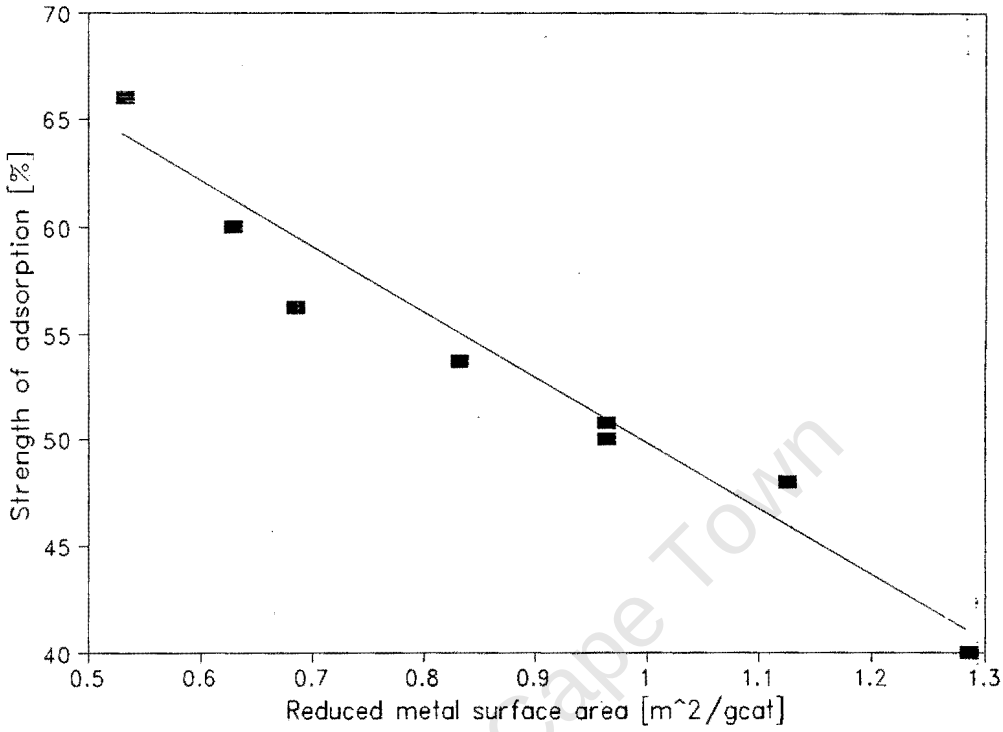

Figure 4.19. Strength of hydrogen adsorption as a function of the metal surface area

The decrease in the strength of adsorption with increasing metal surface area corresponds to an increase in the relative amount of weak adsorption sites (*i.e.* sites from which adsorbed hydrogen can be removed under vacuum). This change in the relative ratio of strong and weak adsorption sites on the metal surface does not change the specific activity for ethanol conversion however it does change the specific activity for ammonia conversion. The adsorption and reaction of ammonia therefore appears to be determined by the strength of the adsorption site.

An increase in the ratio of strong adsorption sites to weak adsorption sites corresponds to an increase in the selectivity to MEA and a decrease in the selectivity to DEA and TEA. If ammonia is preferentially adsorbed on strong sites as opposed to weak sites, an increase in the strength of adsorption would be expected to result in a greater surface coverage of ammonia. From the kinetic evaluation of the SiO_2 supported cobalt catalyst, it was shown

that an increase in the ammonia partial pressure (which results in a greater surface coverage of ammonia) resulted in an increase in the MEA selectivity and a decrease in the selectivities to DEA and TEA. The observed differences can therefore be explained if ammonia shows a preference for strong adsorption sites whereas the rate of ethanol consumption is unaffected by the nature of the adsorption site.

When changing the type of metal from nickel to cobalt to copper, the MEA selectivity decreased and the DEA and TEA selectivities increased. The chemisorption measurements for these catalysts showed a decrease in the relative ratio of strong and weak adsorption sites as the metal was changed in the same order. The change in the specific selectivities of these catalysts is therefore consistent with the findings upon changing the preparation and activation procedures of a number of supported cobalt catalysts (*i.e.* that the rate of ammonia consumption is proportional to the strength of hydrogen adsorption on these metals).

A direct correlation between the strength of hydrogen adsorption as measured by chemisorption and the selectivity during amination does not adequately describe the observed phenomena however. Plotting the specific amine selectivity as a function of the metal surface area for a range of Al_2O_3 supported cobalt catalysts and a range of SiO_2-Al_2O_3 supported catalysts indicates that the chemical nature of the support also influences the selectivity during reductive amination. For the purposes of clarity, these differences in ethylamine selectivity have been represented by plotting the ammonia conversion at an ethanol conversion of 50% as a function of the metallic surface area (Figure 4.20.). Higher ammonia conversions (at constant ethanol conversion) correspond to an increase in the MEA selectivity and a decrease in the selectivity to DEA and TEA.

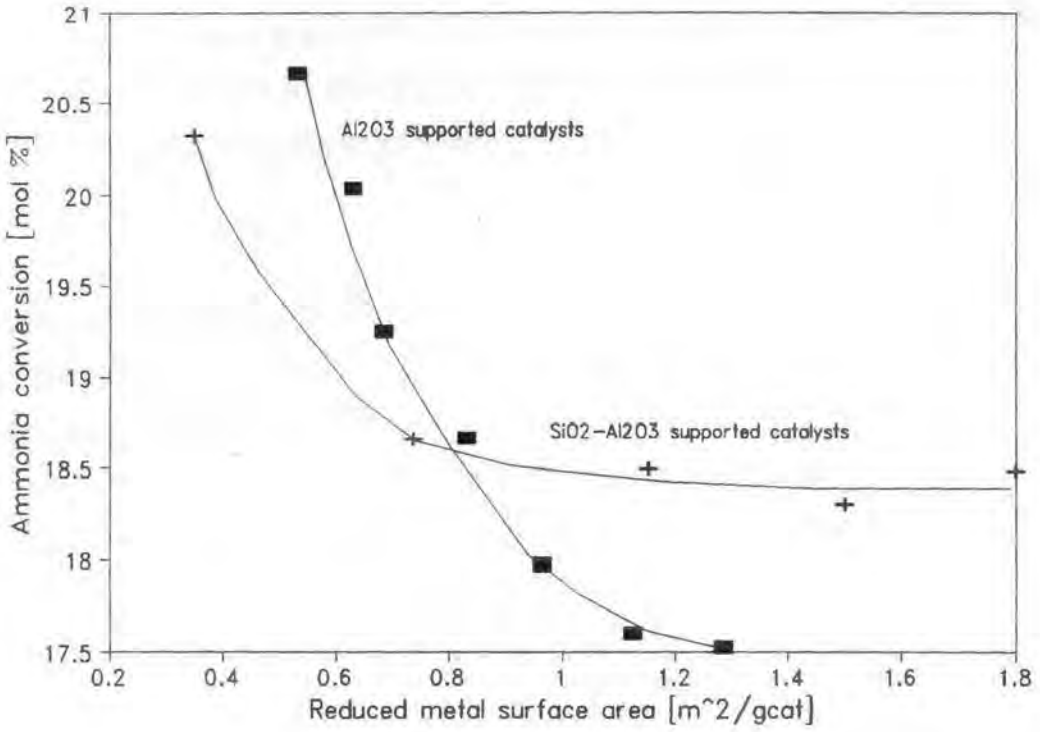

Figure 4.20. Influence of the support on the specific activity for ammonia conversion

From this figure it is clear that the type of support also influences the rate of ammonia consumption during amination, *i.e.* the selectivity is not only determined by the ratio of strong and weak adsorption sites during reaction. In the instance of the Al_2O_3 supported cobalt catalysts in which the time and temperature of hydrogen reduction were varied, a relatively linear correlation between the metal surface area and the rate of ammonia consumption is obtained. Since the same support was used, the concentration of support acid sites is expected to remain constant and any effect of support acidity on the reaction would remain constant.

With the SiO_2-Al_2O_3 supported cobalt catalysts, the support acidity was varied by adjusting the aluminium content of the metal carrier. The specific activity with respect to the conversion of ammonia decreases as the support acidity (aluminium content) is decreased until at very low aluminium contents (1 wt% Al_2O_3 in SiO_2), the selectivity is approximately

the same as that obtained for a SiO_2 supported cobalt catalyst. There therefore appears to be a correlation between the support acidity and the rate of ammonia consumption during amination. Increasing the acidity of the support results in higher MEA selectivities and lower DEA and TEA selectivities.

The contribution of the support towards ammonia conversion may indicate a bifunctional mechanism during amination, *i.e.* some reactions may also be catalysed by support acid sites. These reactions are most likely to be intermediate reactions since reductive amination using only the metal carrier material shows no activity under the reaction conditions used in this study. Another possibility is that upon increasing the acidity of the carrier material, a greater surface concentration of adsorbed ammonia is obtained. This greater surface concentration of ammonia may result in higher rates of MEA formation and may inhibit the formation of DEA and TEA, as observed during the kinetic evaluation of this metal. The role of the support is a secondary effect however since unsupported metals alone are also active for the reductive amination reaction [Kirk-Othmer, 1992].

4.3. Reducibility of Co/SiO_2 Catalysts

During the preparation of SiO_2 supported cobalt catalysts, a number of cobalt species are formed which decrease the reducibility of the supported metal. These species have been proposed to include various surface cobalt oxide [Rosynek and Polansky, 1991] and cobalt silicate species [Ming and Baker, 1995; Matsuzaki *et al*, 1993; Puskas *et al*, 1992]. In this study, a number of different hydrogen consumption peaks were observed during TPR of the SiO_2 supported cobalt catalysts. The type and amount of these cobalt species was shown to be dependent on the particular type of preparation procedure as well as on the catalyst activation procedure. The objective of this discussion is to address the problem of peak assignment and to evaluate the influence of the activation and preparation procedures on the reducibility of Co/SiO_2 catalysts as measured using TPR.

4.3.1. Peak Assignment

Upon changing the temperature of calcination during TPR of Co/SiO_2, six separate hydrogen consumption regions could be distinguished (Chapter 3.3.2.1.). These different regions were separated according to the temperature at which maximum the hydrogen uptake was observed. Peaks I to VI correspond to the hydrogen consumption peaks occurring between 180 and 240°C, 270 and 330°C, 350 and 390°C, 450 and 520°C, 650 and 780°C, and 880 and 990°C respectively. Although the exact size and location of the hydrogen consumption peaks was seen to vary upon changing the catalyst preparation and activation procedures, the different peaks could in general be ascribed to one of the six hydrogen consumption regions listed above.

In order to compare the amount of different cobalt species present in the SiO_2 supported cobalt catalysts accurately, it was important that all cobalt present in the catalyst sample was completely reduced by the time the temperature of 1000°C was reached. If the stoichiometry of the reduction was well established, then simply measuring the hydrogen consumption during TPR would indicate whether all cobalt present is completely reduced. During these studies, the total H_2 : Co molar ratio was seen to vary from 1 to 1.3 mol H_2 / mol Co. This

variation in the total hydrogen consumption during TPR was also observed in the case of Co/Al_2O_3 catalysts [Arnoldy and Moulijn, 1985]. Since it was not clear from the TPR measurements whether the supported cobalt was completely reduced by 1000°C, a combined reduction/oxidation cycle was performed to determine the extent of reduction [Zaborski *et al*, 1989].

Initial reduction of the Co/SiO_2 catalyst to a temperature of 1000°C resulted in a H_2 : Co molar ratio of 1.19. From the measured hydrogen consumption, it can be deduced that the cobalt was present as a mixture of divalent and trivalent cobalt ions following nitrogen calcination at 400°C. It is not clear from the TPR spectrum which hydrogen consumption peaks are caused by the reduction of trivalent cobalt species and which peaks are caused by the reduction of divalent cobalt species. Consequently, the extent of reduction of the supported cobalt cannot be determined. Subsequent oxidation of this reduced sample resulted in an O_2 : Co molar ratio of 0.65. Since complete oxidation of the reduced cobalt in the catalyst sample would result in an O_2 : Co molar ratio of 0.67, it can thus be seen that reduction is essentially complete by 1000°C.

Since trivalent cobalt species are thermally reduced to divalent cobalt species at temperatures greater than 800°C [Perry and Green, 1984] and since the oxidized catalyst was cooled down in an inert helium stream (thereby preventing reoxidation), it follows that cobalt will be present as a divalent ion following the TPO experiment. Reduction of this oxidized catalyst sample up to 1000°C resulted in a measured H_2 : Co ratio of 1.00. This hydrogen consumption corresponds to complete reduction of the supported cobalt which confirms that all cobalt species were completely reduced during the first TPR experiment.

The sharp hydrogen consumption peak (Peak I) occurring between 180 and 240°C is only observed for cobalt catalysts prepared using the cobalt nitrate precursor and which were calcined at temperatures lower than 300°C. Since the cobalt nitrate precursor is completely decomposed by calcination at temperatures greater than 300°C [Lapidus *et al*, 1991], this hydrogen consumption has been ascribed to the reductive decomposition of the cobalt nitrate precursor. The negative peak sometimes occurring prior to this event may be due to the

release of the nitrogen oxides NO_2, NO and N_2O [Sewell *et al*, 1995 b]. Depending on the temperature in the TCD cell, NO_2 can dimerize to form N_2O_4 which has a higher thermal conductivity than hydrogen [Feliciani, 1934].

The amount of hydrogen ascribed to Peak II varied between 0.2 and 0.29 mol H_2 per mol Co. Previous authors have ascribed this hydrogen consumption peak to the one step reduction of Co_3O_4 to Co [Arnoldy and Moulijn, 1985] and to the reduction of small Co_3O_4 particles [Okamoto *et al*, 1991]. Larger Co_3O_4 particles were proposed to be responsible for the subsequent hydrogen consumption peak [Okamoto *et al*, 1991] which would indicate a bimodal distribution of Co_3O_4 crystallites on the SiO_2 supported catalyst. The presence of Co_3O_4 crystallites on Co/SiO_2 catalysts has been confirmed using XRD [Rosynek and Polansky, 1991; Okamoto *et al*, 1991].

In the reduction of unsupported Co_3O_4, two hydrogen consumption maxima were observed (Figure 3.1.). The first hydrogen consumption peak is responsible for approximately 25 % of the total hydrogen consumption [Sexton *et al*, 1986; van Steen, 1993] which indicates that the reduction reaction is a two step process ($Co_3O_4 \rightarrow CoO \rightarrow Co$). This reduction mechanism has been confirmed using XPS measurements [Viswanathan and Gopalkrishnan, 1986]. Since small particles are less likely to be influenced by diffusion limitations during a TPR experiment and since the supported Co_3O_4 particles are expected to have a higher dispersion than their unsupported counterparts, the peak separation observed during TPR of unsupported Co_3O_4 would be expected to be enhanced in the case of the supported Co_3O_4 particles. It is therefore unlikely that this hydrogen consumption peak is due to the complete reduction of Co_3O_4 to metallic cobalt as proposed by Arnoldy and Moulijn [1985] and Okamoto *et al* [1991]. It is more likely that the hydrogen consumption ascribed to Peak II is caused by the reduction of trivalent cobalt species to divalent cobalt species. Not all of this trivalent cobalt is present in the bulk cobalt oxide Co_3O_4, however, since the corresponding hydrogen consumption for the subsequent reduction of CoO to Co is not observed (*i.e.* the ratio of the area of Peak 2 to Peak 3 is less than 25 : 75). The trivalent cobalt species responsible for this hydrogen consumption can therefore be in different surroundings and the reduction of these trivalent species leads to the various divalent cobalt species which are reduced at higher

temperatures.

The hydrogen consumption having a maximum at *ca.* 350°C (Peak III) is most likely caused by the reduction of the divalent cobalt oxide CoO which is formed through the partial reduction of the bulk cobalt oxide Co_3O_4. This assignment is based on the fact that this hydrogen consumption peak occurs at the same temperature as that observed for CoO reduction during TPR of unsupported Co_3O_4 (Figure 3.1.). The species reducing at a slightly higher temperature (Peak IV) is most probably caused by the reduction of divalent cobalt species having a slightly stronger interaction with the SiO_2 support. These cobalt species might be species which are in the coordination sphere of cobalt species having a strong interaction with the SiO_2 support (*i.e.* the cobalt species responsible for the hydrogen consumption in Peak VI). This conclusion is based on the observation that the temperature of the hydrogen consumption maximum of Peak IV increases as the area of Peak VI is increased.

The hydrogen consumption occurring at temperatures greater than 500°C represents cobalt species which interact strongly with the SiO_2 support since bulk unsupported cobalt oxides are reduced completely by this temperature [van't Blik and Prins, 1986]. Under normal reduction conditions (up to 500°C), these species cannot be reduced and are therefore inactive in metal catalyzed reactions. According to the TPR spectra, a number of different cobalt species are responsible for these high temperature hydrogen consumption peaks.

A broad hydrogen consumption peak was observed between temperatures of 500 and 850°C (Peak V) which is probably caused by the reduction of a number of different cobalt species. If this hydrogen consumption was caused by a single cobalt species, a sharper peak would be expected. By mixing a colloidal silica solution (Ludox^R HS 40) with an aqueous solution of cobalt nitrate, a blue precipitate was formed. This solution was dried and then calcined in nitrogen at 400°C. The resulting TPR spectrum was characterized by a number of hydrogen consumption peaks occurring between 550 and 850°C (Figure 4.21.). Since the colloidal silica source contains many silanol groups, it is possible that reaction between dissolved cobalt ions and these silanol groups occurred thereby yielding the blue precipitate.

Upon drying and calcination of this precipitate, it is possible that a number of different Si-O-Co-OH species are formed. Depending on the stoichiometries of the different precipitation reactions (*e.g.* the number of OH groups bonded to the silicon or cobalt atoms), a number of different cobalt hydrosilicate species can be expected. The hydrogen consumption occurring at temperatures between 500 and 800°C is therefore probably due to the reduction of various cobalt hydrosilicate species.

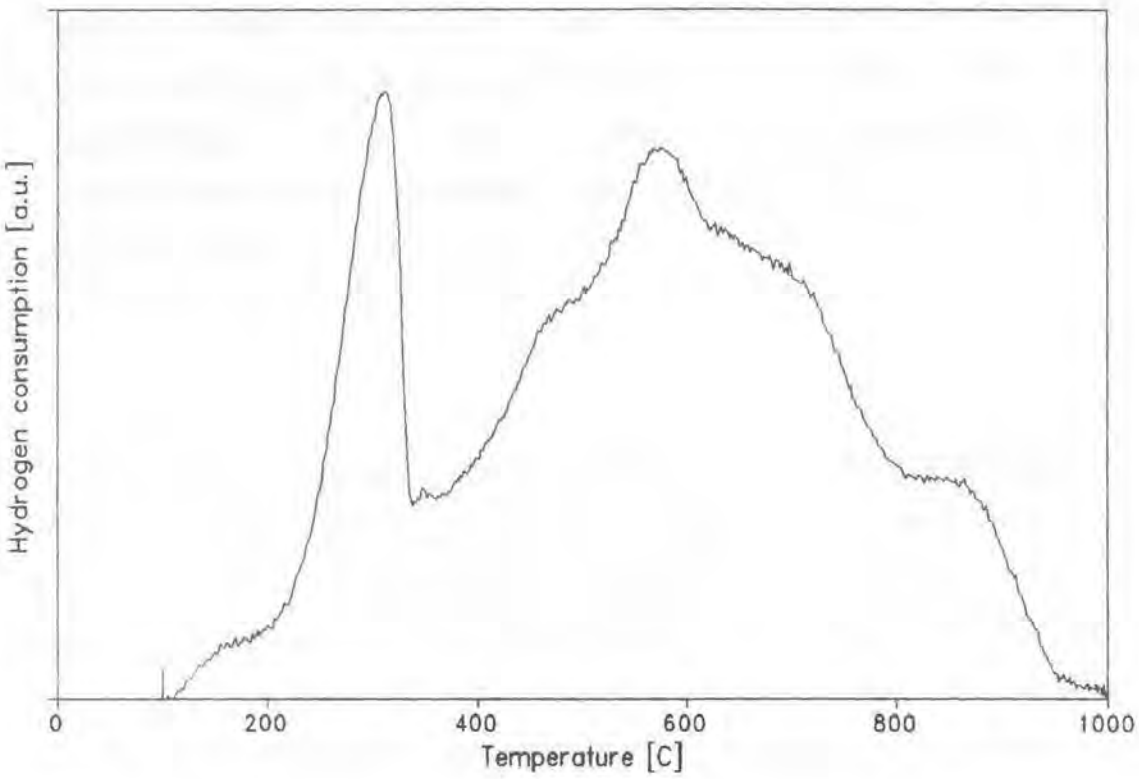

Figure 4.21. TPR spectrum of Ludox^R HS 40 - cobalt nitrate precipitate
(Calcination gas = 60 ml(NTP)/min N_2, calcination temperature = 400°C, reducing gas = 60 ml(NTP)/min 5% H_2/N_2, temperature programming rate = 10°C/min, $m_{cat} \approx 0.15$ g)

The final hydrogen consumption peak occurring at approximately 900°C (Peak VI) is relatively sharp and is therefore probably caused by the reduction of a single cobalt species. Oxidation of the Co/SiO_2 catalyst up to a temperature of 1000°C results in the formation of a purple-pink material. Since Co_3O_4 is black and CoO is grey-black in colour [Perry and Green, 1984], it is evident that cobalt is no longer present as a bulk metal oxide following

oxidation at 1000°C. Since Co_3O_4 is thermally reduced to form CoO at temperatures greater than 800°C [Perry and Green, 1984] and since the solid state reaction between CoO and SiO_2 at these temperatures is well known [Ruger, 1924], it appears that these materials have reacted to form a cobalt orthosilicate surface species. Subsequent reduction of the Co/SiO_2 catalyst oxidized at 1000°C results in a TPR spectrum which is dominated by a hydrogen consumption peak occurring between 900 and 1000°C. The temperature at which this peak occurs indicates that the hydrogen consumption ascribed to Peak VI is due to the reduction of a cobalt orthosilicate species. Measurement of the hydrogen consumption during TPR showed that the H_2 : Co molar ratio was 1.00. The hydrogen uptake during TPR indicates that cobalt is present as a divalent ion in this cobalt orthosilicate species and consequently it can be deduced that the molecular composition of this species is most probably of the form Co_2SiO_4. The formation of cobalt silicide (Co_2Si) species during TPR is unlikely [Chen *et al*, 1991]. If these species were formed, the hydrogen uptake during TPR would be considerably higher.

4.3.2. Influence of the Preparation Variables

The impregnation procedure can be described by the concept of interfacial coordination chemistry as proposed by Che [1993]. The interaction between silica gel and cobalt nitrate is illustrated in Figure 4.22.

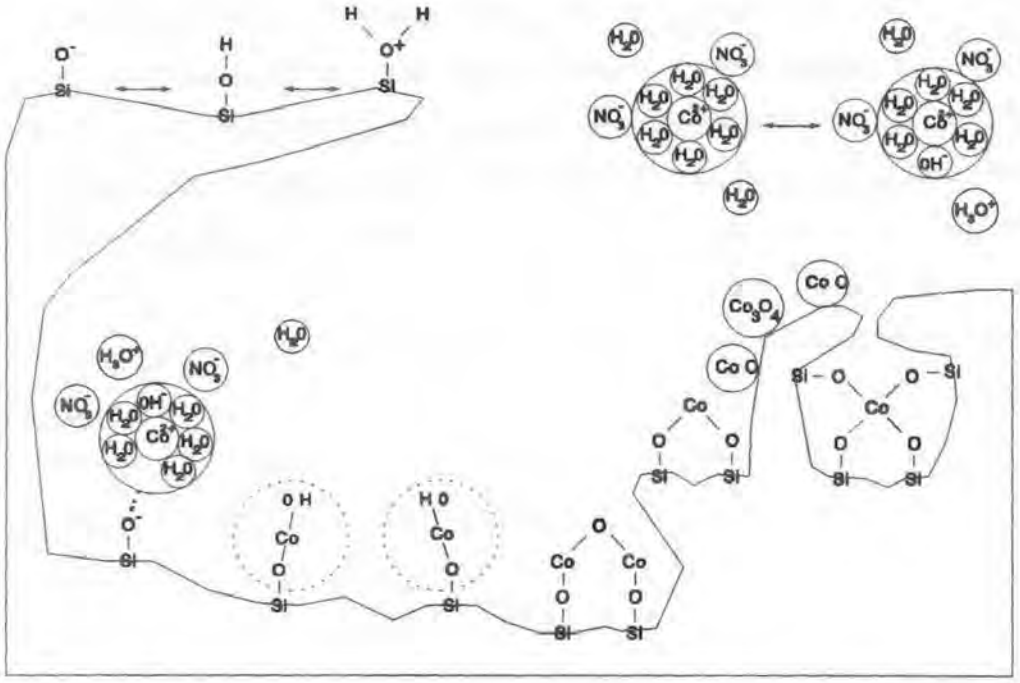

Figure 4.22. Possible interactions between cobalt nitrate and silica gel
(modified according to the concept of interfacial coordination chemistry by Che [1993])

In a non-chelating solution, the cobalt ion is surrounded by water ligands originating from the starting cobalt salt. The water ligands can interact with surface silanol groups to form a surface cobalt complex. If these water ligands are replaced, the interaction between the cobalt ion and the silica surface vanishes and cobalt-silicate species are not formed. The necessity of water ligands in the formation of these surface complexes is underlined by the absence of cobalt-silicate formation when DMSO is used as a solvent during impregnation. DMSO is a strong chelating agent and displaces the water ligands surrounding the cobalt ion. The removal of these ligands by DMSO prevents the interaction between the cobalt ion and the silica surface thus preventing cobalt-silicate formation.

By heating cobalt nitrate ($Co(NO_3)_2 \cdot 6H_2O$) in air at 100°C for 3 hours and measuring the mass loss, it was determined that 90 % of the crystal water had been removed. This partially dehydrated salt was dissolved in n-propanol and impregnated into the SiO_2 support. The TPR spectrum of this catalyst showed a marked decrease in the formation of difficult to reduce

cobalt silicate species in comparison to the corresponding catalyst prepared using the hydrated cobalt nitrate precursor. This result confirms the necessity of the water ligands in the formation of cobalt-silica surface complexes. The importance of the silanol groups in this reaction is underlined by the increase in the contribution of the high temperature hydrogen consumption peaks (Peaks V and VI) as the surface area of the silica support (and therefore the number of silanol groups) is increased.

Silanol groups are amphoteric in nature and depending on the pH of the impregnating solution, can exist as SiOH, SiO^- or $SiOH_2^+$ species. The isoelectric point of silica occurs between a pH of between 1 and 2.2 [Parks and de Bruyn, 1962; Parks, 1965]. At a pH higher than the isoelectric point, the silica surface will be negatively charged and will preferentially adsorb cations. At a pH below the isoelectric point, the surface will be positively charged and will show a greater affinity for the adsorption of anions. In the impregnation step of the catalyst preparation, the solution pH was higher than the isoelectric point of the SiO_2 support and the adsorption process can therefore be described in terms of an electrostatic interaction [Brunelle, 1978].

In a solution of cobalt nitrate, it is apparent that some dissociation of the water ligands has occurred since the solution is acidic. Upon the addition of silica, an increase in the pH is observed. This may be caused by an electrostatic adsorption of cobalt ions and/or an exchange reaction between OH^- ligands for a surface SiO^- group. A similar exchange reaction between a Cl^- ligand and a SiO^- group has been observed upon the adsorption of trans-$Co(en)_2Cl_2^+$ on silica [Burwell *et al*, 1965]. Alternatively, it is possible that the oxolation reaction between SiOH-species and $Co(H_2O)_x(OH)_y^{(2-y)+}$ results in the formation of Co-O-Si species [Che, 1993]. On the basis of the results obtained in this work, it is not possible to conclude whether these strong interactions arise as a consequence of electrostatic adsorption or the oxolation reaction. The oxolation reaction appears to be less important since this reaction only becomes significant at higher pH values [Ming and Baker, 1995].

4.3.3. Influence of the Activation Variables

By increasing the time and temperature of the catalyst drying stage, a decrease in the size of the high temperature hydrogen consumption (Peak VI) was observed. It can therefore be deduced that the precursor of cobalt silicates can be destroyed by a mild thermal treatment. This may occur by the removal of water from the coordination sphere of the cobalt surface complex, thus preventing cobalt silicate formation. By plotting the weight loss of the catalyst during the TPR experiment versus the hydrogen consumption caused by cobalt silicate reduction (Peak VI), a relatively linear correlation is obtained (Figure 4.23.). A decrease in the weight loss during the TPR experiment (which comprises the weight loss occurring during the calcination and reduction steps) corresponds to an increase in the amount of water removed during the drying stage. The correlation between the cobalt silicate content of the catalyst and the amount of water remaining in the catalyst precursor is consistent with the observation that water ligands are required for the interaction between the cobalt complex and the surface silanol groups.

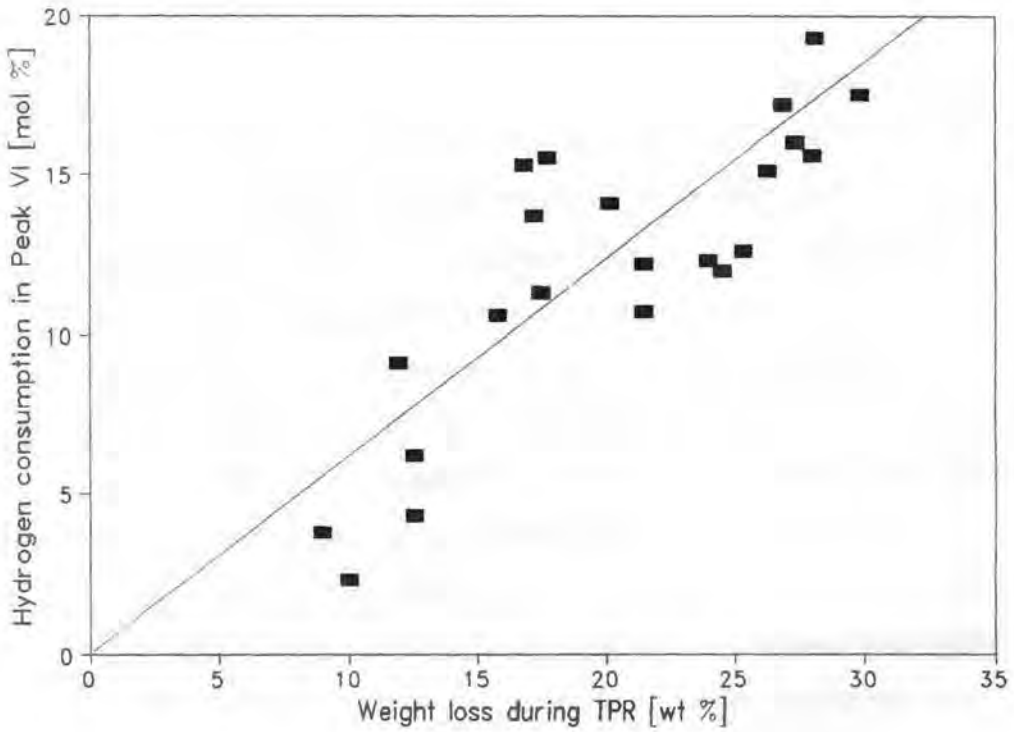

Figure 4.23. Influence of catalyst water content on cobalt silicate formation

By changing the temperature of catalyst calcination, considerable changes in the size of the various hydrogen consumption peaks were observed. In particular, the size of the low temperature hydrogen consumption regions (Peaks II and III) first increased and then decreased with increasing calcination temperature and the size of the high temperature hydrogen consumption region (Peak VI) first decreased and then increased. The destruction of the cobalt silicate species responsible for the hydrogen consumption in Peak VI up to calcination temperatures of approximately 500°C is consistent with the decrease observed upon increasing the severity of the drying step. The increase in the contribution of the high temperature hydrogen consumption peaks at calcination temperatures greater than 500°C may be caused by increased thermal annealing of the supported cobalt and the silica carrier. The intimate contact between the SiO_2 carrier and the cobalt atoms is expected to favour the inclusion of the metal oxide particles by the carrier at high calcination temperatures [Bell, 1987]. The thermal destruction of the surface cobalt silicate with increasing calcination temperature (up to 500°C) results in an increase in the area of Peaks II and III which are ascribed to the reduction of Co_3O_4 and CoO respectively. It is possible that upon destruction of these surface cobalt silicate species, the bulk cobalt oxide Co_3O_4 is formed. This would explain the increase in the area of Peaks II and III. The decrease in the low temperature hydrogen consumption at high calcination temperatures could be caused by the solid state reaction between the supported cobalt oxide and the silica support to form cobalt orthosilicate [Ruger, 1924] which would result in the increase in the hydrogen consumption associated with Peak VI.

The TPR spectra of the Co/SiO_2 catalysts calcined in air and nitrogen were very similar which indicates that the chemical nature of the calcination atmosphere does not influence the reducibility of the supported cobalt significantly. In contrast, the Co/SiO_2 catalyst heated to 400°C without gas flow showed no high temperature hydrogen consumption and the TPR spectrum was similar to that of the bulk unsupported cobalt oxide Co_3O_4. The differences in catalyst reducibility can be ascribed to the increased concentration of nitrogen oxides present during the thermal pretreatment without gas flow. Since these nitrogen oxides are stronger

oxidizing agents than molecular oxygen [Arnoldy and Moulijn, 1985], it appears that these species are able to destroy the surface cobalt silicate precursors to form cobalt oxide.

Increasing the time and temperature of the drying step resulted in a change in the colour of the catalyst precursor from purple to black. This black colour is characteristic of the cobalt oxide Co_3O_4. If the cobalt nitrate precursor was partially decomposed during the drying stage, nitrogen oxides would be released. It has been shown that these nitrogen oxides are capable of destroying the surface cobalt silicate precursors to form cobalt oxide which could explain the change in the colour of the catalyst. Alternatively, if a hydrated cobalt silicate species was formed during the impregnation step and if part of the nitrate evaporated as HNO_3 during the drying stage (B.P. (HNO_3) = 86°C [Perry and Green, 1984]), then the destruction of these hydrated cobalt silicate species could lead directly to cobalt oxide. Since cobalt nitrate only decomposes at a temperature of 275°C [Lapidus *et al*, 1991], it appears that the thermal destruction of the surface cobalt silicate precursor is responsible for the change in catalyst colour.

CHAPTER 5

CONCLUSIONS

5. Conclusions

It has been shown that silica supported cobalt, nickel and copper catalysts can be used successfully for the reductive amination of ethanol using ammonia. Differences in the activity and selectivity of these catalysts were observed, indicating that the catalytic nature of these metals is different. The amination behaviour of the cobalt, nickel and copper catalysts could be described by a typical series reaction mechanism in which MEA was the primary product. This MEA can react with ethanol to form DEA which in turn can react with ethanol to form TEA. Depending on the rates of formation of the reactions to form MEA, DEA and TEA and on the surface concentrations of the various reactants, different activities and selectivities were obtained.

In the case of the Co/SiO_2 catalyst, an increase in the rate of reductive amination was observed upon increasing the partial pressures of ethanol, ammonia and hydrogen. The increase in the rate of reductive amination upon increasing the hydrogen partial pressure was ascribed to the partial deactivation of the Co/SiO_2 catalyst by cobalt nitride formation. The increase in the rate of ethanol consumption with increasing partial pressure of the ammonia feed indicated that ammonia was probably involved in the rate controlling step during reductive amination over Co/SiO_2, as opposed to previous investigations of the reductive amination of various alcohols [Kryukov *et al*, 1967; Baiker *et al*, 1983; Vultier *et al*, 1987; Bassili and Baiker, 1991] in which it was shown that the rate controlling step during reductive amination was the rate of abstraction of the α-hydrogen from the reactant alcohol. Kinetic modelling of the rates of ethylamine formation showed that the rate of MEA formation could be described by a Langmuir-Hinshelwood expression derived for a case where the rate of surface reaction between ethanol and ammonia is the controlling step. The rates of DEA and TEA formation were best described by kinetic expressions derived for a case where the rate of ethanol adsorption was the rate controlling step. The increase in the rate of ethanol consumption with increasing ammonia partial pressure may therefore be ascribed to the increased rate of MEA formation over this catalyst.

The rate of reductive amination over the Ni/SiO_2 catalyst was seen to increase with

increasing ethanol partial pressure whereas the partial pressures of the ammonia and hydrogen feeds did not alter the rate significantly. Although the increase in the rate of reductive amination with increasing ethanol partial pressure may indicate that the dehydrogenation of the reactant alcohol is the controlling step, a corresponding decrease in the reaction rate with increasing hydrogen pressure was not observed. It therefore appears that the rate controlling step over the Ni/SiO_2 catalyst does not involve the abstraction of the α-hydrogen from the reactant alcohol as observed by previous investigators [Kryukov *et al*, 1967; Baiker *et al*, 1983; Vultier *et al*, 1987; Bassili and Baiker, 1991]. Kinetic modelling of the amination behaviour of this catalyst indicated that the reactions forming MEA, DEA and TEA could be described by Langmuir-Hinshelwood kinetic expressions in which the rate of surface reaction is the controlling step.

The Cu/SiO_2 catalyst was characterized by low MEA selectivities which indicated that the rate of conversion of MEA to DEA over this metal was rapid. Besides low MEA selectivities, the formation of an unidentified byproduct was also observed. Kinetic modelling of the amination behaviour of the Cu/SiO_2 catalyst showed that the rate of MEA and DEA formation could be described by a kinetic expression in which the rate of ethanol adsorption was the rate controlling step. The rate of TEA formation could be described by a kinetic expression formulated for a case in which the rate of surface reaction between ethanol and DEA was the rate controlling step. Since the rate of ethanol consumption is determined by the rate of ethylamine formation, it can be seen that the rate controlling step for the conversion of the reactant alcohol over Cu/SiO_2 is not solely determined by the rate of abstraction of the α-hydrogen.

In terms of the overall activity of the three SiO_2 supported metal catalysts, nickel would be preferred over cobalt which would be preferred over copper. These differences in activity are largely caused by changes in the reducibility and the dispersion of the metallic phase. Comparison of the specific activities of the three metals showed however that cobalt had the highest turnover frequency followed by nickel and then copper. Since the metallic dispersion and reducibility can be altered by varying the catalyst preparation and activation steps, it is concluded that cobalt is the most promising catalyst in terms of the overall activity.

The adsorption terms obtained during the kinetic evaluation of the cobalt, nickel and copper catalysts indicated that the strength of ammonia adsorption relative to the strength of ethanol adsorption increased as the metal was changed from copper to cobalt to nickel. The change in the relative strengths of adsorption may be responsible for the changes in ethylamine selectivity. Increasing the ammonia partial pressure at constant ethanol pressure resulted in a decrease in the degree of amine substitution (*i.e.* increased MEA selectivities and decreased DEA and TEA selectivities) and it would be expected that an increase in the strength of ammonia adsorption relative to ethanol would result in a higher concentration ratio of NH_3 : EtOH at the surface. The selectivity behaviours of the three metal catalysts therefore appear to be determined by the relative surface concentrations of ethanol and ammonia, which is consistent with previous observations that the selectivity during reductive amination can be adjusted by varying the ammonia to ethanol feed ratio [Baiker and Kijenski, 1985; Kirk-Othmer, 1992].

Catalyst selection on the basis of ethylamine selectivity would be based on market demands. Since the greatest demand is for MEA [Kirk-Othmer, 1992] and since the specific MEA selectivity decreased as the metal catalyst was changed from Ni/SiO_2 to Co/SiO_2 to Cu/SiO_2, it may be deduced that the catalyst of choice is nickel. Selection of the metal catalyst also depends on the total activity of the metal catalyst and the final choice would depend on the activity of the catalyst as well as the cost of recycling unreacted feed used to alter product selectivity.

By varying the preparation and activation procedures of a number of supported cobalt catalysts, considerable differences in activity were observed. These differences were caused by differences in the extent of cobalt reduction and variations in the dispersion of the metal phase on the inorganic oxide carrier. Even though considerable differences in activity were observed, a linear correlation between the rate of ethanol consumption and the reduced metallic surface area was obtained. This indicates that metallic cobalt is the active catalytic component during reductive amination. No correlation between the concentration of unreduced cobalt species or the support surface area and the rate of ethanol consumption was obtained indicating that these species do not influence the rate of reductive amination

significantly.

The specific ethylamine selectivity (*i.e.* the selectivity measured at the same ethanol conversion) was also seen to change with varying preparation and activation procedures. It was found that the specific ethylamine selectivity was dependent on the reduced metallic surface area of the catalyst with MEA selectivity decreasing and DEA and TEA selectivities increasing with increasing metallic surface area. The only parameter able to be correlated with the metallic surface area was the strength of hydrogen adsorption as measured using hydrogen chemisorption. A decrease in the strength of hydrogen adsorption (as determined by the chemisorption measurements) was observed as the metallic surface area was increased. From this it was concluded that ammonia was preferentially adsorbed on "strong" adsorption sites and, at higher metal surface areas, the relative surface concentration of ammonia to ethanol was decreased. The decrease in the relative surface concentration of ammonia and ethanol resulted in lower MEA selectivities and higher DEA and TEA selectivities. No correlation between the specific ethylamine selectivity and the extent of reduction, the average particle size, the support surface area or the support acidity was observed.

Temperature programmed reduction of SiO_2 supported cobalt catalysts revealed the presence of at least six different cobalt species. The hydrogen consumption peaks occurring during TPR were ascribed to the reduction of residual cobalt nitrate (Peak I), trivalent cobalt species (Peak II), divalent cobalt oxide CoO (Peak III), divalent cobalt ions interacting with cobalt-silicate species (Peak IV), various cobalt hydrosilicate species (Peak V) and cobalt orthosilicate (Peak VI). A combined reduction/oxidation cycle confirmed complete reduction of all cobalt species by the time a temperature of 1000°C was reached.

Cobalt-silicate species were proposed to originate via the interaction between dissolved cobalt ions and surface silanol groups. The importance of water coordinated to the dissolved cobalt ion was underlined by using chelating agents as impregnation solutions (thereby removing ligand water) and by dehydrating the cobalt nitrate precursor salt prior to impregnation. A marked decrease in cobalt-silicate formation was observed in both instances. An increase in cobalt silicate formation was observed upon increasing the surface area of the SiO_2 support

(and therefore the number of silanol groups) which exhibited the importance of support silanol groups in the formation of cobalt-silicate species.

It was shown that a mild thermal pretreatment was capable of destroying cobalt-silicate species. Increasing the time and temperature of the drying stage resulted in a decrease in cobalt silicate formation and a correlation between the residual water content in the catalyst precursor after drying and the amount of cobalt-silicate species was observed, thus emphasizing the importance of water in the formation of cobalt-silicate species. Increasing the temperature of precalcination up to approximately 600°C also decreased cobalt-silicate formation, probably in a similar manner to that occurring during the drying stage. Higher calcination temperatures resulted in increased cobalt-silicate formation due to the diffusion and reaction of supported cobalt ions with the silica carrier.

REFERENCES

Anderson, J.R., Structure of Metallic Catalysts, London, New York, Academic Press, 1975, 275.

Anderson, J.R. and Clark, N.J., *J. Catal.*, **5** (1966) 250.

Arnoldy, P. and Moulijn, J.A., *J. Catal.*, **93** (1985) 38.

Babb, K.H. and White, M.G., *J. Catal.*, **93** (1986) 343.

Baiker, A., *Ind. Eng. Chem., Prod. Res. Dev.*, **20** (1981) 615.

Baiker, A., Caprez, W. and Holstein, W.L., *Ind. Eng. Chem., Prod. Res. Dev.*, **22** (1983) 217.

Baiker, A. and Kijenski, J., *Catal. Rev.-Sci. Eng.*, **27** (1985) 653.

Baiker, A. and Maciejewski, M., *J. Chem. Soc., Faraday Trans. 1*, **80** (1984) 2231.

Baiker, A., Monti, D. and Song Fan, Y., *J. Catal.*, **88** (1984) 81.

Baiker, A. and Richarz, W., *Ind. Eng. Chem., Prod. Res. Dev.*, **16** (1977) 261.

Baiker, A. and Richarz, W., *Helv. Chim. Acta*, **61** (1978) 1169.

Baker, R.T.K., Metal-Support and Metal Additive Effects in Catalysis, Imelik, B. *et al*, Amsterdam, Elsevier, 1982, 37.

Banerjee, A.K., Naidu, S.R., Ganguli, N.C. and Sen, S.P., *Technology*, **11** (1974) 249.

Bartholomew, C.H. and Farrauto, R.J., *J. Catal.*, **45** (1976) 41.

Bartholmew, C.H. and Pannell, R.B., *J. Catal.*, **65** (1980) 390.

Bartholomew, C.H., Pannel, R.B. and Butler, J.L., *J. Catal.*, **65** (1980) 335.

Bartholomew, C.H. and Reuel, R.C., *Appl. Catal.*, **73** (1991) 65.

Bashkirov, A.N., Fridman, R.A., Bogolepova, E.I., Smirnova, R.M. and Kryukov, Y.B., *Dokl. Acad. Nauk. SSSR*, **201** (1971) 847.

Bassili, V.A. and Baiker, A., *Appl. Catal.*, **70** (1991) 325.

Bell, A.T., Supports and Metal-Support Interactions in Catalyst Design, in "Catalyst Design - Progress and Perspectives, ed. Hegedus, L.L., Wiley and Sons, New York, 1987, 103.

Benesi, H.A. and Winquist, B.H.C., *Adv. Catal.*, **17** (1977) 97.

Bessell, S., *Appl. Catal.*, **96** (1993) 253.

Best, D.C., US Patent 4,123,462, 1978.

Boldyrev, V.V., Bulens, M. and Delmon, B., The Control of the Reactivity of Solids, Amsterdam, Elsevier, 1979.

Bond, G.C., Metal-Support and Metal Additive Effects in Catalysis, Imelik, B. *et al* (eds), Amsterdam, Elsevier, 1982, 1.

Bournonville, J.P., Franck, J.P. and Martino, G., Proceedings of the 3rd International Symposium on the Preparation of Catalysts, Louvain-la-Neuve, 1982, Paper A6.1.

Brunelle, J.P., *Pure Applied Chem.*, **59** (1978) 1211.

Burwell Jr., J.L., Pearson, R.G., Haller, G.L., Tjok, P.B. and Chock, S.P., *Inorg. Chem.*, **4** (1965) 1123.

Che, M., in Proc. 10th Int. Congr. on Catalysis, Budapest, 1992, Guczi, L., Solymosi, F. and Tetteny, P., eds, Elsevier, Amsterdam, 1993, 31.

Chen, W.D., Cui, Y.D., Hsu, C.C. and Tao, J., *J. Appl. Phys.*, **69** (1991) 7612.

Chen, Y.Z. and Wang, T.H., *Catal. Lett.*, **22** (1993) 165.

Chin, R.L. and Hercules, D.M., *J. Catal.*, **74** (1982) 121.

Chin, R.L. and Hercules, D.M., *J. Phys. Chem.*, **86** (1982) 360.

Coenen, J.W.E., *Appl. Catal.*, **54** (1989) 65.

Deeba, M., EPA 0 311 900 A2, 1988.

Deeba, M. and Ford, M.E., *Zeolites*, **10** (1990) 794.

Deeba, M., Ford, M.E. and Johnson, T.A., *J. Chem. Soc., Chem. Commun.*, (1987) 562.

Dowden, D.A., Catalysis (Specialist Periodical Report), The Chemical Society, London, 1980, vol. 3, 136.

Engelhard Private Report, "The Amination of Ethanol", 1985.

Feliciani, C., Phys. Z., 6 (1905) 21, in Gmelins Handbuch der Anorganischen Chemie, 8th Ed., Vol. 4, 794, Deutsche Chemische Gesellschaft, Verlag Chemie, Berlin, 1934.

Fenelov, V.B., Neimark, A., Kheifets, L.A. and Samakhov, A.A., in "Preparation of Catalysts II", Delmon, B., Grange, P., Jacobs, P.A. and Poncelet, G., Amsterdam, Elesevier, 1979, 223.

Fierro, G., LoJacono, M., Inversi, M., Porta, P., Lavecchia, R. and Cioci, F., *J. Catal.*, **148** (1994) 709.

Foger, K., in "Catalysis Science and Technology", Anderson, J.R. and Boudart, M., Vol. 6, 1985, 228.

Fowlkes, R.L. and Martinez de Pinillos, J.V., EPA 0 013 176 A1, 1980.

Fuentes, S. and Figueras, F., *J. Chem. Soc. Faraday Trans. I*, **74** (1978) 174.

Fung, S.C., *J. Catal.*, **76** (1982) 225.

Gardner, D.A. and Clark, R.T., US Patent 4,255,357, 1981.

Greegor, R.B. *et al*, *J. Phys. Chem.*, **85** (1981) 1233.

Gruyot, E. and Fournier, M., *C.R. Acad. Sci.*, **189** (1929) 927.

Haberlandt, H., in "Theoretical Aspects of Heterogeneous Catalysis", Moffat, J.B., Van Nostrand Reinhold, New York, 1990, 311.

Heft, B.K., Cooper, C.A., Fowlkes, R.L. and Forester, L.S., EPA 0 379 939 A1, 1990.

Hinshelwood, C.N., in "Kinetics of Chemical Change", Oxford University Press, London, 1940.

Horsley, J.A., *J. Amer. Chem. Soc.*, **101** (1979) 2870.

Howk, B.W., Little. E.L., Scott, S.L., and Whitman, G.M., *J. Am. Chem. Soc.*, **76** (1954) 1899.

Hurst, N.W., Gentry, S.J. and Jones, A., *Catal. Rev. Sci. Eng.*, **24** (1982) 233.

Jacobs, P.A., Tielen, M., Linart, M.P., Uytterhoeven, J.B. and Beyer, H., *J. Chem. Soc., Faraday Trans. I*, **72** (1976) 2793.

Kijenski, K., Burger, J. and Baiker, A., *Appl. Catal.*, **11** (1984) 295.

Kirk-Othmer Encyclopedia of Chemical Technology, Vol. 2, 4th Ed., John Wiley and Sons, New York, 1992, 369 - 386.

Kliger, G.A., Lazutina, L.A., Fridman, R.A., Kryukov, Y.B., Bashkirov, A.N., Snagovskii, Y.S. and Smirnova, R.M., *Kinet. Katal.*, **16** (1975) 660.

Klyuev, M.V. and Khikidel, M.L., *Russ. Chem. Rev.*, **49** (1980) 14.

Ko, E.I., Winston, S. and Woo, C., *J. Chem. Soc. Chem. Commun.*, 1982, 740.

Komiyama, M., Merrill, R.P. and Harnsberger, H.F., *J. Catal.*, **63** (1980) 35.

Kotter, M. and Riekert, L., in "Preparation of Catalysts II", Delmon, B., Grange, P., Jacobs, P.A. and Poncelet, G. (eds), Amsterdam, Elesevier, 1979, 51.

Kryukov, Y.B., Zakirov, N.S., Novak, N.I., Bashkirov, A.N. and Bogolepova, E.I., *Neftekhimiya*, 7 (1967) 124.

Lapidus, A., Krylova, A., Kazanskii, V., Borovkov, V., Zaitsev, A., Rathousky, J., Zukal, A. and Jancalkova, M., *Appl. Catal.*, **73** (1991) 65.

LoJacono, M, Schiavello, M. and Cimino, A., *J. Phys. Chem.*, **75** (1971) 1044.

Malet, P. and Caballero, A., *J. Chem. Soc., Faraday Trans I*, **84** (1988) 2369.

Matsuzaki, T., Takeuchi, K., Taka-aki, H., Hironari, A. and Sugi, Y., *Appl. Catal.*, **105** (1993) 159.

Menon, P.G. and Froment, G.F., *Appl. Catal.*, **1** (1981) 31.

Ming, H. and Baker, B.G., *Appl. Catal.*, **123** (1995) 23.

Mizuno, N., Tabata, M., Uematsu, T. and Iwamoto, M., *J. Catal.*, **146** (1994) 249.

Monti, D.A.M. and Baiker, A., *J. Catal.*, **83** (1983) 323.

Myasaki, E., *J. Catal.*, **65** (1980) 84.

Nekrasova, V.A. and Shuikin, N.I., *Russ. Chem. Rev.*, **34** (1965) 843.

Okamoto, Y., Nagata, K., Adachi, T., Imanaka, T., Inamura, K. and Takya, T., *J. Phys. Chem.*, **95** (1991) 310.

Ono, Y. and Ishida, H., *J. Catal.*, **72** (1981) 121.

Otter, G.J. and Dautzenberg, F.M., *J. Catal.*, **53** (1978) 116.

Parks, G.A., *Chem. Rev.*, **65** (1965) 177.

Parks, G.A. and DeBruyn, P.L., *J. Phys. Chem.*, **66** (1962) 967.

Paryjczak, T., Rynkowski, J. and Karski, S., *J. Chromatogr.*, **188** (1980) 254.

Pasek, J., Kondelik, P. and Richter, P., *Ind. Eng. Chem. Prod. Res. Dev.*, **11** (1972) 333.

Perry, R.H. and Green, D., in Perry's Chemical Engineer's Handbook, 6th ed., McGraw-Hill Book Co., 1984.

Pommersheim, J.M. and Coull, J., *AIChE J.*, **17** (1971) 1075.

Popov, M.A., Candidate's Thesis, Institute of General Chemistry of the USSR Academy of Sciences, Moscow, 1952.

Praliaud, H. and Martin, G.A., *J. Catal.*, **72** (1981) 394.

Puskas, I., Fleisch, T.H., Hall, J.B., Meyers, B.L. and Roginski, R.T., *J. Catal.*, **134** (1992) 615.

Rathousky, J., Zukal, A., Lapidus, A. and Krylova, A., *Appl. Catal.*, **79** (1991) 167.

Reck, R.A., Harwood, H.J. and Ralston, A.W., *J. Org. Chem.*, **12** (1947) 517.

Reuel, R.C. and Bartholomew, C.H., *J. Catal.*, **85** (1984) 63.

Richter, P. and Pasek, J., *Chem. Prum.*, **20** (1970) 426.

Rosynek, P.M., *Catal. Rev.-Sci. Eng.*, **16** (1977) 111.

Rosynek, P.M. and Polansky, C.A., *Appl. Catal.*, **73** (1991) 97.

Runeberg, J., Baiker, A. and Kijenski, J., *Appl. Catal.*, **17** (1985) 309.

Schwoegler, E.J. and Adkins, H., *J. Am. Chem. Soc.*, **61** (1939) 3499.

Sexton, B., Hughes, A., and Turney, T., *J. Catal.*, **97** (1986) 390.

Sewell, G.S., O'Connor, C.T. and van Steen, E., *Appl. Catal.*, **125** (1995) 99.

Sewell, G.S., van Steen, E. and O'Connor, C.T., *Catal. Letters*, accepted for publication.

Shen, J.P., Ma, J., Jiang, D.Z. and Min, E.Z., *Catal. Letters*, **26** (1994) 291.

Shulman, S., Formo, M.W. and Rheineck, A.E., *J. Am. Oil Chem. Soc.*, **38** (1961) 205.

Shyr, Y.S. and Ernst, W.R., *J. Catal.*, **63** (1980) 425.

Smeykal, K., German Patent 637,731 (1936).

Smith, J.M., in "Chemical Engineering Kinetics", 3rd Ed., McGraw-Hill, 1987, 496.

Tatarchuk, B.J. and Dumesic, J.A., *J. Catal.*, **70** (1981) 308.

Trimm, D.L., *Appl. Catal.*, **5** (1983) 263.

Troth, L.E., in "Transition Metals and Carbides", Academic Press, New York, 1971.

van der Grift, C.F.G., Mulder, A. and Geus, J.W., *Appl. Catal.*, **60** (1990) 181.

van Steen, E., PhD Thesis, University Karlsruhe, 1993.

van't Blik, H.F.J. and Prins, R., *J. Catal.*, **97** (1986) 188.

van't Blik, H.F.J., Koningsberger, D.C. and Prins, R., *J. Catal.*, **97** (1986) 210.

Vannice, M.A. and Twu, C.C., *J. Catal.*, **82** (1983) 213.

Viswanathan, B. and Gopalakrishnan, R., *J. Catal.*, **99** (1986) 342.

Volf, J., Pasek, J. and Duraj, N., *Collect. Czech. Chem. Commun.*, **38** (1973) 1038.

Vultier, R., Baiker, A. and Wokaun, A., *Appl. Catal.*, **30** (1987) 167.

Zaborski, M., Vidal, A., Ligner, G., Balard, H., Papirer, E. and Burneau, A., *Langmuir*, **5** (1989) 447.

Zowtiak, J.M. and Bartholomew, C.H., *J. Catal.*, **83** (1983) 107.

Zowtiak, J.M., Weatherbee, G.D. and Bartholomew, C.H., *J. Catal.*, **82** (1983) 230.

APPENDICES

Appendix I - TPR calibration and sample calculation

Calibration of the TPR apparatus was performed using the reduction of the bulk cobalt oxide (Co_3O_4) which is converted to zerovalent cobalt via the following reaction stoichiometry :

$$Co_3O_4 + 4\ H_2 \rightarrow 3\ Co + 4\ H_2O$$

Prior to the TPR experiment, the thermal conductivity of a 60 ml(NTP)/min N_2 stream and the thermal conductivity of a 60 ml(NTP)/min H_2/N_2 gas mixture is recorded relative to a 60 ml(NTP)/min N_2 stream passing through the reference arm of the TCD. The difference in thermal conductivities between the N_2 and H_2/N_2 streams is used as a measure of the hydrogen flowrate in the reducing gas stream. During TPR, the thermal conductivity of the reactor outlet stream and the temperature of the catalyst sample is measured as function of the time elapsed. Changes in the thermal conductivity of the reactor outlet can therefore be directly correlated to changes in the hydrogen flowrate in the reactor outlet and the hydrogen consumption rate as a function of time can be determined.

Since the concentration of H_2 in the gas mixture is not known prior to the calibration, it was assumed that the hydrogen was present as a 5% mixture in nitrogen by volume. From this assumption and from the measured reducing gas flowrate (60 ml(NTP)/min), the rate of hydrogen consumption can be measured as a function of time. The rate of hydrogen consumption of Co_3O_4 (assuming hydrogen is present as a 5 vol% mixture in nitrogen) during TPR is illustrated below.

The area under the curve may be integrated using the trapezoidal rule and is described by the following expression :

$$H_2\ consumption = \Sigma_n \frac{(t_{n+1} - t_n) \times (f_{n+1} + f_n)}{2}$$

where f is the flowrate of hydrogen in mmol/min and t is the time elapsed in minutes.

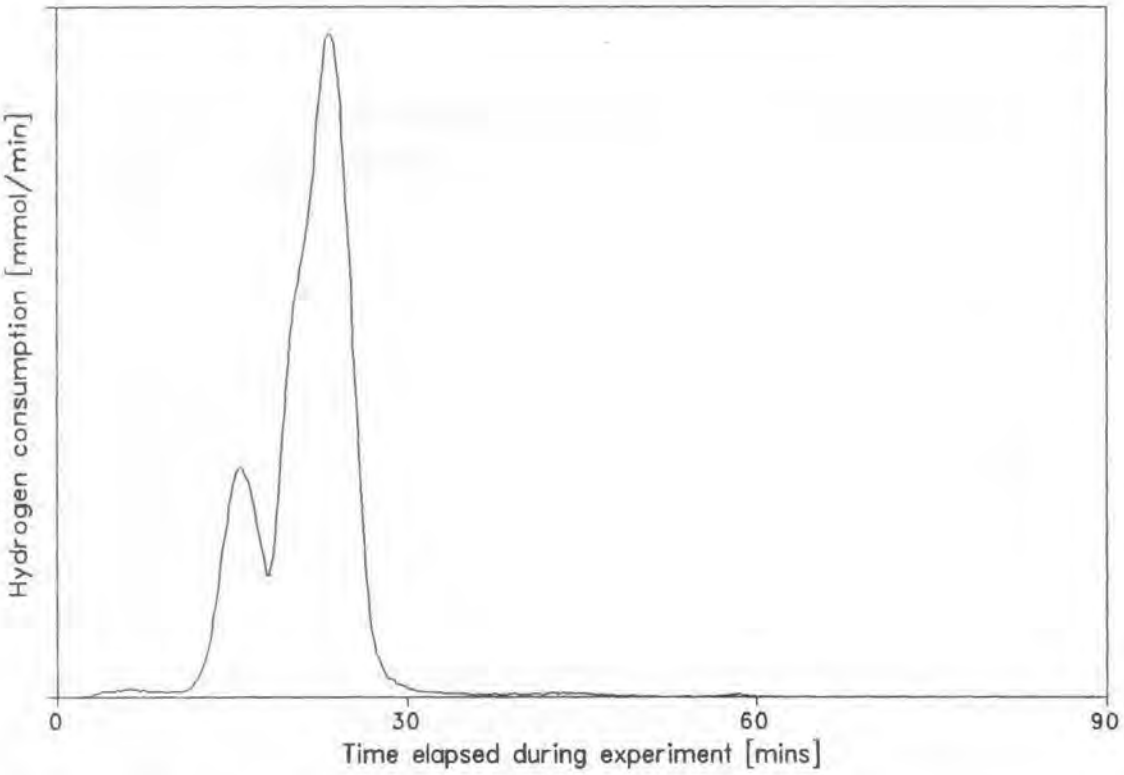

Rate of hydrogen consumption of Co_3O_4 during TPR

Integration of the TCD signal during TPR showed that 1.741 mmol of H_2 was required for the complete reduction of Co_3O_4. From the mass of Co_3O_4 used for the calibration (0.0848 g), it can be calculated that 1.060 mmol of atomic cobalt is present in the TPR sample. The measured hydrogen to cobalt molar ratio during TPR is therefore calculated by the following expression :

$$H_2 : Co = \frac{1.741}{1.056} = 1.649$$

From the reaction stoichiometry it is evident that only 1.33 moles of hydrogen per mole of cobalt are required for complete reduction of Co_3O_4. The assumed concentration of hydrogen in the reducing gas mixture is therefore incorrect and the actual hydrogen concentration can be calculated simply by the following expression :

$$H_2 \text{ concentration} = \frac{1.648}{1.33} \times 5\% = 6.20 \text{ vol\% } H_2/N_2$$

Use of the calculated hydrogen concentration of the reducing gas stream allows direct quantification of the hydrogen consumption during TPR using a similar calculation procedure.

Appendix II - TPO Calibration and Sample Calculation

Calibration of the TPO apparatus was performed using the oxidation of reduced cobalt metal as a standard. The oxidation behaviour of cobalt is characterized by two main phenomena, *viz.* low temperature oxidation to form the bulk oxide Co_3O_4 (reaction 1) and high temperature thermal reduction to form the divalent cobalt oxide CoO (reaction 2). The overall stoichiometry of these two reactions is described by the equations listed below.

$$3\ Co + 2\ O_2 \rightarrow Co_3O_4 \qquad (1)$$

$$Co_3O_4 \rightarrow 3\ CoO + \tfrac{1}{2}\ O_2 \qquad (2)$$

Prior to oxidation of the reduced metal catalyst, the thermal conductivity of a 60 ml(NTP)/min He stream and the thermal conductivity of a 60 ml(NTP)/min O_2/He gas mixture are measured relative to a 60 ml(NTP)/min reference flow of He. The difference in thermal conductivity between the oxidizing gas and the inert helium stream represents the total oxygen flow in the oxidizing gas stream. Variations in the thermal conductivity of the outlet stream during TPO can therefore be correlated directly to the change in oxygen concentration in the oxidizing stream. Since the flowrate of the oxidizing gas stream is known, the oxygen consumption rate can be determined.

Prior to calibration, the concentration of oxygen is not known. It was assumed that the oxygen was present as a 2 vol% mixture in helium which allowed an oxygen consumption rate to be determined as a function of the time elapsed during the TPO experiment. The figure below illustrates the rate of oxygen consumption/release of metallic cobalt during TPO (based on an oxidizing gas stream comprising a 60 ml(NTP)/min 2% O_2/He mixture). A negative rate of oxygen consumption correlates to the oxygen release upon the thermal reduction of Co_3O_4 to CoO.

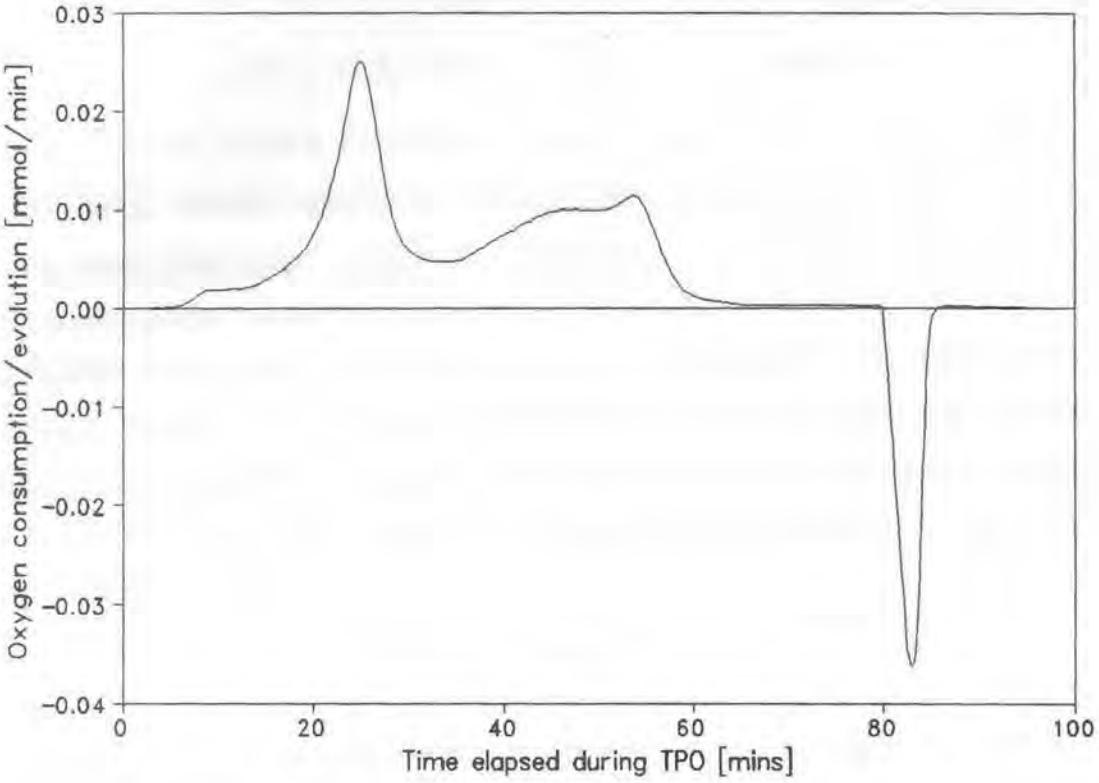

Rate of oxygen consumption/release of cobalt during TPO

Using the trapezoidal rule, the rate of oxygen consumption/release during TPO can be calculated in the following manner :

$$O_2 \text{ consumption} = \Sigma_n \frac{(t_{n+1} - t_n) \times (f_{n+1} + f_n)}{2}$$

where f is the oxygen consumption rate in mmol/min and t is the time elapsed in minutes.

Integration of the oxygen uptake peaks occurring at lower temperatures showed an oxygen uptake of 0.3412 mmol based on an oxidizing gas comprising a 60 ml(NTP)/min 2% O_2/He gas mixture. Since 3 cobalt atoms react with 2 molecules of oxygen, it can be seen that the amount of cobalt oxidized is 0.5118 mmol. The amount of cobalt present during TPO calculated on the basis of an oxygen concentration of 2 vol% is therefore lower than the amount of cobalt added (0.6107 mmol). The actual concentration of oxygen in the TPO

oxidizing gas can therefore be calculated by the following expression :

$$O_2 \text{ concentration} = \frac{0.6107}{0.5118} \times 2\% = 2.39 \text{ vol\% } O_2/He$$

According to the material balance, the amount of oxygen released during the high temperature thermal reduction of Co_3O_4 should also correspond to the total amount of cobalt added during the experiment. Measurement of the high temperature oxygen release showed that 0.0871 mmol of O_2 was released which by the reaction stoichiometry corresponds to 0.5228 mmol Co. The error, which represents the accuracy of the technique, between the amount of cobalt present as determined by the oxygen uptake and the amount of cobalt as determined by the oxygen release is described by the following expression :

$$\text{Difference} = \frac{0.5228 - 0.5118}{0.5228} \times 100\% = 2.1\%$$

In the instance of supported cobalt catalysts, not all of the cobalt is completely reduced following hydrogen reduction at 500°C. This incomplete reduction is caused by the formation of stable cobalt-support species such as cobalt-aluminates [Chin and Hercules, 1982] and cobalt silicates [Puskas *et al*, 1992]. In the measurement of the oxidation behaviour of supported cobalt catalysts in this study, it was established that the oxygen release occurring at high temperatures did not always correspond to the total amount of cobalt in the sample. In other words, not all of the cobalt present had been oxidized to trivalent cobalt by a temperature of approximately 800°C (where thermal reduction of this species begins). This indicates that this cobalt is most likely present as a stable cobalt-support compound which cannot be oxidized up till a temperature of 1000°C.

For a SiO_2 supported cobalt catalyst, an appropriate amount of sample was added such that 0.6072 mmol of Co were present. Measurement of the TCD signal at high temperatures indicated that a total amount of 0.0716 mmol O_2 was released during the thermal reduction of Co_3O_4. From this measurement, the amount of Co_3O_4 being thermally reduced can be calculated by the reaction stoichiometry via the following equation :

Amount Co as Co_3O_4 = 6 × 0.0716 = 0.4296 *mmol Co*

and from the mass balance, the amount of cobalt present as a metal-support compound (non-oxidizable Co^{2+}) can be calculated from the following relationship :

Amount Co as cobalt-support compound = 0.6072 - 0.4296 = 0.1776 *mmol Co*

Besides the presence of cobalt species which cannot be oxidized up till temperatures of 1000°C, it is also possible that a portion of the oxygen uptake in the first peak is due to the oxidation of divalent Co^{2+} species which were not reduced by activation in hydrogen at 500°C. Two types of oxidation reactions can therefore be responsible for the low temperature oxygen uptake during TPO.

$$3\ Co + 2\ O_2 \rightarrow Co_3O_4 \qquad (3)$$

$$3\ CoO + \tfrac{1}{2}\ O_2 \rightarrow Co_3O_4 \qquad (4)$$

If only the first reaction occurs, then the ratio of the area corresponding to the oxygen uptake peak relative to the area resulting from the high temperature oxygen release peak will be 4. If only the second reaction occurs, then this ratio will be 1. In practice, this value has an intermediate value lying between 1 and 4. In the instance of the SiO_2 supported cobalt catalyst, the oxygen uptake during TPO was 0.1990 mmol which results in a relative peak ratio of 2.78. Performing an oxygen balance and assuming that x mmol Co_3O_4 are formed via reaction 3 and y mmol Co_3O_4 are formed via reaction 4, the following simple equations can be derived :

$$2x + \tfrac{1}{2}y = \text{oxygen uptake} = 0.1990 \text{ mmol}$$

$$\tfrac{1}{2}x + \tfrac{1}{2}y = \text{oxygen release} = 0.0716 \text{ mmol}$$

Simultaneous solution of these equations shows that x is equivalent to 0.0849 mmol Co_3O_4 and y is equivalent to 0.0583 mmol Co_3O_4. By definition, it is therefore evident that the amount of cobalt present as a zerovalent metal following reduction is equivalent to 3 x

0.0849 = 0.2547 mmol and the amount of cobalt present as an oxidizable divalent species is 3 x 0.0583 = 0.1749 mmol.

In this manner, the composition of reduced cobalt catalysts can be determined using the TPO technique.

Appendix III - Sample calculation of the conversion and selectivity of the reductive amination reaction

The feed stream during reductive amination comprised a gas phase mixture of ethanol, ammonia, hydrogen and nitrogen. Since nitrogen was present only as an inert diluent, this species was selected as an internal standard during the reductive amination studies. Although hydrogen was included in the feed stream, this species could not be accurately analysed due to the similarity between the thermal conductivities of this species and the helium carrier gas. Since hydrogen is neither consumed nor produced during the reductive amination of alcohols [Kirk-Othmer, 1992], it was assumed that the inlet flowrate of this species was identical to the outlet flowrate.

Based on the volumetric flowrates of the feed gases, mass flowrates can be calculated using the ideal gas law. Furthermore, the total inlet feedrates of atomic carbon and nitrogen can be calculated. These values are required for determining the carbon and nitrogen balances across the reactor system.

Component	Volumetric flowrate (ml/min)	Mass flowrate (g/h)	Carbon flow (mmol/h)	Nitrogen flow (mmol/h)
Nitrogen	90.5	6.32	-	451.6
Ammonia	17.5	0.74	-	43.62
Ethanol	9.8	1.13	49.02	-
Hydrogen	39.8	0.19	-	-
Total	157.5	8.19	49.02	495.22

Using the measured response factors, the area counts obtained upon integration of the TCD signal can be converted into mass percentages. Since the flowrate of the nitrogen internal

standard is known, the flowrates of the individual components can be determined. This conversion process is illustrated below. Nitrogen was assigned a response factor of 1 (since all mass flows are determined relative to the nitrogen internal standard) and the response factor of the unidentified byproduct which was obtained in some instances was assumed to be identical to that of the ethanol feed.

Component	Area (a.u.)	Response factor (-)	Area x RF (a.u.)	Mass % (%)	Mass flow (g/h)
Nitrogen	2904600	1	2904600	78.21	6.322
Ammonia	175034	1.82	318562	8.58	0.693
MEA	39896	0.81	32316	0.87	0.070
Ethanol	497368	0.81	402868	10.85	0.877
DEA	62374	0.65	40543	1.09	0.088
TEA	28586	0.53	15150	0.41	0.033
Byproduct	0	0.81	0	0	0
Total	3707858		3714039	100	8.084

These mass flows can be simply converted into molar flowrates from which the carbon and nitrogen balances across the system can be determined. The conversion of the flowrates into molar flowrates was conducted so that product selectivities could be reported as molar selectivities. The conversion of the mass flows into molar flows and the determination of the total outlet flows of carbon and nitrogen is illustrated below. The molecular weight of the unidentified byproduct was assumed to be the same as that of ethanol for the purposes of calculation.

Component	Mass flow (g/h)	M.W. (A.U.)	Molar flow (mmol/h)	Carbon flow (mmol/h)	Nitrogen flow (mmol/h)
Nitrogen	6.322	28	225.8	-	451.6
Ammonia	0.693	17	40.78	-	40.78
MEA	0.070	45	1.56	3.12	1.56
Ethanol	0.877	46	19.06	38.12	-
DEA	0.088	73	1.21	4.84	1.21
TEA	0.033	101	0.33	1.96	0.33
Byproduct	0	46	0	0	0
Total	8.084		288.74	48.05	43.89

From the calculated outlet molar flowrates of atomic carbon and nitrogen, the molar balances for these two species can be derived using the following expressions :

$$Carbon\ balance = \frac{48.05 - 49.02}{49.02} \times 100\% = -2.0\ mol\%$$

$$Nitrogen\ balance = \frac{43.89 - 43.62}{43.62} \times 100\% = 0.6\ mol\%$$

The nitrogen internal standard was not included in the calculation pertaining to the nitrogen balance since this species was assumed to have the same outlet flowrate and would therefore bias the results of the material balance.

Calculation of the ethanol and ammonia conversions is determined from the atom balances in a similar manner to that which the overall material balances were performed. The

conversion of the ethanol and ammonia feeds can be described by the expressions below.

$$x_{EtOH} = \frac{49.02 - 38.13}{49.02} \times 100\% = 22.2\ mol\%$$

$$x_{NH_3} = \frac{43.62 - 40.79}{43.62} \times 100\% = 6.5\ mol\%$$

Calculation of the product selectivity was made on a molar basis relative to the other products formed during reductive amination. For example, the selectivity to MEA can be calculated using the following expression :

$$S_{MEA} = \frac{1.56}{1.56 + 1.21 + 0.33} \times 100\% = 50.5\ mol\%$$

The selectivities to DEA, TEA and byproducts can be calculated in a similar manner.

Appendix IV - Reaction Data for Reductive Amination Studies

Start-up and Stabilization

Catalyst = Co/SiO2
T = 180 C
P = 1 bar
WHSV = 2
EtOH : NH3 : H2 : N2 = 1 : 2 : 4.1 : 13.6

x(EtOH) (mol %)	x(NH3) (mol %)	s(MEA) (mol %)	s(DEA) (mol %)	s(TEA) (mol %)	s(Other) (mol %)	Time (mins)
21.1	6.1	40	41	14.5	4.5	15
21.3	6	40.5	41.5	14.2	3.8	50
20.3	5.8	41	41.7	14.2	3.1	85
20.7	6.1	41.6	36.9	11.5	10	130
21.2	6.3	43.9	39.7	12.3	4.1	170
21.3	6.2	40.7	41.2	13.5	4.6	210
22.8	5.7	38.3	41.8	14.9	5	275
21.2	6	37.1	42.3	15.1	5.5	315
20.2	5.7	32.4	43.5	17.8	6.3	410
21.8	5.7	33.5	43	17.6	5.9	430
21.3	5.1	19.2	46	27.4	7.4	1395
23.2	5.5	25	43.9	23.9	7.2	1425
22.8	5.5	24.8	44.2	23.5	7.5	1455
22.4	5.5	24.9	44.5	23.1	7.5	1480

Temperature Ramp to Locate Reaction Regimes

Catalyst = Co/SiO2
T = 180 C
P = 1 bar
WHSV = 2
EtOH : NH3 : H2 : N2 = 1 : 2 : 4.1 : 13.6

Temperature (C)	x(EtOH) (mol %)	x(NH3) (mol %)	s(MEA) (mol %)	s(DEA) (mol %)	s(TEA) (mol %)	s(Other) (mol %)
100	2.1	0.7	43.2	56.8	0	0
110	1.1	0.4	57.7	42.3	0	0
120	1.5	0.5	56.1	43.9	0	0
130	2.9	1	49	51	0	0
140	6	1.7	37	49.5	13.5	0
150	9.8	2.6	29.3	47.1	19.5	4.1
160	14.5	3.4	26.3	46.7	22.2	4.8
170	17.2	4.3	23.2	44.7	25.7	6.4
180	22	5.1	21.6	43.3	26.9	8.2
190	24.5	5.6	21.5	42.8	24.1	11.6
200	27.3	6	22.5	41.4	20.4	15.7

Effect of Ammonia Pressure

Catalyst = Co/SiO2
T = 150 C
P = 1 bar
p(EtOH) = 4 kPa
p(H2) = 20 kPa
Total flowrate = 200 ml/min

p(NH3) (kPa)	x(EtOH) (mol %)	x(NH3) (mol %)	s(MEA) (mol %)	s(DEA) (mol %)	s(TEA) (mol %)	s(Other) (mol %)
2.007694	6	4.9	0	37.9	62.1	0
2.597212	7	4.4	3	43.3	56.7	0
3.213726	7.7	4.2	6.9	45	48	0.1
4.083528	8	3.7	10.5	47.2	42.3	0
6.215683	9	2.9	19.2	52.6	28.2	0
8.137799	9.6	2.3	30.8	51.2	18	0
10.76477	8.3	1.8	41.2	47	11.7	0.1

Effect of Ethanol Pressure

Catalyst = Co/SiO2
T = 150 C
P = 1 bar
p(NH3) = 8 kPa
p(H2) = 20 kPa
Total flowrate = 200 ml/min

p(EtOH) (kPa)	x(EtOH) (mol %)	x(NH3) (mol %)	s(MEA) (mol %)	s(DEA) (mol %)	s(TEA) (mol %)	s(Other) (mol %)
1.800866	13	1.9	29.2	51.3	19.5	0
2.23205	12.5	2.1	31	50.5	20	0
2.528167	12.5	2.2	31	50	19.5	0
2.752679	12.7	2.3	31.1	49.1	19.8	0
2.752679	12.7	2.3	31.1	49.1	19.8	0
2.884421	12.5	2.5	31.4	49.2	19.4	0
3.174362	12.2	2.7	31.7	48	19.5	0.8
4.107773	11	3	31	46	23	0
4.454552	10.6	3.1	31	46	23	0
5.61879	9.5	3.2	29.6	44.6	25.6	0.2
6.802896	8.2	3.4	28.6	45.6	25.6	0.2

Effect of Hydrogen Pressure

Catalyst = Co/SiO2
T = 150 C
P = 1 bar
p(EtOH) = 2 kPa
p(NH3) = 8 kPa
Total flowrate = 200 ml/min

p(H2) (kPa)	x(EtOH) (mol %)	x(NH3) (mol %)	s(MEA) (mol %)	s(DEA) (mol %)	s(TEA) (mol %)	s(Other) (mol %)
20.13738	13.8	1.9	32.7	49.5	17.8	0
17.78671	13.8	1.9	36.85	45.75	16.6	0.8
15.74947	12.5	1.9	41	42	15.4	1.6
13.86893	11.6	1.6	51.9	36	13.5	0
12.22347	8.9	1.4	60	33	6.8	0.2
10.42129	6.5	1.1	75	25	0	0
8.932533	6	0.9	83	17	0	0
7.835555	4.9	0.8	90	10	0	0
6.660222	4	0.6	100	0	0	0

Effect of Reaction Temperature

Catalyst = Co/SiO2
P = 1 bar
EtOH : NH3 : H2 : N2 = 1 : 2 : 8.6 : 17.6

Temperature (C)	WHSV (1/h)	x(EtOH) (mol %)	x(NH3) (mol %)	s(MEA) (mol %)	s(DEA) (mol %)	s(TEA) (mol %)	s(Other) (mol %)
150	3.75	8.7	2.1	38.9	46.5	14.6	0
150	3	9.3	2.6	36.4	48.1	15.6	0
150	2.25	10.2	2.9	33.8	47.2	18.9	0.1
150	1.5	13.5	4	31.2	46.9	21.9	0
150	0.75	23	6.7	24.2	47.2	28.6	0
145	3.75	6.3	1.7	40.3	46.9	12.9	0
145	3	7.7	2.1	37.9	47.9	14.2	0
145	2.25	9.9	2.9	37.7	47.5	14.9	0
145	1.5	12.2	4	35.7	47.8	16.5	0
145	0.75	21.8	6.6	30.8	48.3	21	0
140	3.75	5.5	1.3	43.3	44.5	12.2	0
140	3	5.6	1.6	40.5	46.3	13.2	0
140	2.25	5.9	1.8	43.3	39.4	17.2	0.1
140	1.5	9.7	3.1	37	46.9	16.1	0
140	0.75	13.8	4	29.9	45.2	24.9	0
135	3.75	4.6	1.1	49.1	42.1	8.8	0
135	3	5.3	1.5	47.4	44	8.5	0.1
135	2.25	6.4	2.1	45.3	45.1	9.6	0
135	1.5	8.2	3	44.9	45.5	9.6	0
135	0.75	13.9	4.8	38.5	45	16.5	0
130	3.75	2.6	0.7	52.5	39.3	8.2	0
130	3	3.3	1.1	51.6	40.7	7.8	0
130	2.25	4.2	1.4	47.4	43.2	9.4	0
130	1.5	7	2.5	51.4	41.4	7.2	0
130	0.75	10.5	3.6	42.2	45.6	12.1	0.1

Start-up and Stabilization

Catalyst = Ni/SiO2
T = 180 C
P = 1 bar
WHSV = 2
EtOH : NH3 : H2 : N2 = 1 : 2 : 4.1 : 13.6

x(EtOH) (mol %)	x(NH3) (mol %)	s(MEA) (mol %)	s(DEA) (mol %)	s(TEA) (mol %)	s(Other) (mol %)	Time (mins)
43.2	10.1	20.4	48.1	26.2	5.3	15
51.5	13	27.6	49.9	21	1.5	55
51.6	13	29.4	49.8	19.2	1.6	85
44.6	12.2	26.9	51.5	19.6	2	170
47.1	14.5	26.2	50.2	21.6	2	230
43.7	12.1	26.8	50.4	18.8	4	380
40.2	10.9	26.4	51.6	19	3	1390
40.6	11.3	32.1	49.7	15.9	2.3	1420
42	11.4	31	47.1	15.5	6.4	1445
40.9	11.5	32.2	49.3	16.1	2.4	1470
41.5	11.4	31.5	47	15.4	6.1	1500

Temperature Ramp to Locate Reaction Regimes

Catalyst = Ni/SiO2
P = 1 bar
WHSV = 2
EtOH : NH3 : H2 : N2 = 1 : 2 : 4.1 : 13.6

Temperature (C)	x(EtOH) (mol %)	x(NH3) (mol %)	s(MEA) (mol %)	s(DEA) (mol %)	s(TEA) (mol %)	s(Other) (mol %)
100	4.7	1.6	50.4	49.6	0	0
112	2.6	0.9	65.3	34.7	0	0
120	3	1.1	75.8	24.2	0	3.55E-15
130	5.4	1.8	70.8	29.2	0	3.55E-15
140	8.6	2.8	59.1	36	5	-0.1
150	12.3	3.7	51.8	40.3	7.9	5.33E-15
162	20	5.9	42.9	43.3	11.5	2.3
171	28.6	7.7	36.4	44	13.1	6.5
182	40.5	10.9	32.1	48.2	16.9	2.8
191	52.2	13	29.3	49.3	18.2	3.2
200	61.6	15.2	27.2	49.6	18.1	5.1

Effect of Ammonia Pressure

Catalyst = Ni/SiO2
T = 150 C
P = 1 bar
p(EtOH) = 4 kPa
p(H2) = 20 kPa
Total flowrate = 200 ml/min

p(NH3) (kPa)	x(EtOH) (mol %)	x(NH3) (mol %)	s(MEA) (mol %)	s(DEA) (mol %)	s(TEA) (mol %)	s(Other) (mol %)
1.855062	8.5	7.3	4.3	39.1	56.6	0
2.530275	10.4	7.3	12.2	47.4	40.4	0
3.21498	11	6.3	14.6	54.8	30.6	0
3.95796	11.35	5.6	21	54.5	24.5	0
4.902666	11.7	5.1	28.8	54.1	17.1	0
5.896575	11.8	4.8	33.9	52.6	13.5	0
6.843243	12.5	4.7	43.4	47.1	9.5	0
8.158734	12.45	3.9	49.9	42.9	7.1	0.1
9.751021	12.9	3.5	60.8	34.4	4.8	0
10.43519	13.5	3.4	65.8	31.1	3.2	0

Effect of Ethanol Pressure

Catalyst = Ni/SiO2
T = 150 C
P = 1 bar
p(NH3) = 8 kPa
p(H2) = 20 kPa
Total flowrate = 200 ml/min

p(EtOH) (kPa)	x(EtOH) (mol %)	x(NH3) (mol %)	s(MEA) (mol %)	s(DEA) (mol %)	s(TEA) (mol %)	s(Other) (mol %)
1.808946	14.9	2.5	58.9	35.3	5.8	0
2.095555	15	2.8	56.7	37.9	5.4	0
2.376013	14.8	3.2	56.5	37.6	5.9	0
2.554196	14.1	3.2	56.5	38.2	5.3	0
2.899357	13.7	3.5	54.7	38.6	6.6	0.1
3.063025	13.7	3.7	54.1	39.2	6.6	0.1
3.490322	12.9	4	53.9	39.5	6.6	0
4.086088	12.2	4.3	52.7	40.2	7.1	0
4.172284	12.2	4.6	51.7	40.5	7.2	0.6
5.142581	10.5	4.6	51.7	41.1	7.3	0
6.044368	10.3	5	46.8	41	8.3	3.9

Effect of Hydrogen Pressure

Catalyst = Ni/SiO2
T = 150 C
P = 1 bar
p(EtOH) = 2 kPa
p(NH3) = 8 kPa
Total flowrate = 200 ml/min

p(H2) (kPa)	x(EtOH) (mol %)	x(NH3) (mol %)	s(MEA) (mol %)	s(DEA) (mol %)	s(TEA) (mol %)	s(Other) (mol %)
20.13738	20	3	49.2	40.7	9	1.1
20.13738	20	3	49	41	8.6	1.4
17.78671	20.5	3.1	53	40	7.6	0
15.74947	20.5	3.1	56	40	6.3	0
13.86893	20.6	3.2	56.5	37.9	5.6	0
12.22347	21.7	3.4	58.9	36.5	4.6	0
10.42129	21.9	3.2	61	34	4.6	0.4
8.932533	22	3.4	62.5	33.3	4.3	0

Effect of Reaction Temperature

Catalyst = Ni/SiO2
P = 1 bar
EtOH : NH3 : H2 : N2 = 1 : 2 : 8.6 : 17.6

Temperature (C)	WHSV (1/h)	x(EtOH) (mol %)	x(NH3) (mol %)	s(MEA) (mol %)	s(DEA) (mol %)	s(TEA) (mol %)	s(Other) (mol %)
150	0.75	29	10	37	47.3	15.6	0.1
150	1.5	18.1	6.6	47.7	43.1	9.2	0
150	2.25	13.9	4.9	53.9	39.3	6.8	0
150	3	11.7	4	58.4	36.1	5.5	0
150	3.75	9.8	3.2	61.9	33.7	4.5	0
145	0.75	23	5.5	43	42.9	14	0.1
145	1.5	14.5	5	53.4	39.1	7.5	0
145	2.25	10.5	3.5	60.7	34	5.3	0
145	3	8.3	3	65.6	30.5	3.8	0.1
145	3.75	6.5	2.3	67.8	28.7	3.5	0
140	0.75	18.6	6.6	46	41.1	12.9	0
140	1.5	11.2	4.4	58	35.4	6	0.6
140	2.25	8.5	3.6	65	31	3.5	0.5
140	3	6.9	2.6	69	27	2.9	1.1
140	3.75	5.5	2.1	73	24	2.7	0.3
135	0.75	14	4.5	49	39.7	11.2	0.1
135	1.5	8.6	3.8	62.5	33.3	4.3	0
135	2.25	7	2.8	71.2	26.3	2.5	0
135	3	5.7	2.1	76	22.7	1.3	0
135	3.75	4.5	1.6	78	17.7	1	3.3
130	0.75	10.8	4.2	58.7	34.9	6.3	0.1
130	1.5	6.1	2.8	72	27	0.9	0.1
130	2.25	5.2	2.2	80	21	0.3	0
130	3	3.9	1.6	83.6	16.4	0	0
130	3.75	3.7	1.3	85	13	0	2

Start-up and Stabilization

Catalyst = Cu/SiO2
T = 180 C
P = 1 bar
WHSV = 2
EtOH : NH3 : H2 : N2 = 1 : 2 : 4.6 : 13.6

x(EtOH) (mol %)	x(NH3) (mol %)	s(MEA) (mol %)	s(DEA) (mol %)	s(TEA) (mol %)	s(Other) (mol %)	Time (mins)
13	2.5	7.6	33.7	54	4.7	15
10.1	2	9.5	43.9	39.9	6.7	45
7.9	1.7	8.2	47	36.7	8.1	75
8	1.5	5.6	51.8	36.4	6.2	130
6.3	1.3	0	57	34.6	8.4	205
6.2	1.2	0	60.5	32.8	6.7	275
5.1	1.1	0	65	35	0	390
4.7	1	0	64.6	25.9	9.5	1380
4.8	1	0	64.5	26	9.5	1415
4.3	1	0	69.5	30.5	0	1465

Temperature Ramp to Locate Reaction Regimes

Catalyst = Cu/SiO2
T = 180 C
P = 1 bar
WHSV = 2
EtOH : NH3 : H2 : N2 = 1 : 2 : 4.6 : 13.6

Temperature (C)	x(EtOH) (mol %)	x(NH3) (mol %)	s(MEA) (mol %)	s(DEA) (mol %)	s(TEA) (mol %)	s(Other) (mol %)
140	0	0				
150	0.6	0.1	0	100	0	0
161	1.6	0.4	0	80.4	19.6	0
170	2.8	0.5	0	76.8	23.2	0
182	5.6	1.1	6.5	67.3	26.2	0
190	8.8	1.5	5.3	55.4	28.3	11
200	11.1	2.1	4.7	51.3	31.6	12.4
210	14.9	2.8	4.7	45.4	32.3	17.6
222	22.9	3.8	3.5	37.4	30.2	28.9
230	25	4.8	4.1	42.5	33.3	20.1
240	27.8	5.5	3.4	38.2	31.5	26.9

Effect of Ammonia Pressure

Catalyst = Cu/SiO2
T = 190 C
P = 1 bar
p(EtOH) = 4 kPa
p(H2) = 20 kPa
Total flowrate = 200 ml/min

p(NH3) (kPa)	x(EtOH) (mol %)	x(NH3) (mol %)	s(MEA) (mol %)	s(DEA) (mol %)	s(TEA) (mol %)	s(Other) (mol %)
1.901646	8	6.9	9	27.1	57.9	6
2.474168	8.1	5	9.6	33.7	49.7	7
3.366738	7.7	3.7	9.8	38.2	43.6	8.4
3.959244	7.7	3.4	8.1	41.2	42.5	8.2
4.968068	7.2	2.5	7	47	38	8
6.250372	7.2	1.8	6.5	50	34.4	9.1
6.725546	6.9	1.8	5.5	53.2	31.3	10
8.166613	7.6	1.6	5	56	27	12
9.440847	7.6	1.2	5.6	57	21.9	15.5
10.43451	7	1.1	5	59.4	19	16.6

Effect of Ethanol Pressure

Catalyst = Cu/SiO2
T = 190 C
P = 1 bar
p(NH3) = 8 kPa
p(H2) = 20 kPa
Total flowrate = 200 ml/min

p(EtOH) (kPa)	x(EtOH) (mol %)	x(NH3) (mol %)	s(MEA) (mol %)	s(DEA) (mol %)	s(TEA) (mol %)	s(Other) (mol %)
1.618031	9.9	0.9	0	70.9	29.1	0
2.153702	8.6	1.1	0	69.2	30.8	0
2.547639	8.6	1.2	5	65	28	2
2.534262	8.9	1.2	6	61.4	28.6	4
3.087149	7.8	1.3	7	57.3	27	8.7
2.906221	8.5	1.4	6.5	56.9	27.5	9.1
3.787583	6.9	1.4	6	56	29.1	8.9
4.284442	6.8	1.6	5	55	28	12
5.063544	5.9	1.6	5	55	28.7	11.3
5.638065	5.6	1.7	4.2	56	26.5	13.3

Effect of Hydrogen Pressure

Catalyst = Cu/SiO2
T = 190 C
P = 1 bar
p(EtOH) = 2 kPa
p(NH3) = 8 kPa
Total flowrate = 200 ml/min

p(EtOH) (kPa)	x(EtOH) (mol %)	x(NH3) (mol %)	s(MEA) (mol %)	s(DEA) (mol %)	s(TEA) (mol %)	s(Other) (mol %)
20.13738	8	0.8	0	71.4	28.6	0
17.78671	9.3	0.8	0	64.2	24	11.8
15.74947	10.3	0.9	0	64	23.8	12.2
13.86893	9.5	0.9	0	61	22	17
12.22347	8.1	0.8	0	62	20	18
10.42129	7.8	0.7	0	59	18	23
8.932533	7.45	0.65	0	58.4	15.4	26.2
6.660222	7.1	0.6	0	56	14	30

Effect of Reaction Temperature

Catalyst = Cu/SiO2
P = 1 bar
EtOH : NH3 : H2 : N2 = 1 : 2 : 6.6 : 17.6

Temperature (C)	WHSV (1/h)	x(EtOH) (mol %)	x(NH3) (mol %)	s(MEA) (mol %)	s(DEA) (mol %)	s(TEA) (mol %)	s(Other) (mol %)
190	0.75	13.2	3.2	4.4	57.1	32.1	6.4
190	1.5	8.6	2	5.5	59.8	25.4	9.3
190	2.25	6.9	1.5	6	60	22	12
190	3	5.6	1.1	6.8	59	20.5	13.7
190	3.75	4.9	1	7.5	56.4	18.6	17.5
185	0.75	12.8	3.3	4.7	59.3	30.4	5.6
185	1.5	8	1.8	7.1	62	22.5	8.4
185	2.25	5.5	1.4	14.6	55.3	19.6	10.5
185	3	4.2	0.9	0	68.3	21.2	10.5
185	3.75	3.7	0.8	9.6	70.4	20	0
180	0.75	9.4	2.5	6.4	65.2	23.5	4.9
180	1.5	6.1	1.5	15.1	60.3	17.2	7.4
180	2.25	3.9	1	7.6	65.4	18.5	8.3
180	3	3.5	0.7	9.3	73.3	17.4	0
180	3.75	2.9	0.6	18.4	66.3	15.3	0
175	0.75	9.2	2.4	5.6	64.4	24.9	5.1
175	1.5	4.7	1.1	0	71.7	19	9.3
175	2.25	3.2	0.8	9	74.1	16.9	0
175	3	2.5	0.6	0	82.6	17.4	0
175	3.75	2.4	0.5	0	75	15.4	9.6
170	0.75	7.9	2.1	9.9	64.4	20	5.7
170	1.5	3.9	1.1	11.8	65.7	15.1	7.4
170	2.25	2.6	0.6	0	75.6	15.2	9.2
170	3	2	0.5	0	83.2	16.8	0
170	3.75	1.4	0.3	0	100	0	0

Effect of Metal Carrier

Catalyst = Co/SiO2
T = 180 C
P = 1 bar
EtOH : NH3 : H2 : N2 = 1 : 2 : 8.6 : 17.8

WHSV (1/h)	x(EtOH) (mol %)	s(MEA) (mol %)	s(DEA) (mol %)	s(TEA) (mol %)	s(Other) (mol %)	Time (mins)
1	84.9	30	50	16.5	3.5	20
1	77.1	32	49	15.2	3.8	55
1	83.9	34	48	16	2	105
1	81	36	46.5	14.7	2.8	195
1	77.6	36.6	46.3	15.3	1.8	255
1	75.1	37	47.2	14.4	1.4	315
1	64	38	46	15	1	450
1	70.9	37	47	15.9	0.1	525
1	71.2	36.4	45	15.1	3.5	1530
1	65.3	37.4	44.4	13.7	4.5	1570
1	65.6	36.2	45.5	14.5	3.8	1610
1	67.6	38.3	45.7	14.7	1.3	1660
1	66.4	38.4	45.6	13.2	2.8	1690
0.5	94.9	35.1	45.6	15.4	3.7	-
0.5	83.9	33.6	48.3	16.1	2	-
0.5	85.2	35.5	45.6	16.5	2.2	-
0.5	78.3	34.5	44.3	16.2	5	-
2	55.1	45.4	41	10.1	3.5	-
2	57.8	45.2	41.1	12.3	1.4	-
2	56.2	45.2	40.8	10.4	3.6	-
2	52.7	42.1	42.9	11.7	3.3	-

Catalyst = Co/Al2O3
T = 180 C
P = 1 bar
EtOH : NH3 : H2 : N2 = 1 : 2 : 8.6 : 17.8

WHSV (1/h)	x(EtOH) (mol %)	s(MEA) (mol %)	s(DEA) (mol %)	s(TEA) (mol %)	s(Other) (mol %)	Time (mins)
1	62.7	34.7	52.1	10	3.2	20
1	63.2	40.7	46.3	8.5	2.5	50
1	65.3	40.9	47.4	9.3	2.4	85
1	58	41.6	47.1	8.3	3	155
1	63.2	40.8	47	8.7	3.5	255
1	56.6	42	46.5	8.3	3.2	325
1	61.6	42	45.8	7.8	4.6	355
1	49.6	45	46.1	8	0.9	1455
1	49.9	45.2	46.7	6.9	1.2	1500
1	48.4	45.6	44.7	8.4	1.3	1530
1	49.9	45.4	44.4	7	3.2	1560
1	52.4	45.7	45	9.4	0	1585
0.5	57.9	49.5	42.5	6.6	1.4	-
0.5	57.2	51.6	40.8	6.2	1.4	-
0.5	54.7	49.7	40.4	6.2	3.7	-
0.5	57.5	51.3	39.7	5.8	3.2	-
2	39.3	49.1	41	5	4.9	-
2	38	49.9	43.3	5.5	1.3	-
2	39.2	49.3	44	5.5	1.2	-
2	41.2	48.7	44.4	5.4	1.5	-

Catalyst = Co/13SiO2-Al2O3
T = 180 C
P = 1 bar
EtOH : NH3 : H2 : N2 = 1 : 2 : 8.6 : 17.6

WHSV (1/h)	x(EtOH) (mol %)	s(MEA) (mol %)	s(DEA) (mol %)	s(TEA) (mol %)	s(Other) (mol %)	Time (mins)
1	53.4	60	32	7.3	0.7	20
1	49.2	60.5	31.5	6.8	1.2	50
1	49.9	61	31	6.8	1.2	100
1	44.4	60.6	31.4	7.2	0.8	150
1	50	63.4	29.7	6.1	0.8	225
1	44.8	62.8	29.1	6	2.1	280
1	46.8	63.7	28.6	6	1.7	335
1	43.2	65.7	28.9	5.4	0	1310
1	37.8	64.3	26.8	4.7	4.2	1340
1	36.6	67	27.4	4.7	0.9	1380
1	35.8	66	27	5.3	1.7	1430
1	36.2	67.1	26.9	6	0	1465
0.5	45.7	61.6	30.4	6	2	-
0.5	48.9	65.2	28.1	5.4	1.3	-
0.5	44.6	64.5	27.9	4.6	2.8	-
0.5	44.6	64.3	28.7	5	2	-
2	30.6	71.8	24.3	3.9	0	-
2	37.7	68.3	27.4	4.3	0	-
2	33.7	64.3	30.3	5.4	0	-
2	31.5	65.7	29.1	5.2	0	-

Catalyst = Co/MgO
T = 180 C
P = 1 bar
EtOH : NH3 : H2 : N2 = 1 : 2 : 8.6 : 17.6

WHSV (1/h)	x(EtOH) (mol %)	s(MEA) (mol %)	s(DEA) (mol %)	s(TEA) (mol %)	s(Other) (mol %)	Time (mins)
1	12.4	0	5.9	29.6	64.5	20
1	8.7	22.6	6.5	42.8	28.1	50
1	10.6	9.6	3.6	17.9	68.9	95
1	6.8	10.9	6.1	36.4	46.6	160
1	4.9	8.1	6.5	25.6	59.8	290
1	5.4	4.9	18	2.1	75	385
1	1.1	0	0	0	100	1590
1	1.8	0	0	0	100	1710
1	2.2	0	0	0	100	1770

Effect of Support Acidity

Catalyst = Co/1SiO2-Al2O3
T = 180 C
P = 1 bar
EtOH : NH3 : H2 : N2 = 1 : 2 : 8.6 : 17.6

WHSV (1/h)	x(EtOH) (mol %)	s(MEA) (mol %)	s(DEA) (mol %)	s(TEA) (mol %)	s(Other) (mol %)	Time (mins)
1	75.7	34.5	47.8	17.7	0	20
1	73.9	42.1	42.8	12.4	2.7	45
1	73.1	44.2	43.5	12.3	0	75
1	73.3	41.4	44.3	13.6	0.7	120
1	70.6	44	43.5	12.5	0	155
1	70.1	46.5	42.3	11.2	0	180
1	67.9	46.3	42.5	11.1	0.1	200
1	70.5	45.7	42.1	11.6	0.6	235
1	70.5	46.7	42	11.2	0.1	260
1	70.2	43.6	41.4	11.2	3.8	320
1	68.7	44	43.9	12.2	0	500
1	64.3	42.4	44.8	12.8	0	1450
1	65	45.4	42.4	11.3	0.9	1485
1	66.9	48	42.2	10.8	1	1505
1	65.3	44.9	40.8	10.7	3.6	1535
1	64.9	46	42.1	11	0.9	1560
0.5	78.6	36.8	45.4	14.7	3.1	-
0.5	76.9	33.2	50.6	15.7	0.5	-
0.5	77.5	39.5	46.4	14.1	0	-
0.5	79.7	37.9	46.4	14.6	1.1	-
2	58	50.4	41	8.7	0	-
2	55.7	49	41.6	9.4	0	-
2	56.4	49.1	41.7	9.3	0	-
2	56.7	47	43.1	10	0	-

Catalyst = Co/4SiO2-Al2O3
T = 180 C
P = 1 bar
EtOH : NH3 : H2 : N2 = 1 : 2 : 8.6 : 17.6

WHSV (1/h)	x(EtOH) (mol %)	s(MEA) (mol %)	s(DEA) (mol %)	s(TEA) (mol %)	s(Other) (mol %)	Time (mins)
1	59.7	45.6	42.7	11.8	0	20
1	58.5	48.8	41.2	10.2	0	65
1	57.6	50.3	39.9	9.8	0	90
1	57.5	51.3	39.1	9.5	0.1	120
1	56.6	51.2	39.2	9.6	0	150
1	56.2	50.2	39.9	10	0	210
1	53.8	50.8	39.4	9.7	0.1	245
1	53.8	48	41	11.1	0	370
1	51.8	46.6	42.2	11.2	0	1225
1	53.4	50.4	39.8	9.7	0.1	1255
1	51	50	39.9	10	0.1	1285
1	54.4	51.8	38.9	9.4	0	1315
1	50.9	48.7	40.8	10.4	0.1	1365
0.5	67.1	45.3	42.3	12.4	0	-
0.5	67.5	45.9	42.3	11.8	0	-
0.5	67.5	45.3	42.7	12	0	-
0.5	67.1	45.3	42.6	12.1	0	-
2	39.9	54.4	38.1	7.5	0	-
2	40.5	54	38.3	7.7	0	-
2	39.7	54	38	7.9	0.1	-
2	44	54	38.2	7.8	0	-

Catalyst = Co/9SiO2-Al2O3
T = 180 C
P = 1 bar
EtOH : NH3 : H2 : N2 = 1 : 2 : 8.6 : 17.8

WHSV (1/h)	x(EtOH) (mol %)	s(MEA) (mol %)	s(DEA) (mol %)	s(TEA) (mol %)	s(Other) (mol %)	Time (mins)
1	49.4	40.9	43.2	15.9	0	20
1	46.3	52.5	37.1	10.4	0	50
1	46.1	52.9	36.9	10.1	0.1	85
1	44.3	52.4	37.4	10.2	0	190
1	43	52.7	37.1	10.2	0	290
1	45.1	53.8	36.6	9.6	0	340
1	43.9	54.1	36.1	9.8	0	385
1	39.6	50.9	39.3	9.8	0	1320
1	39.1	55.6	36	8.4	0	1345
1	45.7	55.5	35.9	8.6	0	1370
1	41.9	54.5	36.8	8.7	0	1400
1	39.6	56.4	35.2	8.4	0	1430
0.5	56.9	50.4	38.2	11.4	0	-
0.5	56.3	50.1	38.9	11	0	-
0.5	60.1	50.2	38.8	10.9	0.1	-
0.5	55.5	50.2	39	10.8	0	-
2	32.3	60.4	33.5	6	0.1	-
2	30.9	59.8	33.8	6.4	0	-
2	29.9	58.9	34.3	6.8	0	-
2	29.9	59.6	33.7	6.7	0	-

Effect of Reduction Temperature

Catalyst = Co/Al2O3, Reduction Temperature = 300 C
T = 180 C
P = 1 bar
EtOH : NH3 : H2 : N2 = 1 : 2 : 8.6 : 17.8

WHSV (1/h)	x(EtOH) (mol %)	s(MEA) (mol %)	s(DEA) (mol %)	s(TEA) (mol %)	s(Other) (mol %)	Time (mins)
1	11.7	77.2	19.4	0	3.4	30
1	11.6	80.4	16.4	3.2	0	70
1	9.4	78	18.1	0	3.9	110
1	9.4	80.7	15.2	0.5	3.6	155
1	9.1	81.7	14.7	0	3.6	240
1	10.5	68.4	13.4	0	18.2	305
1	8.7	78.9	15.7	0	5.4	455
1	8.5	85	11.2	0	3.8	500
1	6	84.4	15.6	0	0	1460
1	9	76.8	23.2	0	0	1490
1	7	88	12	0	0	1520
1	8.4	84.4	11.6	0	4	1550
1	8.3	86.4	13.6	0	0	1595
0.5	9.6	80.9	14	0	5.1	-
0.5	9.2	82.2	12.9	0	4.9	-
0.5	9.6	82.5	12.9	0	4.6	-
0.5	10	82.8	12.6	0	4.6	-
2	7.2	83.6	12.5	0	3.9	-
2	5.9	86.8	13.2	0	0	-
2	6.3	84.2	15.8	0	0	-
2	6.8	79.6	16	0	4.4	-

Catalyst = Co/Al2O3, Reduction Temperature = 400 C
T = 180 C
P = 1 bar
EtOH : NH3 : H2 : N2 = 1 : 2 : 8.8 : 17.8

WHSV (1/h)	x(EtOH) (mol %)	s(MEA) (mol %)	s(DEA) (mol %)	s(TEA) (mol %)	s(Other) (mol %)	Time (mins)
1	38.6	42.8	46.7	9	1.7	15
1	36.9	50.6	41.3	5.8	2.3	55
1	32.4	53.8	36.8	5.4	2	115
1	31.8	51.7	36.8	5	6.7	185
1	32	54.7	37.7	5.2	2.4	315
1	34	49.7	37.7	5.1	7.5	385
1	30.8	50.5	41.9	5.2	2.4	515
1	24.8	55.6	37	4.6	2.8	1355
1	28.1	58.2	35.4	4	2.4	1390
1	27.3	51.4	34.7	4.8	9.1	1420
1	26.1	59.3	34.1	3.7	2.9	1445
0.5	36	59.1	33	5.4	2.5	-
0.5	32	59	30.7	3.2	7.1	-
0.5	37	53.4	34.8	3.4	8.4	-
0.5	32	61.4	32.5	3.4	2.7	-
2	20.6	60.8	33	3.7	2.5	-
2	21.1	56.8	36.6	4	2.6	-
2	22.9	51.6	35.3	4.6	8.3	-
2	22.1	55.6	37.6	3.9	2.9	-

Catalyst = Co/Al2O3, Reduction Temperature = 450 C
T = 180 C
P = 1 bar
EtOH : NH3 : H2 : N2 = 1 : 2 : 8.8 : 17.8

WHSV (1/h)	x(EtOH) (mol %)	s(MEA) (mol %)	s(DEA) (mol %)	s(TEA) (mol %)	s(Other) (mol %)	Time (mins)
1	59.4	34.9	50.5	10	4.6	15
1	62.6	43.9	46.4	8.4	1.3	45
1	54.1	45.6	45.6	7.5	1.3	95
1	54.2	41.4	45.6	7.7	5.3	145
1	60.9	43.8	46.9	7.7	1.6	185
1	53.1	46.7	46	7.3	0	260
1	40.4	43.9	42.8	6.2	7.1	1280
1	45.6	48.2	40.5	5.6	5.7	1310
1	42.9	46.8	43.3	5.9	2	1340
1	43.9	49.5	43	5.6	1.9	1380
1	44.9	49.8	42.6	5.7	1.9	1410
0.5	55.1	46.7	40.7	6	4.6	-
0.5	52.6	48.8	43.5	5.8	1.9	-
0.5	60.6	52.9	40.2	5.3	1.6	-
0.5	61	51.5	38.9	4.9	4.7	-
2	36.8	52.4	41	4.8	1.8	-
2	38.5	47.9	44.2	6.1	1.8	-
2	38.5	42	45	5.6	7.4	-
2	38.2	47.7	45.7	5.3	1.3	-

Catalyst = Co/Al2O3, Reduction Temperature = 550 C
T = 180 C
P = 1 bar
EtOH : NH3 : H2 : N2 = 1 : 2 : 8.6 : 17.6

WHSV (1/h)	x(EtOH) (mol %)	s(MEA) (mol %)	s(DEA) (mol %)	s(TEA) (mol %)	s(Other) (mol %)	Time (mins)
1	50.8	42.6	47.3	8.7	1.4	15
1	48.4	49.9	41.9	6.4	1.8	50
1	46.3	47.6	43.4	6.9	2.1	110
1	46.9	47.1	40.1	7.1	5.7	145
1	46.6	47.7	40.7	6.1	5.5	185
1	41.2	46.8	41.1	6.2	5.9	520
1	43.5	52	39.9	5.9	2.2	550
1	44.7	49	38.9	5.7	6.4	585
1	43.9	50.7	37.4	5.1	6.8	610
1	36.4	48.4	39.6	5.6	6.4	1365
1	41.7	53.1	36.9	5.6	2.4	1390
1	40.7	52.3	40	5.2	2.5	1410
1	40.6	54.7	38	4.9	2.4	1435
1	40.1	51	37	4.7	7.3	1465
0.5	55.2	54.2	38.8	5	2	-
0.5	50.1	55.7	39.5	4.8	0	-
0.5	52	55.8	37.4	4.8	2	-
2	32.7	56.1	37.3	4.3	2.3	-
2	35.1	48.6	38.4	4.6	8.2	-
2	34.9	47.6	40.6	4.6	7.2	-

Catalyst = Co/Al2O3, Reduction Temperature = 600 C
T = 180 C
P = 1 bar
EtOH : NH3 : H2 : N2 = 1 : 2 : 8.6 : 17.6

WHSV (1/h)	x(EtOH) (mol %)	s(MEA) (mol %)	s(DEA) (mol %)	s(TEA) (mol %)	s(Other) (mol %)	Time (mins)
1	41.3	49.6	43	7.4	0	15
1	44.9	52.8	36.7	4.7	5.8	75
1	41.6	51.9	37.6	5.2	5.3	110
1	50.6	55.6	37.8	4.8	1.8	155
1	40.6	55.5	36	4.1	4.4	220
1	41.2	54.4	39.1	4.5	2	310
1	39.8	56.1	35.9	4.1	3.9	400
1	39.7	55.8	38	4.1	2.1	635
1	33.1	55.7	34.4	3.8	6.1	1460
1	36.2	61.2	33.3	3.7	1.8	1490
1	37.3	59.4	31.8	2.7	6.1	1525
1	39.7	62	32.9	3	2.1	1560
0.5	45.6	58.9	36.1	2.8	2.2	-
0.5	46.8	59.3	32.6	2.8	5.3	-
1	45.7	62.8	32.9	2.2	2.1	-
0.5	42.7	59.6	37.7	2.7	0	-
2	27.2	59.6	37.2	3.2	0	-
2	33.2	59.6	35.4	3.1	1.9	-
2	29.9	53.6	40.5	4.3	1.6	-

Effect of Reduction Time

Catalyst = Co/Al2O3, Reduction Time = 5 hours
T = 180 C
P = 1 bar
EtOH : NH3 : H2 : N2 = 1 : 2 : 8.6 : 17.6

WHSV (1/h)	x(EtOH) (mol %)	s(MEA) (mol %)	s(DEA) (mol %)	s(TEA) (mol %)	s(Other) (mol %)	Time (mins)
1	72	39.5	49.9	9.4	1.2	25
1	67.8	45.4	43.5	8.3	4.8	70
1	68.4	43.1	46.7	8.9	1.3	100
1	77.3	36.6	48.2	9.2	3.8	150
1	69.8	36.7	50.4	9.4	3.5	210
1	78.4	39.7	49.7	9.3	1.3	250
1	67.9	35.6	50.4	10.4	3.6	335
1	63.1	37.5	49.2	9.2	4.1	440
1	57.8	39.5	51.6	8.9	0	1395
1	65.3	39.8	45.9	8.8	5.5	1430
1	63.4	41.6	48.8	7.9	1.5	1460
1	68.9	41.5	50.2	8.3	0	1495
1	60.4	43.2	47.6	7.6	1.6	1520
0.5	71.8	39.5	48.1	8.5	4.9	-
0.5	66.3	35.9	50.2	9.2	4.7	-
0.5	71	43.6	45	7.5	3.9	-
0.5	70.8	44.1	44.5	7.4	4	-
2	47.9	41	46.3	6	6.7	-
2	51.1	43.9	47.5	7	1.6	-
2	48.7	41.8	46.8	6.7	4.9	-
2	48.6	42.7	49.5	6.3	1.5	-

Catalyst = Co/Al2O3, Reduction Time = 20 hours
T = 180 C
P = 1 bar
EtOH : NH3 : H2 : N2 = 1 : 2 : 8.6 : 17.6

WHSV (1/h)	x(EtOH) (mol %)	s(MEA) (mol %)	s(DEA) (mol %)	s(TEA) (mol %)	s(Other) (mol %)	Time (mins)
1	80.6	27.7	56	16.3	0	15
1	75.3	38	50.4	10.7	0.9	45
1	73.9	40.2	49.5	9.5	0.8	70
1	70.1	36.4	50	10.6	3	220
1	71.7	39.3	50.4	10.3	0	290
1	80.1	38.5	47.9	9.5	4.1	325
1	75.2	36.4	48.8	9.4	3.4	375
1	61.9	35.6	51.1	9.5	3.8	1360
1	68	38.5	49.7	9.1	4.7	1390
1	63.6	40.3	49.9	8.5	1.3	1420
1	69.3	39	48	8.6	4.4	1460
1	62.1	37.7	49.1	8.8	4.4	1500
0.5	75.4	38.1	49	9.3	3.6	-
0.5	75.1	40.9	46.2	8.8	4.1	-
0.5	73.6	39.3	50.2	9.4	1.1	-
0.5	80.7	42.4	46.2	8.2	3.2	-
2	52.6	45.9	46.1	6.5	1.5	-
2	53.8	42	46.2	6.4	5.4	-
2	52.5	38.6	52.2	7.4	1.8	-
2	50.9	42.4	49.1	6.8	1.7	-

Appendix V - Sample Calculation of Chemisorption Data Work-up

Hydrogen chemisorption was used to measure the total hydrogen uptake (and therefore the total number of exposed metal atoms) of the reduced metal catalysts. Following the first chemisorption measurement, the sample was evacuated for 15 minutes at the temperature of adsorption and the hydrogen uptake was remeasured. This was performed in order to measure the amount of strongly bound hydrogen on the reduced metal catalyst. This hydrogen uptake represents the amount of hydrogen removed during this 15 minute evacuation and by difference, the amount of strongly adsorbed hydrogen can be determined. Knowledge of the total cobalt content of the sample and the extent of reduction allows the determination of the metallic dispersion and the average particle diameter.

The chemisorption measurements of the Co/SiO_2 catalyst showed that the total hydrogen uptake was 0.4030 cm^3/g_{cat} and the amount of hydrogen not removed by evacuation at the temperature of adsorption (*i.e.* strongly adsorbed hydrogen) was 0.1374 cm^3/g_{cat}. Since hydrogen adsorbs dissociatively on cobalt [Bartholomew *et al*, 1980], the total number of exposed cobalt atoms can be calculated from the following relationship (where N_{Av} is Avogadro's number).

$$N_{Co} = \frac{0.4030\ cm^3\ H_2/g_{cat}}{22414\ cm^3\ H_2/mol\ H_2} \cdot \frac{2\ mol\ Co}{mol\ H_2} \cdot N_{Av} = 2.166 \times 10^{19}\ atoms\ Co/g_{cat}$$

Since the site density of fcc cobalt is 14.6 atoms/nm^2 [Bartholomew *et al*, 1980], the metallic surface area can be easily determined using the following relationship.

$$Surface\ area = \frac{2.166 \times 10^{19}\ atoms}{14.6\ atoms/nm^2} \cdot 10^{-18}\ m^2/nm^2 = 1.48\ m^2/g_{cat}$$

The reversibility (or strength) of hydrogen adsorption is calculated as the percentage of

strongly adsorbed hydrogen relative to the total hydrogen uptake of the catalyst, as illustrated below.

$$Reversibility\ of\ adsorption = \frac{0.1374\ cm^3/g_{cat}}{0.4030\ cm^3/g_{cat}} \cdot 100\% = 34.1\ \%$$

The metallic dispersion is defined as the number of exposed metal atoms relative to the total amount of metal present in the catalyst sample. Since the extent of reduction to zerovalent metal was frequently lower than 100% in these studies, the dispersion calculations were based on the amount of reduced metal in the catalyst sample and not on the total metal content. The number of reduced metal atoms can be determined by multiplying the total number of metal atoms in the catalyst sample by the extent of reduction. The dispersion of the Co/SiO_2 catalyst can be calculated in the following manner :

$$Dispersion = \frac{2.166 \times 10^{19}\ exposed\ Co\ atoms}{2.442 \times 10^{20}\ reduced\ Co\ atoms} \cdot 100\% = 8.9\%$$

The average diameter of the metal particles can be determined by assuming that the supported metal crystallites are spherical. From the volume to surface area relationship of a sphere, the diameter of the particle can be calculated. The volume of reduced cobalt present on the reduced Co/SiO_2 catalyst was using the following relationship using a density of 8.9 g/cm^3 [Perry and Green, 1984].

$$Volume = \frac{2.442 \times 10^{20}\ atoms}{6.023 \times 10^{23}\ atoms/mol} \cdot \frac{58.9\ g/mol}{8.9\ g/cm^3} \cdot 10^{-6}\ m^3/cm^3 = 2.683 \times 10^{-9} m^3$$

From the volume surface area relationship, the average particle diameter can be calculated from the following expression :

$$\textit{Average diameter} = 6 \cdot \frac{2.683 \times 10^{-9}\ m^3/g_{cat}}{1.48\ m^2/g_{cat}} \cdot 10^9\ nm/m = 10.8\ nm$$